Memorial plaque with bust of Albert Einstein in Lesnická No. 7.
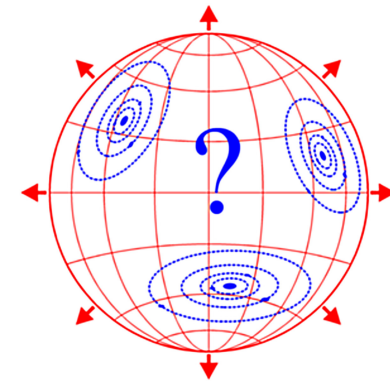
COSMOLOGY ON SMALL SCALES 2022

Proceedings of the International Conference

Cosmology on Small Scales 2022

Dark Energy and the Local
Hubble Expansion Problem

Prague, September 21–24, 2022

Edited by
Michal Křížek and Yurii V. Dumin

Institute of Mathematics
Czech Academy of Sciences

Proceedings of the International Conference
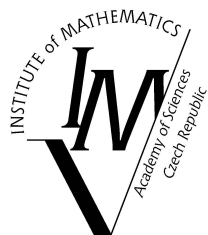
COSMOLOGY ON SMALL SCALES 2022

Dark Energy and the Local
Hubble Expansion Problem

Prague, September 21–24, 2022

Edited by
Michal Křížek and Yurii V. Dumin

Institute of Mathematics
Czech Academy of Sciences
Prague 2022

Dedicated to Alexander Friedmann

CONTENTS

Alternative cosmological theories

Preface

One hundred years ago, Russian mathematician and physicist Alexander A. Friedmann applied the system of Einstein equations to the three-dimensional sphere with a time varying radius. In this way, he obtained a nonlinear ordinary differential equation which is called the Friedmann equation after him and serves now as a cornerstone of the standard cosmological model. Unfortunately, it is well known that this model exhibits a number of paradoxes. Thus, the main goal of the CSS 2022 conference is to discuss whether and how the Friedmann equation can be applied at the various spatial scales, from our local cosmic neighborhood up to the whole Universe; and if the existence of dark matter and dark energy are merely artifacts of the excessive extrapolations. So, it is timely to gather specialists from various branches of astronomy and astrophysics to discuss these issues.

To shed more light onto these topics, we decided to organize the International Conference *Cosmology on Small Scales 2022: Dark Energy and the Local Hubble Expansion Problem.* It is held at the Institute of Mathematics of the Czech Academy of Sciences at Žitná 25, Prague 1, from 21 to 24 September 2022 (see `css2022.math.cas.cz`). It is a continuation of our three previous conferences *Cosmology on Small Scales 2016: Local Hubble Expansion and Selected Controversies in Cosmology*, *Cosmology on Small Scales 2018: Dark Matter Problem and Selected Controversies in Cosmology*, and *Cosmology on Small Scales 2020: Excessive Extrapolations and Selected Controversies in Cosmology* (see `css2016.math.cas.cz`, `css2018.math.cas.cz`, `css2020.math.cas.cz`).

The main topics of the conference "Cosmology on Small Scales 2022" are:

▷ Mathematical aspects of the extrapolations used in cosmology

▷ Arguments for and against dark energy, and revisiting the foundations of physics

▷ Alternative models for dark matter and dark energy

▷ A systematic discord in the value of the Hubble constant derived by different methods

▷ Theoretical possibility and observational evidence for small-scale cosmological effects

▷ Quantum effects on the early Universe and their observational imprints at the present time

This book includes only a small portion of the reports, because other works were either already published or submitted for publication elsewhere. At the end of the Proceedings, there is a couple of papers on "alternative cosmological theories". Although they may be questionable and the Scientific Committee is not responsible for their content, we believe that it is reasonable to present them to the wide audience.

The Scientific Committee consists of

Assoc. Prof. Yurii Dumin (Moscow State University & Space Research Institute of RAS, Russia)
Prof. Itzhak Goldman (Afeka College, Israel)
Prof. Igor Karachentsev (Special Astrophysical Observatory of RAS, Russia)
Prof. Sergei Kopeikin (University of Missouri, USA)
Prof. Pavel Kroupa (University of Bonn, Germany)
Prof. André Maeder (Geneva Observatory, Switzerland)
Assoc. Prof. Attila Mészáros (Charles University, Czech Republic)
Prof. Marek Nowakowski (Universidad de los Andes, Colombia)
Dr. Dmitry Pavlov (Research Institute of Hypercomplex Systems, Russia)
Prof. Lawrence Somer (Catholic University of America, USA)
Prof. Alessandro Spallicci (University of Orleans, CNRS, France)
Prof. Alexei Starobinsky (Landau Institute of RAS, Russia)

Local Organizing Committee consists of

Prof. Michal Křížek — Chair (Czech Academy of Sciences, Czech Republic)
Assoc. Prof. Yurii Dumin — Vice-Chair (Moscow State University & Space Research Institute of RAS, Russia)
Prof. Pavel Kroupa (University of Bonn, Germany)
Assoc. Prof. Tomáš Vejchodský (Czech Academy of Sciences, Czech Republic)
Hana Bílková (Czech Academy of Sciences, Czech Republic)

These Proceedings can be downloaded from the website:

http://users.math.cas.cz/∼krizek/list.html

Michal Křížek and Yurii V. Dumin

LOCAL DYNAMICAL EFFECTS OF SCALE INVARIANCE: THE LUNAR RECESSION

Andre Maeder[1], Vesselin Gueorguiev[2,3]

[1] Geneva Observatory
chemin Pegasi 51, CH-1290 Sauverny, Switzerland
andre.maeder@unige.ch
[2] Institute for Advanced Physical Studies, Sofia, Bulgaria
[3] Ronin Institute for Independent Scholarship, Montclair, NJ, USA
Vesselin@MailAPS.org

Abstract: Scale invariance is expected in empty Universe models, while the presence of matter tends to suppress it. As shown recently, scale invariance is certainly absent in cosmological models with densities equal to or above the critical value $\varrho_{\mathrm{c}} = 3H_0^2/(8\pi G)$. For models with densities below ϱ_{c}, the possibility of limited effects remains open. If present, scale invariance would be a global cosmological property. Some traces could be observable locally. For the Earth-Moon two-body system, the predicted additional lunar recession would be increased by 0.92 cm/yr, while the tidal interaction would also be slightly increased.

The Earth-Moon distance is the most systematically measured distance in the Solar System, thanks to the Lunar Laser Ranging (LLR) experiment active since 1970. The observed lunar recession from LLR amounts to 3.83 (± 0.009) cm/yr; implying a tidal change of the length-of-the-day (LOD) by 2.395 ms/cy. However, the observed change of the LOD since the Babylonian Antiquity is only 1.78 ms/cy, a result supported by paleontological data, and implying a lunar recession of 2.85 cm/yr. The significant difference of (3.83–2.85) cm/yr = 0.98 cm/yr, already pointed out by several authors over the last two decades, corresponds well to the predictions of the scale-invariant theory, which is also supported by several other astrophysical tests.

Keywords: cosmology, dark energy, Earth-Moon system

PACS: 98.80.-k, 96.25.De, 96.90.+c

1. Introduction

The scale-invariant theory aims at responding to a most fundamental principle expressed by Dirac [11]: *"It appears as one of the fundamental principles in Nature*

that the equations expressing basic laws should be invariant under the widest possible group of transformations". Our objective is to explore whether, in addition to Galilean invariance, Lorentz invariance, and general covariance, some effects of scale invariance would also be present in our low density Universe. This is particularly justified since scale invariance is present in Maxwell's equations in absence of charges and currents, while in General Relativity (GR) scale invariance is a property of the empty space in absence of a cosmological constant, a property pointed out by [4].

Clearly, the presence of matter tends to kill scale invariance as shown by [17]. Thus, the question arises about how much matter in the Universe is necessary for suppressing scale invariance. Would one single atom in the Universe be enough to kill scale invariance? Clearly, we do not know whether this is the case, but the way to get an answer to the above questions is to carefully examine the theoretical consequences of this assumption and to perform comparisons with observations. From the scale covariant expressions of the Ricci tensor, curvature scalar and general field equation developped by [11] and [7], cosmological models were obtained by [23] who showed that scale invariance is clearly forbidden for models with matter densities equal and above the critical density $\varrho_c = 3H_0^2/(8\pi G)$. This result was found consistent with considerations [30] on causal connexion in Universe models.

These models also indicate that, as soon that one considers models with a density parameter $\Omega_m > 0$, scale-invariant effects are drastically reduced, before totally disappearing at $\Omega_m = 1$. For a Universe model with $\Omega_m = 0.3$, they are nevertheless sufficient to drive a significant acceleration of the expansion. Several positive results have been obtained, *e.g.* on the distance modulus vs. reshifts z relation, the Hubble rate vs. age and density parameter, the $H(z)$ vs. z relations, even if due to the observed scatter the discrimination from the ΛCDM is difficult at present [23], [28]. The growth of density fluctuations is accounted for without the need of dark matter [27]; the same for the observed mass excess in clusters of galaxies [24]; and the radial acceleration relation for galaxies is reproduced [29]. For a brief summery of the Scale Invariant Vacuum paradigm and its main results and current progress see [20].

The question whether astrophysical systems, such as the solar system and galaxies, follow the Hubble-Lemaître expansion has stimulated a vast literature since the pioneer work of McVittie [33, 34] and the Einstein-Straus theorem [16]. The presence of an expansion at smaller scales has been considered as an open question by Bonnor [5] and recently revisited by us [31]. The fact that the dark-energy dominates the matter-energy content of the Universe and that this energy appears as driving the acceleration of expansion is reviving the interest in the question: If dark energy is uniformly distributed in space would it not imply effects that may be present at small scales? The Earth-Moon system occupies a particular place in this context, since there are direct accurate measurements of the evolution of the distance in this two-body system.

It is thus appropriate to examine whether there are some local effects of scale invariance, *e.g.* in the Solar System. According to several pioneer works [14], [15], [22], [26] the local effects in the Solar System due to scale invariance would have been

of the order of the Hubble-Lemaître expansion or some fraction of it. (The Hubble-Lemaître expansion with $H_0 = 70$ km s^{-1} Mpc^{-1} corresponds to 10.7 m/yr for one astronomical unit, or 2.75 cm/yr for the Earth-Moon distance of $384\,400$ km). For the proper interpretation of these effects in the scale-invariant context, it is necessary to account for the limitations of the λ-variations due to a significant matter density in the Universe, and this implies a refined analysis, which we do here.

Section 2 briefly recalls the main points of the scale-invariant vacuum idea. Section 3 examines the limitations of the scale-factor λ and their impact on timescales. In Section 4, we study the weak-field low-velocity approximation of the scale-invariant field equation and the two-body problem. In Section 5, we compare the predicted and observed lunar recession from Lunar Laser Ranging (LLR) in relation with the data on the length-of-the day (LOD). Section 6 gives the conclusions.

2. Some points on the scale invariant vacuum (SIV) theory

Some recalls on the scale-invariant framework have been given recently [30], with references therein. In short, the theory is expressed in the cotensor framework appropriate to the Integrable Weyl Geometry developed by [11] and [7]. The developments are rather parallel to those of General Relativity (GR), but with the possibility of conformal scale transformations of the form,

$$ds' = \lambda(x^\mu)ds\,, \tag{1}$$

in addition to the general covariance. Primed quantities refer to the GR framework, while quantities without a prime refer to the scale covariant context. Scale covariant first and second derivatives, scale covariant Christoffel symbols, Riemann-Christoffel cotensor, Ricci cotensor and total co-curvature have been developed in the Integrable Weyl Geometry by [11], leading to a general scale covariant field equation [7].

In GR, one needs to define the line element corresponding to the physical system studied, for example the FLWR line element is adopted for expressing the cosmological equations in a homogeneous and isotropic Universe. Similarly, in the scale covariant context, an additional condition is necessary to fix the gauge. Dirac and Canuto et al. had chosen the then in vogue "Large Number Hypothesis" [12]. We prefer to adopt as basic gauging condition the following assumption: *The macroscopic empty space is scale invariant, homogeneous and isotropic.* This is a simple and most reasonable assumption, which is consistent with the scale invariance of the equations of Maxwell and of General Relativity in empty space, as recalled in the introduction. Moreover, the equation of state of the vacuum $p_{\text{vac}} = -\varrho_{\text{vac}}c^2$ is precisely the one equation permitting the vacuum density to remain constant for an adiabatic expansion or contraction [9]. We also note that the assumption of homogeneity and isotropy appears a reasonnable one for the macroscopic empty space.

Within the cotensor framework, our gauging condition can be expressed as follows [23],

$$\kappa_{\mu;\nu} + \kappa_{\nu;\mu} + 2\kappa_\mu\kappa_\nu - 2g_{\mu\nu}\kappa^\alpha_{;\alpha} + g_{\mu\nu}\kappa^\alpha\kappa_\alpha = \Lambda\,g_{\mu\nu}\,. \tag{2}$$

It is what is left from the scale covariant field equation if space is empty[1]. The first member (LHS) results from the scale invariant form of the Ricci tensor [11]. The second member (RHS) contains only the cosmological constant Λ in the scale covariant form, with

$$\Lambda = \lambda^2 \Lambda_{\mathrm{E}} \, . \tag{3}$$

Λ_{E} is the cosmological constant in GR. The first member of Eq. (2) contains terms depending on κ_ν, the coefficient of metrical connection, related to the scale factor λ of Eq. (1),

$$\kappa_\nu \; = \; -\frac{\partial \ln \lambda}{\partial x^\nu} \, . \tag{4}$$

We note that if the scale factor λ is a constant, all terms in κ_ν vanish and Eq. (2) implies $\Lambda_{\mathrm{E}} = 0$. This means that the scale-invariant field equation just becomes the field equation of GR without a cosmological constant.

For reasons of homogeneity and isotropy of the empty space, the scale factor λ should depend on time only, so that the only non-zero component of κ_ν is κ_0,

$$\kappa_\nu = \kappa(t)\, \delta_{0\nu}, \; \kappa_{0,0} = \frac{d\kappa_0}{dt} = \dot{\kappa}_0 = \dot{\kappa} \, . \tag{5}$$

In Weyl's Integrable Geometry, κ_ν is playing a fundamental role alike the $g_{\mu\nu}$. From the time and space components of Eq. (2) one obtains:

$$3\frac{\dot{\lambda}^2}{\lambda^2} \; = \; \lambda^2 \, \Lambda_{\mathrm{E}} \quad \mathrm{and} \quad 2\frac{\ddot{\lambda}}{\lambda} - \frac{\dot{\lambda}^2}{\lambda^2} \; = \; \lambda^2 \, \Lambda_{\mathrm{E}} \, . \tag{6}$$

Thus, the gauging conditions leads to analytical relations between the scale factor λ and the cosmological constant, which represents the energy density of the vacuum. These differential equations give a new physical significance to the cosmological constant, which now appears as the energy density of the relative variations of the scale factor, see the first of Eqs.(6) and [30] for its connection to inflationary stage of the very early Universe. The solution of these differential equations is

$$\lambda(t) \; = \; \sqrt{\frac{3}{\Lambda_{\mathrm{E}}}} \, \frac{1}{ct} \, . \tag{7}$$

We take the present time $t_0 = 1$ and also consider the present scale as a reference to which all scales are referred to. Thus, $\lambda(t)$ may be written as,

$$\lambda(t) \; = \; \frac{t_0}{t} \, . \tag{8}$$

---

[1]The de Sitter metric for empty space with Λ_{E} is conformal to the Minkowski metric, and is identical to it for the condition $3\lambda^{-2}/(\Lambda_{\mathrm{E}} t^2) = c^2$. This condition is consistent with the solution (7).
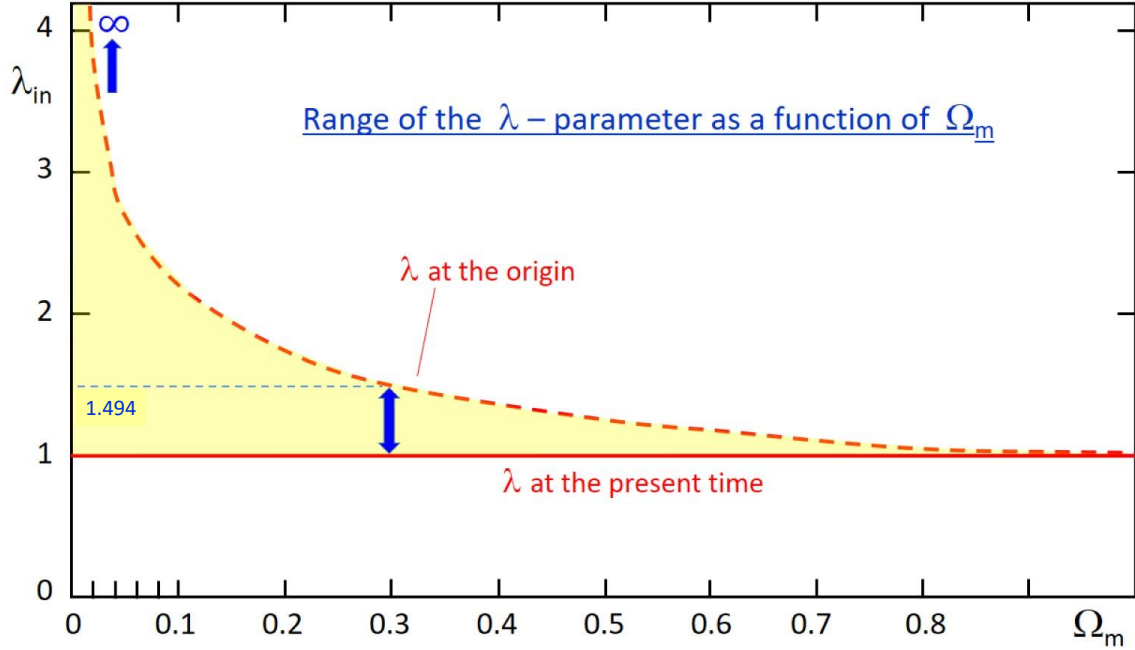
Figure 1: The values of the scale factor $\lambda_{\rm in} = 1/t_{\rm in}$ at the initial time $t_{\rm in} = \Omega_{\rm in}^{1/3}$, as a function of the density parameter $\Omega_{\rm m}$. The yellow zone shows, at each value of $\Omega_{\rm m}$, the range of $\lambda(t)$ from the Big-Bang (broken red line) to the present time (continuous red line). The blue arrow illustrates that for $\Omega_{\rm m} = 0.3$, the value of $\lambda(t)$ varies only between 1.494 at the origin and 1.0 at present. We see the drastic reduction of the effects of scale invariance with increasing $\Omega_{\rm m}$.

Remarkably, the gauging condition, which implies the two equations (6), lead to major simplifications of the cosmological equations derived by [7] on the basis of the general field equations. One obtains [23]:

$$\frac{8\pi G\varrho}{3} = \frac{k}{a^2} + \frac{\dot{a}^2}{a^2} + 2\frac{\dot{a}\dot{\lambda}}{a\lambda}, \tag{9}$$

$$-8\pi Gp = \frac{k}{a^2} + 2\frac{\ddot{a}}{a} + \frac{\dot{a}^2}{a^2} + 4\frac{\dot{a}\dot{\lambda}}{a\lambda}. \tag{10}$$

On the right side of both, we note an additional term. For a constant λ, Friedmann's equations are recovered. A third equation may be derived from the above two,

$$-\frac{4\pi G}{3}(3p + \varrho) = \frac{\ddot{a}}{a} + \frac{\dot{a}\dot{\lambda}}{a\lambda}. \tag{11}$$

Since $\dot{\lambda}/\lambda$ is negative, the extra term represents an additional acceleration in the direction of the motion. Thus, the effects of the scale invariance are fundamentally different from those of a cosmological constant. For an expanding Universe, this extra

force produces an accelerated expansion, without requiring dark energy. For a contraction, the additional term favors collapse. This is exactly what the corresponding term in the weak-field approximation is also doing, as verified in the study of the growth of density fluctuations [27]. There, the additional term favors contraction and allows an early formation of galaxies in absence of dark matter.

3. Limits on the variations of the scale factor

3.1. Solutions of the cosmological equations for $k = 0$

Analytical solutions for the flat scale-invariant models with $k = 0$ have been obtained by [21] in the case of matter dominated models, with the corresponding equation of conservation,

$$a(t) = \left[\frac{t^3 - \Omega_{\mathrm{m}}}{1 - \Omega_{\mathrm{m}}}\right]^{2/3}. \tag{12}$$

It is noticeable that an analytical solution exists. It is expressed in the timescale where at present $t_0 = 1$ and $a(t_0) = 1$. Such solutions are illustrated in [23] and [30]. Along with $\Omega_{\mathrm{m}} = \varrho/\varrho_{\mathrm{c}}$ with $\varrho_{\mathrm{c}} = 3H_0^2/(8\pi G)$ as usual. There is no meaningful scale-invariant solution for Ω_{m} equal or larger than 1, consistently with causality relations [30]. We see that the initial time when $a = 0$, the Big Bang, is at:

$$t_{\mathrm{in}} = \Omega_{\mathrm{m}}^{1/3}. \tag{13}$$

This dependence in $1/3$ produces a rapid increase of t_{in} for increasing low matter density. For $\Omega_{\mathrm{m}} = 0, 0.01, 0.1, 0.3, 0.5$, the values of t_{in} are 0, 0.215, 0.464, 0.669, 0.794. Since $\lambda \sim 1/t$, this leads to a strong reduction of the range of $\lambda(t)$-variations for increasing matter densities as illustrated in Fig. 1. While the range of scale variations is infinite between the Big Bang and now for an empty Universe model, the range would be very limited for significant Ω_{m}-values, for example from only 1.494 to 1.0 for $\Omega_{\mathrm{m}} = 0.3$. The Hubble parameter, in the same timescale, is

$$H(t) = \frac{2\,t^2}{t^3 - \Omega_{\mathrm{m}}}. \tag{14}$$

Thus, $H_0 = H(t_0)$ varies between 2 and the infinite for Ω_{m} between 0 and 1. We also write

$$\Omega_{\mathrm{k}} = -\frac{k}{a^2 H_0^2} \quad \text{and} \quad \Omega_\lambda = -\frac{2}{H_0}\left(\frac{\dot{\lambda}}{\lambda}\right)_0 = \frac{2}{H_0\,t_0}. \tag{15}$$

These are respectively the normalized contributions (vs. ϱ_{c}) of the matter, space curvature, and scale factor λ. With these definitions equation (9) leads to,

$$\Omega_{\mathrm{m}} + \Omega_{\mathrm{k}} + \Omega_\lambda = 1. \tag{16}$$

These quantities are usually considered at the present time. In the case of energy-density dominated by radiation and relativistic matter, for flat scale-invariant models with $k = 0$, analytical solutions for the expansion factor, the matter density, the radiation density and temperature have been obtained by [25].

3.2. Some essential properties of the scale-invariant solutions

Let us further examine the conditions of applicability of the above results:

1. Case of $\lambda(t)$ for homogeneous and isotropic Einstein-like empty space, but not necessarily empty Universe with homogeneous and isotropic cosmological space. The two equations (6) and their solution (7) for $\lambda(t)$ have been derived for the macroscopic empty space, under the assumption that it is homogeneous and isotropic, which implies a dependence of λ on time t only. The empty space obeys an equation $p_{\mathrm{vac}} = -\varrho_{\mathrm{vac}}\, c^2$ and in the scale-invariant theory the vacuum density is also related to the cosmological constant by $\Lambda = 8\pi G\, \varrho_{\mathrm{vac}}$. For $\Omega_{\mathrm{m}} = 0$ one has $\lambda = 1/t$ and $a = t^2$ and the cosmological equation (11) then implies $3p + \rho = 0$, which is the trace of the matter energy-momentum tensor.

Alike in GR, the properties of the vacuum and thus of the cosmological constant are intrinsic characteristics of the vacuum space, not depending on any matter content and distribution, and so was it also in the derivation of Eqs. (6). Thus, these equations and their solution apply everywhere in the Universe, independently of Ω_{m}. As a consequence, *the solution $\lambda(t)$ is a universal function, characteristic of the empty space.* Let us note that the energy density of the empty space can be expressed in term of a scalar field ψ,

$$\varrho = \frac{1}{2}\, C\, \dot{\psi}^2 \quad \text{with } \dot{\psi} = \kappa_0 = -\frac{\dot{\lambda}}{\lambda} \tag{17}$$

with the constant $C = 3/(4\pi G)$. The field ψ obeys a modified Klein-Gordon equation and ψ is advantageously playing the role of the "inflaton" during inflation [30].

2. Case of $\lambda(t)$ in presence of matter. The presence of matter could be viewed as space inhomogeneities below certain scale but absent at larger scales and especially at cosmic scales. The presence of matter is determined by the density parameter $\Omega_{\mathrm{m}} = \varrho/\varrho_{\mathrm{c}}$, which influences the interval of time between the initial time $t_{\mathrm{in}} = \Omega_{\mathrm{m}}^{1/3}$ and $t_0 = 1$. For a higher Ω_{m}-value (between 0 and 1), the interval $(t - t_{\mathrm{in}})$ is smaller and so does the range of the λ-values. In this indirect way, the presence of matter drastically reduces the range of variation of the scale factor λ (Fig. 1). Most importantly, we easily verify that in the scale-invariant context (Section 3.1), Ω_{m} does not change during the evolution of the Universe, both in the matter and radiation eras. As long as the radiation era is very short and negligible compared to the full age of the Universe, then the initial time t_{in} defines Ω_{m} as a constant for the Universe.

Thus, steps 1 and 2 show that the function $\lambda(t)$ has a form which is universal $\lambda(t) \sim 1/t$, but the range of the time variations, and thus of λ, is strongly limited by the matter content.

3. Case of $\lambda(t)$ for comoving galaxies. Now, comouving galaxies have the same timescale and thus the same age (the cosmic time). Thus, the $\lambda(t)$ parameter, its first, second derivatives and the coefficient of metrical connection are the same in all comoving galaxies:

$$\kappa(t) = -\dot{\lambda}/\lambda = 1/t. \tag{18}$$

Therefore, we are led to the following global conclusion: *The universal function $\lambda(t)$ and its limitations apply the same way in all comouving galaxies*. Thus, the effects of the variations of $\lambda(t)$ with their limitations could also be expected locally, *e.g.* in the Solar System, which is a low velocity subpart of a comoving galaxy.

3.3. Relations between timescales

We have two different timescales (both concerning the cosmic time): (1.) The age t of the above cosmological model, with $t_0 = 1$ at the present time and $t_{\rm in} = \Omega_{\rm m}^{1/3}$ at the origin. (2.) The usual timescale τ, with $\tau_0 = 13.8$ Gyr at the present time [18] and $\tau_{\rm in} = 0$ at the Big-Bang. The relation between ages in the two timescales is,

$$\frac{\tau - \tau_{\rm in}}{\tau_0 - \tau_{\rm in}} = \frac{t - t_{\rm in}}{t_0 - t_{\rm in}}. \tag{19}$$

This means that for an event at a given epoch, the age fraction with respect to the present age is the same in both timescales. This gives the two following relations between particular times t and τ,

$$\tau = \tau_0 \frac{t - t_{\rm in}}{t_0 - t_{\rm in}}, \quad \text{and } t = t_{\rm in} + \frac{\tau}{\tau_0}(t_0 - t_{\rm in}). \tag{20}$$

For the derivatives of these two timescales, we have,

$$\frac{d\tau}{dt} = \frac{\tau_0}{t_0 - t_{\rm in}}, \quad \text{and } \frac{dt}{d\tau} = \frac{t_0 - t_{\rm in}}{\tau_0}. \tag{21}$$

These derivatives have constant values, implying that the two times are linearly connected. For larger $\Omega_{\rm m}$-values, $t_{\rm in}$ is also larger (13) and the timescale t is squeezed over a smaller fraction of the interval [0,1] as $[t_{\rm in}, t_0 = 1]$. The above expressions are useful to express the relative variations of the scale factor $\lambda(t)$ as function of ages.

4. The dynamical equation and the two-body problem

4.1. The weak-field low-velocity approximation of the equation of motion

This approximation in the scale-invariant framework is leading to a modified expression of the Newton's Law [26], [24]. In spherical coordinates, it is

$$\frac{d^2\mathbf{r}}{dt^2} = -\frac{G_t\, M(t)}{r^2}\frac{\mathbf{r}}{r} + \kappa(t)\frac{d\mathbf{r}}{dt}. \tag{22}$$

16

This expression for a weak field is derived from the geodesic equation by Dirac in the reference [11], which was also obtained from an action principle by [6]. The conservation law for a dust Universe in the scale invariant context imposes a relation of the form [23]: $\varrho R^3 \lambda = const$. This means that the inertial mass of a particle or of an object is not necessarily a constant, a situation which also occurs in GR and Special Relativity where the inertial mass of an object depends on its velocity. Within SIV the mass is evolving like t in the same way as the length, so that, interestingly enough, the gravitational potential $\Phi = G_t M(t)/R(t)$ of an object is a scale-invariant quantity. We call $M(t)$ the mass that varies like $M(t) \sim (1/\lambda) \sim t$, where t is the cosmic time. In a Universe model with $\Omega_{\rm m} = 0.3$, a mass $M(t_0)$ at the present time was at time $t_{\rm in} = \Omega_{\rm m}^{1/3}$, $M(t_{\rm in}) = (t_{\rm in}/t_0)M(t_0) = \Omega_{\rm m}^{1/3} M(t_0) = 0.6694\ M(t_0)$ at the Big-Bang. Over small and moderate time intervals, the mass may often be considered as a constant.

With respect to the classical expression, there is an additional acceleration term in the direction of motion. This term proportional to the velocity is favoring collapse in an accretion system and favoring expansion in a two-body system. From here onwards, we call G_t the gravitational constant (a true constant), expressed in the appropriate units t in the above cosmological models, while G wil now on be reserved to the value expressed in the current time units (years, seconds).

Equation (22) contains terms and derivatives which are functions of the universal $\lambda(t)$, the range of which is squeezed by the limited range of the adopted t-scale in the cosmological models. As $\Omega_{\rm m}$ increases, a given range $\Delta\tau$ in the current time units (e.g. 2 Gyr) is expressed in terms of the corresponding smaller Δt interval. We need to convert the equation of motion (22) expressed with variable t into terms of the cosmic time τ in the current units (years, seconds) with an origin at $\tau = 0$ and a present value $\tau_0 = 13.8$ Gyr. Equation (22) becomes,

$$\frac{d^2\mathbf{r}}{d\tau^2}\left(\frac{d\tau}{dt}\right)^2 = -\frac{G_t M(t)}{r^2}\frac{\mathbf{r}}{r} + \frac{1}{t_{\rm in} + \frac{\tau}{\tau_0}(t_0 - t_{\rm in})}\frac{d\tau}{dt}\frac{d\mathbf{r}}{d\tau}\ . \tag{23}$$

The corresponding units of G in the usual τ-scale are $[{\rm cm}^3 \cdot g^{-1}{\rm s}^{-2}]$. Thus, we have the correspondence $G_t\left(\frac{dt}{d\tau}\right)^2 = G$ with the usual units conversion. At the present epoch t_0 or τ_0 in the current units, the masses $M(t_0)$ and $M(\tau_0)$ are evidently equal. At other epochs, the relation is,

$$M(t) = \frac{t}{t_0} M(t_0)\,, \qquad \text{thus} \quad M(\tau) = [\Omega_{\rm m}^{1/3} + \frac{\tau}{\tau_0}(1 - \Omega_{\rm m}^{1/3})]\,M(\tau_0)\,. \tag{24}$$

This results in the correct scaling of expected mass at the Big Bang $M(t_{\rm in}) = \Omega_{\rm m}^{1/3}M(t_0)$ to be compared with $M(\tau_{\rm in} = 0) = \Omega_{\rm m}^{1/3}M(\tau_0)$; therefore, $M(t_{\rm in}) = M(\tau_{\rm in} = 0)$.

Thus, multiplying both members of Eq. (23) by $\left(\frac{dt}{d\tau}\right)^2$, we get at time τ/τ_0,

$$\frac{d^2\mathbf{r}}{d\tau^2} = -\frac{G M(\tau)}{r^2}\frac{\mathbf{r}}{r} + \frac{1}{t_{\rm in} + \frac{\tau}{\tau_0}(t_0 - t_{\rm in})}\frac{t_0 - t_{\rm in}}{\tau_0}\frac{d\mathbf{r}}{d\tau}\ . \tag{25}$$

17

We see that the presence of matter ($t_{in} > 0$) always reduces the effect of the additional acceleration term, for $\Omega_m = 1 \Rightarrow t_{in} = 1 = t_0$ it disappears. Now, let us consider the situation at the present time τ_0. We define the numerical factor $\psi = \psi(\tau_0)$ using:

$$\psi(\tau) = \frac{t_0 - t_{in}}{t_{in} + \frac{\tau}{\tau_0}(t_0 - t_{in})} \Rightarrow \psi_0 = \psi(\tau_0) = 1 - \Omega_m^{1/3}. \tag{26}$$

The modified Newton's equation at present time τ_0, currently 13.8 Gyr, is then:

$$\frac{d^2\mathbf{r}}{d\tau^2} = -\frac{G\,M(\tau_0)}{r^2}\frac{\mathbf{r}}{r} + \frac{\psi_0}{\tau_0}\frac{d\mathbf{r}}{d\tau}. \tag{27}$$

The small additional term depends on the global cosmology, in particular on parameter Ω_m, as discussed above. In an empty Universe, $\psi_0 = 1$. For $\Omega_m \to 1$, one has $\psi_0 \to 0$. For higher Ω_m values, consistently with the discussion of the Eq. (12) the additional term would be absent [30]. In the case with $\Omega_m = 0.30$, one has $\psi_0 = 0.331$. Thus, the additional acceleration term is significantly reduced.

4.2. The two-body problem with λ-limitations

Let us now consider a two-body system within the SIV theory with $k = 0$ and a density parameter Ω_m. From Eq. (22) in the t-scale, the orbital motion was found to be still described by the Binet equation (the mass change being accounted for) and thus obeying the equation of conics [24] and [26]

$$r(\vartheta) = \frac{p}{1 + e\cos\vartheta}. \tag{28}$$

The parameter p is related to the semi-major axis a, semi-minor axis b, and eccentricity e via the relationships:

$$p = \frac{b^2}{a}, \quad b = a\sqrt{1 - e^2}, \quad \text{thus } p = a(1 - e^2). \tag{29}$$

The eccentricity e is a scale-invariant quantity. For $e = 0$, one has a circular orbit with a radius $r = p$. There is a small growth of the parameter p, or r for $e = 0$ as we consider here, first in the time t-scale,

$$\frac{\dot{r}}{r} = \left(-\frac{\dot{\lambda}}{\lambda}\right) = 1/t \quad \text{implying } r \sim t, \text{ and } \frac{\Delta r}{r} = \frac{\Delta t}{t}. \tag{30}$$

Thus, the orbital motion of a bound system is described by a circle (or an ellipse) with a slight superposed outwards spiraling motion. Quite interestingly, the small cosmological expansion keeps the orbital velocity constant. This reminiscent of the behaviour in MOND, where the speed on an orbit becomes asymptotically independent of the size of the orbit [35].

The above expressions formally only apply within an empty Universe with $\Omega_m = 0$. The limitations of the range of t- and λ-variations given by Eqs. (20) are not yet included. Clearly, we have to account for them in a Universe with a density parameter

different from zero. Thus, with Eqs. (20) and (21) we may write the relative change of the orbital radius (or parameter p),

$$\frac{dr}{r} = \frac{dt}{t} = \frac{dt}{d\tau}\frac{d\tau}{t} = \frac{(t_0 - t_{\rm in})}{\tau_0}\frac{d\tau}{(t_{\rm in} + \frac{\tau}{\tau_0}(t_0 - t_{\rm in}))} = \psi(\tau)\frac{d\tau}{\tau_0}. \tag{31}$$

This applies at a time τ. Let us consider, at the present epoch τ_0, where the orbital radius is r_0, an interval of time $\Delta\tau$ (say one year) very small with respect to $\tau_0 = 13.8\,\mathrm{Gyr}$. We may thus write the relative change of the orbital distance $\Delta r/\Delta\tau$ during this small interval of time,

$$\frac{\Delta r}{\Delta\tau} = \psi_0\,\frac{r_0}{\tau_0}. \tag{32}$$

For $\Omega_{\rm m} = 0$, we would get $\psi_0 = 1$ and thus $\Delta r/\Delta\tau = r_0/\tau_0$. In a Universe model with a density parameter $\Omega_{\rm m} > 0$, the temporal increase of the orbital parameter is smaller than that in an empty universe ($\psi_0 = 1 - \Omega_{\rm m}^{1/3} < 1$). For $\Omega_{\rm m}$ tending to 1, the relative orbital increase tends to zero. For $\Omega_{\rm m} = 0.2, 0.3, 0.4$, the factor ψ_0 is equal to 0.4152, 0.3306, 0.2632, respectively. Below, we will consider the standard model with $\Omega_{\rm m} = 0.30$. On the whole, the account of matter strongly reduces the expected effects of scale invariance.

5. Study of the Earth-Moon system

5.1. The LLR data

Let us turn to the observations. Since March 1970, the Earth-Moon distance has been intensively measured by Lunar Laser Ranging (LLR), first at Mc Donald Observatory and since the 80's at several other observatories around the world. A total of 20 138 ranges up to September 2015 have been performed leading to an average lunar recession of 3.83 (± 0.009) cm/yr [43, 44]. We note the impressive accuracy. The value of the lunar recession has not much changed since the first determination more than three decades ago [8], which illustrates the quality of the measurements. The Earth-Moon distance is the most intensively and systematically measured distance in the Solar System and the only one by a direct laser signal.

The main effect producing this recession is the Earth-Moon tidal coupling: the tidal bump of the Earth embarked by the fast Earth axial rotation, with an angular velocity faster than that of the Moon on its orbits, generates a forward pull on the Moon. This pull is transferring some axial terrestrial angular momentum to the lunar orbital one. Over geological times, the lunar recession has likely changed since the Moon was closer to the Earth and thus the tidal exchanges were larger. For example, a lunar recession of about 6.5 cm/yr was estimated for the Ediacaran – Early Cambrian period (about 600 Myr ago) by [1].

5.2. The LOD data

According to the theoretical modeling of the tidal waves, lunar motion, and terrestrial rotation by [43], the observed lunar recession of 3.83 cm/yr implies an increase of the length of the day (LOD) of 2.395 ms/cy (millisecond per century). The LOD is defined as the excess of the length of the day with respect to 86 400 SI seconds. We note that the value of 2.395 ms/yr for the change of the LOD over centuries is consistent with the calculation of the tidal coupling under the assumption of conservation of the global angular momentum of the Earth-Moon system [14], [31]. This theoretical value of the increase of the LOD has also been very well confirmed recently by [2]. These authors revisited the Earth rotation theories with a two-layer deformable Earth model, including dissipative effects at the core-mantle boundary and account of the coupling torque between the two. The deceleration is numerically estimated with frequency-dependent modeling of the various solid and oceanic tides. In the assumption of the long-term coupling of the core and mantle, they obtain a deceleration of the Earth rotation corresponding to an increase of the LOD of 2.418 ms/cy in very good agreement with the above modeling by [43].

The best and longest studies on the change of the LOD in History have been performed by Stephenson et al. [40], who analyzed the lunar and solar eclipses from 720 BC up to 1600 AD and found an average shift of the LOD by 1.78 (±0.03) ms/cy. Such a shift, apparently very small, is acting every day and progressively produces large effects over a long period. When cumulated over 2000 yr, differences in the time of solar and lunar eclipses are amounting to about 18 000 s. Such time differences are leading to big shifts in the eclipse locations, up to thousands of km. The constraints on the eclipse locations and indications (when available) about the time of the eclipse allowed Stephenson et al. to make the above determination, which had only slightly changed in their successive papers since 1984, see references in [40]. These authors also suggested the existence of a slight undulation around the mean with a period of 1500 yr, possibly related to the effect of magnetic core-envelope coupling [13].

Various other effects may contribute to the LOD, with different timescales: atmospheric effects, ice melting and change of the sea level, glacial isostatic adjustment, and core-envelope coupling. The most uncertain contribution is that of the core coupling which seems responsible for the 1500 yr undulation. Over the long term, the various negative and positive effects appear to balance each other before the year 1990, see data by [36], [37] and our recent detailed review of the problem [31], (since 1990, the fast melting of even the polar ice fields contribute to an increase of the Earth momentum of inertia). The reality of the difference between the above observed mean value of the LOD (1.78 ms/cy) and the value due to the tidal interaction (2.395 ms/cy) has recently been further emphasized by [41].

We note that other estimates of the change of the LOD have been made from lunar occultations, however on a shorter time basis. The observations of lunar occultations from 1656 to 1986 have been analyzed by [32], they indicate a slowing down of the Earth of 0.73 (±0.018) ms/cy. The data show some decadal variations around

the mean, which were also present in the further analyses. Various astronomical telescopic observations over the last 350 yr were analyzed by [39], which led to a mean increase of the LOD of 0.9 ms/cy. A new determination of the change of the LOD based on the data from [40] for occultations since 1680 complemented by IERS data for the period 1970 to 2020 has been performed recently by us [31]. We showed an average increase of 1.09 ($\pm$0.012) ms/cy for the LOD over that period. All these determinations based on relatively limited durations are more subject to decadal fluctuations than the ancient eclipse observations.

Interestingly enough, another independent very long-term determination of the deceleration of the Earth rotation has been established on the basis of paleontological studies by Deines and Williams [10]. These authors examined all available paleontological fossils and deposits for direct measurements of Earth's rotation, in particular they used corals, bivalves, brachipods, rythmites, and stromatolites. These fossils are keeping the traces of phases of daily growth due to the alternance of days and nights. The oldest records go back to 1.85 Gyr ago, however such very ancient data are highly uncertain. Much more reliable data are availablle since the Cambrian explosion of the forms of life, when animals with hard shells first appeared, about 542 Myr ago. From their whole sample, [10] found a clear decrease of the number of days in one year. For example, 400 Myr ago, an epoch where there are lots of data, the mean number of days in one year (considered of constant duration, but see below) was about 405 days (with an uncertainty σ of about $\pm$ 7 days). From their sample of collected data, Deines and Williams found a mean deceleration corresponding to a change of the LOD 1.642 ($\pm$ 0.48) ms/cy. This mean value is quite interesting, although not taken at present time it concerns an age differing by less 3% of the present age of the Universe. The error is larger than the one by Stephenson et al. [40] (1.78 $\pm$ 0.03 ms/cy). Nevertheless, it gives another value consistent with and independent of the value by Stephenson et al. [40]. Based on an incredibly much longer time period, the result by Deines and Williams is supporting the discrepancy between the change of the LOD and the value of the lunar recession.

5.3. Theoretical predictions of the two-body problem

Let us consider the possible increase of the Earth-Moon distance during one year in the scale-invariant context. For an empty Universe with an age of $\tau_0 = 13.8$ Gyr and a mean Earth-Moon distance of $r_0 = 384\,400$ km, the lunar recession would be

$$\left(\frac{\Delta r}{\Delta \tau}\right)_{\text{vac}} = \frac{r_0}{\tau_0} = 2.78 \text{ cm} \cdot \text{yr}^{-1}. \tag{33}$$

This is close to the Hubble-Lemaître expansion rate with $H_0 = 70$ km/(s Mpc), corresponding to a lunar recession of 2.75 cm $\cdot$ yr^{-1}. For a Universe with $\Omega_{\text{m}} = 0.30$, $\psi_0 = 0.3306$ and the predicted cosmological expansion of the Earth-Moon system is,

$$\left(\frac{\Delta r}{\Delta \tau}\right)_{\text{cosm}} = 0.92 \text{ cm} \cdot \text{yr}^{-1}, \tag{34}$$

a value substantially smaller than the Hubble-Lemaître expansion.

Let us also shortly consider the Earth-Mars distance. The relevant parameters are:

Mars : $a = 227944000$ km, $e = 0.09339$, $p = 225.956 \cdot 10^6$ km.
Earth: $a = 149598000$ km, $e = 0.01671$, $p = 149.556 \cdot 10^6$ km.

The difference of parameters p for Mars and the Earth is $d = p_{\mathrm{Mars}} - p_{\mathrm{Earth}} = 76.4 \cdot 10^6$ km. The estimate of the Mars-Earth recession based on this distance d would be in an empty Universe, $\left(\frac{\Delta d}{\Delta \tau}\right)_{\mathrm{vac}} = \frac{d}{\tau_0} = 5.54$ m $\cdot$ yr^{-1}. With the factor $\psi = 0.3306$ for $\Omega_{\mathrm{m}} = 0.30$, we get

$$\left(\frac{\Delta d}{\Delta \tau}\right)_{\mathrm{cosm}} = 1.83 \,\mathrm{m} \cdot \mathrm{yr}^{-1}. \tag{35}$$

5.4. The tidal interaction in the scale invariant context

Let us also examine the tidal interaction in the Earth-Moon system. The law of angular momentum conservation for a given mass element in the scale invariant framework [26], is $\kappa(t)\, r^2\, \Omega = const$, while both r and M, are scaling like t, e.g. $M = M_0(t/t_0)$. Let us examine the conservation of the total angular momentum of the Earth (E)–Moon (M) system at time t [14],

$$\zeta \cos \varphi\, I_{\mathrm{E}} \Omega_{\mathrm{E}} + M_{\mathrm{M}} R^2 \Omega_{\mathrm{M}} = L, \quad \text{with } L = L_0 \frac{t^2}{t_0^2} \tag{36}$$

The angle φ is the variable angle between the lunar orbital plane and the Earth equator. The numerical factor ζ accounts for the consequences of the eccentricity $e = 0.055$ of the lunar orbit, see numerical value below. Quantities I_{E} and $\Omega_{\mathrm{E}} = 2\pi/T_{\mathrm{E}}$ are respectively the moment of inertia and the axial angular velocity of the Earth, M_{M} is the mass of the Moon and Ω_{M} its orbital angular velocity, R is the mean distance between the Earth and Moon, L_0 is the total angular momentum at the present time t_0. We neglect the axial angular momentum of the Moon, since its mass is 1.2 % of that of the Earth and its axial rotation period (equal to its orbital period) is 27.3 days. Thus, the lunar axial angular momentum is a fraction of about $4 \cdot 10^{-4}$ of that of the Earth.

Let us evaluate the time derivative of the above expression (36),

$$-\zeta \cos \varphi \frac{2\pi}{T_{\mathrm{E}}^2} I_{\mathrm{E}} \frac{dT_{\mathrm{E}}}{dt} + \zeta \cos \varphi \frac{2\pi}{T_{\mathrm{E}}} \frac{dI_{\mathrm{E}}}{dt} + \frac{d}{dt}(M_{\mathrm{M}} R^2 \Omega_{\mathrm{M}})$$
$$= 2 \left(\zeta \cos \varphi\, I_{\mathrm{E}} \Omega_{\mathrm{E}} + M_{\mathrm{M}} R^2 \Omega_{\mathrm{M}} \right)_0 \frac{t}{t_0^2}. \tag{37}$$

Account has been given to the change of the moment of inertia due to the mass variation. Here T_{E} is the axial rotation period of the Earth. For Ω_{M}, we have the relation $\Omega_{\mathrm{M}}^2 = G M_{\mathrm{E}} R^{-3}$, which also applies in the SIV context, there M_{E} is the

Earth's mass. We can develop the third term on the left of the above expression (37),

$$\frac{d}{dt}(M_{\mathrm{M}}R^2\Omega_{\mathrm{M}}) = \frac{d}{dt}(G^{\frac{1}{2}}M_{\mathrm{E}}^{\frac{1}{2}}R^{\frac{1}{2}}M_{\mathrm{M}}) = G^{\frac{1}{2}}M_{\mathrm{E}}^{\frac{1}{2}}M_{\mathrm{M}}\frac{d}{dt}(R^{\frac{1}{2}}) + G^{\frac{1}{2}}R^{\frac{1}{2}}\frac{d}{dt}(M_{\mathrm{E}}^{\frac{1}{2}}M_{\mathrm{M}})$$
$$= G^{\frac{1}{2}}M_{\mathrm{E}}^{\frac{1}{2}}M_{\mathrm{M}}R^{-\frac{1}{2}}\frac{1}{2}\frac{dR}{dt} + \frac{3}{2}G^{\frac{1}{2}}M_{\mathrm{E}}^{\frac{1}{2}}M_{\mathrm{M}}R^{\frac{1}{2}}\frac{1}{t}. \qquad (38)$$

Indeed, $dM/dt = M/t$ as well as M_0/t_0. Introducing this expression in Eq. (37) and explicating the time dependence of the various terms leads to

$$\zeta\,\cos\varphi\,\left(\frac{2\,\pi}{T_{\mathrm{E}}}\frac{dI_{\mathrm{E}}}{dt} - \frac{2\,\pi I_{\mathrm{E}}}{T_{\mathrm{E}}^2}\frac{dT_{\mathrm{E}}}{dt}\right) + \frac{G^{\frac{1}{2}}M_{\mathrm{E}}^{\frac{1}{2}}M_{\mathrm{M}}}{2R^{\frac{1}{2}}}\frac{dR}{dt} + \frac{3}{2}G^{\frac{1}{2}}M_{\mathrm{E}}^{\frac{1}{2}}M_{\mathrm{M}}R^{\frac{1}{2}}\frac{1}{t}$$
$$= \zeta\,\cos\varphi\,I_{\mathrm{E}}\frac{4\,\pi}{T_{\mathrm{E}}}\frac{t}{t_0^2} + 2G^{\frac{1}{2}}M_{\mathrm{E}}^{\frac{1}{2}}M_{\mathrm{M}}R^{\frac{1}{2}}\frac{t}{t_0^2}. \qquad (39)$$

From this relation, we now extract the lunar recession dR/dt, which becomes after some simplifications,

$$\frac{dR}{dt} = \frac{4\,\pi\zeta\,\cos\varphi\,R^{\frac{1}{2}}I_{\mathrm{E}}}{G^{\frac{1}{2}}M_{\mathrm{E}}^{\frac{1}{2}}M_{\mathrm{M}}T_{\mathrm{E}}^2}\frac{dT_{\mathrm{E}}}{dt} + \frac{4\,\pi\zeta\,\cos\varphi R^{\frac{1}{2}}I_{\mathrm{E}}}{G^{\frac{1}{2}}M_{\mathrm{E}}^{\frac{1}{2}}M_{\mathrm{M}}T_{\mathrm{E}}}\left(\frac{2t}{t_0^2} - \frac{1}{I_{\mathrm{E}}}\frac{dI_{\mathrm{E}}}{dt}\right) + R\left(\frac{4t}{t_0^2} - \frac{3}{t}\right). \qquad (40)$$

We may write it in a more condensed form by defining a constant k_{E},

$$k_{\mathrm{E}} = 4\,\pi\left(\zeta\,\cos\varphi\frac{R^{1/2}I_{\mathrm{E}}}{T_{\mathrm{E}}^2\,G^{1/2}\,M_{\mathrm{M}}\,M_{\mathrm{E}}^{1/2}}\right). \qquad (41)$$

By using $dI_{\mathrm{E}}/dt = 3\,I_{\mathrm{E}}/t$ (since I_{E} is scaling like $I_{\mathrm{E}} = I_0(t^3/t_0^3)$ Eq. (40) can now be written as:
$$\frac{dR}{dt} = k_{\mathrm{E}}\frac{dT_{\mathrm{E}}}{dt} + k_{\mathrm{E}}T_{\mathrm{E}}\left(\frac{2\,t}{t_0^2} - \frac{3\,t^2}{t_0^3}\right) + R\left(\frac{4t}{t_0^2} - \frac{3}{t}\right). \qquad (42)$$

For a time t differing very little from t_0, e.g. by one year, one has $\frac{t_0}{t} \to 1$, and thus with a high accuracy we write,

$$\frac{dR}{dt} = k_{\mathrm{E}}\frac{dT_{\mathrm{E}}}{dt} - k_{\mathrm{E}}\frac{T_{\mathrm{E}}}{t_0} + \frac{R}{t_0}. \qquad (43)$$

The first term on the right represents the tidal effect linking the change of the LOD and the lunar recession, the second term results from the increase of the moment of inertia of the Earth (which reduces the lunar recession), the third term expresses the global expansion of the system. Interestingly enough, this third term is just the same as that predicted by the study of to the two-body problem, which shows the internal consistency of both approaches. We note that the change of the mass of the Moon is also contained in this third term, it was intervening through the last term in Eq. (40).

We have now to bring the above equation in the current time units, seconds and years. With Eqs. (20) and (21), we get

$$\frac{dR}{d\tau} = k_{\mathrm{E}}\frac{dT_{\mathrm{E}}}{d\tau} - k_{\mathrm{E}}\,\psi_0\,\frac{T_{\mathrm{E}}}{\tau_0} + \psi_0\,\frac{R}{\tau_0}\,. \tag{44}$$

In a cosmological Universe model with $\Omega_{\mathrm{m}} = 0.30$, the ratio $\psi_0 = \frac{(t_0 - t_{\mathrm{in}})}{t_0} = 0.331$. The constant k_{E} is here in the units of t^{-1}, while T_{E} is in the units of t. Thus, both have to be turned τ-units and the scaling factors simplify. Thus, k_{E} and T_{E} can finally be both expressed in current time units (seconds or years).

5.5. Numerical values and discussion

We adopt the following numerical values of the various astronomical quantities

$$\begin{aligned}
M_{\mathrm{E}} &= 5.973 \cdot 10^{27}\mathrm{g}, \quad R_{\mathrm{E}} = 6.371 \cdot 10^{8}\mathrm{cm}, \\
M_{\mathrm{M}} &= 7.342 \cdot 10^{25}\mathrm{g}, \quad R = 3.844 \cdot 10^{10}\mathrm{cm}, \\
I_{\mathrm{E}} &= 0.331 \cdot M_{\mathrm{E}}R_{\mathrm{E}}^2 = 8.0184 \cdot 10^{44}\mathrm{g}\cdot\mathrm{cm}^2.
\end{aligned} \tag{45}$$

The value 0.331 is obtained from precession data [42]. Coefficient $k_{\mathrm{E}} = 1.806 \cdot 10^5 \cdot \zeta\cos\varphi\ \mathrm{cm}\cdot\mathrm{s}^{-1}$. The angle φ varies between 18.16 and 28.72 degrees, thus we adopt a mean value of $\cos\varphi = 0.91$. We have to estimate the value of ζ. The tidal effects behave like $1/r^3$, thus they depend on the eccentricity like $(1 + e\cos\vartheta)^3$. The time spent in an interval of angles $\Delta\vartheta$ goes like $r^2\Delta\vartheta$, thus like $(1 + e\cos\vartheta)^{-2}$. The product of the two leads to a dependence of the form $(1 + e\cos\vartheta)$. For $\cos\vartheta$, let us take a value of -0.5 which leads to $\zeta = 1 - 0.03 \approx 0.97$. We thus obtain for the coefficient $k_{\mathrm{E}} = 1.60 \cdot 10^5\ \mathrm{cm}\cdot\mathrm{s}^{-1}$.

Let us evaluate numerically the various contributions. With the LOD of $1.78\,\mathrm{ms/cy}$ from the antique data by [40], the first term contributes to a lunar recession of $2.85\,\mathrm{cm/yr}$, while the LOD of $1.09\,\mathrm{ms/cy}$ from 1680 to the present [31] leads to a recession of 1.74 cm/yr. The second term in Eq. (44) gives for the case of $\Omega_{\mathrm{m}} = 0.3$,

$$0.33 \cdot k_E\frac{T_{\mathrm{E}}}{\tau_0} = 0.33 \cdot 1.60 \cdot 10^5\ \mathrm{cm}\cdot s^{-1}\,\frac{86400\ \mathrm{s}}{13.8 \cdot 10^9\ \mathrm{yr}} = 0.33\left[\frac{\mathrm{cm}}{\mathrm{yr}}\right]. \tag{46}$$

The direct expansion effect $\frac{R}{t_0}$ is

$$0.33 \cdot \frac{R}{\tau_0} = 0.33 \cdot \frac{3.844 \cdot 10^{10}\ \mathrm{cm}}{13.8 \cdot 10^9\ \mathrm{yr}} = 0.92\left[\frac{\mathrm{cm}}{\mathrm{yr}}\right]. \tag{47}$$

This term corresponds to a third of the general Hubble-Lemaître expansion. Summing the various contributions, we get

$$\frac{dR}{d\tau} = (2.85 - 0.33 + 0.92)\,\mathrm{cm/yr} = 3.44\,\mathrm{cm/yr},\ \text{from historical data [40].} \tag{48}$$

24

Thus, we see that the scale invariant analysis is giving a relatively good agreement with the lunar recession of 3.83 cm/yr obtained from LLR observations. The difference amounts only to 10 % of the observed lunar recession. This is clearly much better than in the standard case, where the predicted LOD of 2.395 ms/cy corresponding to the observed recession diverges from the observed one of 1.78 ms/cy by 35 %. Thus, the scale invariant analysis appears to give more consistent results that the standard case. We do not consider this as a proof of the scale invariant theory, but this shows that the SIV theory deserves some attention, especially since more than several other astrophysical tests (see introduction) are successful.

We point out that the discrepancy between the observed LOD from historical records and the observed lunar recession has already been mentioned by several authors. Munk [38] has emphasized the interest of the discrepancy between the LLR lunar recession and the LOD data, invoking climatic effects. However, this would not be consistent with the data by Deines and Williams [10] which cover a much longer period of time over the geological epochs. Dumin [14] has also clearly demonstrated the above discrepancy between the LLR and the LOD results, showing that there was an excess of lunar recession of about 1.3 cm/yr not accounted by the slowing down of the Earth, an excess which would correspond to a fraction of about the half of the Hubble expansion. Dumin further studied this discrepancy and discussed some possible origins of it [15]. Krizek and Somer [22] have supported a local expansion of at least the order of the half of Hubble rate from an analysis of various properties in the Solar System. Also, the reality of the discrepancy between the observed LOD and the lunar recession was emphasized by Stephenson et al. [41].

On one side, we may of course wonder whether this small effect of about 1.3 cm/yr is sufficient to claim for an additional symmetry property in Physics. On the other side, steps forward often come by scrutinizing minute differences. Also, a larger effect would have already been found by more people than the few above precursors.

6. Conclusions

We have studied several mechanical properties in the scale invariant context, in particular we have shown the large reduction of the additional dynamical effects with the matter density. We have considered the two-body problem and the tidal interaction in the Earth-Moon system. As examples in the two-body system, independently of tidal effects, there would be a cosmological increase of 0.92 cm/yr for the Earth-Moon distance.

The observed lunar recession from LLR data amounts to 3.83 (± 0.009) cm/yr and the corresponding theoretical tidal change of the LOD is 2.395 ms/cy, [43], [44]. Now, the observed change of the LOD since the Babylonian Antiquity is only 1.78 ms/cy, leading to a significant difference of 35 %, see [41]. Moreover, the value of 1.78 ms/cy is supported by the data from paleontology over hundreds million years. Such a change of the LOD would correspond to a lunar recession of 2.85 cm/yr, instead of 3.83 cm/yr as observed. The difference in the lunar recession is well accounted for

within the dynamics of the SIV theory (48). *A minima*, the above results shows that the problem of scale invariance is worth of some attention.

7. Acknowledgments:

8. APPENDIX: A note on the result of Banik and Kroupa

A criticism of the scale invariant theory was expressed by Banik and Kroupa [3] with the argument that "the predicted expansion of the Earth–Moon orbit is incompatible with lunar laser ranging data at $> 200\sigma$". They used the following expression for the change of the lunar angular velocity,

$$\frac{\dot{\Omega}}{\Omega} = -\frac{\dot{r}_{\text{SIV}} + (3/2)\dot{r}_{\text{Tide}}}{r} \,. \tag{49}$$

The correct expression in the scale invariant theory (SIV) is according to the unmodified expression of the orbital velocity $v^2 = GM_{\text{E}}/r$, and thus via $\Omega^2 = GM_{\text{E}}r^{-3}$ one has:

$$\frac{\dot{\Omega}}{\Omega} = \frac{1}{2}\frac{\dot{M}_{\text{E}}}{M_{\text{E}}} - \frac{3}{2}\frac{\dot{r}}{r} \,. \tag{50}$$

Now, $\dot{r}$ is given by Eq. (44), where the first term on the right of this equation corresponds to $\dot{r}_{\text{Tide}}$ in (49),

$$\frac{\dot{\Omega}}{\Omega} = \frac{1}{2}\frac{\dot{M}_{\text{E}}}{M_{\text{E}}} - \frac{3}{2}\frac{\dot{r}_{\text{Tide}}}{r} + \frac{3}{2\,r}\,k_{\text{E}}\,\psi\,\frac{T_{\text{E}}}{\tau_0} - \frac{3}{2}\psi\,\frac{1}{\tau_0} \,. \tag{51}$$

The first and last terms on the right simplify, we get

$$\frac{\dot{\Omega}}{\Omega} = -\psi\,\frac{1}{\tau_0} - \frac{3}{2}\frac{\dot{r}_{\text{Tide}}}{r} + \frac{3}{2\,r}k_{\text{E}}\,\psi\,\frac{T_{\text{E}}}{\tau_0} \,. \tag{52}$$

The first two terms are identical with those of Banik and Kroupa, however the last term, which is an important one, is absent in their equation. This clearly invalidate their claim. On the contrary, the results of the present work confirm the remarkable compatibility of the scale invariant theory with the observed lunar recession, an agreement which does not exist in the standard theory.

References

[1] Azarevich, M. B., Lopez, V. L.: Lunar recession encoded in tidal rhythmites: a selective overview with examples from Argentina. Geo-Marine Letters. *37* (2017), 333–344.

[2] Baenas, T., Escapa, A., Ferrandiz, J. M.: Secular changes in length of day: Effect of the mass redistribution. Astron. Astrophys. *648* (2021), 89–98.

[3] Banik, I., Kroupa, P.: Scale invariant dynamics in the Solar system. MNRAS, *407* (2020), L62–66.

[4] Bondi, H.: The cosmological scene 1945-1952. *Modern Cosmology in Retrospect* (1990) Bertotti, B., Balbinot, R., Bergia, S., eds., Cambridge Univ. Press., 189.

[5] Bonnor, W. B.: Local dynamics and the expansion of the Universe. Gen. Rel. Grav. *32* (2000) 1005.

[6] Bouvier, P., Maeder, A.: Consistency of Weyl's geometry as a framework for gravitation. Astroph. Space Sci. *54* (1978), 497–508.

[7] Canuto, V., Adams, P. J., Hsieh, S.-H., Tsiang, E.: Scale-covariant theory of gravitation and astrophysical applications. Phys. Rev. D. *16* (1977), 1643–1663.

[8] Christodoulidis, D. C., Smith, D. E., Williamson, R. G. et al.: Observed tidal braking in the Earth/moon/sun system. J. Geophys. Res. *93(B6)* (1988), 6216–6236.

[9] Carroll, S. M., Press, W. H., Turner, E. L.: The cosmological constant. Ann. Rev. Astron. Astrophys. *30*, 499–542.

[10] Deines, S. D., Williams, C. A.: Earth's rotational deceleration: determination of tidal friction independent of timescales. Astron. J. *151* (2016). 103–114.

[11] Dirac, P. A. M.: Long range forces and broken symmetries. Proc. Roy. Soc. London Ser. A, *333* (1973), 403–418.

[12] Dirac, P. A. M.: Cosmological models and the large numbers hypothesis. Proc. Roy. Soc. London Ser. A, *338* (1974), 439–446.

[13] Dumberry, M., Bloxham, J.: Azimuthal flows in the Earth's core and changes in length of day at millennial timescales. Geophys. J. *165* (2006), 32–46.

[14] Dumin, Yu. V.: A new application of the lunar laser retroreflectors: Searching for the "local" hubble expansion. Adv. Space Res. *31* (2003), 2461–2466.

[15] Dumin, Yu. V.: Local Hubble expansion: current state of the problem. In *Cosmology on Small Scales* (2016), eds. M. Křížek and Y. Dumin, Institute of Math. CAS, Prague, 23–40.

[16] Einstein, A., Straus, E. G.: The influence of the expansion of space on the gravitation fields surrounding the individual stars. Rev. Mod. Phys. *17* (1945), 120.

[17] Feynman, R. P.: Mainly mechanics, radiation, and heat. Feynman lectures on physics, *1* (1963).

[18] Frieman, J. A., Turner, M. S., Huterer, D.: Dark energy and the accelerating universe. Ann. Rev. Astron. Astrophys. *46* (2008), 385–437.

[19] Gross, R.: Earth rotation variations - long period. In *Treatise of Geophysics, vol 3, Geodesy* (2009) Ed. G. Schubert, Elsevier, Amsterdam, p. 239.

[20] Gueorguiev, V. G., Maeder, A.: The scale invariant vacuum paradigm: main results and current progress. Universe *8* (2022), 213.

[21] Jesus, J. F.: Exact solution for flat scale-invariant cosmology. Rev. Mex. Astron. Astrophys. *55* (2018), 17–20.

[22] Křížek, M., Somer, L.: Anthropic principleand the local Hubble expansion. In *Cosmology on Small Scales* (2016), Eds. M. Křížek and Y. Dumin, Institute of Math. CAS, Prague, 65–94.

[23] Maeder, A.: An alternative to the LambdaCDM model: the case of scale invariance. Astrophys. J. *834* (2017a), 194–210.

[24] Maeder, A.: Dynamical effects of the scale invariance of the empty space: the fall of dark matter? Astrophys. J. *849* (2017c), 158–177.

[25] Maeder, A.: Evolution of the early Universe in the scale-invariant theory. arXiv:1902.10115.

[26] Maeder, A., Bouvier, P.: Scale invariance, metrical connection and the motions of astronomical bodies. Astron. Astrophys., *73* (1979), 82–89.

[27] Maeder, A., Gueorguiev, V. G.: The growth of the density fluctuations in the scale-invariant vacuum theory. Physics of the Dark Universe, *25* (2019), 100315–100330.

[28] Maeder, A., Gueorguiev, V. G.: The scale-invariant vacuum (SIV) theory: a possible origin of dark matter and dark energy. Universe, *6* (2020a), 46.

[29] Maeder, A., Gueorguiev, V. G.: Scale-invariant dynamics of galaxies, MOND, dark matter, and the dwarf spheroidals. MNRAS *492* (2020b), 2698.

[30] Maeder, A., Gueorguiev, V. G.: Scale invariance, horizons, and inflation. MNRAS *504* (2021a), 4005–4014.

[31] Maeder, A., Gueorguiev, V. G.: On the relation of the lunar recession and the length-of-the-day. Astroph. Space Sci. *366* (2021b), 101–125.

[32] McCarthy, D. D., Babcock, A.: The length of day since 1656. Physics of the Earth and Planetary Interiors *44* (1986), 281–292.

[33] McVittie, G. C.: Condensations in an expanding Universe. MNRAS *92* (1932), 500.

[34] McVittie, C. G.: The mass-particle in an expanding universe. MNRAS *93* (1933), 325.

[35] Milgrom, M.: MOND laws of galactic dynamics. MNRAS *437* (2014), 2531–2541.

[36] Mitrovica, J. X., Wahr, J.: Ice age Earth rotation. Ann. Rev. Earth Planetary Sci. *39* (2011), 577–616.

[37] Mitrovica, J. X., Hay, C. C., Morrow, E. et al.: Reconciling past changes in Earth's rotation with 20th century global sea-level rise: resolving Munk's enigma. Sci. Adv. *1* (2015), e1500679–1500684.

[38] Munk, W. H.: Twentieth century sea level: an enigma. Proc. Natl. Acad. Sci. USA *99* (2002), 6550–6555.

[39] Sidorenkov, N. S.: The effect of the El Nino Southern oscillation on the excitation of the Chandler motion of the Earth's pole. Astron. Reports (in Russian), *41* (1997), 705–708.

[40] Stephenson, F. R., Morrison, L. V., Hohenkerk, C. Y.: Measurement of the Earth's rotation: 720 BC to AD 2015. Proc. Roy. Soc. *A472* (2016), 404–430.

[41] Stephenson, F. R., Morrison, L. V., Hohenkerk, C. Y.: Eclipses and the Earth's rotation. General Assembly, Proceedings of the IAU *XXX* (2020), 160–162.

[42] Williams, J. G.: Contribution to the Earth's obliquity rate, precession, and nutation. Astron. J. *108* (1994), 71.

[43] Williams, J. G., Boggs, D. H., Ratcliff, J. T.: Lunar Tidal recession. 47th Lunar and Planetary Science Conference (2016a), 1096-1100.

[44] Williams, J. G., Boggs, D. H.: Secular tidal changes in lunar orbit and Earth rotation. Celestial Mechanics and Dynamical Astron. *126* (2016b), 89–129.

RECALCULATION OF THE MOON RETREAT VELOCITY SUPPORTS EXPANSION OF GRAVITATIONALLY BOUND LOCAL SYSTEMS

Heikki Sipilä[1]

[1] Physics Foundations Society, https:www.physicsfoundations.org
Espoo, Finland
hjsipila@gmail.com

Abstract: The current paradigm of astronomy and cosmology denies the expansion of gravitationally bound local systems. The increase of the Earth to Moon distance, 3.82 cm/yr measured in the Lunar Laser Ranging program [1] for the last 50 years is explained as a tidal effect. If local systems expanded at a rate corresponding to Hubble constant 71 (km/s)/Mpc, 2.8 cm/yr of the increase resulted from the expansion and only about 1 cm/yr from the tidal interaction. An independent method to measure the retreat value is based on the ancient tidal sediment layers which give the development of the number of months in a year. The most accurate of those are the studies by [2], [3]. Based on the unchanged length of a year, he has obtained the average retreat value of 2.1 ± 0.1 cm/yr over 635 Myr, which is less than the value expected from expansion. The conclusion from the result has been that there cannot be any Hubble expansion and the current high retreat value is caused by a special ocean resonance. When the retreat from tidal sediment data is recalculated by assuming expansion of local systems and observing that the expansion is associated with a change in the length of a year, a perfect agreement between the Laser Ranging result and the sediment layer result is obtained.

Keywords: cosmology, celestial mechanics

PACS: 98.80.-k, 6.10.+i, 95.10., 96.15.Wx, 96.20.-n

1. Introduction

It is known that the rotation of the Earth is slowing down with time. This was shown convincingly as the development of the number of days in a year obtained from coral fossils by [4] in 1963. The fossil data shows that the Earth's rotation rate has been slowing down smoothly for the last 800 million years without major changes or jumps. In the Earth-Moon system, the slowing rotation of the Earth is associated with an increasing angular momentum of the Moon resulting in the increasing orbital radius of the Moon. Because Earth's rotation is slowing down

almost linearly at present, it means that the retreat of the Moon must be also linear. In the current theoretical framework, there is a major conflict between the laser-measured retreat value and the value obtained from tidal sediment layers. In the framework of the Dynamic Universe (DU) theory by T. Suntola [5] all gravitationally bound local systems expand in direct proportion to the expansion of space which means that also the length of a year increases with the expansion. When solved in the DU framework, a coherent result is obtained from the coral fossil data, sediment layer data, and the Laser Ranging data.

2. Calculation of the Moon retreat value based on the current paradigm with non-expanding local systems and the associated constant length of a year

In Southern, Australia there is a well-preserved 635 Ma old tidal layer formation. G.E. Williams studied drilling cores from this formation and found a continuous 60-year footprint of lunar cycles. Typically, similar deposits contain a few months of continuous layers maximum. The current average distance to Moon is 384 400 km and the length of the sidereal month (rotation time of the Moon with relative to the fixed stars) is 27.3 days corresponding to 13.38 sideral months in a year.

The sediment layers are caused by tides. The observed number of months in a year in the 635-million-year-old samples is 14.1 ± 0.1, corresponding to the sidereal month of 25.9 current days in a year when assuming that the length of a year has been unchanged. This means that the sidereal month 635 million years ago was 0.944 times the present sidereal month. Based on Kepler's laws the orbital radius of the Moon corresponding to orbital period 635 Myr ago was 371 143 km which is 13 257 km less that the current orbital radius. This gives the average change of 2.1 cm/yr, which is substantially less than today's measured value of 3.82 cm/yr.

The number of months per year is theory-free; it is obtained from direct counting from layers. The interpretation of the result is theory dependent. It is that the length of the year does not change i.e. the Solar system does not expand. By using a theory that follows the current paradigm, we cannot find the reason for the conflict in the results between laser distance measurement and results from sediment layers.

3. Calculation based on Suntola's Dynamic Universe theory

DU theory is based on the balance of the gravitational and kinetic energy in spherically closed space. Space expands uniformly including gravitationally bound local systems. Applying the Hubble constant 71 (km/s)/Mpc the length of a year 635 million years ago was 349 current days, and the length of a month was 349/14.1 = 24.8 current days. The current length of a sidereal month is 27.39 days and the mean distance of the Moon is 384 400 km. Applying Keppler's law, the distance to the moon 635 Myr ago was 359 575 km, which means that the distance has increased by 24 825 km in 635 million years corresponding to the average annual change of 3.91±0.2 cm. It should be noted that in this calculation we had no need to separate

the tidal component and the cosmic expansion on the retreat of the Moon. In the DU framework, the expansion of space corresponding to Hubble constant Hubble constant 71 (km/s)/Mpc gives a 2.8 cm annual retreat, which leaves about 1 cm annual retreat to the tidal interactions in a good agreement with both the sediment results and the Lunar Laser results.

When assuming the tidal effect only, the high rate of the Moon's retreat has created a problem with the age of the Moon. We do not have reliable tidal data from the deeper in history. When incorporating the cosmic expansion, the tidal component today is about 26% of the total retreat value which presumably is low enough to solve the age problem.

4. Conclusions

This study gives strong support to the expansion of the Solar system in direct proportion to cosmic expansion. This study gives also a fully independent method to determine the Hubble constant. Calculations here indicate the accuracy of 71 ± 2 km/s/Mpc, see [6]. Future more thorough statistical analysis may give an even more strict error limit for the Hubble constant.

References

[1] Dickey, J. O. et.al.: Lunar laser ranging: A continuing legacy of the Apollo program. Science 265 (1994), 482.

[2] Williams, G. E.: Geological constraints on the Precambrian history of Earth's rotation and the Moon's orbit. Rev. Geophys. 38 (2000), 37–39.

[3] Williams, G. E.: Age of the Elatina deposit is 635 Myr according the latest aging determination. Private information (2021).

[4] Wells, J. W.: Coral growth and geochronometry. Nature 197 (1963), 948.

[5] Suntola, T.: The dynamic Universe, toward a unified picture of physical reality. 4th ed. Physics Foundations Society, Espoo (2018), https:www.physicsfoundations.org/dynamic-universe.

[6] Sipilä, H.: Is the Solar system expanding? J. Phys. Conf. Ser. 1466 (2020).

UNDERESTIMATION OF HUBBLE-LEMAÎTRE CONSTANT ERROR BARS: A HISTORICAL ANALYSIS

Martín López-Corredoira[1,2], Timothy Faerber[3]

[1] Instituto de Astrofísica de Canarias
38205 La Laguna, Tenerife, Spain
martin@lopez-corredoira.com
[2] Departamento de Astrofísica, Universidad de La Laguna
38206 La Laguna, Tenerife, Spain
[3] Department of Physics and Astronomy, West Virginia University
Morgantown, WV 26506-6315, US
tf00014@mix.wvu.edu

Abstract: The aim of this analysis of a historical compilation of Hubble–Lemaître constant (H_0) values in the standard cosmological model is to determine whether or not the stated error bars truly represent the dispersion of values given. For this analysis, a chi-squared test was executed on a compiled list of past measurements. It was found through statistical analyses of the data (163 data points measured between 1976 and 2019), that the χ^2 values (between 480.1 and 575.7) have an associated probability that is very low: $Q = 1.8 \times 10^{-33}$ for a linear fit of the data vs. epoch of measurement and $Q = 1.0 \times 10^{-47}$ for the weighted average of the data. This means that either the statistical error bars associated with the observed parameter measurements have been underestimated or the systematic errors were not properly taken into account in at least 15–20% of the measurements.

The fact that the underestimation of error bars for H_0 is so common might explain the apparent 4.4σ discrepancy formally known today as the Hubble tension. Here we have carried out a recalibration of the probabilities with the present sample of measurements and we find that $x\sigma$s deviation is indeed equivalent in a normal distribution to the $x_{\text{eq.}}\sigma$s deviation, where $x_{\text{eq.}} = 0.83x^{0.62}$. Hence, the tension of 4.4σ, estimated between the local Cepheid–supernova distance ladder and cosmic microwave background (CMB) data, is indeed a 2.1σ tension in equivalent terms of a normal distribution, with an associated probability $P(> x_{\text{eq.}}) = 0.036$ (1 in 28). This can be increased to an equivalent tension of 2.5σ in the worst cases of claimed 6σ tension, which may in any case happen as a random statistical fluctuation.

Keywords: cosmological parameters; history and philosophy of astronomy

PACS: 98.80.Es

1. Introduction

The Hubble–Lemaître constant, H_0, is one of the fundamental cosmological parameters. We know its approximate value, but there is not yet any widely accepted accurate estimate of the parameter.

From the beginning of the discovery of the apparent magnitude relation of the galaxies in the 1920s, first by Lemaître and later by Hubble (the so-called Hubble–Lemaître diagram), H_0 has decreased in value by almost an order of magnitude. In the 1980s, two preferred values were defended by different teams: either 50 or $100 \, \mathrm{km \, s^{-1} \, Mpc^{-1}}$. Later, in the 1990s and 2000s, a value of around $70 \, \mathrm{km \, s^{-1} \, Mpc^{-1}}$ became dominant, with preference for the value of $72 \, \mathrm{km \, s^{-1} \, Mpc^{-1}}$ obtained by the Hubble Space Telescope (HST) Key Project using supernovae [1]. Nonetheless, discordant values were later published. A period–luminosity bias for the calibration of distances with nearby galaxies would justify a reduction of the Hubble–Lemaître constant to values of around $60 \, \mathrm{km \, s^{-1} \, Mpc^{-1}}$, see [2], [3]. Even supernova data with HST were fitted with these values. As to the possible (non-)universality of the Cepheid period–luminosity relation, it was argued that low metallicity Cepheids have flatter slopes, and that the derived distance would depend on what relation is used [4].

We must also bear in mind that the value of H_0 is determined without knowing on what scales the radial motion of galaxies and clusters of galaxies relative to us is completely dominated by the Hubble–Lemaître flow [5]. The homogeneity scale may be much larger than expected [6], [7], thus giving important net velocity flows on large scales that are incorrectly attributed to cosmological redshifts. Hence, some differences in H_0 measured on different scales might be due to this neglect of net radial motions of galaxies. Also, values of H_0-derived cosmic microwave background (CMB) analyses are subject to the errors in the cosmological interpretation of this radiation [8].

Yet another controversy arose more recently on the value of H_0. The Hubble–Lemaître constant estimated from the local Cepheid–supernova distance ladder is at odds with the value extrapolated from CMB data, assuming the standard cosmological model (74.0 ± 1.4 and $67.4 \pm 0.4 \, \mathrm{s^{-1} \, Mpc^{-1}}$, respectively), which gives an incompatibility at the 4.4σ level [9]. This tension can even be increased up to 6σ depending on the datasets considered [10]. Given the number of systematic errors that may arise in the measurements, this should not be surprising. However, this problem has motivated hundreds of papers since 2019: many solutions to the problem have been proposed (review in Refs. [10], [11]), either discussing the method to estimate H_0 or new theoretical scenarios.

Here we will not contribute with a new solution to this Hubble tension in physical terms. Instead we will carry out a historical investigation to determine whether or not the given error bars truly represented the dispersion of values in a historical compilation of H_0 values between 1976 and 2019. We also show how we can use this knowledge to recalibrate the probabilities of some tension of this kind.

2. Bibliographical data

We compile 163 values for H_0 between the years of 1976 and 2019. In addition to the values themselves, we were interested in a few other details about the measurements, namely, the years in which those measurements were made and the sizes of the error bars corresponding to the observed values. The list of observed values can be found in Ref. [12], where 120 measurements between 1990 and 2010 were taken from the compilation by Ref. [13][1], plus other 8 measurements between 1976 and 1989 and 35 measurements between 2011 and 2019. The latest measurement we use is the value given by Ref. [9], which marked the origin of the present-day Hubble tension.

3. Statistical analysis

For the statistical analysis of this data, a simplifying assumption was made that each observed measurement is independent of the other observed measurements, thus eliminating the need for a covariance term. It should also be noted that the given error bars account for all statistical effects. In order to analyse the trends in our datasets when viewed in scatter plots (see Figure 1), we used a chi-squared test to examine the probabilities of the deviations and determine whether the simplifying assumption made that the measurements were independent of one another was correct.

The chi-squared value of a set of data gives the likelihood that the trend observed in the data occurred due to chance, and is also known as a 'goodness of fit' test [15]. The probability that a calculated χ^2 value for a dataset with d degrees of freedom is due to chance is represented by Q and is given by the following expression:

$$Q_{\chi^2,d} = \left[2^{d/2} \Gamma \left(\frac{d}{2} \right) \right]^{-1} \int_{\chi^2}^{\infty} (t)^{\frac{d}{2}-1} e^{\frac{-t}{2}} dt, \tag{1}$$

$$\Gamma(x) = \int_0^{\infty} t^{x-1} e^{-t} dt.$$

The covariance term is not included owing to the simplifying expression made that all of the observed measurements are independent of one another. This independence of data is precisely the hypothesis we want to test. In any case, non-independency of our data would make the spread of the points lower than is indicated by the error bars, making the probability Q of higher deviations even lower, and thus the number of points to reject in order to have a distribution compatible to the error bars even larger. Therefore, our simplified approach may be considered a conservative calculation.

This calculation was carried out twice, first using the weighted average H_0 values as the theoretical values (x_t), and then again using the best-fit values from a linear

---

[1]All of the data except the measurement of $93 \pm 1 \, \mathrm{km \, s^{-1} \, Mpc^{-1}}$ by Ref. [14], which we excluded for being $> 20\sigma$ away from the average.
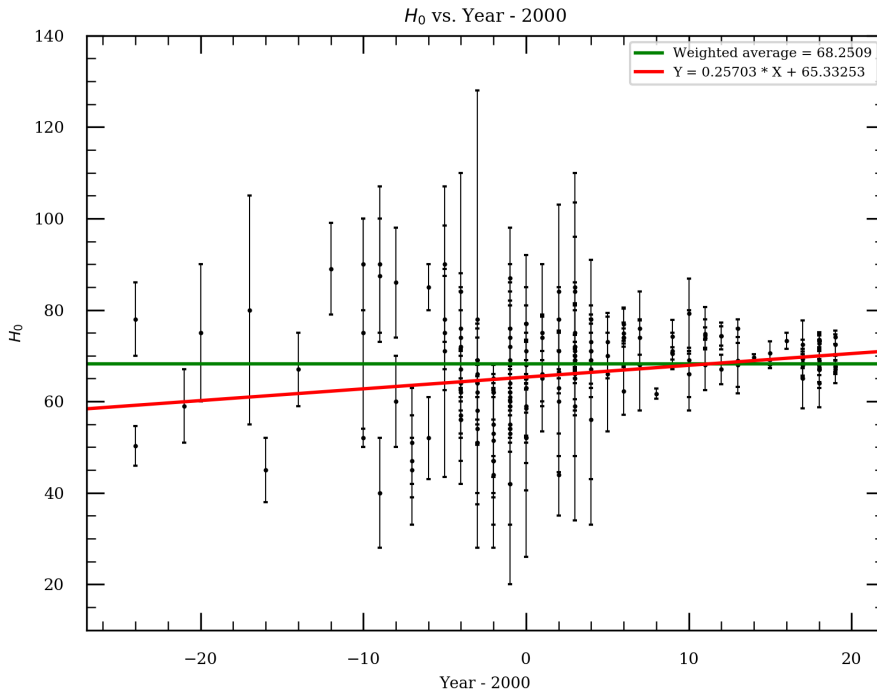
Figure 1: Data of H_0 vs. time (year - 2000) data, weighted average, and best linear fit.

fit. Lines representing both the weighted average of the dataset (green) and the best fit for the dataset (red) that were used to calculate chi-squared can be seen with the data points in Figure 1. The weighted averages (λ_w) of the parameters in question were calculated by weighting each point by the variance of that value. We get $\lambda_w \approx 68.26 \pm 0.40$ km s^{-1} Mpc^{-1} and $\chi^2 = 575.7$.

Also, a linear fit of the form $Y = A + B \times X$ is used, where Y is the theoretical value for the parameter being analyzed and X is the year of that measurement minus 2000. We get a $\chi^2 \approx 480.1$ for the linear fit:

$$H_0 \left(\text{km s}^{-1} \text{Mpc}^{-1} \right) = 65.3 + 0.26 \times [t(\text{yr}) - 2000], \tag{2}$$

as can be seen in Figure 1, represented by the red line.

For the value of χ^2 calculated using the best linear fit function designed to minimize χ^2, $Q = 1.8 \times 10^{-33}$. In order to reach a statistically significant value for Q, 24 bad values must be removed ($n = 139$, $\chi^2 \approx 164.1$), producing a value for Q of 0.057. In order to determine which values should be removed as bad values, all values were ranked based on their contributions to χ^2 by increasing value of $[x - (\text{best fit } x)]/(\text{error of } x)$ and then again by $[x - (\text{weighted average } x)]/(\text{error of } x)$, where x is the observed value for the parameter in question. Values with the
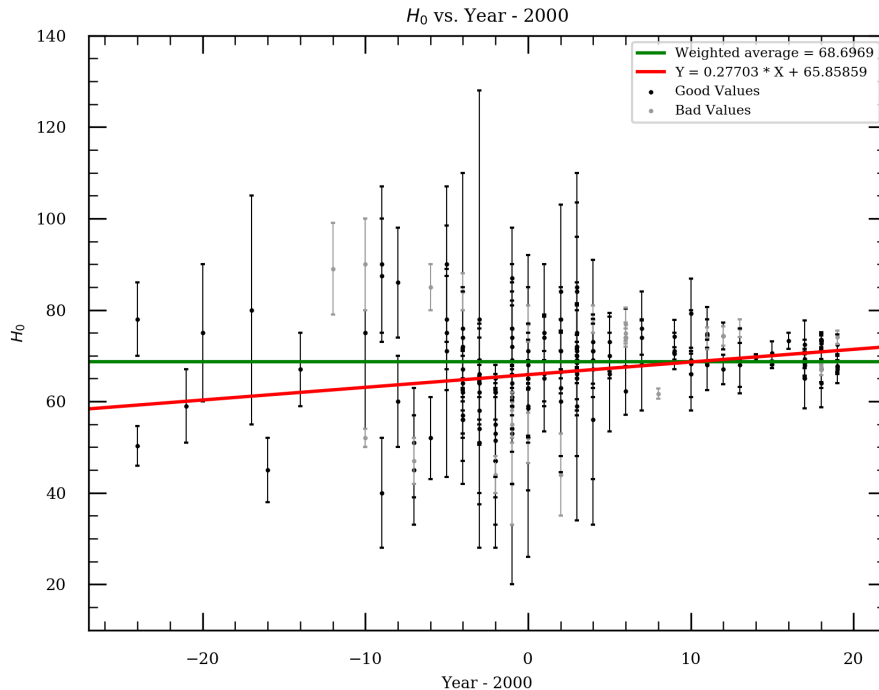
36

Figure 2: Data of H_0 vs. time (year $-$ 2000) separating the $N = 139$ good values that make the χ^2 linear fit compatible with the error bars, and the rest of the points ($N = 24$) plotted as bad values. Here, we only use the good values for the weighted average and best linear fit.

largest contribution to χ^2 (bad values) were removed first. With this last subsample of 139 points, the best linear fit of H_0 returned an A value of 65.9 ± 0.4 and a B value of $0.277^{+0.032}_{-0.034}$; see Figure 2.

The correlation factor of H_0 with time[2] is $c = 0.027 \pm 0.013$, a 2σ significant correlation. Two sigma correlation is not a highly significant detection and is possibly a statistical fluctuation. If a more significant correlation had been obtained, it would have been proof that the measurements of the parameter are not independent, and that there are systematic common errors that vary with time or social biases.[3]

---

[2]For two independent variables X and Y, the correlation factor is defined as $c = \frac{\langle X Y \rangle}{\langle X \rangle \langle Y \rangle} - 1$, with error $Err(c) = \frac{\sigma_X \sigma_Y}{\sqrt{N} \langle X \rangle \langle Y \rangle}$. The Pearson correlation coefficient would be $\frac{c}{\sqrt{N} Err(c)}$.

[3]Richard Feynman gives an example of Nobel Laureate Robert Millikan measuring the charge of an electron: "it's interesting to look at the history of measurements of the charge of the electron, after Millikan. If you plot them as a function of time, you find that one is a little bigger than Millikan's, and the next one is a little bit bigger than that, and the next one's a little bit bigger than that, until finally they settle down to a number which is higher"[16]. Feynman goes on to ask why the final higher number was not discovered right away, and comes to the conclusion, when "[scientists] got a number that was too high above Millikan's, they thought something must be wrong and they would look for and find a reason why something might be wrong, leading them to eliminate values that were too far off, and did other things like that".

We will neglect the variation with time of H_0, and we will continue our analysis with the weighted average. For the value of χ^2 calculated using the weighted average, the probability that the observed trend is due to chance is $Q = 1.0 \times 10^{-47}$. In order to reach a value for Q that is statistically significant ($Q \geq 0.05$), 27 bad values (with more than 2.8σ deviation from the average value) must be removed from the data ($n = 136$, $\chi^2 = 161.3$), producing a value for Q of 0.061. These numbers are slightly different from those given by Ref. [12] owing to a minor error correction. Table 1 [17] lists the 27 values with more than 2.8σ deviation.

See Ref. [12] for further details of this analysis.

Table 1: Bad values: measurements of H_0 in which $|H_0 - \overline{H_0}| > 2.8\sigma$, where $\overline{H_0} = 68.26$ km s^{-1} Mpc^{-1} is the weighted average of the 163 values of the literature.

| Year	H_0 (km s^{-1} Mpc^{-1})	$\frac{|H_0 - \overline{H_0}|}{\sigma}$	Reference
1976	50.3 ± 4.3	4.2	Sandage & Tammann; [18]
1984	45.0 ± 7.0	3.3	Jõeveer; [19]
1990	52.0 ± 2.0	8.1	Sandage & Tammann; [13]
1993	47.0 ± 5.0	4.3	Sandage & Tammann; [13]
1994	85.0 ± 5.0	3.3	Lu et al.; [13]
1996	84.0 ± 4.0	3.9	Ford et al.; [13]
1996	57.0 ± 4.0	2.8	Branch et al.; [13]
1996	56.0 ± 4.0	3.1	Sandage et al.; [13]
1998	65.0 ± 1.0	3.3	Watanabe et al.; [13]
1998	44.0 ± 4.0	6.1	Impey et al.; [13]
1999	60.0 ± 2.0	4.1	Saha et al.; [13]
1999	55.0 ± 3.0	4.4	Sandage; [13]
1999	54.0 ± 5.0	2.9	Bridle et al.; [13]
1999	42.0 ± 9.0	2.9	Collier et al.; [13]
2000	65.0 ± 1.0	3.3	Wang et al.; [13]
2000	52.0 ± 5.5	3.0	Burud et al.; [13]
2004	78.0 ± 3.0	3.2	Wucknitz et al.; [13]
2006	74.9 ± 2.3	3.0	Ngeow & Kanbur; [13]
2006	74.0 ± 2.0	2.9	Sánchez et al.; [13]
2008	61.7 ± 1.2	5.7	Leith et al.; [13]
2012	74.3 ± 2.1	2.9	Freedman et al.; [20]
2013	76.0 ± 1.9	4.1	Fiorentino et al.; [21]
2016	73.2 ± 1.7	2.9	Riess et al.; [22]
2018	73.5 ± 1.7	3.1	Riess et al.; [23]
2018	73.3 ± 1.7	3.0	Follin & Knox; [24]
2018	73.2 ± 1.7	2.9	Chen et al.; [25]
2019	74.0 ± 1.4	4.1	Riess et al.; [9]
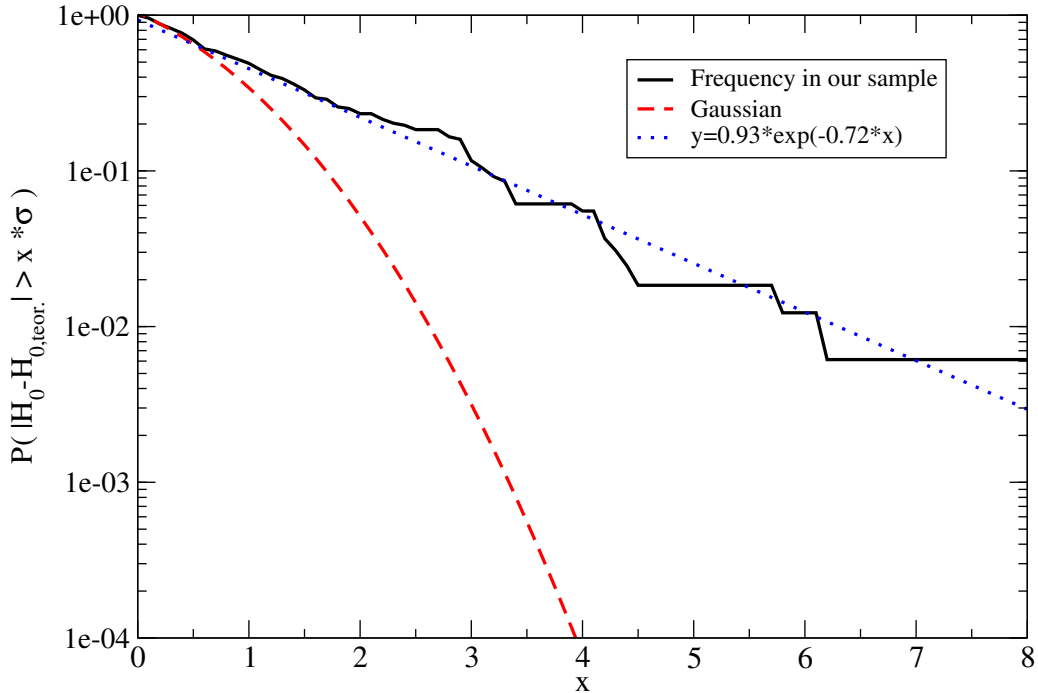
Figure 3: Probability of deviation larger than x sigmas, assuming $H_{0,\text{teor.}} = 68.26\,\text{km}\,\text{s}^{-1}\,\text{Mpc}^{-1}$ (the weighted average value). The dotted line shows the best exponential fit. In dashed line shows the expected probability if the errors are Gaussian.

4. Recalibration of probabilities

In Figure 3, we plot the frequency of deviation larger than $x\sigma$ from the weighted average value $H_{0,\text{teor.}} = 68.26\,\text{km}\,\text{s}^{-1}\,\text{Mpc}^{-1}$ derived used the whole sample of 163 measurements (including the bad ones) [17]. Clearly, the probabilities are much higher than those expected in a normal Gaussian error distribution. For example, in a Gaussian error distribution we should get a $P = 2.7 \times 10^{-3}$ of obtaining a deviation higher than 3σ (where σ is the error of the measurement), but instead we observe that 11.7% of our measurements get deviations higher than 3σ. The fit of our probability with the frequencies we obtain from the real measurements is:

$$P(|H_0 - \overline{H_0}| > x\,\sigma) = (0.93 \pm 0.06) \times \exp[-(0.720 \pm 0.013)x]. \qquad (3)$$

This is equivalent (fit in the range of x between 1 and 12) to a number of σs deviation in a normal distribution:

$$x_{\text{eq.}} = (0.830 \pm 0.004)x^{0.621 \pm 0.003}, \qquad (4)$$

where x is the number of σs in the measurement, i.e. $x = \frac{|H_0 - \overline{H_0}|}{\sigma}$. Hence, for instance, a datum which is 3.0σ away for the expected value should not be interpreted as a 3.0σ tension, but a 1.6σ one in equivalent terms of a normal distribution

$(P(> x_{\text{eq.}}) = 0.11)$. Likewise, a tension of 4.4σ (as for instance claimed by Ref. [9]) for a Hubble tension) is indeed a 2.1σ tension in equivalent terms of a normal distribution, with an associated $P(> x_{\text{eq.}}) = 0.036$ (1 in 28), which is not large but it may happen as a random statistical fluctuation. For an even larger limit of the tension, at 6σ, as pointed by using some different datasets [10], we would have a equivalent 2.5σ with an associated $P(> x_{\text{eq.}}) = 0.012$ (1 in 83), still not amazing.

5. Conclusions and discussion

We have examined the trend and dispersion of values of 163 measurements of H_0 during 43 years (1976–2019). We observed a slightly growing trend (at 2σ level) in the value of the measurements of H_0, for which a random fluctuation interpretation is not excluded. More significantly, the probabilities Q for the distribution of different measurements of H_0 and their errors are extremely low, both with respect to a constant value (weighted average of all the measurements) and with a linear fit. We needed to remove 24–27 measurements to reach a statistically significant dataset $(Q \geq 0.05)$.

In addition to the increasing precision of measurements, it is concluded from this analysis that the error bars of the observed parameters have been largely underestimated in 15–20% of the measurements, or the systematic errors of the observation techniques were not fully considered. It should also be stated that, because of the simplifying assumption made about the covariance of each observed measurement, it is a conservative percentage.

In the light of the analysis carried out here, one would not be surprised to find cases like the 4.4σ discrepancy seen between the best measurement using Supernovae Ia in Ref. [9]. It is likely that the underestimation of error bars for H_0 in many measurements contributes to the apparent 4.4σ discrepancy. Here we have carried out a recalibration of the probabilities with the present sample of measurements and we find that the $x\sigma$s deviation is indeed equivalent in a normal distribution to $x_{\text{eq.}}\sigma$s deviation, where $x_{\text{eq.}} = 0.83x^{0.62}$. Hence, the tension of 4.4σ, estimated between the local Cepheid–supernova distance ladder and cosmic microwave background (CMB) data is indeed a 2.1σ tension in equivalent terms of a normal distribution with an associated $P(> x_{\text{eq.}}) = 0.036$ (1 in 28), which is not large but it may happen as a random statistical fluctuation. This can be increased up to a equivalent tension of 2.5σ in the worst of cases.

References

[1] Freedman, W. L., Madore, B. F.: The Hubble constant. Annu. Rev. Astron. Astrophys. 48 (2010), 673–710.

[2] Paturel, G.: Some difficulties for measuring and interpreting the expansion of the universe. In: Y. Baryshev, I. Taganov, and P. Teerikorpi (Eds.), Practical Cosmology, vol. 2, pp. 178–184, TIN, St.-Petersburg, 2008.

[3] Sandage, A., Tammann, G. A., Reindl, B.: New period-luminosity and period-color relations of classical Cepheids. III. Cepheids in SMC. Astron. Astrophys. 493 (2009), 471–479.

[4] Tammann, G. A., Sandage, A., Reindl, B.: New period-luminosity and period-color relations for classical Cepheids: I. Cepheids in the Galaxy. Astron. Astrophys. 404 (2003), 423–448.

[5] Matravers, D. R., Ellis, G. F. R., Stoeger, W. R.: Complementary approaches to cosmology – relating theory and observations. Quaterly J. R. Astron. Soc. 36 (1995), 29–45.

[6] Yadav, J. K., Bagla, J. S., Khandai, N.: Fractal dimension as a measure of the scale of homogeneity. Mon. Not. R. Astron. Soc. 405 (2010), 2009–2015.

[7] Sylos Labini, F.: Inhomogeneities in the Universe. Class. Quantum Grav. 28 (2011), id. 164003.

[8] López-Corredoira, M.: Peaks in the CMBR power spectrum II: Physical interpretation for any cosmological scenario. Int. J. Mod. Phys. D 22 (2013), id. 1350032, 18 pp.

[9] Riess, A. G., Casertano, S., Yuan, W., Macri, L. M., Scolnic, D.: Large magellanic cloud cepheid standards provide a 1% foundation for the determination of the Hubble constant and stronger evidence for physics beyond ΛCDM. Astrophys. J. 876 (2019), id. 85, 13 pp.

[10] Di Valentino, E., Mena, O., Pan, S., et al.: Class. Quantum Grav. **38** (2021), id. 153001, 110 pp.

[11] Perivolaropoulos, L., Skara, F.: Challenges for ΛCDM: An update. [arXiv:2105.05208].

[12] Faerber, T., López-Corredoira, M.: A Chi-squared analysis of the measurements of two cosmological parameters over time. Universe 6(8) (2020), id. 114.

[13] Croft, R. A., Dailey, M.: On the measurement of cosmological parameters. Quaterly Phys. Rev. 1 (2015), 1–14 [arXiv:1112.3108].

[14] Chiba, M., Yoshii, Y.: A technique for determining the extragalactic distance scale. Astrophys. J. 442 (1995), 82–86.

[15] Plackett, R. L.: Karl Pearson and the chi-squared test. Int. Stat. Rev. **51** (1983), 59-72.

[16] Feynman, R.: Cargo cult science. Engineering and Science 37(7) (1974), 10–13.

[17] López-Corredoira, M.: Hubble tensions: a historical statistical analysis. Submitted (2022).

[18] Sandage, A., Tammann, G.: Steps toward the Hubble constant. VII-Distances to NGC 2403, M101, and the Virgo cluster using 21 centimeter line widths compared with optical methods: The global value of H_0. Astrophys. J. 210 (1976), 7–24.

[19] Jõeveer, M.: The type I supernovae absolute magnitude brightness decline rate relation and the Hubble constant. Publ. Tartu Astrofiz. Obs. 50 (1984), 327–334.

[20] Freedman, W. L., Madore, B. F., Scowcroft, V., Burns, C., Monson, A., Persson, S. E., Seibert, M., Rigby, J.: Carnegie Hubble program: A mid-infrared calibration of the Hubble constant. Astrophys. J. 758 (2012), id. 24, 10 pp.

[21] Fiorentino, G., Musella, I., Marconi, M.: Cepheid theoretical models and observations in HST/WFC3 filters: The effect on the Hubble constant H_0. Mon. Not. R. Astron. Soc. 434 (2013), 2866–2876.

[22] Riess, A. G., Macri, L. M., Hoffmann, S. L., et al. A 2.4% determination of the local value of the Hubble constant. Astrophys. J. 826 (2016), id. 56, 31 pp.

[23] Riess, A. G., Casertano, S., Yuan, W., et al.: New parallaxes of Galactic Cepheids from spatially scanning the Hubble Space Telescope: Implications for the Hubble constant. Astrophys. J. 855 (2018), id. 136, 18 pp.

[24] Follin, B., Knox, L.: Insensitivity of the distance ladder Hubble constant determination to Cepheid calibration modelling choices. Mon. Not. R. Astron. Soc. 47 (2018), 4534–4542.

[25] Chen, H. Y., Fishbach, M., Holz, D. E.: A two per cent Hubble constant measurement from standard sirens within five years. Nature 562 (2018), 545–547.

THE WEAK FIELD APPROXIMATION OF GENERAL RELATIVITY, RETARDATION, AND THE PROBLEM OF PRECESSION OF THE PERIHELION FOR MERCURY

Asher Yahalom

Ariel University
Ariel 40700, Israel
asya@ariel.ac.il

Abstract: In this paper we represent a different approach to the calculation of the perihelion shift than the one presented in common text books. We do not rely on the Schwarzschild metric and the Hamilton-Jacobi technique to obtain our results. Instead we use a weak field approximation, with the advantage that we are not obliged to work with a definite static metric and can consider time dependent effects. Our results support the conclusion of Křížek [1] regarding the significant influence of celestial parameters on the indeterminacy of the perihelion shift of Mercury's orbit. This shift is thought to be one of the fundamental tests of the validity of the general theory of relativity. In the current astrophysical community, it is generally accepted that the additional relativistic perihelion shift of Mercury is the difference between its observed perihelion shift and the one predicted by Newtonian mechanics, and that this difference equals 43" per century. However, as it results from the subtraction of two inexact numbers of almost equal magnitude, it is subject to cancellation errors. As such, the above accepted value is highly uncertain and may not correspond to reality.

Keywords: general relativity, retardation, Mercury

PACS: 04.20.-q, 04.25.Nx, 95.10.Ce

1. Introduction

Under Newtonian physics, an object in an (isolated) bounded two-body system, consisting of the object orbiting a spherical mass, would trace out an ellipse with the massive object at a focus of the ellipse. The point of closest approach, called the periapsis (or, because the central massive body in the Solar system is the Sun, perihelion), is fixed. Hence, the major axis of the ellipse remains fixed in space. Both objects orbit around the center of mass of this system, so they each have their own ellipse, but the heavier body trajectory is smaller. In fact it can be much smaller if the ratio between the masses is considerable. However, a number of effects in the

Solar System cause the perihelia of planets to precess (rotate) around the Sun, or equivalently, cause the major axis to rotate, hence changing its orientation in space. The principal cause is the presence of other planets which perturb one another's orbit. Another (much less significant) effect is solar oblateness.

Mercury deviates from the precession predicted from these Newtonian effects. This anomalous rate of precession of the perihelion of Mercury's orbit was first recognized in 1859 as a problem in celestial mechanics, by Urbain Le Verrier. His re-analysis of available timed observations of transits of Mercury over the Sun's disk from 1697 to 1848 demonstrated that the actual rate of the precession disagreed from that predicted from Newton's theory by 38" (arcseconds) per tropical century [4] (later it was estimated to be 43" by Simon Newcomb in 1882 [5]). A number of ad hoc and ultimately unsuccessful solutions were proposed, but they seemed to cause more problems. Le Verrier speculated that another hypothetical planet might exist to account for Mercury's behavior [6]. The previously successful search for Neptune based on its perturbations of the orbit of Uranus led astronomers to place some faith in this possible explanation, and the hypothetical planet was even named Vulcan. Finally, in 1908, W. W. Campbell, Director of the Lick Observatory, after meticulous photographic observations by Lick astronomer, Charles D. Perrine, at three different solar eclipse expeditions, stated, "In my opinion, Dr. Perrine's work at the three eclipses of 1901, 1905, and 1908 brings the observational side of the famous intramercurial-planet problem definitely to a close," see [7]. Since no evidence of Vulcan was found and Einstein's 1915 general theory accounted for Mercury's anomalous precession. Einstein could write to his friend Michael Besso, "Perihelion motions explained quantitatively...you will be astonished" [7].

In general relativity, this remaining precession, or change of orientation of the orbital ellipse within its orbital plane, is explained by gravitation being mediated by the curvature of spacetime, and by the fact that the trajectory must be a geodesic in the curved space-time. Einstein showed that general relativity [8], [9] agrees closely with the observed amount of perihelion shift. This was a powerful factor motivating the adoption of general relativity.

Although earlier measurements of planetary orbits were made using conventional telescopes, more precise measurements are now made using a radar. The total observed precession of Mercury is 574.10"±0.65" per century [10] relative to the inertial International Celestial Reference System (ICRS) (the current standard celestial reference system adopted by the International Astronomical Union (IAU). Its origin is at the barycenter of the Solar System, with axes that are intended to be oriented with respect to the stars.)

This precession can be attributed to the causes [10], [11] described in Table 1. Thus, despite the efforts, theoretical predictions of the precession of perihelion for Mercury do not full within observational results error bars and the discrepancy is at best 0.56" per century or about 0.1%. This is not much but still requires explanation.

Causes of the precession of perihelion for Mercury (arcsec/Julian century)	Cause
532.3035	Gravitational tugs of other solar bodies
0.0286	Oblateness of the Sun (quadruple moment)
42.9799	General Relativity effect (Schwarzschild - like)
−0.0020	Lense-Thirring precession
575.31	**Total predicted**
574.10 ± 0.65	**Observed**

Table 1: The different contributions to the precession of perihelion for Mercury amount (arcsec/Julian century), theory vs. prediction.

In general relativity the perihelion shift $\delta\theta$, expressed in radians per revolution, is approximately given by [12]:

$$\delta\theta = \frac{6\pi GM}{ac^2\left(1 - e^2\right)}, \tag{1}$$

where $G \simeq 6.67 \cdot 10^{-11}\,\mathrm{m^3 kg^{-1} s^{-2}}$ is the universal gravitational constant and $c \simeq 3 \cdot 10^8\,\mathrm{ms^{-1}}$ indicates the velocity of light in the absence of matter, M is the mass of the Sun, a is the semi-major axis of the ellipsoidal trajectory and e is its orbital eccentricity. The above is based on calculating a geodesic in a Schwarzschild geometry, that is in a geometry created by a static point mass. The framework of Schwarzschild geometry does not allow us to take into account effects such as the motion of the Sun with respect to the frame.

The other planets experience perihelion shifts as well, but, since they are farther from the Sun and have longer periods, their shifts are lower, and could not be observed accurately until long after Mercury's. For example, the perihelion shift of Earth's orbit due to general relativity is theoretically 3.83868" per century and experimentally 3.8387±0.0004"/cy, Venus's is 8.62473"/cy and 8.6247±0.0005"/cy. Both values have now been measured, with results in good agreement with theory [13].

Einstein's general relativity (GR) is known to be invariant under general coordinate modifications. This group of general transformations has a Lorentz subgroup, which is valid even in the weak field approximation. This is seen through the field equations containing the d'Alembert (wave) operator, which can be solved using a retarded potential solution.

It is known that GR is verified by many types of observations. However, currently, Newton–Einstein gravitational theory is at a crossroads. It has much in its favor observationally, and it has some very disquieting challenges. The successes that it has achieved in both astrophysical and cosmological scales have to be considered in light of the fact that GR needs to appeal to two unconfirmed ingredients, dark matter and energy, to achieve these successes. Dark matter has not only been with us since

the 1920s (when it was initially known as the missing mass problem), but it has also become severe as more and more of it had to be introduced on larger distance scales as new data have become available. Moreover, 40-year-underground and accelerator searches and experiments have failed to establish its existence. The dark matter situation has become even more disturbing in recent years as the Large Hadron Collider was unable to find any super symmetric particle candidates, the community's preferred form of dark matter. While things may still take turn in favor of the dark matter hypothesis, the current situation is serious enough to consider the possibility that the popular paradigm might need to be amended in some way if not replaced altogether. In our recent work we have sought such a modification. Unlike other ideas such as Milgrom's MOND [14], Mannheim's Conformal Gravity [15], [16], [17], Moffat's MOG [18] or $f(R)$ theories and scalar-tensor gravity [19], the present approach is, the minimalist one adhering to the razor of Occam. It suggests to replace dark matter by the retardation effect within standard GR. Fritz Zwicky noticed in 1933 that the velocities of Galaxies within the Comma Cluster are much higher than those predicted by the virial calculation that assumes Newtonian theory [20]. He calculated that the amount of matter required to account for the velocities could be 400 times greater with respect to that of visible matter, which led to suggesting dark matter throughout the cluster. In 1959, Volders, pointed out that stars in the outer rims of the nearby galaxy M33 do not move according to Newtonian theory [21]. The virial theorem coupled with Newtonian Gravity implies that $MG/r \sim Mv^2$, thus the expected rotation curve should at some point decrease as $1/\sqrt{r}$. During the seventies Rubin and Ford [22], [23] showed that, for a large number of spiral galaxies, this behavior can be considered generic: velocities at the rim of the galaxies do not decrease— but they attain a plateau at some unique velocity, which differs for every galaxy. We have shown that such velocity curves can be deduced from GR if retardation is not neglected. The derivation of the retardation force is described in previous publications [24], [25], [26], [27], [28], [29], [30], [31], see for example Figure 1. It should be noted that "dark matter" effects on light rays (gravitational lensing) are well handled when taking into account retardation [32]. The effects of gravitational lensing and the explanation of the anomalous perihelion advance of the planet Mercury where the first corroborated predictions of GR. Einstein made unpublished work on gravitational lensing as early as 1912 [33] (see Figure 2). As we mentioned previously in 1915 Einstein showed how GR explained the anomalous perihelion advance of the planet Mercury without any arbitrary parameters [34] (for a detailed account of Einstein's previous unsuccessful attempts to obtain the same see Weinstein [3]) , in 1919 an expedition led by Eddington confirmed GR's prediction for the deflection of starlight by the Sun in the total solar eclipse of May 29, 1919, see [35], [36], making Einstein famous [34] instantly. The reader should recall that there was a special significance to a British scientist confirming the prediction of a German scientist after the bloody battles of world war I.

Gravitational retardation effects do not seem to be very important in the Solar system, up to small corrections the dynamics is well described by Newtonian me-
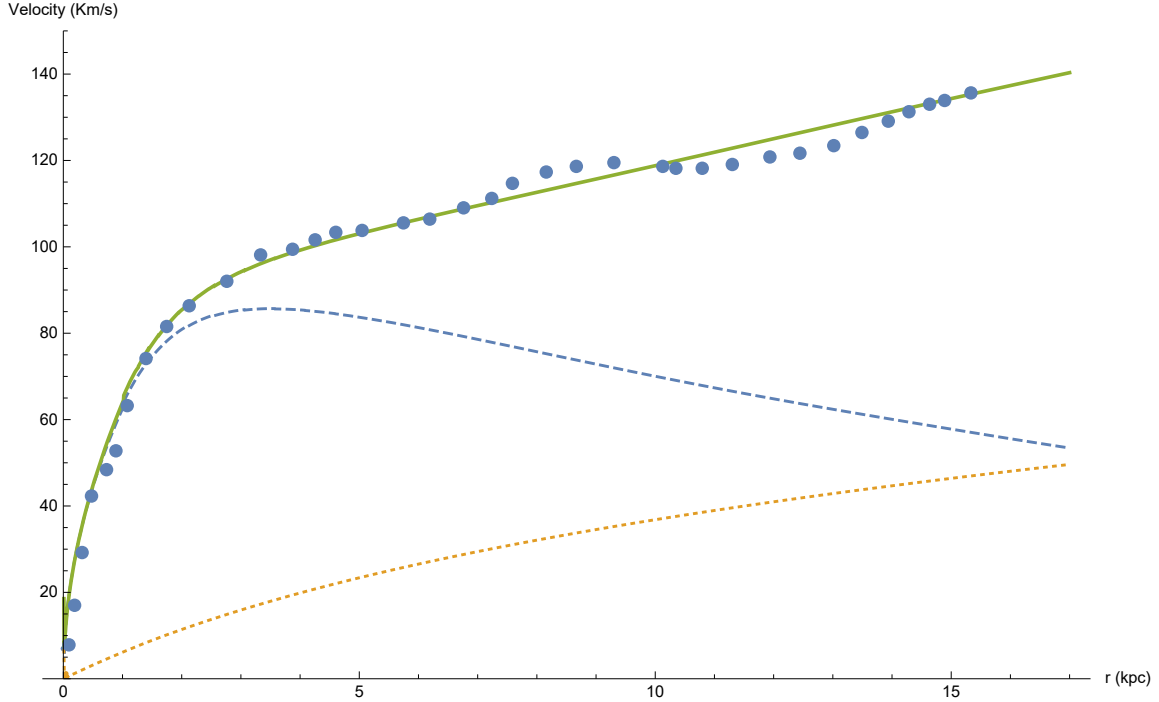
Figure 1: Velocity curve for M33. Observational points were obtained by Dr. Michal Wagman, a former PhD student under my supervision, using [44]; the full line describes the rotation curve, which is the sum of the dotted line, describing the retardation contribution, and the dashed line, which is Newtonian.

chanics, and even the small GR effects observed can be well explained by a constant Schwarzschild metric, that is without time dependency effects of the metric. Still, it is perhaps too early to dismiss any time dependent effects on account of the discrepancy described in Table 1 with regard to the perihelion precession of Mercury which is the reason for our study.

2. General relativity

The general theory of relativity is based on two fundamental equations, the first being Einstein equations [37], [39], [40], [38]:

$$G_{\mu\nu} = -\frac{8\pi G}{c^4} T_{\mu\nu}, \tag{2}$$

where $G_{\mu\nu}$ stands for the Einstein tensor (see equation (8)), $T_{\mu\nu}$ indicates the stress–energy tensor (see equation (4)), (Greek letters are indices in the range $0-3$). The second fundamental equation that GR is based on is the geodesic equation

$$\frac{d^2 x^\alpha}{dp^2} + \Gamma^\alpha_{\mu\nu} \frac{dx^\mu}{dp} \frac{dx^\nu}{dp} = 0, \tag{3}$$
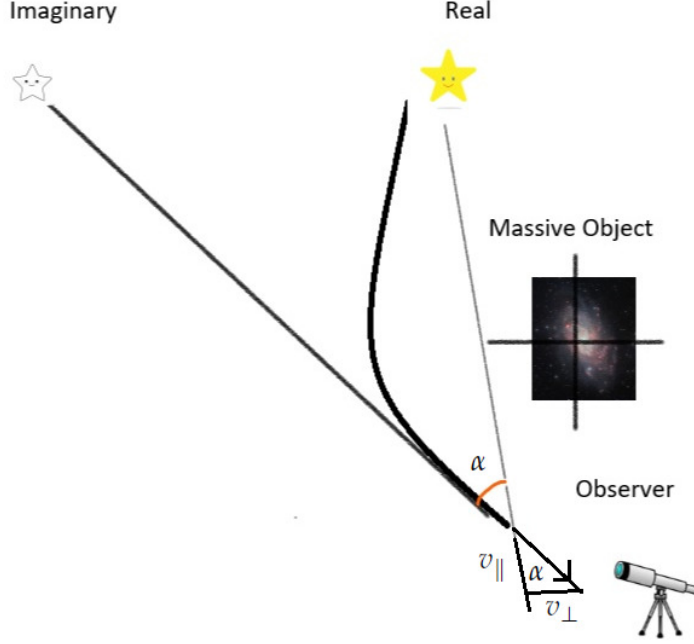
47

Figure 2: Light travelling toward the observer is bent due to the gravitational field of a massive object, thus a distant star appears to the observer at an angle α with resect to its true location.

where $x^\alpha(p)$ are the coordinates of the particle in spacetime, p is a typical parameter along the trajectory that for massive particles is chosen to be the length of the trajectory $(p = s)$, $\tilde{u}^\mu = \frac{dx^\mu}{ds}$ or the proper time $(p = \tau = \frac{s}{c})$ $u^\mu = \frac{dx^\mu}{d\tau} = c\tilde{u}^\mu$ is the μ-th component of the 4-velocity of a massive particle moving along the geodesic trajectory (increment of x per p) and $\Gamma^\alpha_{\mu\nu}$ is the affine connection (Einstein summation convention is assumed). The stress–energy tensor of matter is usually taken in the form

$$T_{\mu\nu} = (pr + \rho c^2)\tilde{u}_\mu \tilde{u}_\nu - pr\ g_{\mu\nu}. \tag{4}$$

In the above, pr is the pressure and ρ is the **mass** density. We remind the reader that lowering and raising indices is done through the metric $g_{\mu\nu}$ and inverse metric $g^{\mu\nu}$, such that $u_\mu = g_{\mu\nu}u^\nu$. The same metric serves to calculate s

$$ds^2 = g_{\mu\nu}dx^\mu dx^\nu. \tag{5}$$

The affine connection is connected to the metric as follows

$$\Gamma^\alpha_{\mu\nu} = \frac{1}{2}g^{\alpha\beta}\left(g_{\beta\mu,\nu} + g_{\beta\nu,\mu} - g_{\mu\nu,\beta}\right), \qquad g_{\beta\mu,\nu} \equiv \frac{\partial g_{\beta\mu}}{\partial x^\nu}. \tag{6}$$

Using the affine connection we calculate the Riemann and Ricci tensors and the curvature scalar

$$R^\mu_{\nu\alpha\beta} = \Gamma^\mu_{\nu\alpha,\beta} - \Gamma^\mu_{\nu\beta,\alpha} + \Gamma^\sigma_{\nu\alpha}\Gamma^\mu_{\sigma\beta} - \Gamma^\sigma_{\nu\beta}\Gamma^\mu_{\sigma\alpha}, \quad R_{\alpha\beta} = R^\mu_{\alpha\beta\mu}, \quad R = g^{\alpha\beta}R_{\alpha\beta} \tag{7}$$

48

which, in turn, serves to calculate the Einstein tensor

$$G_{\alpha\beta} = R_{\alpha\beta} - \frac{1}{2} g_{\alpha\beta} R. \tag{8}$$

Hence, the given matter distribution determines the metric through equation (2) and the metric determines the geodesic trajectories through equation (3).

3. Linear approximation of GR – justification

Only in extreme cases of compact objects (black holes and neutron stars) and the primordial reality or the very early universe does one need not consider the solution of the full non-linear Einstein equation [24]. In typical cases of astronomical interest[1] (certainly everywhere in the Solar system) one can use a linear approximation to those equations around the flat Lorentz metric $\eta_{\mu\nu}$ such that

$$g_{\mu\nu} = \eta_{\mu\nu} + h_{\mu\nu}, \quad \eta_{\mu\nu} \equiv \text{diag}(1, -1, -1, -1), \quad |h_{\mu\nu}| \ll 1, \tag{9}$$

$$ds^2 = (\eta_{\mu\nu} + h_{\mu\nu}) dx^\mu dx^\nu. \tag{10}$$

In order to appreciate the above statements, let us look at the Schwarzschild metric [39]. This metric describes a static spherically symmetric mass distribution and thus is less general than the approach we intend to develop in this paper. It does have one advantage, however, and this is the ability to take into account strong gravitational fields and not just weak ones. This advantage is irrelevant in most astronomical cases in which gravity is weak and must be only considered for trajectories near compact objects (black holes and neutron stars). Here we introduce it just for the sake of making an order of magnitude estimate. The Schwarzschild squared interval can be written as

$$ds^2_{\text{Schwarzschild}} = \left(1 - \frac{r_s}{r'}\right) c^2 dt^2 - \left(1 - \frac{r_s}{r'}\right)^{-1} dr'^2 - r'^2 \left(d\theta^2 + \sin^2\theta\, d\Phi^2\right). \tag{11}$$

In which r', θ, Φ are spherical coordinates and the point massive body is located at $r' = 0$. The Schwarzschild radius is defined as

$$r_s = \frac{2GM}{c^2} \tag{12}$$

in which M is the mass of the point particle. The most massive object in the Solar system is the Sun with a Solar mass of $M_{\text{sun}} \simeq 1.99 \cdot 10^{30}$ kg leading to $r_s \simeq 2950$ m $\simeq$ 3 km. The deviation of the metric from the empty space Minkowski metric according to equation (11) is

$$h_{00} = -\frac{r_s}{r'}. \tag{13}$$

Here h_{00} is strongest on the Sun's surface where $r' = 6.96 \cdot 10^8$ m in which $h_{00} \simeq 4.27 \cdot 10^{-6}$, this is quite small (with respect to unity) indeed. For Mercury the closer distance to the Sun (perihelion) is $r' = 4.6 \cdot 10^{10}$ m hence $h_{00} \simeq 6.41 \cdot 10^{-8}$ at most. Neglecting second order terms thus means neglecting terms of order 10^{-15} and seems quite justified.

---

[1] Private communication with the late Professor Donald Lynden-Bell.

4. Linear approximation of GR – the metric

One then defines the quantity

$$\bar{h}_{\mu\nu} \equiv h_{\mu\nu} - \frac{1}{2}\eta_{\mu\nu}h, \quad h = \eta^{\mu\nu}h_{\mu\nu}, \tag{14}$$

where $\bar{h}_{\mu\nu} = h_{\mu\nu}$ stands for non diagonal terms. For diagonal terms

$$\bar{h} = -h \Rightarrow h_{\mu\nu} = \bar{h}_{\mu\nu} - \frac{1}{2}\eta_{\mu\nu}\bar{h}. \tag{15}$$

It can be shown ([37] page 75, exercise 37, see also [38], [39], [40]) that one can choose a gauge such that the Einstein equations are

$$\bar{h}_{\mu\nu,\alpha}{}^{\alpha} = -\frac{16\pi G}{c^4}T_{\mu\nu}, \qquad \bar{h}_{\mu\alpha,}{}^{\alpha} = 0. \tag{16}$$

Equation (16) can always be integrated to take the form [41]:

$$\bar{h}_{\mu\nu}(\vec{x}, t) = -\frac{4G}{c^4}\int \frac{T_{\mu\nu}(\vec{x}', t - \frac{R}{c})}{R}d^3x',$$

$$t \equiv \frac{x^0}{c}, \quad \vec{x} \equiv x^a, \quad a, b \in [1, 2, 3],$$

$$\vec{R} \equiv \vec{x} - \vec{x}', \quad R = |\vec{R}|. \tag{17}$$

For reasons why the symmetry between space and time is broken, see [42], [43]. The factor before the integral is small: $\frac{4G}{c^4} \simeq 3.3 \cdot 10^{-44}$ in MKS units; hence, in the above calculation one can take $T_{\mu\nu}$, which is zero order in $h_{\alpha\beta}$. In the zeroth order:

$$\tilde{u}^0 = \frac{1}{\sqrt{1 - \frac{v^2}{c^2}}} \equiv \gamma, \quad \vec{\tilde{u}} \equiv (\tilde{u}^1, \tilde{u}^2, \tilde{u}^3) = \frac{\frac{\vec{v}}{c}}{\sqrt{1 - \frac{v^2}{c^2}}} = \vec{\beta}\gamma,$$

$$v^\mu \equiv \frac{dx^\mu}{dt}, \quad \vec{v} \equiv \frac{d\vec{x}}{dt}, \quad v = |\vec{v}|, \quad \vec{\beta} \equiv \frac{\vec{v}}{c}, \quad \beta = |\vec{\beta}|. \tag{18}$$

And also

$$u^0 = c\gamma, \quad \vec{u} \equiv (u^1, u^2, u^3) = \vec{v}\gamma. \tag{19}$$

Assuming the reasonable assumption that the said massive body is composed of particles of non relativistic velocities

$$\tilde{u}^0 \simeq 1, \qquad \vec{\tilde{u}} \simeq \vec{\beta}, \qquad \tilde{u}^a \ll \tilde{u}^0 \qquad \text{for} \quad v \ll c, \tag{20}$$

and also

$$u^0 \simeq c, \qquad \vec{u} \simeq \vec{v}, \qquad u^a \ll u^0 \qquad \text{for} \quad v \ll c. \tag{21}$$

Let us now look at equation (4). We assume $\rho c^2 \gg pr$ and, taking into account equation (20), we arrive at $T_{00} = \rho c^2$, while other tensor components are significantly

smaller. Thus, $\bar{h}_{00}$ is significantly larger than other components of $\bar{h}_{\mu\nu}$ which are ignored from now on. One should notice that it is possible to deduce from the gauge condition in equation (16) the relative order of magnitude of the relative components of $h_{\mu\nu}$

$$\bar{h}_{\alpha 0,}{}^0 = -\bar{h}_{\alpha a,}{}^a \qquad \Rightarrow \qquad \bar{h}_{00,}{}^0 = -\bar{h}_{0a,}{}^a, \quad \bar{h}_{b0,}{}^0 = -\bar{h}_{ba,}{}^a. \tag{22}$$

Thus, the zeroth derivative of $\bar{h}_{00}$ (which contains a $\frac{1}{c}$ as $x^0 = ct$) is the same order as the spatial derivative of $\bar{h}_{0a}$ meaning that $\bar{h}_{0a}$ is of order $\frac{v}{c}$ smaller than $\bar{h}_{00}$. And the zeroth derivative of $\bar{h}_{0a}$ (which appears in Equation (22)) is the same order as the spatial derivative of $\bar{h}_{ab}$. Meaning that $\bar{h}_{ab}$ is of order $\frac{v}{c}$ with respect to $\bar{h}_{0a}$ and of order $(\frac{v}{c})^2$ with respect to $\bar{h}_{00}$.

In the current approximation, the following results hold:

$$\bar{h} = \eta^{\mu\nu}\bar{h}_{\mu\nu} = \bar{h}_{00}, \tag{23}$$

$$h_{00} = \bar{h}_{00} - \frac{1}{2}\eta_{00}\bar{h} = \frac{1}{2}\bar{h}_{00}, \tag{24}$$

$$h_{\underline{aa}} = -\frac{1}{2}\eta_{\underline{aa}}\bar{h} = \frac{1}{2}\bar{h}_{00}. \tag{25}$$

(The underline $\underline{aa}$ signifies that the Einstein summation convention is not assumed.)

$$h_{\mu\nu} = \bar{h}_{\mu\nu} = 0, \qquad \mu \neq \nu. \tag{26}$$

We can summarize the above results in a concise formula

$$h_{\mu\nu} = h_{00}\delta_{\mu\nu}. \tag{27}$$

in which $\delta_{\mu\nu}$ is Kronecker's delta. Thus,

$$ds^2 = (\eta_{\mu\nu} + h_{\mu\nu})dx^\mu dx^\nu = (\eta_{\mu\nu} + h_{00}\delta_{\mu\nu})dx^\mu dx^\nu = (1 + h_{00})c^2 dt^2 - (1 - h_{00})d\vec{x}^2, \tag{28}$$

and the proper time is

$$d\tau = dt\sqrt{(1 + h_{00}) - (1 - h_{00})\beta^2} \simeq dt\left[\sqrt{1 - \beta^2} + \frac{1}{2}h_{00}\frac{1 + \beta^2}{\sqrt{1 - \beta^2}}\right], \tag{29}$$

for slow particles this reduces to

$$d\tau = dt\left[1 + \frac{1}{2}h_{00}\right], \tag{30}$$

and thus

$$\vec{u} = \frac{d\vec{x}}{d\tau} = \frac{d\vec{x}}{dt}\frac{dt}{d\tau} = \frac{\vec{v}}{\sqrt{1 - \beta^2} + \frac{1}{2}h_{00}\frac{1 + \beta^2}{\sqrt{1 - \beta^2}}}. \tag{31}$$

The above somewhat complex relation is the main reason that we will prefer to perform our analysis with $\vec{u}$ rather than $\vec{v}$ keeping in mind that in the Solar system $\vec{u} \simeq \vec{v}$ for slow moving bodies (with respect to the speed of light).

It will be useful to introduce the gravitational potential ϕ which is defined below and can be calculated using Equation (17),

$$\phi \equiv \frac{c^2}{4}\bar{h}_{00} = -\frac{G}{c^2}\int \frac{T_{00}(\vec{x}', t - \frac{R}{c})}{R}d^3x' = -G\int \frac{\rho(\vec{x}', t - \frac{R}{c})}{R}d^3x'. \tag{32}$$

From the above definition and equation (24) it follows that

$$h_{00} = \frac{2}{c^2}\phi, \qquad \phi = \frac{c^2}{2}h_{00}. \tag{33}$$

Let us now calculate the affine connection in the linear approximation

$$\Gamma^\alpha_{\mu\nu} = \frac{1}{2}\eta^{\alpha\beta}\left(h_{\beta\mu,\nu} + h_{\beta\nu,\mu} - h_{\mu\nu,\beta}\right). \tag{34}$$

Taking into account equation (27), we arrive at the result

$$\Gamma^a_{\mu\nu} = \frac{1}{2}\left(\eta^{a\mu}h_{00,\nu} + \eta^{a\nu}h_{00,\mu} + h_{00,a}\delta_{\mu\nu}\right). \tag{35}$$

The above equation is only correct for a Latin index a. This is our main concern, as we will concentrate on the analysis of u^a (rather than u^0).

5. Linear approximation of GR – the trajectory

Let us start calculating the trajectory by inserting equation (35) into equation (3), we arrive at the equation

$$\frac{du^a}{d\tau} = -\Gamma^a_{\mu\nu}u^\mu u^\nu = u^a u^\nu h_{00,\nu} - \frac{1}{2}u^\nu u^\nu h_{00,a}. \tag{36}$$

We may write

$$u^\nu h_{00,\nu} = h_{00,\nu}\frac{dx^\nu}{d\tau} = \frac{dh_{00}}{d\tau}. \tag{37}$$

Thus

$$\frac{du^a}{d\tau} = u^a\frac{dh_{00}}{d\tau} - \frac{1}{2}u^\nu u^\nu h_{00,a}. \tag{38}$$

As the current analysis is only valid to first order in h_{00} and since the right-hand side of the equation is already linear in h_{00}, we only need to consider the other expressions in the right-hand side to zeroth order in h_{mn}, thus

$$\frac{du^a}{d\tau} = u^{(0)a}\frac{dh_{00}}{d\tau} - \frac{1}{2}u^{(0)\nu}u^{(0)\nu}h_{00,a}. \tag{39}$$

It follows that according to equation (5),

$$c^2 = \frac{ds^2}{d\tau^2} = \eta_{\mu\nu}u^{(0)\mu}u^{(0)\nu} = (u^{(0)0})^2 - u^{(0)a}u^{(0)a} \tag{40}$$

52

and also
$$u^{(0)\nu}u^{(0)\nu} = (u^{(0)0})^2 + u^{(0)a}u^{(0)a} = 2(u^{(0)0})^2 - c^2. \tag{41}$$

Thus we obtain
$$\frac{du^a}{d\tau} = u^{(0)a}\frac{dh_{00}}{d\tau} + \left(\frac{1}{2}c^2 - (u^{(0)0})^2\right)h_{00,a}, \tag{42}$$

or in vector form
$$\frac{d\vec{u}}{d\tau} = \vec{u}^{(0)}\frac{dh_{00}}{d\tau} + \left(\frac{1}{2}c^2 - (u^{(0)0})^2\right)\vec{\nabla}h_{00}, \tag{43}$$

In term of the potential ϕ this takes the form
$$\frac{d\vec{u}}{d\tau} = \frac{2\vec{u}^{(0)}}{c^2}\frac{d\phi}{d\tau} + \left(1 - \frac{2(u^{(0)0})^2}{c^2}\right)\vec{\nabla}\phi. \tag{44}$$

If the body is slowly moving such that $\beta \to 0$ it follows that $\tau \simeq t$, $\vec{u} \simeq \vec{v}$, $u^{(0)0} \simeq c$ and thus
$$\frac{d\vec{v}}{dt} = \frac{2\vec{v}^{(0)}}{c^2}\frac{d\phi}{dt} - \vec{\nabla}\phi. \tag{45}$$

If ϕ does not depend explicitly on time: $\frac{d\phi}{dt} = \vec{v} \cdot \vec{\nabla}\phi$ and we obtain
$$\frac{d\vec{v}}{dt} = 2\vec{\beta}(\vec{\beta} \cdot \vec{\nabla}\phi) - \vec{\nabla}\phi \simeq -\vec{\nabla}\phi. \tag{46}$$

Thus we are back to the Newtonian equation of motion, which can be used as a good approximation for most purposes to derive planetary motion.

5.1. "Angular Momentum"

Let us perform a vector multiplication of equation (43) with the vector $\vec{r} = (x^1, x^2, x^3)$. We obtain
$$\vec{r} \times \frac{d\vec{u}}{d\tau} = \vec{r} \times \vec{u}^{(0)}\frac{dh_{00}}{d\tau} + \left(\frac{1}{2}c^2 - (u^{(0)0})^2\right)\vec{r} \times \vec{\nabla}h_{00}. \tag{47}$$

Now suppose that $h_{00} = h_{00}(r)$ in which $r = |\vec{r}|$, in this case $\vec{r} \cdot \vec{\nabla}h_{00} = 0$. And thus
$$\frac{d(\vec{r} \times \vec{u})}{d\tau} = \vec{r} \times \frac{d\vec{u}}{d\tau} = \vec{r} \times \vec{u}^{(0)}\frac{dh_{00}}{d\tau} = (\vec{r} \times \vec{u})\frac{dh_{00}}{d\tau}, \tag{48}$$

the last equation sign is correct to first order in h_{00} (which is the order of our entire analysis). We now define an "angular momentum"
$$\vec{J} \equiv m\vec{r} \times \vec{u} \simeq m\vec{r} \times \vec{v} \tag{49}$$

in which m is the mass of the particle under consideration. The right-hand side of the equation is correct for slow bodies, in the Solar system. It follows that
$$\frac{d\vec{J}}{d\tau} = \vec{J}\,\frac{dh_{00}}{d\tau}. \tag{50}$$

Hence, for each cartesian component

$$\frac{dJ_x}{d\tau} = J_x \frac{dh_{00}}{d\tau}, \quad \frac{dJ_y}{d\tau} = J_y \frac{dh_{00}}{d\tau}, \quad \frac{dJ_z}{d\tau} = J_z \frac{dh_{00}}{d\tau}. \tag{51}$$

Or also

$$\frac{d(\ln J_x - h_{00})}{d\tau} = 0, \quad \frac{d(\ln J_y - h_{00})}{d\tau} = 0, \quad \frac{d(\ln J_z - h_{00})}{d\tau} = 0. \tag{52}$$

Thus

$$\vec{J} = \vec{J}_0 e^{h_{00}} \simeq \vec{J}_0(1 + h_{00}) \tag{53}$$

in which $\vec{J}_0$ is constant. This implies that the "angular momentum" has a size that depends on h_{00}

$$J \equiv |\vec{J}| = |\vec{J}_0| e^{h_{00}} \equiv J_0 e^{h_{00}} \tag{54}$$

and a fixed direction

$$\hat{J} \equiv \frac{\vec{J}}{J} = \frac{\vec{J}_0}{J_0} \equiv \hat{J}_0. \tag{55}$$

We conveniently choose this direction to point in the z axis, hence,

$$\vec{J} = \vec{J}_0 e^{h_{00}} = J_0 e^{h_{00}} \hat{z}, \qquad J_x = J_y = 0. \tag{56}$$

Since the direction of $\vec{J}$ is fixed and perpendicular to the direction of both $\vec{r}$ and $\vec{u}$, it follows that both vectors lie in the $x - y$ plane. Thus we can conveniently describe their motion using the standard polar coordinates r, θ. We underline that unlike the angular momentum vector of classical mechanics this vector is only fixed in direction but not in size. We also underline that nowhere did we imply that the velocity of the particle must be small with respect to the velocity of light.

5.2. "Energy"

Let us make a scalar multiplication of equation (43) with $\vec{u}$ to obtain

$$\vec{u} \cdot \frac{d\vec{u}}{d\tau} = \vec{u}^2 \frac{dh_{00}}{d\tau} + \left(\frac{1}{2}c^2 - (u^0)^2\right) \vec{u} \cdot \vec{\nabla} h_{00}. \tag{57}$$

For a h_{00} without explicit time dependence we have

$$\frac{dh_{00}}{d\tau} = \vec{u} \cdot \vec{\nabla} h_{00} + \tilde{u}^0 \frac{\partial h_{00}}{\partial t} = \vec{u} \cdot \vec{\nabla} h_{00}. \tag{58}$$

It follows that

$$\frac{1}{2}\frac{d\vec{u}^2}{d\tau} = \left(\frac{1}{2}c^2 + \vec{u}^2 - (u^0)^2\right) \frac{dh_{00}}{d\tau}, \tag{59}$$

the term in parenthesis in the right-hand side needs only to be evaluated to zeroth order in h_{00} and this can be done using equation (40),

$$\frac{1}{2}\frac{d\vec{u}^2}{d\tau} = \left(\frac{1}{2}c^2 - c^2\right) \frac{dh_{00}}{d\tau} = -\frac{1}{2}c^2 \frac{dh_{00}}{d\tau} = -\frac{d\phi}{d\tau}, \tag{60}$$

54

in which we use the definition for the potential given in equation (33). Hence, we obtain the conserved "energy"

$$E \equiv \frac{1}{2}m\vec{u}^2 + m\phi \simeq \frac{1}{2}mv^2 + m\phi. \tag{61}$$

The "energy" is defined for either fast or slow bodies, while the right hand $\simeq$ relates only to slow bodies.

5.3. Polar coordinates

Introducing polar coordinates, we may write equation (49) and equation (61) as follows

$$E = \frac{1}{2}m\left[\dot{r}^2 + r^2\dot{\theta}^2\right] + m\phi, \qquad J = mr^2\dot{\theta}, \qquad \dot{r} \equiv \frac{dr}{d\tau}, \quad \dot{\theta} \equiv \frac{d\theta}{d\tau}. \tag{62}$$

The above forms seem quite classical, however, one should remember that the derivatives are with respect to the proper time of the body and not with respect to the global t coordinate. One should also recall that J is not constant and can vary to a small extent. Thus we eliminate $\dot{\theta}$ and obtain

$$E = \frac{1}{2}m\dot{r}^2 + \frac{J^2}{2mr^2} + m\phi = \frac{1}{2}m\dot{r}^2 + \frac{J_0^2 e^{2h_{00}}}{2mr^2} + m\phi \simeq \frac{1}{2}m\dot{r}^2 + \frac{J_0^2}{2mr^2} + m\phi + \frac{2J_0^2\phi}{mc^2r^2}. \tag{63}$$

The above result is quite classical except the last term which is a relativistic correction as is disclosed by the $\frac{1}{c^2}$ appearing there. To put the above result in a form which is closer to the forms which are found in the literature [12, 40] we make the following observation. We have written $d\vec{x}^2 = dr^2 + r^2\left(d\theta^2 + \sin^2\theta d\Phi^2\right)$ as is usually done for spherical coordinates. But notice that r in the above is not strictly a radial coordinate which is defined as the circumference, divided by 2π, of a sphere centered around the massive body. In fact from equation (28) it is clear that the appropriate radial coordinate is

$$r' = r\sqrt{1 - h_{00}} \tag{64}$$

which is a small correction to r. Now calculating the differential dr' it follows that

$$dr' = dr\sqrt{1 - h_{00}} + rd\sqrt{1 - h_{00}} = dr\frac{1 - h_{00} - \frac{1}{2}r\frac{dh_{00}}{dr}}{\sqrt{1 - h_{00}}}. \tag{65}$$

If we assume a Schwarzschild metric according to equation (13),

$$h_{00} = -\frac{r_s}{r'} = -\frac{r_s}{r\sqrt{1 - h_{00}}} \Rightarrow h_{00}\sqrt{1 - h_{00}} = -\frac{r_s}{r} \Rightarrow h_{00} = -\frac{r_s}{r}, \qquad r' \simeq r \gg r_s, \tag{66}$$

where the last equality is correct to first order. Alternatively one can use equation 32 to calculate the gravitational potential for a static point mass to obtain

$$\phi = -G\frac{M}{r} \tag{67}$$

and then plug this into equation (33) to obtain again

$$h_{00} = \frac{2}{c^2}\phi = -\frac{2GM}{c^2 r} = -\frac{r_s}{r}. \tag{68}$$

It now follows that

$$\frac{dh_{00}}{dr} = \frac{r_s}{r^2} = -\frac{h_{00}}{r}. \tag{69}$$

Plugging equation (69) into equation (65) leads to

$$dr' = dr\frac{1 - h_{00} - \frac{1}{2}r\frac{dh_{00}}{dr}}{\sqrt{1 - h_{00}}} = dr\frac{1 - \frac{1}{2}h_{00}}{\sqrt{1 - h_{00}}}. \tag{70}$$

Hence, to first order in h_{00},

$$dr' = dr. \tag{71}$$

Using the results equation (64) and equation (71), the interval given in equation (28) can be rewritten as

$$\begin{aligned} ds^2 &= (1 + h_{00})c^2 dt^2 - (1 - h_{00})d\vec{x}^2 \\ &= (1 + h_{00})c^2 dt^2 - (1 - h_{00})dr'^2 - r'^2 \left(d\theta^2 + \sin^2\theta d\phi^2\right). \end{aligned} \tag{72}$$

As to first order in h_{00}

$$1 - h_{00} = \frac{1}{1 + h_{00}}, \tag{73}$$

and taking into account equation (13) we obtain

$$ds^2 = (1 - \frac{r_s}{r'})c^2 dt^2 - (1 - \frac{r_s}{r'})^{-1}dr'^2 - r'^2 \left(d\theta^2 + \sin^2\theta d\phi^2\right) = ds^2_{\text{Schwarzschild}}. \tag{74}$$

Thus to first order our metric is identical to Schwarzschild's for the case of a static point particle. This makes our analysis superior as it addresses the case of a general density distribution and does not ignore the possibility of time dependence which is crucial for retardation effects to take place.

In terms of r' we may write the energy as

$$\begin{aligned} E &= \frac{1}{2}m\dot{r}'^2 + \frac{J_0^2 e^{2h_{00}}}{2mr'^2}(1 - h_{00}) + m\phi = \frac{1}{2}m\dot{r}'^2 + \frac{J_0^2}{2mr'^2}(1 + h_{00}) + m\phi \\ &= \frac{1}{2}m\dot{r}'^2 + \frac{J_0^2}{2mr'^2} + m\phi + \frac{J_0^2\phi}{mc^2 r'^2} = \frac{1}{2}m\dot{r}'^2 + \frac{J_0^2}{2mr'^2} - \frac{GMm}{r'} - \frac{GMJ_0^2\phi}{mc^2 r'^3}. \end{aligned} \tag{75}$$

The relativistic correction has a $\frac{1}{r'^3}$ dependence and the is greater the more the object is close to the gravitating point mass which represents the Sun. We also notice that in terms of r' one may write up to first order in h_{00},

$$J_0 = mr'^2\dot{\theta} \tag{76}$$

which is reminiscent of the well-known classical result regrading the conservation of angular momentum.

5.4. Integration of the equations of motion

Using equation (76), we may write

$$\dot{r}' = \dot{\theta}\frac{dr'}{d\theta} = \frac{J_0}{mr'^2}\frac{dr'}{d\theta}. \tag{77}$$

Defining[2]

$$u' \equiv \frac{1}{r'} \Rightarrow \dot{r}' = -\frac{J_0}{m}\frac{du'}{d\theta}. \tag{78}$$

Plugging equation (78) into equation (75), we arrive at the result

$$\tilde{E} \equiv \frac{2mE}{J_0^2} = \left(\frac{du'}{d\theta}\right)^2 + u'^2 - \frac{2GMm^2}{J_0^2}u' - \frac{2GM}{c^2}u'^3, \tag{79}$$

or

$$\left(\frac{du'}{d\theta}\right)^2 = \tilde{E} - u'^2 + \frac{2GMm^2}{J_0^2}u' + \frac{2GM}{c^2}u'^3. \tag{80}$$

Which is exactly Padmanabhan [12] equation 7.114 (page 318), with a slightly different notation

$$L_{\text{Padmanabhan}} = J_0, \qquad \varepsilon_{\text{Padmanabhan}} = mc^2\sqrt{1 + 2\frac{E}{mc^2}}. \tag{81}$$

The analysis of Padmanabhan [12] of equation (80) leads to equation (1) and will not be repeated here due to lack of space. The interested reader is referred to the original text. We only mention that the semi-major axis can be calculated by

$$a = \frac{J_0^2}{GM(1 - e_{\text{eccentricity}}^2)m^2} \tag{82}$$

and the eccentricity can be calculated as:

$$e_{eccentricity} = \sqrt{1 + \frac{2E_N J_0^2}{G^2 M^2 m^3}}, \qquad E_N \equiv \varepsilon_{\text{Padmanabhan}} - mc^2. \tag{83}$$

Recently Křížek [2] has commented regarding the uncertainties related the approximation needed in order to derive equation (1) from equation (80). The integration of equation (80) involves elliptic functions, and the derivation of equation (1) is not exact but involves approximations to those integrals, thus errors are introduced which should be accounted for.

---

[2]The symbol u' has nothing to do with the previously defined u^ν and is chosen this way in order to comply with the symbol used in the literature [12].

6. Metric correction and the gravitational potential

So far we have considered only a naive model in which the Sun was taken to be a static point particle in the inertial frame, this has led us from equation (67) to equation (1). However, we can certainly do better, as it is well known that equation (32) can be integrated for a particle p of mass M_p moving in an arbitrary trajectory with velocity $\vec{v}_p(t)$, resulting in a Liénard-Wiechert potential [46], [47], [41],

$$
\phi_{LWp} = -\frac{GM_p}{R_p(1 - \hat{R}_p \cdot \vec{\beta}_p)}\bigg|_{t_{rp}}, \quad \hat{R}_p = \frac{\vec{R}_p}{R_p}, \quad t_{rp} = t - \frac{R_p(t_{rp})}{c}, \quad R_p(t) = |\vec{x} - \vec{x}_p(t)|.
$$
(84)

The peculiar thing about this equation is that it must be evaluated at a retarded time t_{rp} which is only given in terms of an implicit equation. This equation requires a knowledge of the evaluation point of the potential and the knowledge of the particles trajectory for its solution, which is highly inconvenient. The derivative of the global time coordinate t with respect to the particular retardation time related to a certain particle is

$$
\frac{dt}{dt_{rp}} = \frac{1}{1 - \hat{R}_p \cdot \vec{\beta}_p}\bigg|_{t_{rp}} \simeq 1.
$$
(85)

Which implies that for a slow moving particle with $\beta_p \ll 1$ we arrive at the classical gravitational potential

$$
\phi_{LWp} \simeq \phi_p = -\frac{GM_p}{R_p(t)}.
$$
(86)

If many slow moving bodies affect a particular body, this body will move under the influence of a potential

$$
\phi = \sum_{p=1}^{N} \phi_p = -\sum_{p=1}^{N} \frac{GM_p}{R_p(t)}.
$$
(87)

This is essentially Křížek's [1] equation (7) (given in terms of potential rather than force). In the Mercury case the most dominant body influencing its trajectory is the Sun which is much more massive than the other planets in the Solar system, thus to a zeroth order approximation we can ignore the other planets altogether. However, for more subtle effects such as the precession of the perihelion for Mercury they cannot be ignored. Indeed most of the precession can be attributed to the effect of the various planets as is indicate in the first row of Table 1, see [10], [11]. Křížek's [1] has correctly criticized the lack of any error bar to this number which must result from the uncertainty in the other planet masses and trajectories. This should be contrasted with the uncertainty attributed to the observed precession of the perihelion for Mercury in the same table.

As indicated previously relativistic corrections in equation (84) are only relevant for fast moving bodies with a considerable β. The highest β in the Solar system is for Mercury itself with $v \simeq 47.36 \cdot 10^3$ km/s yielding a $\beta \simeq 1.6 \cdot 10^{-4}$. However, the

highest velocity among the other planets affecting, Mercury's orbit is Venus, with $v \simeq 35.0 \cdot 10^3$ km/s yielding a $\beta \simeq 1.2 \cdot 10^{-4}$. Thus the relativistic corrections are small corrections to the contribution the other planets make to the gravitational potential experienced by Mercury, those contributions are quite small even before a relativistic correction is applied. It thus remains to analyze the corrections to the gravitational potential of the Sun.

The Schwarzschild based analysis, as well as the one presented in the previous sections assumes that the Sun is static and is located at the origin of axes. The Liénard-Wiechert potential described above allows us to take into account various corrections to the above simplified assumptions. The Sun need not be located at the origin of axis, and it can be moving with respect to the inertial frame. The motion of the Sun as well as the time gravity propagates from the Sun to Mercury all affect the gravitational potential. All those effects are small but not necessarily of the same magnitude, hence we need to evaluate there relative strengths.

Classical mechanics teaches us that a frame in which the Sun is located at the origin of axis is not inertial. A classical system which is inertial is one in which the origin of axis is located at the center of mass. This is only true in classical mechanics, however, the relativistic engine effect described in [48], [49], [50], [51], [52], [53], [54] shows that the relativistic retardation phenomena may cause even the center of mass to accelerate, and thus cannot be used in strictly fixing an inertial frame.

Never the less, we shall assume for now that the center of mass does define an inertial frame and discuss the effect of the motion of the Sun with respect to it. The velocity of the Sun from the center of mass is estimated to be $v \simeq 11$ m/s, see [55], yielding a $\beta \simeq 3.7 \cdot 10^{-8}$. The difference between the potential $\phi_{LW\text{sun}}$ and the potential ϕ given in equation (67) is defined as

$$\Delta\phi \equiv \phi_{LW\text{sun}} - \phi, \qquad \phi_{LW\text{sun}} = \phi + \Delta\phi. \tag{88}$$

The difference can be written in terms of three terms

$$\Delta\phi = \Delta\phi_\beta + \Delta\phi_{tr} + \Delta\phi_d,$$
$$\Delta\phi_d = -GM_{\text{sun}}\left(\frac{1}{R_{\text{sun}}(t)} - \frac{1}{r}\right), \qquad R_{\text{sun}}(t) = |\vec{x} - \vec{x}_{\text{sun}}(t)|,$$
$$\Delta\phi_{tr} = -GM_{\text{sun}}\left(\frac{1}{R_{\text{sun}}(t_r)} - \frac{1}{R_{\text{sun}}(t)}\right), \qquad t_r = t - \frac{R_{\text{sun}}(t_r)}{c},$$
$$\Delta\phi_\beta = -GM_{\text{sun}}\left(\frac{1}{(1 - \hat{R}_{\text{sun}}(t_r) \cdot \vec{\beta}_{\text{sun}}(t_r))R_{\text{sun}}(t_r)} - \frac{1}{R_{\text{sun}}(t_r)}\right). \tag{89}$$

Those terms can be approximated to first order as follows

$$\Delta\phi_d \simeq -\phi\,(\hat{x} \cdot \hat{x}_{\text{sun}})\frac{x_{\text{sun}}}{r}, \qquad \hat{x} \equiv \frac{\vec{x}}{|\vec{x}|} = \frac{\vec{x}}{r}, \quad \hat{x}_{\text{sun}} \equiv \frac{\vec{x}_{\text{sun}}}{|\vec{x}_{\text{sun}}|},$$
$$\Delta\phi_{tr} = -\Delta\phi_\beta = \phi\,(\hat{x} \cdot \vec{\beta}_{\text{sun}}), \tag{90}$$

59

where the equality holds only to first order. It is apparent that $\Delta\phi_{tr}$ and $\Delta\phi_\beta$ cancel each other to first order in β as expected, while second order corrections in β are negligible. Thus we may write a more accurate potential due to the Sun as

$$\phi_{LW\text{sun}} = \phi\left(1 - (\hat{x}\cdot\hat{x}_{\text{sun}})\frac{x_{\text{sun}}}{r}\right), \tag{91}$$

where the equality holds only to first order. Taking into account the distance of the Sun from the barycenter (see Figure 3 of Křížek [1]) it follows that it of the order of the Sun's diameter, while the exact trajectory of the Sun with respect to the Solar system barycenter is quite complex. Thus

$$\frac{x_{\text{sun}}}{r} \simeq \frac{2\ \text{Sun}\ \ \text{Radius}}{\text{Mercury Perihelion}} \simeq 2\frac{6.96\cdot 10^8}{4.60\cdot 10^{10}} \simeq 3\%. \tag{92}$$

The analytical approach described above is not useful for calculating the trajectory in the presence of the $\Delta\phi$ potential correction. As now the potential depends on time and thus the energy is not strictly conserved, moreover, the potential depends on the polar angle and thus angular momentum is not conserved in an exact sense. Thus it seems best to integrate the equations numerically, however, this is beyond the scope of the present paper. A crude model that can accommodate the present approach would be to replace the Sun's mass with an effective mass

$$\phi_{LW\text{sun}} = -\frac{GM_{\text{eff}}}{r}, \qquad M_{\text{eff}} \equiv M_{\text{sun}}(1 \pm 0.03). \tag{93}$$

Thus the anomalous perihelion shift is not the value given by equation (1) but rather by

$$\delta\theta = \frac{6\pi GM_{\text{eff}}}{ac^2\left(1-e^2\right)}, \tag{94}$$

for Mercury the semi-major axis is $a \simeq 57.909\cdot 10^6$ km and the eccentricity is $e \simeq 0.2056$ thus:

$$\delta\theta = 43"/\text{cy} \pm 1.3"/\text{cy}. \tag{95}$$

Thus the calculated value can be easily put within the error bar of the observed value as we recall that the discrepancy is only about 0.56" per century. Other uncertainties may arise regarding the Newtonian contributions of the other planets to the gravitational potential [1].

7. Conclusions

We have shown that one can solve the Mercury trajectory problem using the weak gravitational approximation to GR and without using the Schwarzschild metric. This is contrary to the claims that this problem can only be solved in the framework of strong gravity [12]. In fact it can easily be seen that the weak gravity approximation will suffice anywhere in the Solar system, and Mercury is no exception to this rule.

We have presented a solution to the current discrepancy between the observed and calculated perihelion shift although the solution is crude and numerical simulations may reveal more details.

The weak field approximation takes in account retardation, however, the retardation correction is of order β^2 as should be expected and is thus unimportant in the Mercury trajectory problem, certainly comparing to the corrections related to the motion of the center of the Sun with respect to the barycenter of the Solar system. In this respect the Mercury perihelion problem is quite different than the "dark matter" problem, although the weak gravity approach can handle them both.

References

[1] Křížek, M.: Influence of celestial parameters on Mercury's perihelion shift. Bulg. Astron. J. *27* (2017), 41–56.

[2] Křížek, M.: Relativistic perihelion shift of Mercury revisited. Astron. Nachr. *343* (2022), e20220016, 1–7.

[3] Weinstein, G.: Einstein and the problem of confirmation by previously known evidence: A comment on Michel Janssen and Jurgen Renns Einstein and the Perihelion Motion of Mercury (2022), 1–16, arXiv: 2201.00807v1.

[4] Le Verrier, U.: Lettre de M. Le Verrier à M. Faye sur la théorie de Mercure et sur le mouvement du périhélie de cette planète. Comptes rendus hebdomadaires des séances de l'Académie des sciences (Paris) *49* (1859), 379–383.

[5] Carter, B. Carter, M.S.: Simon Newcomb, America's first great astronomer. Physics Today, *62 (2)* (February 2009), 46, doi:10.1063/1.3086102.

[6] Levenson, T.: The hunt for vulcan. And how Albert Einstein destroyed a planet, discovered relativity, and deciphered the Universe. Random House Publishing Group (2015), 80.

[7] Baum, R. P., Sheehan, W.: In search of planet vulcan: the ghost in Newton's Clockwork. Basic Books (2003).

[8] Einstein, A.: The foundation of the general theory of relativity. Ann. Phys. *49 (7)* (1916), 769–822.

[9] Einstein, A.: Näherungsweise Integration der Feldgleichungen der Gravitation. Sitzungsberichte der Königlich Preussischen Akademie der Wissenschaften Berlin, Part 1. The Prusssian Academy of Sciences, Berlin, Germany, (1916) 688–696.

[10] Clemence, G. M.: The relativity effect in planetary motions. Rev. Modern Phys. *19 (4)* (1947), 361–364.

[11] Park, R. S. et al.: Precession of Mercury's perihelion from ranging to the MESSENGER Spacecraft. Astron. J. *153 (3)* (2017), 121.

[12] Padmanabhan, T.: Gravitation – foundations and frontiers. Cambridge University Press (2010).

[13] Biswas, A., Mani, K. R. S.: Relativistic perihelion precession of orbits of Venus and the Earth. Cent. Eur. J. Phys. *6 (3)* (2008) 754–758.

[14] Milgrom, M.: A modification of the Newtonian dynamics as a possible alternative to the hidden mass hypothesis. Astrophys. J. *270* (1983), 365-–370, doi:10.1086/161130.

[15] Mannheim, P. D., Kazanas, D.: Exact vacuum solution to conformal Weyl gravity and galactic rotation curves. Astrophys. J. *342* (1989), 635.

[16] Mannheim, P. D.: Linear potentials and galactic rotation curves. Astrophys. J. *149* (1993), 150.

[17] Mannheim, P. D.: Are galactic rotation curves really flat? Astrophys. J. *479* (1997), 659.

[18] Moffat, J. W.: Scalar-tensor-vector gravity theory. J. Cosmology and Astroparticle Physics. *3* (2006), 4, arXiv:gr-qc/0506021.

[19] Corda, C.: Interferometric detection of gravitational waves: the definitive test for general relativity. Int. J. Mod. Phys. *D 18* (2009), 2275, arXiv:0905.2502.

[20] Zwicky, F.: On a new cluster of nebulae in pisces. Proc. Natl. Acad. Sci. USA *23*, (1937), 251-–256.

[21] Volders, L. M. J. S.: Neutral hydrogen in M33 and M101. Bull. Astr. Inst. Netherl. *14* (1959), 323.

[22] Rubin, V. C., Ford, W. K., Jr.: Rotation of the Andromeda Nebula from a spectroscopic survey of emission regions. Astrophys. J. *159* (1970), 379.

[23] Rubin, V. C., Ford, W. K., Jr.: Thonnard, N.: Rotational properties of 21 Sc Galaxies with a large range of luminosities and radii from NGC 4605 (R = 4 kpc) to UGC 2885 (R = 122 kpc). Astrophys. J. *238* (1980), 471.

[24] Yahalom, A.: The effect of Retardation on Galactic rotation curves. J. Phys. Conf. Ser. 1239 (2019) 012006.

[25] Yahalom, A.: Retardation effects in electromagnetism and gravitation. In Proceedings of the Material Technologies and Modeling the Tenth International Conference, Ariel University, Ariel, Israel, 20–24 August 2018, arXiv:1507.02897v2.

[26] Yahalom, A.: Dark matter: reality or a relativistic illusion? In Proceedings of Eighteenth Israeli-Russian Bi-National Workshop 2019, The Optimization of Composition, Structure and Properties of Metals, Oxides, Composites, Nano and Amorphous Materials, Ein Bokek, Israel, 17–22 February 2019.

[27] Wagman, M.: Retardation theory in Galaxies. Ph.D. Thesis, Senate of Ariel University, Samria, Israel, 23 September 2019.

[28] Yahalom, A.: Lorentz symmetry group, retardation, intergalactic mass depletion and mechanisms leading to Galactic rotation curves. Symmetry *12(10)* (2020), 1693, https://doi.org/10.3390/sym12101693

[29] Yahalom A.: Effects of higher order retarded gravity. Universe *7(7)* (2021), 207. https://doi.org/10.3390/universe7070207, https://arxiv.org/abs/2108.08246

[30] Yahalom, A.: The cosmological decrease of galactic density and the induced retarded gravity effect on rotation curves. Proceedings of IARD 2020, J. Phys.(2021), Conf. Ser. 1956 012002.

[31] Yahalom, A.: Tully-Fisher relations and retardation theory for Galaxies. International Journal of Modern Physics D, (2021), Volume No. 30, Issue No. 14, Article No. 2142008 (8 pages). World Scientific Publishing Company. https://doi.org/10.1142/S0218271821420086, https://arxiv.org/abs/2110.05935.

[32] Yahalom, A.: Lensing effects in retarded gravity. Symmetry 2021, 13, 1062. https://doi.org/10.3390/sym13061062, https://arxiv.org/abs/2108.04683.

[33] Sauer, T.: Nova Geminorum 1912 and the origin of the idea of gravitational lensing. Archive for History of Exact Sciences *62 (1)* (2008), 1–22, arXiv:0704.0963. doi:10.1007/s00407-007-0008-4. S2CID 17384823.

[34] Pais, A.: 'Subtle is the Lord ...' The science and life of Albert Einstein. Oxford University Press (1982), ISBN 978-0-19-853907-0.

[35] Dyson, F. W., Eddington, A. S., Davidson, C. R.: A determination of the deflection of light by the Sun's gravitational field, from observations made at the Solar eclipse of May 29, 1919. Phil. Trans. Roy. Soc. A. *220* (1920), 291–333.

[36] Kennefick, D.: Not only because of theory: Dyson, Eddington and the competing myths of the 1919 Eclipse expedition. Proceedings of the 7th Conference on the History of General Relativity, Tenerife, 2005, 0709, (2007), 685.

[37] Narlikar, J. V.: Introduction to cosmology, 2nd ed. Cambridge University Press: Cambridge, UK, 1993.

[38] Eddington, A. S.: The mathematical theory of relativity. Cambridge University Press, Cambridge, UK, 1923.

[39] Weinberg, S.: Gravitation and cosmology: principles and applications of the general theory of relativity. John Wiley & Sons, Inc., Hoboken, NJ, USA, 1972.

[40] Misner, C. W., Thorne, K. S., Wheeler, J. A.: Gravitation. W. H. Freeman & Company, New York, NY, USA, 1973.

[41] Jackson, J. D.: Classical electrodynamics, 3rd ed. Wiley, New York, NY, USA, 1999.

[42] Yahalom, A.: The geometrical meaning of time. Found. Phys. *38* (2008), 489–497.

[43] Yahalom, A.: The gravitational origin of the distinction between space and time. Int. J. Mod. Phys. D *18* (2009), 2155–2158.

[44] Corbelli, E.: Dark matter and visible baryons in M33. Mon. Not. Roy. Astron. Soc. *342* (2003), 199–207, doi:10.1046/j.1365-8711.2003.06531.x.

[45] Goldstein, H., Poole, Jr., C. P., Safko, J. L.: Classical mechanics, 3rd Edition. (2002), Pearson.

[46] Liénard, A.: Champ électrique et magnétique produit parune charge concentrée en un point et animée d'un mouvement quelconque, L'éclairage Electrique' 16 p.5; ibid. p. 53; ibid. p. 106 (1898).

[47] Wiechert, E.: Elektrodynamische elementargesetze. Annalen der Physik *309 (4)* (1901), 667–689.

[48] Tuval, M., Yahalom, A.: Newton's third law in the framework of special relativity. Eur. Phys. J. Plus *129* (11 Nov 2014), 240. (arXiv:1302.2537 [physics.gen-ph]).

[49] Yahalom, A.: Retardation in special relativity and the design of a relativistic motor. Acta Physica Polonica A *131 (5)* (2017), 1285–1288.

[50] Tuval, M., Yahalom, A.: Momentum conservation in a relativistic engine. Eur. Phys. J. Plus *131* (2016): 374.

[51] Yahalom, A.: Preliminary energy considerations in a relativistic engine. Proceedings of the Israeli-Russian Bi-National Workshop The optimization of composition, structure and properties of metals, oxides, composites, nano - and amorphous materials, page 203–213, 28–31 August 2017, Ariel, Israel.

[52] Rajput, S., Yahalom, A.: Material engineering and design of a relativistic engine: how to avoid radiation losses. Advanced Engineering Forum ISSN: 2234-991X *36*, 126–131. Submitted: 2019-06-16, Accepted: 2020-05-18, Online: 2020-06-17. 2020 Trans. Tech. Publications Ltd, Switzerland.

[53] Rajput, S., Yahalom, A., Qin, H.: Lorentz symmetry group. Retardation and Energy Transformations in a Relativistic Engine, Symmetry 13 (2021), 420. https://doi.org/10.3390/sym13030420.

[54] Rajput, S. Yahalom, A.: Newton's third law in the framework of special relativity for charged bodies. Symmetry *13 (7)* (2021), 1250. https://doi.org/10.3390/sym13071250

[55] Wright, J. T., Kanodia, S.: Barycentric corrections for precise radial velocity measurements of sunlight planet. Sci. J. *1* (2020), 38.

IN A HOLISTIC PERSPECTIVE EVERYTHING
IN SPACE IS INTERCONNECTED

Tuomo Suntola

Physics Foundations Society, https:www.physicsfoundations.org
Espoo, Finland
tuomo.suntola@gmail.com

Abstract: Description of space as the 3D surface of a 4D ball allows a dynamic solution to the cosmological development of space and opens the linkage between local structures and space as a whole. In such a holistic perspective, all velocities in space are linked to the 4D velocity of space and the expansion of local gravitationally bound structures to the expansion of the spherical structure. Space works as a spherical pendulum: Mass in space has gained its rest energy as the energy of motion against the release of gravitational energy in a contraction phase and pays it back to gravitational energy in the ongoing expansion phase. Following the zero-energy principle, local structures in space are formed against release of the global gravitational energy via local tilting of space resulting in a system of nested energy frames that relates all energy states in space to the state of rest in hypothetical homogeneous space. The zero-energy approach referred to as the Dynamic Universe (DU) model [1], honors time and distance as universal coordinate quantities. Local gravitational systems expand in direct proportion to the expansion of space. Atomic clocks in motion or at a lowered gravitational potential run slower due to their different energy state, the state of motion and gravitation. DU produces precise, parameter-free predictions for cosmological observables and local physical phenomena in full agreement with observations and allows an understandable picture of the physical reality. Mass appears as the wavelike substance for the expression of energy and Mach's principle obtains a quantitative expression as the work an accelerating object does against the global gravitation arising from the rest of space.

Keywords: cosmology, relativity, philosophy of science, unifying theory

PACS: 01.30.Cc, 95.30.Sf, 98.80.-k, 98.80.Bp, 98.80.Es, 98.80.Jk

1. Introduction

A primary challenge of natural sciences in the new millennium is to cure the gap between metaphysics and empiricism – and puzzle out the obstacles to a unified theory and an understandable picture of reality. Antique science flourished via its strong

philosophical impact but faded away due to the lack of supporting empirical science. The fast development of mathematical physics has led to the opposite; theories are diversified, they are more like mathematical descriptions of observations; they provide precise predictions but lack a solid metaphysical basis and an understandable picture of reality. Modern science has increased our understanding of physics from elementary particles to cosmological structures and produced information that allows re-evaluation of the basis. By switching from the observer-oriented perspective of the theory of relativity to a system-oriented perspective, relativity is expressed in terms of locally available energy – without scarifying absolute time and distance as central base units in physics and coordinate quantities essential for human comprehension. Such a holistic perspective is obtained by describing the 3D space as the surface of a 4D ball with the energies of motion and gravitation in balance. For maintaining the zero-energy balance of motion and gravitation, local phenomena are linked to the rest of space; motion in space is linked to the motion of space in the fourth dimension, and local gravitation is linked to the gravitation arising from space as a whole. Relativity is a direct consequence of the conservation of the overall zero-energy balance in the system. The buildup of local kinetic energy in space is counterbalanced by a reduction in the rest energy of the object in motion which results in a reduction of the characteristic frequency of atomic oscillators. Close to mass centers in space, local bending of space reduces the local velocity of light and locally available rest energy observed, e.g., as the gravitational shift of clock frequencies. There is no need for distorted time and distance needed in the kinematic solution of relativity. In the holistic perspective, relativity is relativity between a local and the whole rather than relativity between an object and the observer. Everything in space is interconnected.

2. Energy buildup in space

Global gravitational energy

The gravitational energy of mass m in spherically closed space is expressed in terms of the mass equivalence $M'' = 0.776 \cdot M_\Sigma$ at the center of the 4D ball closing space, Fig. 1. It is obtained by integrating the gravitational energy in homogeneous space,

$$E_{g(m)} = -\frac{2}{\pi} \frac{GmM_\Sigma}{R_4} \int\limits_0^\pi \frac{\sin^2\theta}{\theta} \, d\theta = -\frac{0.776 \cdot GmM_\Sigma}{R_4} = -\frac{GmM''}{R_4}, \qquad (1)$$

where $G = 6.67 \cdot 10^{-11}$ [Nm^2/kg^2] is the gravitational constant, R_4 the 4-radius of space, $M_\Sigma = \Sigma m$ the total mass in space, and M'' the mass equivalence at the 4-center of space.

The dynamic zero-energy balance

The primary energy buildup is described as a contraction-expansion process of spherically closed space. The rest energy appears as the energy of motion obtained against the release of gravitational energy in the contraction of spherical space towards sin-
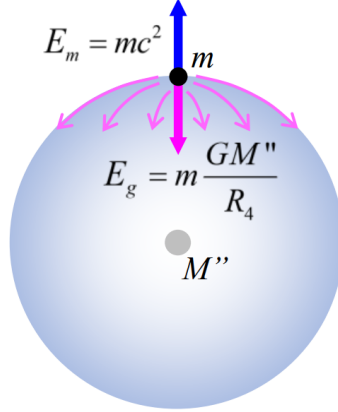
Figure 1: The dynamics of spherically closed space is determined by the balance between the energies of gravitation and motion. The rest energy of a local object is counterbalanced by the gravitational energy arising from the rest of space. The gravitational energy of mass m due to the rest of space is expressed as the effect of the mass equivalence M'' representing the total mass M_Σ at the 4-center of space.

gularity; in the ongoing expansion phase, the energy of motion is paid back to gravitational energy. Such an interpretation assumes a metric fourth dimension, representing the direction of the 4-radius of space and time as a universal scalar allowing the study of velocity and momentum equally in the three space directions and in the fourth dimension. Applying the zero-energy principle, the sum of the total gravitational energy and the total energy of motion, expressed as $E = c|\mathbf{p}|$ in the fourth dimension, the direction of the 4-radius, is zero, Fig. 2,

$$E_m + E_g = M_\Sigma c_0^2 - \frac{GM_\Sigma M''}{R_4} = 0. \tag{2}$$

As a demand of the zero-energy balance, the maximum velocity in space is equal to the velocity of space in the fourth dimension,

$$c_0 = \pm\sqrt{GM''/R_4} \approx 300\,000\,[\text{km/s}]. \tag{3}$$

The current estimate for today's 4-radius $R_4 \approx 13.7 \cdot 10^9$ [ly], resulting in $M_\Sigma \approx 2.3 \cdot 10^{53}$ [kg] and the average mass density $\rho \approx 5 \cdot 10^{-27}$ [kg/m^3] which is the Friedmann critical mass density equivalence in DU framework. The buildup of the rest energy in the pre-singularity contraction phase cancels the assumed instant Big Bang event of the standard model of cosmology (SC). The singularity in DU is a state of extreme excitation of the energies of gravitation and motion, followed by the turn to expansion at extreme velocity (like the inflation in SC) which has gradually slowed down to the present velocity of light. The deceleration rate of the present velocity of light is $dc_4/c_4 \approx -3.6 \cdot 10^{-11}$/year. Such a change is observable only indirectly
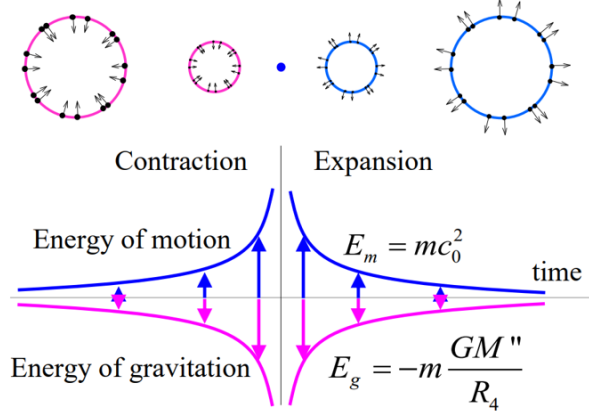
Figure 2: The buildup and release of the rest energy of matter as the energy of motion via contraction and expansion of spherically closed space.

because the frequency of atomic clocks and the rate of physical processes, in general, are directly proportional to the velocity of light.

Buildup of local structures in space

For conserving the balance of the energies of gravitation and motion in a local mass center buildup, the total gravitational energy is divided, via tilting of local space, into orthogonal components with the local gravitational energy in the local space direction and the reduced global gravitational energy in the local fourth dimension. The velocity of free fall, v_{ff}, of mass m is obtained against the reduction of the velocity of space in the fourth dimension, and the corresponding kinetic energy against the release of the rest energy of the falling object and the release of local gravitational energy related to the reduction of the global gravitational energy

$$E_{\text{kin}} = \Delta E_g = E_{g(0)} \left(1 - \cos\varphi\right) = \frac{GMm}{R}, \tag{4}$$

where φ is the tilting angle of local space at distance R from mass center M, Fig. 3.

The local gravitational state is characterized by the gravitational factor δ, the ratio of the local gravitational energy and the global gravitational energy

$$\delta = \frac{GMm/R}{GM''m/R_4} = \frac{\Delta E_g}{E_{g(0)}} = 1 - \cos\varphi = \frac{GM}{c_0^2 R}, \tag{5}$$

where the last form is obtained by applying equation (3). As illustrated in Fig. 3, the velocity of space in the local fourth dimension, determining the local velocity of light, c, at gravitational state δ is

$$c = c_0 \cos\varphi = c_0(1 - \delta). \tag{6}$$

Any motion and momentum in space is associated with the motion and momentum of space in the local fourth dimension as orthogonal components. Using
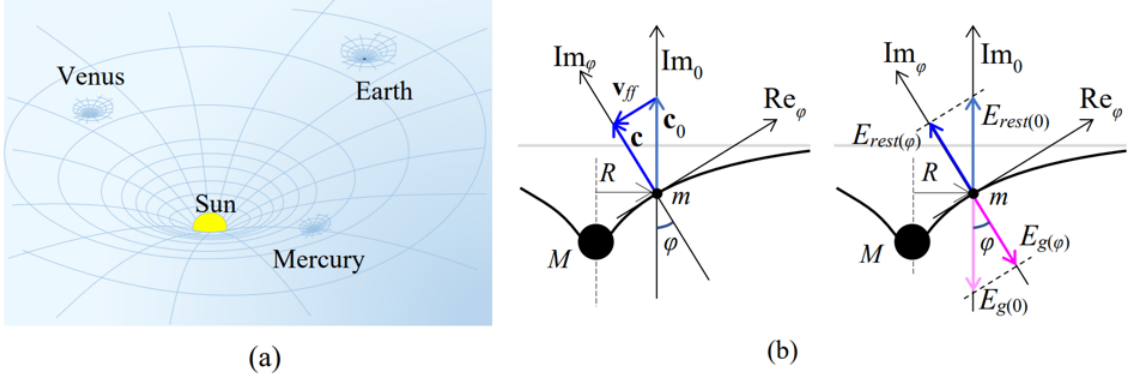
69

Figure 3: (a) The overall energy balance in space is conserved via tilting of space in local mass center buildup creating the kinetic energy of free fall and the local gravitational energy. (b) Due to the tilting, the velocity of free fall, $\mathbf{v}_{ff}$, is obtained against a reduction of the velocity of space in the local fourth dimension.

a complex quantity notation, with i as the imaginary unit, the quantity in the fourth dimension as the imaginary part, and the quantity in a space direction as the real part, the total momentum of mass m moving at velocity $\beta = v/c$ in space is

$$p_{\text{total}} = |\mathbf{p} + \mathbf{i}\, mc| = \sqrt{p^2 + (mc)^2} \tag{7}$$

and the total energy of motion

$$E_{m(\text{total})} = c_0 |\mathbf{p} + \mathbf{i}\, mc| = c_0 \sqrt{p^2 + (mc)^2}, \tag{8}$$

which is formally identical to the corresponding equation in special relativity.

As illustrated in Fig. 4, the buildup of momentum in space is counterbalanced with a reduction of the rest momentum p_{Im} of the moving object

$$p_{\text{Im}}(\beta) = p_{\text{Im}}(0)\sqrt{1 - \beta^2} \tag{9}$$

which means that the rest energy of an object moving at velocity β is reduced as

$$E_{\text{rest}(\beta)} = c_0 |p_{\text{Im}}(0)| = E_{\text{rest}(0)} \sqrt{1 - \beta^2}. \tag{10}$$

Combining the effect of the gravitational state on the local velocity of light, the rest energy of mass m moving at velocity $\beta = v/c$ at gravitational state δ is

$$E_{\text{rest}(\delta,\beta)} = E_{\text{rest}(0,0)}(1 - \delta)\sqrt{1 - \beta^2}. \tag{11}$$

The system of nested energy frames

Mass center buildup occurs in several steps; dents around planets are dents in the larger dent around the Sun – which is a local dent in the much larger Milky Way dent. The energy structure of space can be illustrated as a system of nested energy frames extending from hypothetical homogeneous space to any local structure, Fig. 5. In each step, the energy available in a subframe formed is reduced.
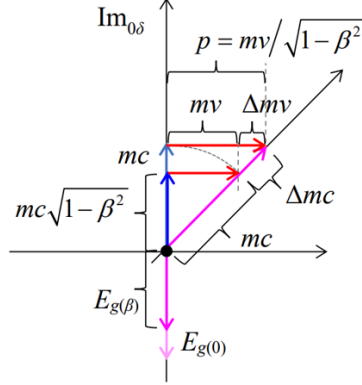
Figure 4: In DU space, buildup of velocity v at constant gravitational potential requires insertion of the energy $c_0 \Delta mc$ which results in the total energy $E_{\text{tot}} = c_0 (m + \Delta m) c$, and momentum $\mathbf{p} = (m + \Delta m)\mathbf{v}$ in the direction of the real axis (in a space direction)

.

3. Relativity in DU framework

In DU, relativity is a direct consequence of the conservation of the zero-energy balance in space. The quantum mechanical solution of the frequency of atomic oscillators is

$$f = \frac{E_{e(\text{rest})}}{h} F\left[\alpha, \Delta\left(n, j\right)\right], \tag{12}$$

where $E_{e(\text{rest})}$ is the rest energy of the oscillating electrons, α is the fine structure constant, and $\Delta(n, j)$ gives the difference of the quantum states related to the oscillation. In the DU framework, the rest energy is a function of the local state of motion and gravitation as given in equation (11) which means that, in a local frame, the frequency of a clock moving at velocity β at gravitational potential δ is

$$f = f_0 \left(1 - \delta\right) \sqrt{1 - \beta^2}, \tag{13}$$

where f_0 is the frequency of the clock in the parent frame of the local energy frame. Equation (13) is the DU replacement of Schwarzschild's equation for the time dilation in general relativity

$$dt = dt_0 \sqrt{1 - 2\delta - \beta^2}. \tag{14}$$

In the Earth's gravitational frame, the difference between equations (13) and (14) appears only in the 18th to 20th decimal.

In DU space, the local velocity of light is locked to the local 4D velocity of space. Bending of the light path passing a mass center as well as the Shapiro delay are direct consequences of the slower velocity of light and the increased distance due to the dent around a mass center. The motion of a mass center in its parent frame, like the Earth in the solar gravitational frame draws the local dent with the motion thus conserving
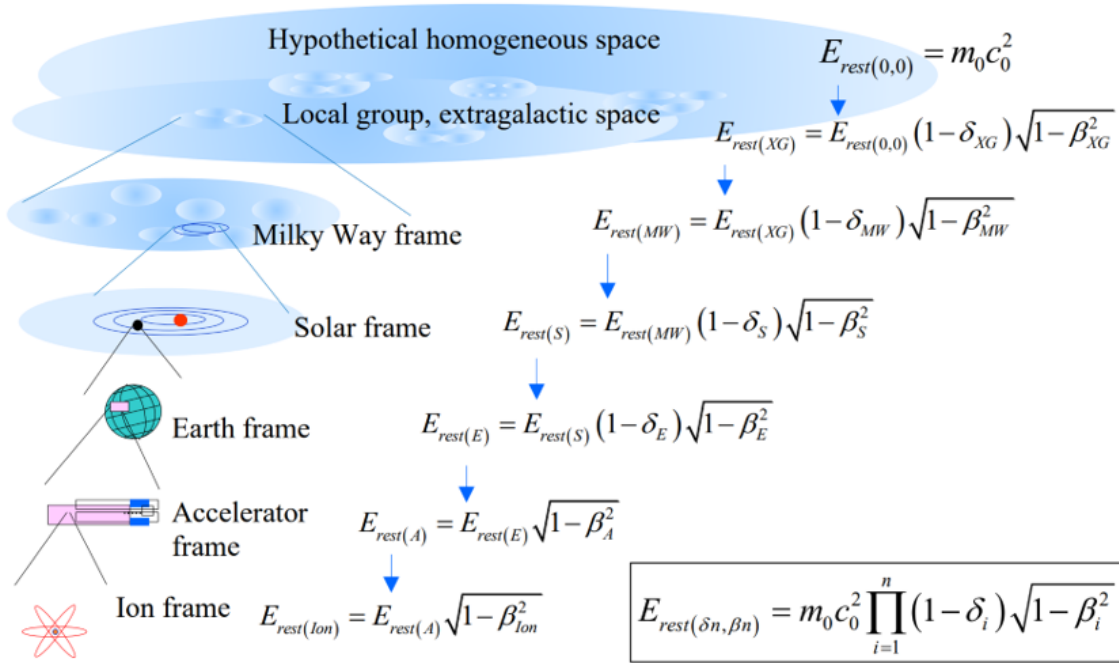
71

Figure 5: The system of nested energy frames. The rest energy in the nth (local) frame is subject to reductions due to the motions and gravitational states of the local frame in all its parent frames – and is finally related to the rest energy the object would have at rest in hypothetical homogeneous space.

the velocity of light at a fixed gravitational state in the Earth gravitational frame, which gives a simple explanation to the zero-result in the early experiments on the velocity of light like the Michelson-Morley experiment. The frequency of atomic clocks is directly proportional to the local velocity of light which means that the velocity of light is observed unchanged when measured with atomic clocks.

The signal transmission time, e.g., from a satellite to a receiver on the rotating Earth can be calculated from the actual distance from the satellite at the time the signal is sent to the location of the receiver at the time the signal is received. Such a calculation conveys the Sagnac correction needed in the GR/SR framework as a separate correction for the motion of the receiver during the signal transmission.

Rather than relativity between an object and the observer like in the SR/GR framework, relativity in DU is relativity between a local and the whole. Any state of gravitation and motion in space has its history that links it to the state of rest in the local frame, the state of the local frame in the parent frame, and finally to the state of rest in hypothetical homogeneous space. Time and distance are universal coordinate quantities of the observational reality essential for an understandable picture of physical reality.

Planck's constant and the nature of quantum and matter wave

Without any assumptions tied to DU, Planck's equation can be formally solved from Maxwell's equations by solving the energy that a single electron transition in a one-wavelength dipole emits into a cycle of electromagnetic radiation. A point source can be regarded as a one-wavelength dipole in the fourth dimension, where space moves the distance $cdt = \lambda$ (equal to the 4D line element in the SR/GR framework) in one cycle

$$h = 1.1049 \cdot 2\pi^3 e^2 \mu_0 \cdot c. \tag{15}$$

The solution links Planck's constant to primary electrical constants; the unit charge e and vacuum permeability μ_0, and shows that the velocity of light, c, is a hidden factor in the Planck constant. We define the intrinsic Planck constant by removing the velocity of light from h as $h_0 = h/c$, which allows writing the Planck equation in the form

$$E = \frac{h_0}{\lambda}c^2 = m_\lambda c^2, \tag{16}$$

where the quantity $h_0 = h/c$ has the physical dimension of kilogram [kg] and is the mass equivalence of a quantum of radiation or a cycle of radiation emitted by a unit charge transition in the emitter. The mass equivalence of radiation is the counterpart of the Compton wavelength $\lambda_m = h_0/m$ as the wavelength equivalence of mass m. The reformulation does not change physics but allows an illustrative picture of the nature of mass and quantum, and the unified expressions of energy:

$$\text{Rest energy of mass } E = \frac{h_0}{\lambda_m}c^2 = mc^2. \tag{17}$$

$$\text{Electromagnetic radiation } E = \frac{h_0}{\lambda}c^2 = m_\lambda c^2. \tag{18}$$

$$\text{Coulomb energy } E = \frac{e^2\mu_0}{4\pi r}\,c^2 = \alpha\frac{h_0}{2\pi r}\,c^2 = m_{EM} \cdot c^2. \tag{19}$$

As shown by a detailed analysis, the factor c^2 in equations (16) to (19) is the product of the 4D velocity c_0 of homogeneous space and the local velocity of light c equal to the 4D velocity of local space. In the Earth's gravitational frame c differs from c_0 at ppm-level. Following the new formulation, e.g., quantum states (like solutions of Schrödinger's equation in closed systems) appear as energy minima of mass wave states fulfilling the relevant resonance conditions. The de Broglie wave is described as a mass wave carrying the momentum of a moving mass object – much in the way de Broglie was looking for.

4. Cosmological consequences

Dynamics of the expansion

DU gives a precise prediction for the development of the rate of the expansion of space

$$c_0 = \frac{dR_4}{dt} = \left(\frac{2}{3}GM''\right)^{1/3}t^{-1/3} = \frac{2}{3}\frac{R_4}{t}, \tag{20}$$

where t is the time from the singularity. Today, the 4-radius R_4 is about 14 billion light-years. Due to the faster expansion in the past, the age of the expanding space is about 9.3 billion present years.

All gravitationally bound local systems, as well as the wavelength of electromagnetic radiation propagating in space, expand in direct proportion to the expansion, Fig. 6. Atoms and material objects do not expand. The distance 2.8 cm of the measured 3.8 cm annual increase of the Earth to Moon distance comes from the expansion of space and only 1 cm from tidal interactions. Earth and Mars have been closer to the Sun in their infancy, which offers an obvious solution to the early faint Sun paradox.
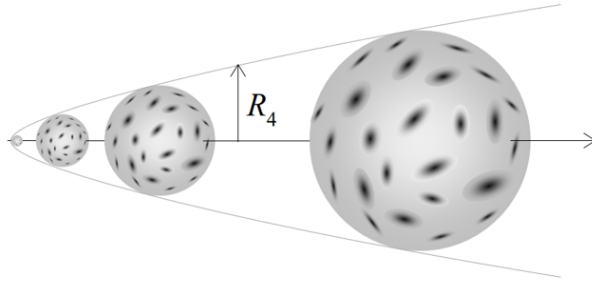

Figure 6: In DU, all gravitationally bound local systems like galaxies and planetary systems expand in direct proportion to the expansion of space.

Cosmological distances

The linkage of the velocity of light in space to the expansion velocity of space in the fourth dimension means, e.g., that the optical distance in space is equal to the increase of the 4-radius during the light traveling time from the object. Such a situation allows a simple, closed-form expression for the optical distance versus redshift

$$D = R_0 \frac{z}{1+z}, \tag{21}$$

where R_0 is the 4-radius of space at the time of the observation, Fig. 7.

The optical distance applies to the angular size distance and when corrected with the Doppler dilution, to the luminosity distance. In DU, luminosity distance applies directly to the observed bolometric magnitudes (without reduction to the emitter's rest frame by the K-correction like in SC) and produces precise predictions, e.g., to Ia supernovae magnitudes without hypothetical dark energy. In DU, there is no basis for the reciprocity [2] of Standard Cosmology.

The spherical geometry, the linkage of the velocity of light to the expansion velocity, and the linkage of the size of quasars and galaxies to the expansion of space result in the Euclidean appearance of galactic space, supported by observations on galaxies and quasars [3], Fig. 8.
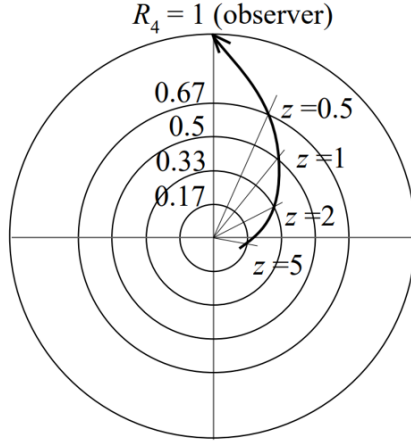
Figure 7: Lightpath in expanding space. The optical distance is the integrated tangential component of the lightpath. The radial direction in the picture is the fourth dimension showing the development of the expansion.

Magnitude of standard candle

DU produces a precise prediction for the magnitude of standard candles without mass density, dark energy, or any other adjustable parameters

$$m_{DU} = M + 5 \log \left(\frac{R_4}{10 \text{pc}} \right) + 5 \log (z) - 2.5 \log (1 + z). \tag{22}$$

The DU prediction applies to bolometric magnitudes excluding the "conversion to emitters rest frame" applied in standard cosmology via the K-correction. K-correction is used to compensate for losses due to atmospheric attenuation and spectral mismatch of filters or photographic plates, which are technical corrections. Also, K-correction converts the observed magnitudes of the objects into their respective rest frames, which, in SC, means an extra $(1 + z)^2$ reduction to the observed power density. The resulting reduction of power density corresponds to $5 \log(1 + z)$ correction to the observed magnitudes. The inclusion of the redshift effect in the K-correction was first introduced by Hubble and Tolman in 1935, see [4] and is still the praxis "as the conversion to emitter's rest frame" in Standard Cosmology [5].

The magnitude prediction in standard cosmology is based on power loss proportional to the comoving distance squared and the effects of redshift by the factor $(1+z)$ due to the Doppler effect and another $(1 + z)$ due to dilution based on Planck's equation. Physically, the Planck equation describes energy conversion at the emission [6], which means that the energy carried by a cycle of radiation does not change when the wavelength is increased but is diluted as observed via the Doppler effect. In DU, the magnitude prediction applies to bolometric magnitudes. It is based on the optical distance (21) and Doppler dilution, which together result in a $5 \log(1 + z)$
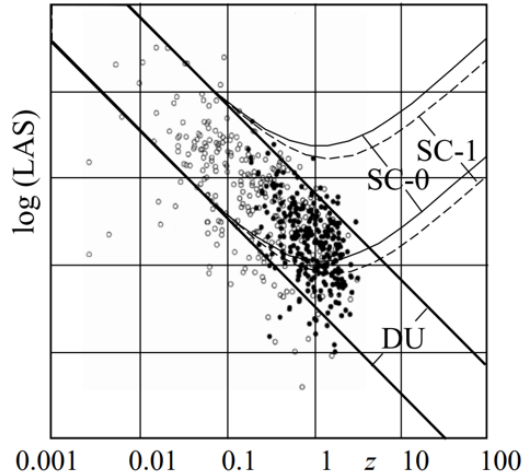
75

Figure 8: Angular size of galaxies (open circles) and quasars (filled circles). The data points fall well between the Euclidean DU prediction lines. The SC-0 and SC-1 curves showing increasing angular sizes for z higher than 1 are the Standard Cosmology predictions without and with dark energy, respectively.

difference [1] compared to the SC prediction that applies to magnitudes "converted to emitter's rest frame" by the factor $5 \log (1 + z)$ in the K-correction.

Fig. 9 (a) shows the K-corrected observations (dots) of Ia supernovae by Riess et al. [7], and the DU prediction (22) (solid line) corrected by factor $5 \log (1 + z)$ to correspond to the K-corrected magnitudes. Fig. 9 (b) shows the K-corrections applied by Riess et.al. to the observed magnitudes.

An ideal bolometric detector is a wideband detector with flat spectral response. Detection systems, based on multi-bandpass filters, produce closest to bolometric magnitudes by matching each filter to the redshift of the object observed, or by following the envelope curve obtained from the minimum magnitude readings of each filter channel over the whole redshift range. Such an analysis, based on observed magnitudes in bandpass filters B, V, R, I, Z, J by Tonry et al. [8], is shown in Fig. 10. The envelope curve shows a complete match to the DU prediction (22) for bolometric magnitudes. The SC prediction (dashed curve) deviates from the envelope curve by factor $5 \log (1 + z)$.

---

[1]In the redshift range $0 \ldots 2$, compared to DU optical distance, the comoving distance in SC is higher by the factor $\approx \sqrt{1 + z}$, resulting in extra attenuation by the factor $(1 + z)$. Another $(1 + z)$ difference comes from the application of both Doppler and Planck dilutions in SC. DU prediction applies to bolometric magnitudes, SC prediction to bolometric magnitudes corrected with the factor $5 \log (1 + z)$ included in the K-correction as "the conversion to emitter's rest frame".
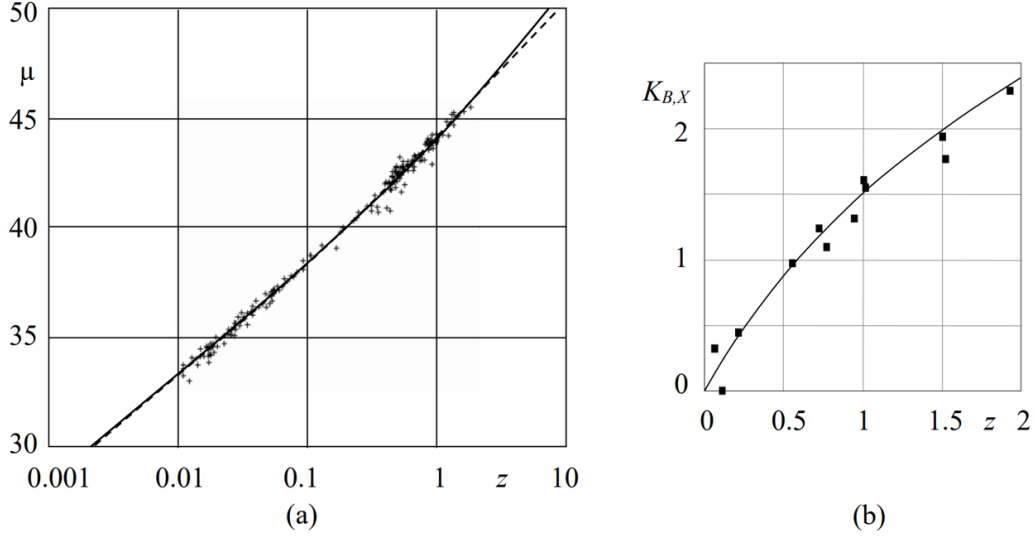
Figure 9: (a) Distance modulus $\mu = m - M$, vs. redshift for Riess et al. "high-confidence" dataset and the data from the HST14. The SC prediction is shown by the dashed curve. The DU prediction (solid curve) is based on equation (22) corrected with $5\log(1+z)$ to correspond the data points converted to emitter's rest frame. (b) Average $K_{B,X}$ -corrections (black squares) collected from the $K_{B,X}$ data in Table 2 used by Riess for the K-corrected distance modulus data shown in (a). The solid curve gives the $5\log(1+z)$ correction "converting observations to emitter's rest frame".

Supernova light-curve broadening

The duration of distant supernova explosions is observed as being proportional to the redshift as $T_z = T_0(1+z)$ [9]. In standard cosmology, the broadening is referred to as cosmological time dilation. Supernova explosions are considered standard candles which means that we can assume that the duration of an explosion corresponds to a fixed number of cycles measured with an atomic clock at the time of the event. The ticking frequency of atomic clocks is directly proportional to the velocity of light, which decreases with the expansion of space. Light redshifted by z has been emitted when the velocity of light was $c_z = c_0\sqrt{1+z}$, and the ticking rate of clocks $f_z = f_0\sqrt{1+z}$, respectively. It means that the duration of an explosion was $dt_z = dt_0/\sqrt{1+z}$ compared to the duration of a similar explosion at $z \approx 0$. The expansion of space during an explosion is

$$dR_z = c_z dt_z = c_0\sqrt{1+z} \cdot dt_0 / \sqrt{1+z} = c_0 dt_0 \qquad (23)$$

which means that the expansion of space during an explosion is independent of the redshift. Expansion dR_z at redshift z corresponds to expansion $dR_{0(z)} = dR_z(1+z)$ at the time of the observation, and the corresponding observed time, Fig. 11,

$$dt_{0(z)} = dR_{0(z)}/c_0 = c_0 dt_0/c_0 = dt_0(1+z). \qquad (24)$$

77
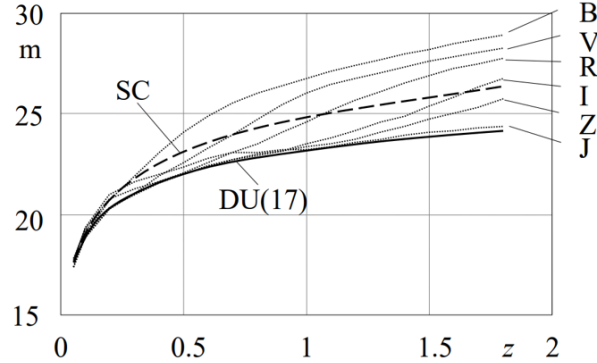
Figure 10: Observed magnitudes in bandpass filters B, V, R, I, Z, J by Tonry et al. The data is collected from Table 7 in [8] (dotted curves). The envelope curve shows the bolometric magnitude with a complete match to the DU prediction (22) (solid curve). The SC prediction (dashed curve) deviates from the envelope curve by the factor $5 \log (1 + z)$.
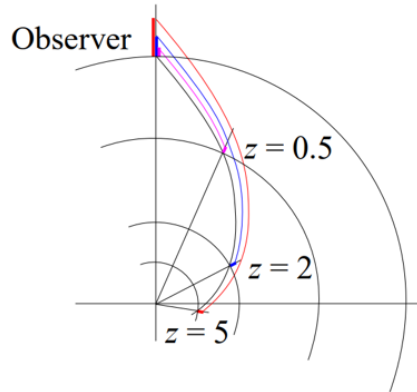
Figure 11: The duration of a supernova explosion has been shorter in the past, but it is observed lengthened.

Days in a year

Perhaps the most convincing cosmological support for the linkage of planetary systems to the expansion of space comes from paleo-anthropological data available back to almost 1000 million years in the past. Fossil layers preserve both the daily and annual variations, thus giving the development of the number of days in a year [10], [11].

According to the standard cosmology model, the orbital radius of the Earth is constant, which means that the reduction in the number of days in a year comes only from the tidal interaction which increases the length of a day via reduced rotation speed of the Earth. In the DU framework, the orbital radius and the length of

78

a year increase with the expansion, which compensates a part of the tidal effect on the number of days in a year. The tidal effect on the lengthening of a day is about 2.5 ms/100y [12]. A change of 2.5 ms/100y is too fast when compared to the data from coral fossils. When corrected with the increase in the length of a year by 0.6 ms/100y due to the expansion of space, we end up with the lengthening 1.9 ms/100y which gives a perfect match to the coral fossil data, Fig. 12. The 0.6 ms/100y correction due to the expansion is based on the expansion corresponding to Hubble constant 71 (km/s)/Mpc.
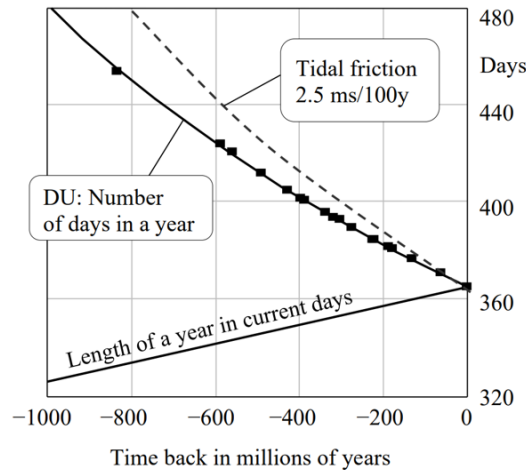
Figure 12: The development of the length of a year in the number of days. Black squares are data points from [10], [11]. The DU prediction combines the effects of tides and the change in the length of a year due to the expansion of the Solar system.

Further observational evidence on the development of the Earth's rotation is available from ancient Babylonian and Chinese eclipse observations extending almost 3000 years back [13]. The average lengthening of a day calculated from the eclipse observations is 1.8 ms/100y which is about 0.7 ms/100y less than the estimated effect of tidal friction. Adding the effect of the lengthening of a year, 0.6 ms/100y, we end up to 1.9 ms/100y, which is essentially the same as the result from coral fossils.

The length of a day has been measured with atomic clocks since 1955. An announced result for the lengthening by NASA is 1.5 ms/100y. When the result is corrected with the change in the clock frequency, 0.3 ms/100y, we get 1.8 ms/100y, which is in a good agreement with the solar eclipse and coral fossil data, Fig. 13.

The faint young Sun paradox

At the time of the early development of the planets about 4 billion years ago, solar insolation is estimated to be about 25% fainter than it is today [14]. Based on geological observations, the temperature of oceans on the Earth has been about 30–40°C. Also, there is evidence of liquid water on Mars at that time. According to DU, Earth and Mars have been about 30% closer to the Sun than they are today. Combining

79

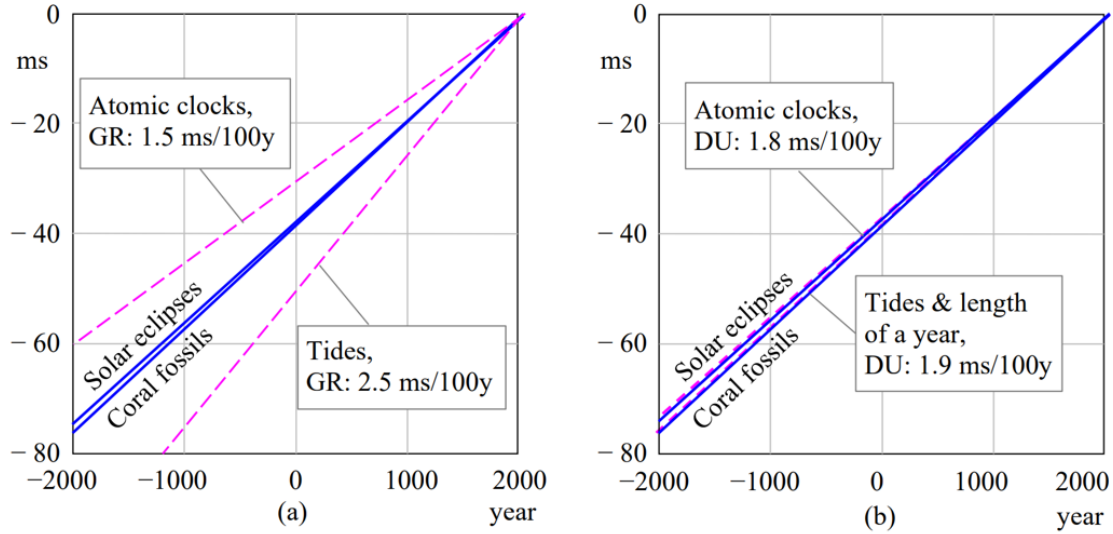Figure 13: Lengthening of a day obtained from solar eclipses and coral fossil data is 1.8 ms/100/y and 1.9 ms/100y, respectively (solid lines in (a) and (b)). Atomic clock measurement for the lengthening of a day is 1.5 ms/100y if assumed that the frequency of the clock is unchanged (dashed line in (a)). In the DU framework, the frequency of an atomic clock has been higher in the past. The corrected lengthening of a day is 1.8 ms/100y, consistent with the solar eclipse and coral fossil results (dashed line in (b)). According to the standard model, the lengthening of the day is due to tidal interactions, which give about 2.5 ms/100y prediction to the lengthening of a day (dashed line in (a)). In DU, the lengthening of a year shall be taken into account, which together with the tidal effects results in the 1.9 ms/100y lengthening of the day (dashed line in (b)).

that with the fainter luminosity of the Sun, 30–40°C ocean temperature on the Earth, and liquid water on Mars are well in line with the DU prediction [15], Fig. 14.

Distances to the moon and planets

The distance of the Moon has been monitored in the Lunar Laser Ranging program since the 1970s [16]. In the DU framework, 2.8 cm of the measured 3.8 cm annual increase of the Earth to Moon distance comes from the expansion of space and only 1 cm from the tidal interactions.

Reported analyses of transponder measurements of planetary distances apply an "Einstein effect" to eliminate the expansion shown by the direct transmission time data [17]. The "Einstein effect" is justified as a relativistic correction for matching the timescales in measurements at different epochs. In the DU framework, there is no basis for time-scale corrections; in the transponder measurement, the number of clock cycles is directly proportional to the distance just as applied in the case of Laser Ranging in the Earth to Moon distance monitoring.
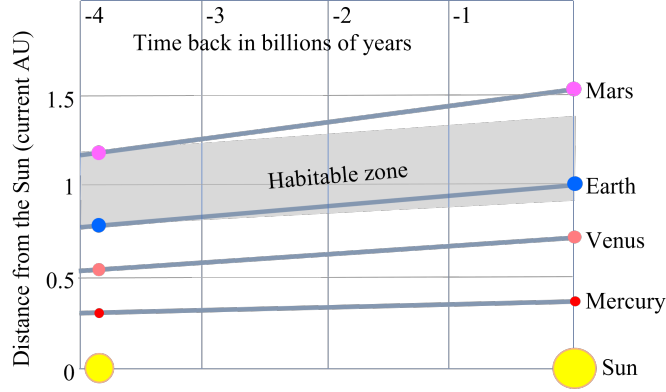
Figure 14: The development of the habitable zone in the expanding solar system. The expansion overcompensates the fainter solar luminosity in the past; the early temperatures on the planets have been higher than they are today [15]

Orbital decay

In the DU framework, the decay of the period of an elliptic orbit can be solved as a consequence of the periastron rotation and the related rotation of the orbital angular momentum in the fourth dimension, Fig. 15(a). Interestingly, the prediction derived from the rotation of the 4D orbital angular momentum gives essentially the same prediction as the GR prediction based on the change of the quadrupole moment [18], [19]. The only difference is that DU predicts orbital decay for eccentric orbits only, GR predicts decay for circular orbits, too, Fig. 15 (b). To the author's knowledge, all observations on orbital decay are related to orbits with non-zero eccentricity.

The possible energy radiation (gravitational radiation) by the rotating 4D angular momentum in the DU has not been analyzed.

$$\frac{dP}{dt}_{(DU)} \approx 120 \cdot \frac{G^{5/3}}{c^5} \left(\frac{P}{2\pi}\right)^{-5/3} \left(2 \cdot \frac{\sqrt{1+e_{0\delta}} - \sqrt{1-e_{0\delta}}}{\left(1-e^2\right)^2}\right) \cdot \frac{m_p m_c}{\left(m_p + m_c\right)^2} \left(m_p + m_c\right)^{5/3}$$

(25)

$$\frac{dP}{dt}_{(GR)} \approx 123 \cdot \frac{G^{5/3}}{c^5} \left(\frac{P}{2\pi}\right)^{-5/3} \left(\frac{1 + (73/24)\,e^2 + (37/96)\,e^4}{\left(1-e^2\right)^{7/2}}\right) \cdot \frac{m_p m_c}{\left(m_p + m_c\right)^2} \left(m_p + m_c\right)^{5/3}$$

(26)

5. Philosophical considerations

The essence of mass

Breaking down Planck's constant into its constituents opens up the essence of mass as the wavelike "substance" for the expression of energy. Mass is not a form of energy, but it expresses the energy related to motion and potentiality. In the DU framework,
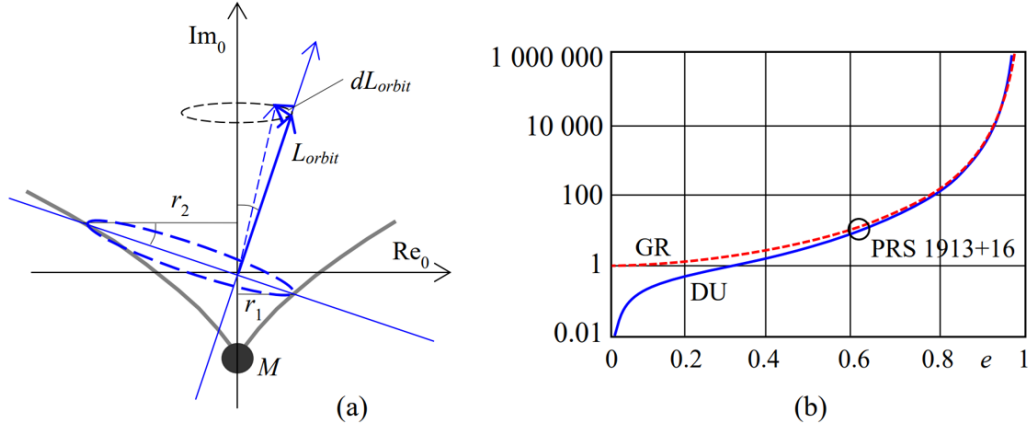
Figure 15: (a) In the DU framework the orbital decay of binary stars is calculated from the energy related to the rotation of orbital angular momentum due to the periastron advance. (b) The eccentricity factor of the decay of binary star orbit period in equations (25) for DU and (26) for GR, respectively. At the eccentricity $e = 0.616$ of the PSR 1913+16 orbit, the eccentricity factor of the GR and DU for the orbit decay are essentially the same. According to the DU prediction, the eccentricity factor goes to zero at zero eccentricity.

mass is conserved also in annihilation; the mass equivalence of the emitted photons is equal to the rest mass of annihilated particles. The total mass in space is the primary conservable. The contraction of space builds up the excitation of the complementary energies of motion and gravitation. The anti-energy of the rest energy of a localized mass particle is the negative gravitational energy arising from all other mass in space.

Inertia and Mach's principle
In the DU framework, inertial work is the work done against the global gravitational energy via the interaction in the fourth dimension, which means a quantitative explanation of Mach's principle. Inertia is not a property of mass; in the DU framework, the "relativistic mass increase" Δmc introduced in the SR framework is the mass contribution by the accelerating system to the buildup of kinetic energy. In the complex quantity presentation, the real part of kinetic energy increases the momentum observed in space, and the imaginary part of kinetic energy reduces the global gravitational energy and the rest energy of the moving object, which is observed as the reduced ticking frequency of atomic clocks in motion.

Any motion in space is central motion relative to the barycenter of space in the center of the 4D ball defining space. Inertial work can be understood as the work that the central force created by motion in space does against the global gravitational force in the fourth dimension. Electromagnetic radiation propagating at the velocity of light in space moves like in a satellite orbit around the barycenter of whole space; radiation is weightless but not massless.

Occam's razor
DU omits all central postulates of the relativity theory and standard cosmology like the relativity principle, Lorentz covariance, equivalence principle, the constancy of the velocity of light, dark energy, an instant of the Big Bang, inflation hypothesis, and the space-time concept and replaces them with the assumption of zero-energy balance in spherically closed space. DU gives at least as precise predictions as SR/GR/SC but uses fewer postulates and more straightforward mathematics [20], [21]. Most importantly, DU uses time and distance as universal coordinate quantities essential for human comprehension and offers a framework for a unified framework for physics from cosmology to quantum phenomena.

Aristotle's entelecheia and the linkage of local to the whole
In the spirit of Aristotle's entelecheia, the primary energy buildup is described as the "actualization of potentiality", the conversion of gravitational energy into the energy of motion – and follows the same, as the zero-energy principle, in all interactions in space. Any state of motion in space has its history that links it, through the system of nested energy frames, to the state of rest in hypothetical homogenous space. In the kinematic analysis of SR, a velocity in space is related to an observer, but in the dynamic analysis of DU, a state of motion is related to the state where the energy building up the kinetic energy was released. There are no independent objects in space, any local object is linked to the rest of space; the rest energy of any energy object is balanced by the global gravitational energy arising from space as a whole.

Acknowledgements

References

[1] Suntola, T.: The Dynamic Universe, Toward a Unified Picture of Physical Reality, 4th ed. Physics Foundations Society, Espoo (2018)
https:www.physicsfoundations.org/dynamic-universe.

[2] Etherington, J. M. H.: Phil. Mag. *15* (1933), 761.

[3] Nilsson, K. et al.: Astrophys. J. *413* (1993), 453.

[4] Hubble, E., Tolman, R. C.: ApJ *82* (1935) 302.

[5] Kim, A. Goobar, A., Perlmutter, S.: PASP *108* (1996), 190.

[6] Suntola, T.: Proceedings of SPIE *5866* (2005), 18.

[7] Riess, A.G.: et al., Astrophys. J. *607* (2004), 665.

[8] Tonry, J.T.: et al., ApJ, *594* (2003), 1.

[9] Goldhaber, G et.al.: Astrophys. J. *558* (2001), 359.

[10] Wells, J. W.: Nature *197* (1963), 948.

[11] Wells, J. W.: In S. K. Runcorn (Eds.), Paleogeophysics, Academic Press, London 1970.

[12] Stephenson, F. R., Morrison, L. V.: Phil. Trans. R. Soc. A *351* (1995), 165.

[13] Stephenson, F. R., Morrison, L. V., Hohenkerk, C. Y.: Proc. R. Soc. A 2016.

[14] Bahcall, J. N. et.al: arXiv:astro-ph/0010346v2 13 Mar (2001).

[15] Sipilä, H.: J. Phys. Conf. Ser. *1466* (2020).

[16] Dickey, J. O. et.al.: Science *265* (1994), 482.

[17] Krasinsky, G. A., Brumberg, V. A.: Celestial mechanics and dynamical astronomy *90* (2004), 267.

[18] Peters, P. C., Mathews, J.: Phys. Rev. *131* (1963), 435.

[19] Weisberg, J. M., Taylor, J. H.: ASP Conference series *328* (2005), 25.

[20] Styrman, A.: Economical unification as a method of philosophical analysis. Ph.D. thesis, University of Helsinki, (2016) http://urn.fi/URN:ISBN:978-951-51-2697-9.

[21] Styrman, A.: Only a unified ontology can remedy disunification. J. Phys. Conf. Ser. 1466 012001 (2020). https://iopscience.iop.org/article/10.1088/1742-6596/1466/1/012001.

A DEMONSTRATION OF THE DIFFERENCE BETWEEN THE NORMALIZED AND NON-LIMITED SOLUTIONS OF THE FIELD EQUATIONS IN THE MODELING OF RELATIVISTIC COMPACT OBJECTS

Luboš Neslušan

Astronomical Institute, Slovak Academy of Sciences
05960 Tatranská Lomnica, Slovakia
ne@ta3.sk

Abstract: When a relativistic compact object (RCO), like a neutron star, is modeled, it is prescribed that its matter must be distributed from the outer surface down to the center, i.e., only the normalized solutions of the field equations are allowed to be used. The arguments to obey this demand are crucially based on the identification of the radial component of metric tensor (its special form) with the mass of RCO. However, this identification of the tensor component (its value depends on a choice of coordinate frame) with the mass, which is a scalar quantity (its value does not depend on the used frame for a static RCO), must never be done. Constructing a model of spherically symmetric, super-massive RCO, when the demand of the normalization is abolished, we demonstrate some important consequences of the new approach. Namely, there are stable-equilibrium RCOs with outer radius above the event horizon, the RCO's mass can be several orders of magnitude larger than the observed mass-equivalent of the tensor component, the object in center of a galaxy and its dark-matter halo can be modeled as a single whole, within the same numerical integration of field equations, etc. A way how to include the dark matter into the RCO modeling is also outlined.

Keywords: general relativity, relativistic compact object, galactic halo, dark matter

PACS: 04.90.+e, 04.20.Cv, 04.40Dg, 98.62.-g, 95.35.+d

1. Introduction

It is well-known that the neutron stars are the objects significantly curving the spacetime, therefore the general theory of relativity (GR, hereafter) has to be used in a creation of their models. In sixties of the 20th century, some researchers (e.g. [8], [18], [7], [19]) tried to construct also the models of the super-massive (SM, hereafter) objects, detected in the centers of galaxies and quasars, on the basis of GR. In

this paper, these objects, significantly curving the spacetime, are referred to as the relativistic compact objects (RCOs, hereafter). We are going, here, to deal only with the RCOs, which are measured to be spherically symmetric by an observer in their centers.

When a model of a realistic RCO has been constructed, it has been demanded that only the normalized solution of the Einstein field equations (EFEs) could be used. In other words, it has been demanded that the matter of the RCO had to be distributed from the outer physical surface down to its center; it had to be a fulfilled-sphere object. We found that this demand has a character of a postulate, which we name "normalization postulate" and which can be abolished. Actually, there is no reason why the RCO has always to acquire the form of the fulfilled sphere. The arguments for a necessity of such configuration are wrong, because they are based on the following false identity.

Oppenheimer and Volkoff [13] in their modeling of a spherically symmetric neutron star re-wrote g_{rr} component of metric tensor with the help of metric function u:

$$u = \frac{1}{2} r \left(1 - e^{-\lambda}\right), \tag{1}$$

where $g_{rr} = -e^{\lambda}$. If function u is multiplied with the square of the speed of light, c, and divided with the Newton gravitational constant, G, we obtain quantity in unit of mass,

$$U = \frac{c^2}{G} u, \tag{2}$$

which is, hereafter, referred to as "metric mass-equivalent". Notice, since u is the re-written component of g_{rr}, it must also be the tensor quantity and U must be the tensor quantity as well. Although the unit of this quantity is the unit of mass, the metric mass-equivalent must not be represented as any mass.

The mass of RCO, M, is the scalar quantity. It is the integral of energy density, E, through the RCO's volume, ranging from an inner radius R_{in} to outer radius R_{out}, divided by the square of the light speed (in accord to the well-known Einstein's formula that energy is the product of mass and c^2). Specifically,

$$M = \frac{4\pi}{c^2} \int_{R_{\text{in}}}^{R_{\text{out}}} E r^2 \, dr. \tag{3}$$

The normalization postulate requires $R_{\text{in}} = 0$, but if it is abolished, then there may be considered $R_{\text{in}} > 0$. The relation between U and M is given and discussed in Section 2.2.

In our previous paper [11], we showed that there can occur $M > 0$ and, at the same time, $U < 0$ in a distance r inside a RCO. The same quantity cannot be positive, when calculated in one way, and at the same time negative when calculated in other way, regardless a realistic or only a theoretical model of RCO was constructed.

If one numerically integrates the EFEs in course to model a RCO, whereby the integration is started in a finite RCO-centric distance and performed in two stages,

stepping outward and stepping inward, there appears that not only the outward, but also the inward stepped integration reaches a finite RCO-centric distance where the pressure and energy density are vanished. This fact means that RCO is bordered not only with an outer, but also with an inner physical surface. Below the inner surface, there is a vacuum void. Besides our earlier papers [9, 10, 11], the models of RCOs in the form of hollow sphere, with the inner physical surface, have been published by Ni [12] and deLyra et al. [4], [5].

We would like to emphasize that the inner surface occurs due to the normal, attractive, GR gravity. No exotic assumption is needed to be adopted. The example of this gravity is the gravity acting on an astronaut on the Lunar surface, when the astronaut stays on the surface between the centers of Earth and Moon (i.e., the Earth is in his zenith) and we describe his gravitational acceleration in the coordinate frame with the origin identical with the center of the Earth. The astronaut is accelerated away from the Earth, i.e. away from the origin of the coordinate frame, but this outward oriented (outward in respect to the coordinate origin) gravitational acceleration is not caused by any repulsion of the Earth. The outward oriented acceleration occurs simply due to the fact that the dominant matter acting on the astronaut, matter of the Moon, is situated beyond the astronaut from the point of view of observer in the center of Earth.

The same situation exists deeply inside any RCO. A test particle situated close to the inner RCO' surface or in the central void of RCO is attracted away from the void center by the dominant matter, which is distributed in a volume beyond the particle from the point of view of an observer in the center.

One could, perhaps, argue with the spherical symmetry of RCO. In the Euclidean space of the Newtonian physics, an asymmetry leading to the dominant matter beyond the test particle from the point of view of observer in the center actually does not exist. However, the concept of the spherical symmetry in the GR is more complicated. A distribution of matter, e.g. a spherical shell, which is measured as spherically symmetric by an observer in the center (of the shell), is not, generally, measured as spherically symmetric by an observer located aside the center. The asymmetry leading to the outward-from-center oriented gravitational attraction occurs in the relativistic object. The mechanism of the outward oriented gravitational attraction was more explained in our previous paper [11].

In this contribution, we present a model of SM RCO constructed when the normalization postulate is not valid. We discuss some cosmological consequences of such a model. One section (Section 4) is devoted to a discussion about an inclusion of the dark matter into the RCO modeling.

2. Modeling an energetic SM RCO

2.1. Fundamental equations

We consider a spherically symmetric object, therefore we use the EFEs simplified for the spherical symmetry. These equations are [15]

$$\kappa P = e^{-\lambda} \left(\frac{1}{r} \frac{d\nu}{dr} + \frac{1}{r^2} \right) - \frac{1}{r^2}, \tag{4}$$

$$\kappa P = e^{-\lambda} \left[\frac{1}{2} \frac{d^2\nu}{dr^2} - \frac{1}{4} \frac{d\lambda}{dr} \frac{d\nu}{dr} + \frac{1}{4} \left(\frac{d\nu}{dr} \right)^2 + \frac{1}{2r} \frac{d\nu}{dr} - \frac{1}{2r} \frac{d\lambda}{dr} \right], \tag{5}$$

$$\kappa E = e^{-\lambda} \left(\frac{1}{r} \frac{d\lambda}{dr} - \frac{1}{r^2} \right) + \frac{1}{r^2}, \tag{6}$$

where $\kappa = 8\pi G/c^4$ is the Einstein gravitational constant (G is the gravitational constant in the Newton law and c is the speed of light in a vacuum), P is the pressure, E is the energy density, r is the distance from the center of the object, and $\lambda = \lambda(r)$, $\nu = \nu(r)$ are the auxiliary metric functions. It is valid $g_{rr} = -e^{\lambda}$ and $g_{tt} = e^{\nu}$; g_{rr} and g_{tt} are the components of the metric tensor.

From the EFEs, the radial component of the gradient of pressure can be given as

$$\frac{dP}{dr} = -\frac{E+P}{2} \frac{d\nu}{dr}. \tag{7}$$

The EFEs (4)−(6) have often been re-written with the help of metric function u (see relation (1)). Using this function, the EFEs can be given in form

$$\frac{du}{dr} = \frac{1}{2} \kappa E r^2, \tag{8}$$

$$\frac{d\nu}{dr} = \frac{2}{r^2 - 2ru} \left(\frac{1}{2} \kappa P r^3 + u \right), \tag{9}$$

$$\frac{dP}{dr} = -\frac{E+P}{r^2 - 2ru} \left(\frac{1}{2} \kappa P r^3 + u \right), \tag{10}$$

which is appropriate for the numerical integration. (Or, the last equation can be re-written for the direct integration of material density ρ, when its derivative in respect to r is calculated taking into account the validity of $dP/dr = (dP/d\rho)(d\rho/dr)$, see relations (22) and (23) in Section 2.3.)

We note that equations (8)−(10) are the tensor equations. Let us deal with the last one to demonstrate the tensor character. It is the equation for the diagonal rr-component. In the case of spherical symmetry, we can regard the spatial diagonal components, rr, $\vartheta\vartheta$, and $\varphi\varphi$, as the components of a vector and establish unit vector $\vec{r}_o$ in the radial direction (corresponding to rr component of the metric tensor). The left-hand side of Eq. (10) is the radial component of the gradient of pressure in fact. To obtain a vector component also on the right-hand side of this equation, we

write variable r and quantity u in their ordinary, i.e. vectorial, forms $\vec{r} = r\vec{r}_o$ and $\vec{u} = u\vec{r}_o$. Eq. (10) can, then, be re-written to

$$\operatorname{grad} P|_r = -\frac{E+P}{(r\vec{r}_o)^2 - 2(u\vec{r}_o)(r\vec{r}_o)}\left[\frac{1}{2}\kappa P(r\vec{r}_o)^2(r\vec{r}_o) + u\vec{r}_o\right] \tag{11}$$

or (using $\vec{r}_o.\vec{r}_o = 1$)

$$\operatorname{grad} P|_r = -\frac{E+P}{r^2 - 2ur}\left(\frac{1}{2}\kappa Pr^3\vec{r}_o + u\vec{r}_o\right). \tag{12}$$

Besides other arguments, also this equation implies that function u, exactly $u\vec{r}_o = \vec{u}$, cannot be regarded as a scalar function; therefore, c^2u/G cannot be identified with any mass.

2.2. On the concept of mass in the unlimited GR

Eq. (8) can be used to calculate integral (3), i.e. the mass of the RCO. From (8), we can express $Er^2 = 2(du/dr)/\kappa$ and supply this into (3). Then, the integral can be easily calculated and mass M can be given as

$$M = \frac{8\pi}{c^2\kappa}(u_{\text{out}} - u_{\text{in}}) = \frac{c^2}{G}u_{\text{out}} - \frac{c^2}{G}u_{\text{in}} = U_{\text{out}} - U_{\text{in}}, \tag{13}$$

where $u_{\text{in}} = u(R_{\text{in}})$, $u_{\text{out}} = u(R_{\text{out}})$, $U_{\text{in}} = U(R_{\text{in}})$, and $U_{\text{out}} = U(R_{\text{out}})$. If the coordinate frame with the origin in the center of the RCO is used, then it is always true that $U_{\text{in}} < 0$ and $U_{\text{out}} > 0$. Therefore, mass can be given as

$$M = |U_{\text{out}}| + |U_{\text{in}}|. \tag{14}$$

It implies that the mass is always positive.

Beside the mass, a RCO can be further characterized with the rest mass, M_o. It is the sum of the rest masses of constituting particles. The rest mass of whole RCO is

$$M_o = 4\pi\bar{m}\int_{R_{\text{in}}}^{R_{\text{out}}} nr^2 e^{\lambda/2}\,dr, \tag{15}$$

where $\bar{m}$ is the mean mass of the particles, which equals $\bar{m} = \mu_b m_a$, and n is the number density of particles. We denoted the molecular weight of the gas by μ_b and atomic mass unit by m_a. Integral (15) gives the number of the particles in the proper volume of RCO, $V = 4\pi\int_{R_{\text{in}}}^{R_{\text{out}}} r^2 e^{\lambda/2}\,dr$. Since the number density, n, is related to the material density, ρ, as $n = \rho/(\mu_b m_a)$, the rest mass can also be given as

$$M_o = 4\pi\int_{R_{\text{in}}}^{R_{\text{out}}} \rho r^2 e^{\lambda/2}\,dr = 4\pi\int_{R_{\text{in}}}^{R_{\text{out}}} \frac{\rho r^2}{\sqrt{1 - \frac{2u}{r}}}\,dr. \tag{16}$$

Further, one could show that $R_{\text{in}} \to 0$ and $U_{\text{in}} \to 0$ in the limit of weak field. Then, $M \to U_{\text{out}}$, numerically. It means that the normalization postulate is redundant, in fact. The GR itself implies that a non-rotating, gaseous object tends to acquire the form of fulfilled sphere, with the mass approaching the metric mass-equivalent, in the limit of weak field. We need not to prescribe the fulfilled-sphere solution in advance.

2.3. Equation of state; polytrope

It appears that even the maximum density inside a RCO is relatively low and, thus, the gas constituting a SM RCO is, probably, similar to a common stellar plasma. Hence, in modeling of a SM RCO, we use the equation of state (EoS) in form of a combination of polytrope and EoS for radiation ($E = 3P$). It means that the pressure is given by [16]

$$P = K_P \rho^\gamma + \frac{1}{3} a T^4, \tag{17}$$

and energy density

$$E = N K_P \rho^\gamma + c^2 \rho + a T^4, \tag{18}$$

where a is the radiation constant, T is the temperature of plasma, N is the polytropic index, $\gamma = 1 + 1/N$, and constant K_P equals

$$K_P = \frac{k_B T_{\text{max}}}{\mu_b m_a \rho_{\text{max}}^{1/N}}. \tag{19}$$

In the last relation, k_B is the Boltzmann constant, ρ_{max} and T_{max} are the maximum density and maximum temperature inside the RCO (these constants are more specified below). For the sake of simplicity, we consider the same composition of plasma as in the zero-age, main sequence stars throughout the RCO volume. Hence, the weight abundances of hydrogen and helium are equal to $X_H = 0.73$ and $X_{He} = 0.25$, respectively. The abundance of heavy chemical elements is $Z = 0.02$.

Since we model a RCO assuming the normalization postulate abolished, the maximum pressure, P_{max}, and maximum energy density, E_{max}, occur in a finite RCO-centric distance, r_o. The local extreme of the pressure is given by equality $dP/dr = 0$ and this is valid, according to relation (10), if $\kappa P_{\text{max}} r_o^3 / 2 + u_o = 0$. From the latter, $u_o = u(r_o)$ can be expressed as

$$u_o = -\frac{1}{2} \kappa P_{\text{max}} r_o^3. \tag{20}$$

When $dP/dr = 0$, then also $d\nu/dr = 0$ according to relation (7). Since the gravitational acceleration is proportional to $d\nu/dr$, it is zero in r_o. It means that distance r_o is the distance of zero net gravity.

It is reasonable to start each stage of the numerical integration of EFEs just from the distance r_o, where the maximum material density, ρ_{max}, and maximum

temperature, T_{max}, of RCO are assumed. In the case of polytrope, temperature T can be given with the help of density ρ as

$$T = T_{\mathrm{max}} \left(\frac{\rho}{\rho_{\mathrm{max}}} \right)^{1/N}.$$

(21)

The common formula for the calculation of pressure of a gas is $P = k_B \rho T / (\mu_b m_a)$. Hence, for the maximum pressure of gas, we have $P_{\mathrm{max}} = k_B \rho_{\mathrm{max}} T_{\mathrm{max}} / (\mu_b m_a)$ and, at the same time (see the first term of relation (17)), $P_{\mathrm{max}} = K_P \rho_{\mathrm{max}}^{\gamma}$. Comparing these two relations, we can express constant K_P in form (19).

If we now establish the auxiliary variable ξ equal to

$$\xi = \frac{\rho}{\rho_{\mathrm{max}}},$$

(22)

the EFEs for the numerical integration can be given in form (8), (9) and

$$\frac{d\xi}{dr} = \frac{-\frac{E+P}{r^2-2ru} \left(\frac{1}{2}\kappa P r^3 + u \right)}{\gamma K_P \rho_{\mathrm{max}}^{\gamma} \xi^{1/N} + \frac{4}{3N} K_r \xi^{(4/N)-1}},$$

(23)

where we supply

$$P = K_P \xi^{\gamma} + \frac{1}{3} K_r \xi^{4/N},$$

(24)

$$E = N K_P \xi^{\gamma} + K_r \xi^{4/N} + K_c \xi,$$

(25)

for P and E. We denoted $K_r = a T_{\mathrm{max}}^4$ and $K_c = c^2 \rho_{\mathrm{max}}$.

2.4. Calibration of g_{tt} component of metric tensor

In the inner and outer radii of RCO, the metrics of the RCO's interior (IM) should be smoothly tailored with an appropriate vacuum metrics; according to the Birkhoff [1] theorem, it should be tailored with the outer Schwarzschild metrics (OSM). The smooth tailoring means that all components of the metric tensor of IM and OSM, as well as their derivatives in respect to r, should equal each other, correspondingly. For a spherically symmetric object, the transversal components, $g_{\vartheta\vartheta}$ and $g_{\varphi\varphi}$, are identical in both the metrics, therefore, the demand of smooth tailoring is apriori obeyed. Component g_{rr} and its derivative dg_{rr}/dr also obey the demand due to the intrinsic consistency of GR.

However, the EFEs do not contain g_{tt} component itself, only the derivative of auxiliary function ν, therefore this component is not completely determined by the EFEs and its tailoring deserves an attention.

Since only the derivative $d\nu/dr$ of function ν is present in the EFEs, the behavior of ν inside the RCO's body is the same for the initial values of, e.g., $\nu_{o,1}$ and $\nu_{o,2}$, except of a constant difference $\Delta\nu_{1,2}$. Thus, we can suppose whatever initial value $\nu_{o,1}$ and perform the integration. In the outer radius of RCO, integration

yields the value $\nu_1(R_\mathrm{out})$. This value has to be smoothly tailored to value ν_OSM of the OSM in R_out, i.e., to value $\nu_\mathrm{OSM}(R_\mathrm{out}) = \ln(1 - 2u_\mathrm{out}/R_\mathrm{out})$. Since the numerical integration also yields values u_out and R_out, $\nu_\mathrm{OSM}(R_\mathrm{out})$ can be calculated and, then, difference $\Delta\nu_{1,2} = \nu_1(R_\mathrm{out}) - \nu_\mathrm{OSM}(R_\mathrm{out})$ is also known. Therefore, we can calculate the appropriate initial value of ν in r_o:

$$\nu_{o,2} = \nu_{o,1} - \nu_1(R_\mathrm{out}) + \ln\left(1 - \frac{2u_\mathrm{out}}{R_\mathrm{out}}\right). \tag{26}$$

Using this initial value, we repeat the numerical integration. The repetition yields the behavior of function $\nu(r)$, which can be smoothly tailored to the OSM in R_out.

The general form of g_{rr} and g_{tt} components of metric tensor in the OSM is

$$g_{tt} = -\frac{K_\nu}{g_{rr}} = K_\nu\left(1 - \frac{2u}{r}\right), \tag{27}$$

where K_ν and u are the constants. There is the convention to put $K_\nu = 1$ for the OSM in the vacuum above the outer surface of RCO, i.e. in the region $r \geq R_\mathrm{out}$. The convention was established to achieve the convergence of the GR to the Newtonian physics in the limit of weak field. (This convention is not, however, necessary. We could choose whatever value of constant K_ν and establish the gravitational constant $\widetilde{G}$. Then, the Newtonian gravitational acceleration would be proportional to $K_\nu\widetilde{G}$. In the experiments to determine the effective gravitational constant, we always measure the effective gravitational constant, G, which is just the product of K_ν and $\widetilde{G}$, i.e., $G = K_\nu\widetilde{G}$. If we did not demand K_ν to equal unity, we could anyway denote $G = K_\nu\widetilde{G}$ and achieve the standard form of the acceleration in this way, i.e., via establishing the appropriate denotation.)

The OSM can smoothly be tailored to the IM also in the inner radius R_in. Since we already chose the initial value of ν, it cannot be chosen again to achieve $K_\nu = 1$ in $r = R_\mathrm{in}$. Constant $K_{\nu,\mathrm{in}}$ in this RCO-centric distance is

$$K_{\nu,\mathrm{in}} = \frac{1 - \frac{2u_\mathrm{out}}{R_\mathrm{out}}}{1 - \frac{2u_\mathrm{in}}{R_\mathrm{in}}}. \tag{28}$$

The effective gravitational constant in the inner vacuum void, i.e. in the region $r \leq R_\mathrm{in}$, is $G_\mathrm{in} = K_{\nu,\mathrm{in}}G$. A modeling shows that $K_{\nu,\mathrm{in}} \neq 1$, therefore $G_\mathrm{in} \neq G$. It implies that the strong, relativistic, accumulation of matter changes the value of the gravitational constant.

3. Example of a very energetic RCO

3.1. Basic properties and overall structure

Here, we present a model of SM RCO, which was constructed by performing the numerical integration of EFEs (8), (9), and (23). The Runge-Kutta integration algorithm was used. Polytrope index $N = 3$ was considered. The integration in each

of two stages started in the zero-gravity distance $r_o = 1$ au. In this distance, we put $\rho_{max} = 1.0 \cdot 10^5 \, \mathrm{kg \, m^{-3}}$ and $T_{max} = 5.0 \cdot 10^{10}$ K. In the starting distance r_o, value ξ equals unity according to (22) and u_o is given by relation (20).
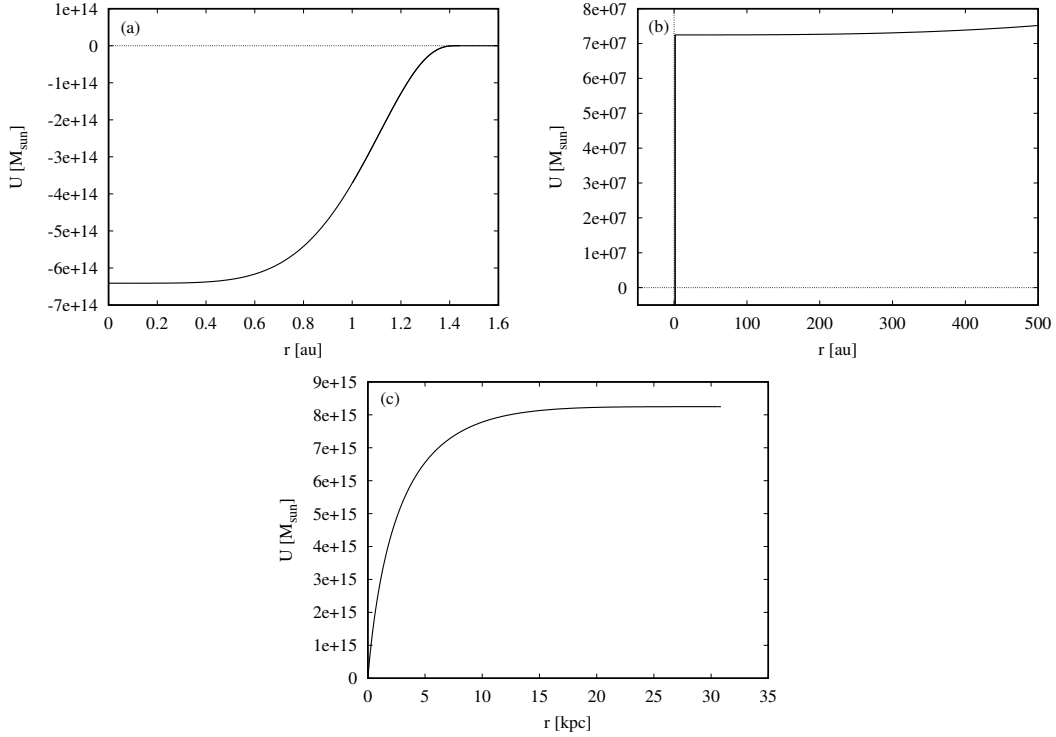
Figure 1: The behavior of the metric mass-equivalent, U, in the example of SM RCO. The behavior is described in more detail in Sect. 3.1. Notice the different scales of the panels.

Since the radiation was included into our considerations (the EoS contained the term corresponding to the radiation), pressure and energy density did not vanish exactly at the borders of RCO. Because of this circumstance, the sphere, where the material density, ρ, dropped to $10^{-9}\rho_{max}$, was regarded as the surface. This definition implies the inner radius $R_{in} = 125.022$ km. The outer radius of central condensation of RCO (CC-RCO, hereafter), where $\rho = 10^{-9}\rho_{max}$, equals $R_{cc} = 1.44214$ au. (The reason why we established term "CC-RCO" is clarified below.)

To explain better the characteristics obtained from the integration, let us deal, firstly, with the behavior of metric mass-equivalent U as the function of RCO-centric distance, r. This behavior can be seen in Fig. 1. In panel (a) of this figure, the beginning of the $U = U(r)$ curve in R_{in} can be seen. In R_{in}, $U_{in} = -6.410 \cdot 10^{14}$ M$_\odot$.

The outer border of the CC-RCO is seen in plot (b). In R_{cc}, the metric mass-equivalent equals $U_{out} = 7.248 \cdot 10^7$ M$_\odot$. This value, which is about seven orders of magnitude lower than the size of U_{in}, characterizes the metrics above the outer surface of the CC-RCO. In this region, the motion of various objects is observed and U_{out} is determined (via a reverberation mapping or other method). Here, we

can see that the mass of CC-RCO, which is the difference $U_{\text{out}} - U_{\text{in}}$ according to relation (13), is much larger than the metric mass-equivalent in the region above the outer CC-RCO surface. Specifically, the CC-RCO mass is equal to $6.410 \cdot 10^{14}\,\text{M}_\odot$. The CC-RCO rest mass, M_o, equals only $9.379 \cdot 10^5\,\text{M}_\odot$.

We note that integral (3) can be obtained within the numerical integration. The mass can also be calculated as $U_{\text{out}} - U_{\text{in}}$. Both values can be compared and used to estimate the precision of the numerical integration. In the presented example, we obtained values $6.410185 \cdot 10^{14}\,\text{M}_\odot$ and $6.410186 \cdot 10^{14}\,\text{M}_\odot$, respectively. So, the mass was determined with the precision of six decimal digits.

In Fig. 1b, one can further notice a constant behavior of the metric mass-equivalent above the CC-RCO' surface, up to the distance of $\sim$200 au. The constancy implies the OSM. A detailed inspection revealed, that the metrics was not exactly the OSM, but the approximation with this vacuum metrics was a very good approximation of the actual metrics in the above-mentioned region. The region seems to be an analogy of the region in the Milky Way, where the S-stars orbit the central compact object, SgrA*. (The extent of the region can be larger, up to several thousands of astronomical units according to some speculative models including the dark matter; see Section 4.)

If one goes on with the integration beyond $\sim$200 au, the value of the metric mass-equivalent increases, up to the distance of $\sim$22 kpc (Fig. 1c). Then the metric mass-equivalent is again practically constant up to the outer border of the RCO. This border appears to be in the RCO-centric distance of $R_{\text{out}} = 30.854$ kpc. Here, the material density, ρ, abruptly decreases and if the numerical integration went on, it would imply a negative material density in a larger distance. (It is similar to the Oppenheimer and Volkoff's [13] neutron stars. There is an inflex point in the outer border of star and a further integration beyond this point, if was performed, would also yield a negative energy density.) In the region $r > R_{\text{out}}$, the material density is postulated to be zero. Of course, the total energy density is not exactly zero because of escaping photons. However, it is negligible and the metrics can, again, be well approximated with the OSM.

At the outer RCO's border, the value of the metric mass-equivalent reaches $U_{\text{out}} = 8.247 \cdot 10^{15}\,\text{M}_\odot$ and mass equals $M = 8.888 \cdot 10^{15}\,\text{M}_\odot$. The region in the interior of the sphere with this radius resembles the dark-matter galactic halo, although, in our example, it consists exclusively of the baryonic matter. (We considered the EoS of the common, hydrogen-helium, stellar type of plasma with the EoS for radiation added.)

The model of the RCO in this example was constructed within a single integration of EFEs, it is a single whole. Formally, we can divide the RCO structure to three substructures, in three regions: the central condensation (CC-RCO) in the region between the spheres of radii R_{in} and R_{cc}, the region of OSM (OSM-RCO) extending from the outer CC-RCO surface to the end of constant U behavior, which is in the distance of about 200 au in our example, and the halo of the RCO (H-RCO) extending from the outer border of the OSM-RCO to the outer border of whole RCO, i.e., from about 200 au to 30.854 kpc in our example RCO.

94

3.2. Evaluation of the RCO's stability

Let us now evaluate the stability of the RCO. It was constructed by using the EFEs for a static case. Such the EFEs provide only a solution for an object in an equilibrium configuration. However, the object can be in stable or unstable equilibrium. It acquires the stable-equilibrium configuration if its binding energy, $W_o - W$ [17], is positive. It means that the rest energy, $W_o = M_o c^2$, is larger than the total energy, $W = Mc^2$.

Since the radiation is also considered in our example RCO, we correct the condition $W_o - W > 0$. Namely, if the condition is obeyed, the free energy, $W - W_o$, of the RCO is negative. The RCO could become unstable, if the free energy of gas, $W_{gas} - W_o$, would be positive (W_{gas} is the total energy of gas; it equals $W_{gas} = W - W_{rad}$, where W_{rad} is the energy of radiation inside the RCO). If the radiation energy was transformed to the energy of gas, then the latter could become larger than W_o and RCO could be unstable. However, the radiation energy, W_{rad}, cannot be transformed to W_{gas}, since this would be a violation of the second law of thermodynamics (in a gas, the temperature of gas cannot increase and temperature of radiation decrease; the radiation must be in an equilibrium with the gas). In the stability criterion, we therefore replace the total energy, W, with the energy of gas, and obtain condition

$$W_o - W_{gas} > 0. \tag{29}$$

In our example, $W_{gas} = 1.217 \cdot 10^{63}$ J (mass equivalent $W_{gas}/c^2 = 6.806 \cdot 10^{15}$ M$_\odot$) and $W_o = 1.367 \cdot 10^{63}$ J (mass equivalent equals $7.649 \cdot 10^{15}$ M$_\odot$), therefore the condition of stability is obeyed.

In our previous paper [11], we found several models of neutron stars which were not only in a stable configuration, but also in the minimum-energy configuration. In the current modeling, it is impossible to create a series of models with the same rest energy and investigate the dependence of the total energy on the zero-gravity distance, since the rest energy of CC-RCO is not constant. At the considered high maximum temperature, the nuclear reactions happen. Two photons can transmute to a pair of particle-antiparticle and vice versa, for example.

It is worth to note that the CC-RCO, when regarded as an autonomous object, is in an unstable-equilibrium in our example (and, probably, in all models that can be created). While the energy of gas on our CC-RCO equals $2.426 \cdot 10^{56}$ J (mass equivalent is $1.357 \cdot 10^9$ M$_\odot$), the rest energy is equal to only $1.677 \cdot 10^{53}$ J (mass equivalent equals $9.379 \cdot 10^5$ M$_\odot$). Hence, the CC-RCO is obviously kept as a stable object by an interaction with the other parts of RCO.

3.3. An estimate of the RCO's luminosity

Further, let us estimate the bolometric luminosity of the RCO in our example. We assume that the RCO-constituting radiation fluid can be approximately regarded as a grey stellar photosphere. Then, we can calculate the opacity by using the relations, which are approximation of tabulated opacity values [6],

$$\chi_e = 0.02(1 + X), \tag{30}$$

$$\chi_{ff} = 1.0 \cdot 10^{19} \frac{\rho}{\mu_e \mu_i} \frac{X + Y}{A_{He}} T^{-3.5}, \tag{31}$$

$$\chi_{bf} = 4.0 \cdot 10^{21} Z(1 + X)\rho T^{-3.5}, \tag{32}$$

where χ_e, χ_{ff}, and χ_{bf} are the free-electrons, free-free transitions, and bound-free transitions opacities, respectively, X, Y, and Z are the weight abundances of hydrogen, helium, and metals, respectively, μ_e is the mean molecular weight per free electron, μ_i is the total mean molecular weight of ions, and $A_{He} = 4$ is the atomic mass of helium. All quantities are in the SI units. The total opacity, χ, is the sum of the above given components, i.e., $\chi = \chi_e + \chi_{ff} + \chi_{bf}$.

At the outer border of the RCO, in about 30 kpc, the temperature is only few kelvins and the density of the gas is also extremely low. (The identification of the gas with the stellar plasma fails in this region, because the gas is obviously neutral; we ignored this fact since this region is small, with a negligible energy content, not significantly influencing the other parts of RCO, and in sake of simplicity.) Therefore, the above-mentioned relations can scarcely be extrapolated to such the extreme conditions. However, one can draw some, at least qualitative, conclusion estimating the appropriate parameters of layer, in which the temperature is, say, 5000 K. We chose such a geometrical thickness of the layer, h, that its optical thickness is $\tau = 1$. Then, we found that $h \sim 8.8$ pc and luminosity equals $\sim 1.1 \cdot 10^{47}$ W. The RCO could, constantly, emit so intensive radiation only during about 0.0024 current age of the universe. This fact in a combination with the tremendous estimated luminosity implies that the galactic halos must consist of the dark matter.

The optical thickness, τ, in the spherically symmetric curved spacetime was calculated as

$$\tau = -\int_{r_5}^{r_5 - h} \chi \rho e^{\lambda/2} \, dr, \tag{33}$$

since we had to consider the proper element of length, $e^{\lambda/2} dr$, in the curved spacetime. r_5 is the radius of the layer with the temperature equal to 5000 K ($r_5 \sim 4.9$ kpc in our example).

The outer radius of the CC-RCO equals $1.0078 \, R_g$, where R_g is the gravitational radius calculated as $R_g = 2GU_{\text{out}}/c^2$. (In each step of the integration, we checked if inequality $r > 2u$ is valid. If the inequality did not hold, the integration would fail.) Since the outer surface is situated above the event horizon, the CC-RCO can emit a radiation from its upper layer, photosphere. Let us assume that OSM-RCO and H-RCO prevailingly consist of the dark matter and, thus, these parts are transparent for the radiation emitted by the plasma in the photosphere of CC-RCO. Assuming further that this part mostly consists of baryonic matter, we give a rough, order-of-magnitude, estimate of geometrical thickness of the photosphere and luminosity of the CC-RCO. The bolometric luminosity, L, can be calculated as

96

$$L = \frac{16}{3}\pi ac\frac{r^2}{\chi\rho}\sqrt{g_{tt}}T^3\frac{dT}{dr}. \tag{34}$$

The square root of g_{tt} component of metric tensor has to occur in this relation because the frequency of each emitted photon is gravitationally redshifted. It means, the photon has the frequency $\sqrt{g_{tt}}f_s$ in a large distance (of observer on the Earth), when the frequency at the source is f_s.

The geometrical thickness of the CC-RCO photosphere in our example model was about $26\,\text{km}$. The luminosity was estimated to be about $\sim 9.0{\cdot}10^{42}\,\text{W}$ ($\sim 2.4{\cdot}10^{16}\,\text{L}_\odot$). If the luminosity was assumed to be constant during the period equal to the current age of the universe, $\approx 14\,\text{Gyr}$, then the CC-RCO would loose only 0.035 of its initial total energy during this period. If the phenomenon of quasar was the radiation from the photosphere of CC-RCO, then the most energetic quasars would have enough energy to emit the radiation, with the high observed luminosity, during the whole age of the universe. Yet, they would have spent only a small fraction of their initial total energy.

The luminosity estimated above is larger than even the maximum luminosity observed at the quasars. (For example, it is about 5900 times larger that the luminosity of the well-known, bright quasar 3C 273.) Maybe, these astrophysical objects consist not only of baryonic, but of the dark matter as well. Then their actual bolometric luminosity would be lower.

4. Note on the inclusion of dark matter into the modeling

At the present, we have no direct evidence that the dark matter (DM) exists. However, this concept enables to explain some puzzles, as e.g. the rotation curves of spiral galaxies. In the following, we hypothesize that the DM exists. Based on the explanations of some effects assumed to occur due to the DM, only few fundamental properties of the DM have been derived: it is a subject of the gravitational interaction, it does not emit any electromagnetic radiation, and the efficient cross-section in its collision with the normal, baryonic matter (BM) is extremely small. Despite our not very good knowledge of the properties of DM, it appears, surprisingly, that we have a quite a lot of information that we need to create a reasonable model of RCO consisting of both BM and DM.

Assuming that the DM can constitute a gas, which can be characterized in a similar way than a gas consisting of BM, i.e., its pressure, temperature, material density, and energy density are well defined, then the DM can be included into a modeling of RCOs. Below, we outline such the modeling.

Since there is no pressure of the DM on the BM and vice versa, each of these two kinds of matter must balance the gravity in a RCO autonomously. In a RCO being in an equilibrium configuration, it means that the gradient of pressure of DM, $\mathrm{grad}\,P_d$, must be the same as the gradient of pressure of BM, $\mathrm{grad}\,P$. When we assume a spherically symmetric, non-rotating, RCO, only the radial component of

the pressure gradient is non-zero. So, we have the equation

$$\frac{dP_d}{dr} = \frac{dP}{dr}. \tag{35}$$

After the integration of this equation in respect to r, one obtains

$$P_d = P + C_d, \tag{36}$$

where C_d is an integration constant.

Completing EFE (4) with the cosmological constant, Λ, we can use this equation to calculate the difference $P_d - P$. Since the same gravity is efficient in the case of DM as BM, i.e., functions λ and $d\nu/dr$ are the same in the equations for both P_d and P, the difference is equal to

$$P_d - P = \Lambda_d - \Lambda_b. \tag{37}$$

Symbols Λ_d and Λ_b stand for the cosmological constant for the DM and BM, respectively, and the difference of $\Lambda_d - \Lambda_b$, equal to our constant C_d in fact, is the actual cosmological constant. From various measurements we know that this constant, if non-zero, is very small. Obviously we can put $C_d = 0$ on the scale of RCO in our example. Relation (36) then implies $P_d = P$.

Because of the equality of the pressures, it is reasonable to assume the same functional dependence of the DM pressure on DM material density as in the case of BM. Therefore, the DM pressure, P_d, will be given by a polytrope. Specifically,

$$P_d = K_d \rho_d^\gamma. \tag{38}$$

In this relation, symbol ρ_d stands for the DM material density and K_d is a constant of proportionality. In analogy with constant K_P given by relation (19), the constant K_d can obviously be given as

$$K_d = \frac{k_d T_{d,\mathrm{max}}}{\mu_d m_d \rho_{d,\mathrm{max}}^{1/N}}. \tag{39}$$

Since we do not know if the Boltzmann constant for the DM is identical to that for the BM, we assume that it equals k_d. The molecular weight and atomic mass unit for the DM are also unknown; we denoted them by symbols μ_d and m_d, respectively. Symbol $T_{d,\mathrm{max}}$ denotes the maximum temperature and $\rho_{d,\mathrm{max}}$ the maximum density of the DM. Relation (38) does not contain the radiation term (an analog of term $aT^4/3$ in the case of BM) because the DM does not emit the electromagnetic radiation, which causes the radiation pressure.

Obviously, constants k_d, μ_d, and m_d for the DM are the multiples of constants k_B, μ_b, and m_a for the BM, respectively. When we denote these multiples by C_k, C_μ, and C_m, respectively, we can write

$$k_d = C_k k_B, \tag{40}$$

$$\mu_d = C_\mu \mu_b, \tag{41}$$

$$m_d = C_m m_a. \tag{42}$$

Denoting

$$C_3 = \frac{C_k}{C_\mu C_m},\tag{43}$$

the constant K_d can be re-written as

$$K_d = \frac{C_k k_B T_{d,\max}}{C_\mu \mu_b C_m m_a \rho_{d,\max}^{1/N}} = C_3 \frac{k_B T_{d,\max}}{\mu_b m_a \rho_{d,\max}^{1/N}}.\tag{44}$$

We see that constants k_b, k_μ, and k_m can be merged to a single constant, C_3. This constant can be regarded as a free parameter in the modeling of RCO.

Because of the equality of the DM and BM pressures, the DM material density, ρ_d, is related to the BM material density, ρ, as

$$\rho_d = \left(\frac{K_P}{K_d} + \frac{aT_{\max}^4}{3K_d \rho_{\max}^{4/N}} \rho^{\frac{3-N}{N}} \right)^{\frac{N}{N+1}} \rho.\tag{45}$$

This relation can be derived, after an algebraic handling, from the equality of the right-hand sides of relations (17) and (38). In (17), temperature of BM gas can be re-written with the help of relation (21). In a special case, when the polytropic index $N = 3$, the DM density is

$$\rho_d = \left(\frac{K_P}{K_d} + \frac{aT_{\max}^4}{3K_d \rho_{\max}^{4/3}} \right)^{3/4} \rho.\tag{46}$$

We see that the DM density is linearly proportional to the BM density, since the form in the parentheses is constant.

Further, the equality of DM and BM pressures means that also the maximum DM pressure, $P_{d,\max}$, must equal the maximum BM pressure, $P_{\max}$. In other words, the right-hand side of relation (17) for $\rho = \rho_{\max}$ (again, temperature T can be re-written with the help of relation (21)) is equal to the right-hand side of relation (38) for $\rho_d = \rho_{d,\max}$. From this equality, one can find that

$$\rho_{d,\max} = \frac{\mu_b m_a}{k_B C_3 T_{d,\max}} \left(K_P \rho_{\max}^\gamma + \frac{1}{3} aT_{\max}^4 \right).\tag{47}$$

Now, only independent parameter is the maximum temperature, $T_{d,\max}$, of the DM. This parameter can be merged with free parameter C_3, i.e., we can put

$$K_T = C_3 T_{d,\max}\tag{48}$$

and regard constant K_T as a single free-parameter input into a numerical integration to model a RCO.

The description of the thermodynamic state of the DM by the polytrope implies the energy density of the DM, E_d, in form

$$E_d = NK_d \rho_d^\gamma + c^2 \rho_d.\tag{49}$$

99

Again, the radiation term is omitted, because there is no electromagnetic radiation of the DM.

The absence of the ability of DM to emit an electromagnetic radiation is important in the cosmological evolution of galactic halos. We know that the electromagnetic radiation is the main mechanism of cooling of the macroscopic objects in the universe. It is well-known that a more massive star, a shorter its active life. If the galactic halos could emit the electromagnetic radiation, they would likely loose their internal energy and collapsed within a period much shorter than the age of the universe. Since these halos consist of DM, prevailingly, they can probably loose their energy only when produce the gravitational waves (e.g. when galaxies collide), but this mechanism is much less efficient than the emission of the electromagnetic radiation. Thus, the galactic DM halos can exist for eons.

Accounting for the DM, the EFEs to model a spherically symmetric RCO can be given, in an analogy with Eqs. (8), (9), and (10), in the form

$$\frac{du}{dr} = \frac{1}{2}\kappa(E + E_d)r^2, \tag{50}$$

$$\frac{d\nu}{dr} = \frac{2}{r^2 - 2ru}\left(\kappa Pr^3 + u\right), \tag{51}$$

$$\frac{dP}{dr} = -\frac{E + E_d + 2P}{r^2 - 2ru}\left(\kappa Pr^3 + u\right). \tag{52}$$

The total energy density is the sum $E + E_d$ of the energy densities of both BM and DM. Term $E + E_d + 2P$ in the nominator of fraction in the right-hand side of Eq. (52) acts as an inertial mass density and term in the parentheses (which is also in relation (51)) acts as a gravitational mass density [14]. Since both BM and DM pressures contribute to both these densities, there appears the sum $P + P_d = 2P$ (because $P_d = P$ as argued above) instead of single P in the aforementioned relations as well as further relations for a mixture of BM and DM.

In the zero-gravity distance, r_o, the function u can be calculated, in a BM-DM model of RCO, in analogy with its calculation for a pure BM (see relation (20)) as

$$u_o = -\kappa Pr_o^3. \tag{53}$$

Equations (50)–(52) can be used to model a RCO consisting of both BM and DM. However, a construction of the BM-DM models, their analysis and description of results exceed the scope of this article. We stop this part of our considerations, here.

5. Instead of conclusion: is there an implication of new cosmology of quasars and galaxies?

The outlined properties of the very energetic RCO resemble some properties of quasars and galaxies. On the basis of implied qualitative properties of the example RCO, it is thus possible to hypothesize that the galaxies and quasars did not form by an accumulation of dispersed matter, filling in the intergalactic space, during

a certain period after the Big Bang, but they occurred as the stupendously large RCOs in a very short time after the Big Bang. Carr et al. [2] and Carr and Kühnel [3] concluded that the stupendously large primordial black holes with the masses in the interval ranging from $10^{12}\,\mathrm{M}_\odot$ to $10^{18}\,\mathrm{M}_\odot$ could occur. These black holes were the collapsed primordial objects of such the high masses. Assuming in accord to the indications pointed out in this work, these objects did not collapse below their event horizon, they can still exist, being evolved meanwhile, and can be identified with the galaxies and, those with the most energetic central condensations, with the quasars.

Actually, the CC of the SM RCO in the presented example indicates that a quasar with a comparable energy content could have emitted a radiation with the luminosity of the brightest quasars during a period comparable to the current age of the universe and, yet, it has spent only a small fraction of its initial total energy. One should not be surprised if a clear evidence of dark age is never found and quasars in distances corresponding to a very young universe (e.g., $z = 15$ or 20, or even higher values) will be discovered.

Since there is no event horizon, the CC-RCOs could eject some material into a neighboring space. If such a CC-RCO ejected only a small fraction of its mass (energy), there was enough material to form even a giant galaxy.

In the end, we again emphasize that the above-mentioned concepts are the implications of unlimited GR. The revision of the arguments to demand, that only the normalized solutions of the EFEs can be used in modeling of real objects, is needed. In astrophysics, we should utilize the whole, unlimited, Einstein's GR, not only a limiting case of this theory.

Acknowledgements

References

[1] Birkhoff, G. D., Langer, R. E.: Relativity and modern physics. Harvard University Press, Cambridge, 1923.

[2] Carr, B. J., Kühnel, F., Visinelli, L.: Constraints on stupendously large black holes. Mon. Not. Royal Astron. Soc. *501* (2021), 2029–2043.

[3] Carr, B. J., Kühnel, F.: Primordial black holes as dark matter candidates. arXiv:2110.02821 (2021).

[4] deLyra, J. L., Orselli, R. de A., Carneiro, C. E. I.: Exact solution of the Einstein field equations for a spherical shell of fluid matter. arXiv:2101.02012v2 (2021).

[5] deLyra, J. L., Carneiro, C. E. I.: Complete solution of the Einstein field equations for a spherical distribution of polytropic matter. arXiv:2101.07214v3 (2021).

[6] Hansen, C. J., Kawaler, S. D.: Stellar interiors. Physical principles, structure, and evolution. Springer-Verlag, New York, 1994.

[7] Hoyle, F.: Highly condensed objects. Quarterly Journal of the Royal Astronomical Society *10* (1969), 10–20.

[8] Hoyle, F., Fowler, W. A., Burbidge, G. R., Burbidge, E. M.: On relativistic astrophysics. Astrophys. J. *139* (1964), 909–928.

[9] Neslušan, L.: The Ni's solution for neutron star and outward oriented gravitational attraction in its interior. J. Modern Phys. *6* (2015), 2164–2183.

[10] Neslušan, L.: Outline of the concept of stable relativistic radiation sphere. A model of quasar? Astrophys. Space Sci. *362* (2017), art.id. 48.

[11] Neslušan, L.: The second rise of general relativity in astrophysics. Modern Phys. Lett. A *34* (2019), id. 1950244-356.

[12] Ni, J.: Solutions without a maximum mass limit of the general relativistic field equations for neutron stars. Science China: Physics, Mechanics, and Astronomy *54* (2011), 1304–1308.

[13] Oppenheimer, J. R., Volkoff, G. M.: On massive neutron cores. Phys. Rev. *55* (1939), 374–381.

[14] Schwab, J., Hughes, S. A., Rappaport, S.: The self-gravity of pressure in neutron stars. arXiv:0806.0798v1 (2008).

[15] Tolman, R. C.: Static solutions of Einstein's field equations for spheres of fluid. Phys. Rev. *55* (1939), 364–373.

[16] Tooper, R. F.: Stability of massive stars in general relativity. Astrophys. J. *140* (1964), 811–814.

[17] Tooper, R. F.: Adiabatic fluid spheres in general relativity. Astrophys. J. *142* (1965), 1541–1562.

[18] Tooper, R. F.: The "standard model" for massive stars in general relativity. Astrophys. J. *143* (1966), 465–482.

[19] Tooper, R. F.: Adiabatic fluid spheres in general relativity. II. Massive configurations of ideal gas and radiation. Astrophys. J. *155* (1969), 145–161.

DETERMINATION OF THE LOCAL VALUE OF THE HUBBLE CONSTANT AND COSMOLOGICAL CONSTRAINTS WITH LOCAL GIANT HII REGIONS AND HIGH-REDSHIFT HII GALAXIES

David Fernández-Arenas[1], Ana Luisa González-Morán[2,3], Ricardo Chávez[4,5], Elena Terlevich[1], Roberto Terlevich[1,6], Jorge Melnick[7,8], Fabio Bresolin[9], Eduardo Telles[8], Manolis Plionis[10,11] and Spyros Basilakos[12]

[1] Instituto Nacional de Astrofísica, Óptica y Electrónica, Tonantzintla, México
arenas@inaop.mx
[2] Instituto de Astrofísica de Canarias, Spain
[3] Departamento de Astrofísica, Universidad de La Laguna, Spain
algonzalez@iac.es
[4] Instituto de Radioastronomía y Astrofísica, UNAM, Campus Morelia, C.P. 58089, Morelia, México
[5] Consejo Nacional de Ciencia y Tecnología, Av. Insurgentes Sur 1582, 03940 Mexico City, Mexico
r.chavez@irya.unam.mx
[6] Institute of Astronomy, University of Cambrige, Cambridge, CB3 0HA, UK
[7] European Southern Observatory, Santiago de Chile, Chile
[8] Observatorio Nacional, Rua José Cristino 77, 20921-400 Rio de Janeiro, Brasil
[9] Institute for Astronomy, University of Hawaii, 2680 Woodlawn Drive, 96822 Honolulu, HI USA
[10] National Observatory of Athens, P. Pendeli, Athens, Greece
[11] Physics Dept., Aristotle Univ. of Thessaloniki, Thessaloniki 54124, Greece
[12] Academy of Athens, Research Center for Astronomy & Applied Mathematics, Soranou Efessiou 4, 11-527 Athens, Greece

Abstract: In this work, we describe the use of the H II galaxies redshift – distance relation, measured by means of the $L - \sigma$ relation and the resulting Hubble expansion cosmological probe of low-z HII galaxies and giant HII regions and of samples of high-z (up to $z \sim 4$) HII galaxies, to constrain the Dark Energy Equation of State (DE EoS) parameters solution space and to measure the Hubble constant as an alternative to the cosmological use of type Ia Supernovae (SNIa) and in a joint likelihood analysis with other well tested cosmological probes (CMB, BAOs).

Keywords: Hubble constant, Cosmological parameters – Dark Energy, H II galaxies, H II regions

PACS: 98.80.-k, 95.35.+d

1. Introduction

HII Galaxies (HIIG) are compact and massive systems experiencing luminous bursts of star formation generated by the formation of young super clusters (SSCs) with a high luminosity per unit mass and with properties similar, if not identical, to Giant HII Regions (GHIIRs). The potential of GHIIRs as distance indicators was originally realized from the existence of a correlation between the GHIIR diameter and the luminosity [15], [16] see also [11].

Most HIIG were discovered in objective-prism surveys thanks to their strong narrow emission lines. Currently, in spectroscopic surveys like Sloan Digital Sky Survey (SDSS), they are selected by very large equivalent widths in the Balmer lines. Since the luminosity of HIIG is dominated by the starburst component they can be observed even at large redshifts becoming interesting standard candles.

In 1981, [17] found a tight correlation between the turbulent emission lines velocity dispersion and their integrated luminosity: the $L - \sigma$ relation. This correlation, valid for HIIG and GHIIRs, links a distance dependent parameter, the integrated Hβ line luminosity, with a parameter that is independent of distance, the velocity dispersion of the ionized gas, therefore defining a redshift independent distance estimator.

The relationship between the integrated Hβ line luminosity and the velocity dispersion of the ionized gas of H II galaxies and giant H II regions represents an exciting standard candle. Locally it is used to obtain precise measurements of the Hubble constant by combining the slope of the relation obtained from nearby ($z \leq 0.2$) H II galaxies with the zero point determined from GHIIRs belonging to an "anchor sample" of galaxies for which accurate redshift-independent distance moduli are available [4], [7], [12].

On the other hand, HIIG are alternative and effective tracers of the Hubble relation, because they can be observed up to high redshifts $z \sim 3.5$, where the distance modulus is more sensitive to the cosmological parameters and despite the fact that the scatter of the HIIG distance modulus is larger (by a factor of 2) than that of high-z SNIa, this demerit is fully compensated by the fact that HIIG are observed to larger redshifts than SNIa, where the degeneracies for different DE models are reduced [13].

Indeed, it has been proven that this relation can be used as an alternative cosmological tracer with promising results in constraining cosmological parameters and determining the local value of the Hubble constant in recent years; not only by our group (cf. [6], [8], [9], [18], [19]) but also by independent groups, cf. [2], [3], [14], [20], [21].

2. Analysis

We have analyzed a sample of HIIG and GHIIRs containing 217 objects, which can be split into: the anchor sample (36 GHIIRs in 13 local galaxies with distances from primary indicators, [7]), the local sample of HIIG (107 with $z < 0.16$, [5]) and a high-z sample based on 29 KMOS, 15 MOSFIRE, 6 XShooter and 24 literature

objects (see [9] for more details). We used these data to make constrain cosmological parameters and to determine the local value of the Hubble constant by means of the distance indicator defined by the $L - \sigma$ relation.

2.1. Determination of the Hubble constant

The Hubble constant is determined as follows: first we fix the slope of the $L - \sigma$ relation using the velocity dispersions and luminosities of the HIIG. The slope is independent of the actual value of H_0.

To estimate the Hubble constant we use the slope (α) of the $L - \sigma$ relation of the HIIG and new GHIIR data (anchor sample) to calibrate the zero point (Z_p) of the distance indicator as follows

$$Z_p = \frac{\sum_{i=1}^{36} W_i(\log L_{\text{GHR,i}} - \alpha \times \log \sigma_{\text{GHR,i}})}{\sum_{i=1}^{36} W_i}, \tag{1}$$

where $L_{GHR,i}$ is the Hβ luminosity of each GHIIR and $\sigma_{\text{GHR,i}}$ is the corresponding velocity dispersion. The statistical weights W_i are calculated as

$$W_i^{-1} = \left(0.4343\frac{\delta L_{\text{GHR,i}}}{L_{\text{GHR,i}}}\right)^2 + \left(0.4343\alpha\frac{\delta\sigma_{\text{GHR,i}}}{\sigma_{\text{GHR,i}}}\right)^2 + (\delta\alpha)^2(\sigma_{\text{GHR,i}} - <\sigma_{\text{HIIG}}>)^2, \tag{2}$$

where $<\sigma_{\text{HIIG}}>$ is the average velocity dispersion of the HIIG that define the slope of the relation. Thus, the calibrated $L - \sigma$ relation or distance estimator is: $\log L(H\beta) = \alpha \log \sigma + Z_p$. To calculate the Hubble constant we minimize the function,

$$\chi^2(H_0) = \sum_{i=1}^{N}[W_i(\mu_i - \mu_{H_0,i})^2 - \log(W_i)], \tag{3}$$

where μ_i is the logarithmic distance modulus to each HIIG calculated using the distance indicator and the Hβ flux $F(H\beta)$ as

$$\mu_i = 2.5[Z_p + \alpha \times \log \sigma_i - \log F_i(H\beta) - \log 4\pi] \tag{4}$$

and $\mu_{H_0,i}$ is the distance modulus calculated from the redshift using either the linear relation $D_L = zc/H_0$ or the full cosmological prescription with $\Omega_\Lambda = 0.71$.

The best value of H_0 is then obtained minimising χ^2 with statistical weights $W_i^{-1} = \delta\mu_i^2 + \delta\mu_{H_0,i}^2$ calculated as,

$$W_i^{-1} = 6.25[(\delta Z_p)^2 + \left(0.4343\frac{\delta F_i}{F_i}\right)^2 + \left(0.4343\alpha\frac{\delta\sigma_i}{\sigma_i}\right)^2 + (\delta\alpha)^2(\sigma_i - <\sigma>)^2]. \tag{5}$$

2.2. Determination of the Hubble constant: Systematics

Genuine systematic errors are difficult to estimate. However, we include a range of parameters to quantify at least part of the systematic error component. In particular,

we explore alternative parametrizations that cannot be easily included in the error budget, in order to include: the sensitivity to the Hβ photometry, extinction laws, evolution corrections due to the cluster stellar evolution, the robustness of the slope by means of bootstrap sample test and the sensitivity of H_0 to changes in the sample.

- Two samples: S1 with 107 or S2 with $z < 0.1$ 92 HIIGs;

- Two different sources for the Hβ photometry: [5] (Ch14) or SDSS;

- Two formulations for the luminosity distance for the HIIG: $D_L = H_0/cz$ (LR) or full ΛCDM cosmology with $\Omega_\Lambda = 0.71$.

- For all cases we use two different extinction laws: [1] (C00) or [10] (G03).

- We have included in the estimate of the evolution correction the contribution of an underlying older stellar population and of the differential extinction.

2.3. Cosmological parameters constraints

To calculate the parameters of the $L - \sigma$ relation in a unified way including HIIGs and GHIIRs, we define the following likelihood function

$$\mathcal{L} \propto \exp\left(-\frac{1}{2}\chi^2_{HII}\right), \tag{6}$$

where

$$\chi^2_{HII} = \sum_n \frac{(\mu_0(\log f, \log \sigma | \alpha, \beta) - \mu_\theta(z|\theta))^2}{\epsilon^2} \tag{7}$$

and where μ_0 is the distance modulus calculated from a set of observables as

$$\mu_0 = 2.5(\alpha + \beta \log \sigma - \log f - 40.08). \tag{8}$$

Here α and β are the $L - \sigma$ relation's intercept and slope, respectively, $\log \sigma$ is the logarithm of the measured velocity dispersion and $\log f$ is the logarithm of the measured flux. For HIIG the theoretical distance modulus, μ_θ, is given as

$$\mu_\theta = 5 \log d_L(z, \theta) + 25, \tag{9}$$

where z is the redshift, d_L is the luminosity distance in Mpc and θ is a given set of cosmological parameters. For GHIIRs, the value of μ_θ is inferred from primary indicators and finally ϵ^2 are the weights in the likelihood function.

The luminosity distance d_L of the sources tracing the Hubble expansion is employed to calculate the theoretical distance moduli. We define, for convenience, an extra parameter independent of the Hubble constant as:

$$D_L(z, \theta) = (1 + z) \int_0^z \frac{dz'}{E(z', \theta)}, \tag{10}$$

106

i.e., $d_L = cD_L/H_0$. Here $E(z.\theta)$ for a flat Universe is given by

$$E^2(z, \theta) = \Omega_r(1 + z)^4 + \Omega_m(1 + z)^3 + \Omega_w(1 + z)^{3y} \exp\left(\frac{-3w_a z}{1 + z}\right) \qquad (11)$$

with $y = 1 + w_0 + w_a$. The parameters w_0 and w_a refer to the DE EoS, the general form of which is

$$p_w = w(z)\rho_w \qquad (12)$$

with ρ_w the pressure and ρ_w the density of the postulated Dark Energy fluid. Different DE models have been proposed and many are parametrized using a Taylor expansion around the present epoch:

$$w(a) = w_0 + w_a(1 - a) \Longrightarrow w(z) = w_0 + w_a\frac{z}{1 + z}. \qquad (13)$$

The cosmological constant is just a special case of DE, given for $(w_0, w_a) = (-1, 0)$, while the so called wCDM models are such that $w_a = 0$ but w_0 can take values $\neq -1$.

2.4. Joint analysis

A joint-likelihood analysis with the CMB and BAO probes is performed on the full sample using the h-free likelihood method. Combining HIIG, CMB and BAO yields $\Omega_m = 0.298 \pm 0.012$ and $w_0 = -1.005 \pm 0.051$, fully consistent with the ΛCDM model. It is clear that the solution space of HIIG/CMB/BAO, although less constrained, is certainly compatible with the solution space of SNIa/CMB/BAO.

3. Results

This work presents observational constraints of the cosmological parameters and the determination of the local value of the Hubble constant making use of the GHIIRs in nearby galaxies and HIIG local and at high-z, the results are summarized in the Figures 1, 2, 3, 4 and 5, where we describe the local $L - \sigma$ relation followed by GHIIRs, the determination of the local value of the Hubble constant, the local $L - \sigma$ relation, the Hubble diagram tracing local GHIIRs up to high-z HIIG, the space of solutions in the cosmological parameters and the joint analysis of the other tracers of the Hubble expansion.

4. Conclusions and future perspectives

- Our best estimate of the Hubble parameter is 71.0 ± 2.8 (random) ± 2.1 (systematic) km s^{-1} Mpc^{-1}. This result is the product of an independent approach and, although at present less precise than the latest SNIa results, it is amenable to substantial improvement.

- We have used the $L - \sigma$ distance indicator to derive an independent local value of the Hubble parameter H_0. To this end we have combined new data for 36 GHIIRs in 13 galaxies of the "anchor sample" that includes the megamaser
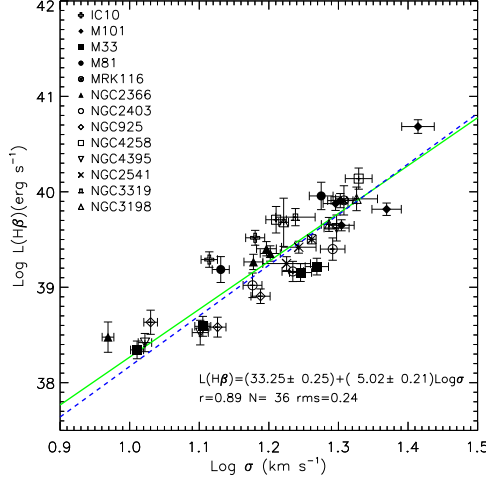
Figure 1: $L - \sigma$ relation for the GHIIRs. The adopted distances to the parent galaxies come from of Cepheids. The green solid line is the fit to the data given in the inset and the dashed line is the fit to the anchor sample of [4]. Taken from [7]
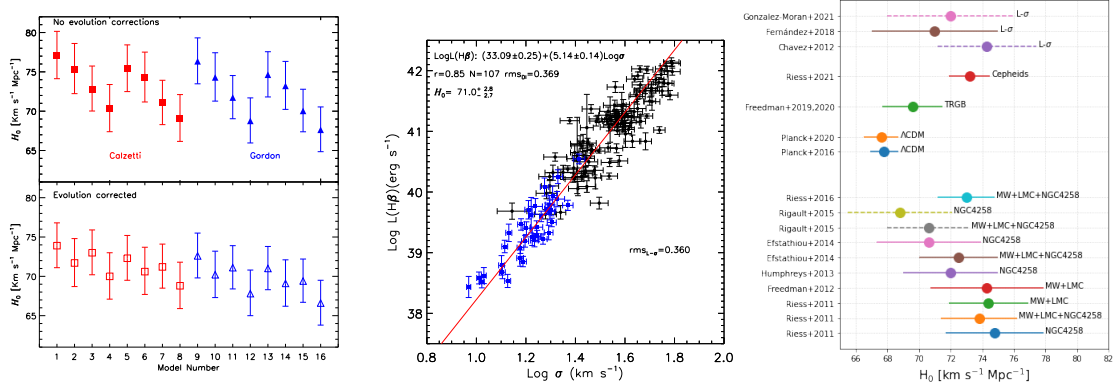
Figure 2: Left upper: Resulting H_0 without correcting the luminosities for evolution. Left Bottom: Same as the top panel, but using the fluxes corrected for evolution. As discussed in [7], the difference between models 1-8 (in red) and models 9-16 (in blue) is the adopted extinction law as indicated by the figure legends. Middle: The $L - \sigma$ relation for the [5] sample using the velocity dispersions in the original paper; the fluxes have been corrected using [10] extinction law. The solid line is the fit to the HIIGs. The inset equation is the distance indicator, where the slope is obtained from the fit to the HIIG and the Zp determined following the procedure described in the text. Right: Our main result incorporating the evolution correction, is $H_0 = 71.0 \pm 3.5$ km s^{-1} Mpc^{-1} (random+systematic) a value that is half way between the most recent determination from Planck and SNIa. Taken and updated from [7].

108
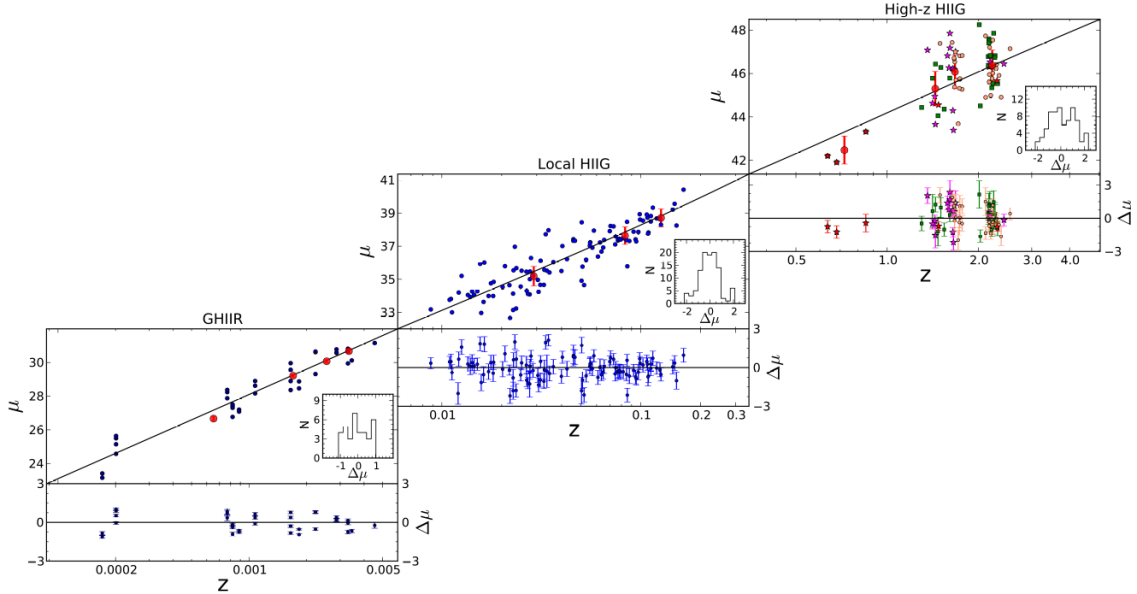
Figure 3: Hubble diagram connecting our local and high redshift samples up to $z \sim 2.6$. Red circles represent averages of the distance moduli in redshift bins. The continuous line corresponds to $\Omega_m = 0.249$ and $w_0 = -1.18$ (our best cosmological model using only HIIG). The insets show the distribution of the residuals of the fit that are plotted in the bottom panels. Taken from [9].

galaxy NGC 4258, with the data for 107 HIIG from [5]. Our new data is the result of the first four years of observation of our primary sample of 130 GHIIRs in 73 galaxies with Cepheid distances.

- Regarding future improvement of the $L-\sigma$ distance indicator, our first priority is to increase the anchor sample from the present 13 galaxies to the 43 galaxies of our primary sample. Much of the error in the value of H_0 is related to the uncertainty in the value of the slope of the $L-\sigma$ relation, thus it will be important to include low luminosity HIIG, i.e., those with luminosities similar to the luminosity of GHIIR, and also GHIIR in more distant galaxies.

- The addition of a second parameter in the $L-\sigma$ relation can lead to an important improvements in the distance indicator. In particular the size of the starforming region has proven to be a real possibility potentially reducing the scatter by about 40%. We also plan to expand the analysis to include TRGB distances to the galaxies in the primary sample. Finally the evolution correction needs a quantitative approach that takes into account the underlying stellar continuum and differential reddening effect in the measurement of the EW of the emission lines.

109
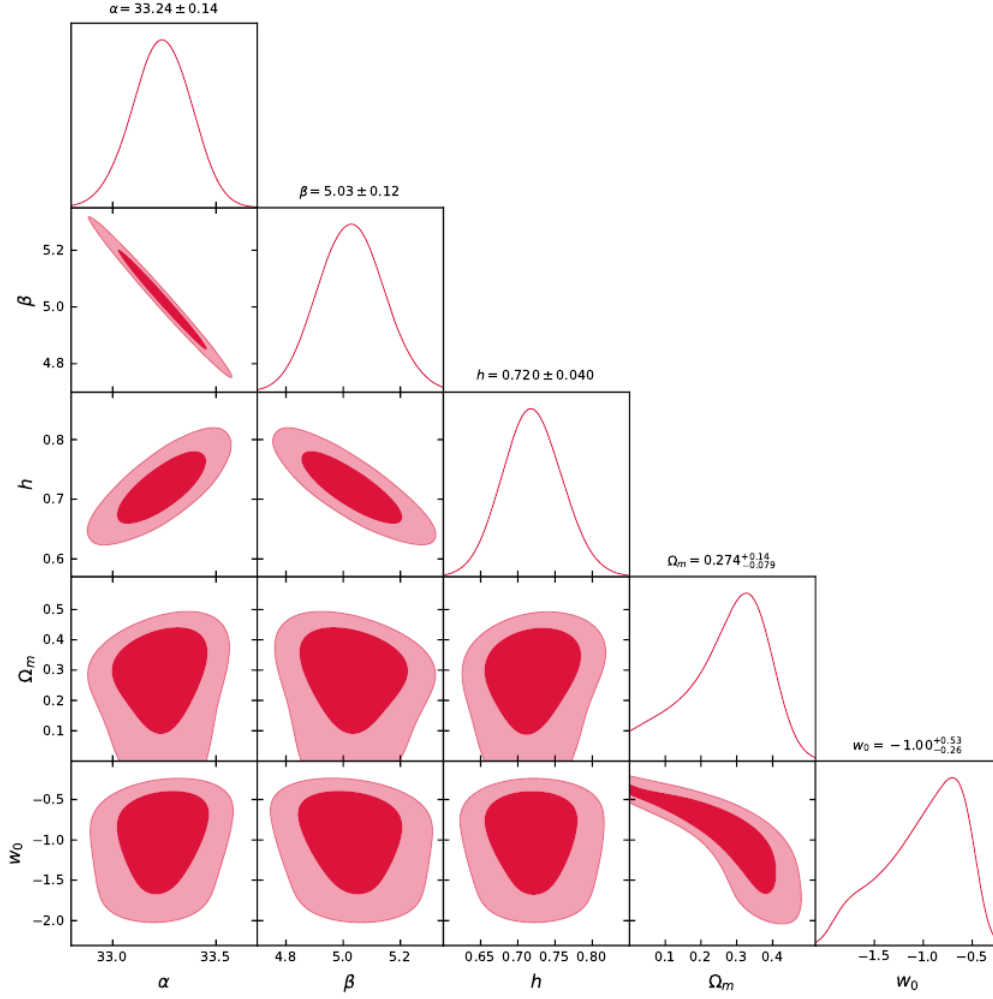
Figure 4: Likelihood contours corresponding to the 1σ and 2σ confidence levels in the $\{\alpha, \beta, h, \Omega_m, w_0\}$ space for the Global sample. Taken from [9].

- We have analyzed a set of 181 HIIG in the redshift range $0.01 < z < 2.6$. The sample includes a new set of 41 HIIG observed with KMOS at the VLT in the range of redshift $1.3 < z < 2.6$. Using the $L - \sigma$ distance indicator, we have constrained cosmological parameters independently of the value of the Hubble constant.

- Regarding the restrictions of the Ω_m parameter we found that HIIG alone constrain the matter density to high significance. Using the Full sample of 181 HIIG and the MultiNest MCMC procedure, we find $\Omega_m = 0.244^{+0.040}_{-0.049}$ (stat).

- HIIG also constrain the value of the DE EoS parameter in the $\{\Omega_m, w_0\}$ plane independently of the value of the Hubble constant and we find $\Omega_m = 0.249^{+0.11}_{-0.065}$ and $w_0 = -1.18^{+0.45}_{-0.41}$ (stat).

110

$\Omega_m = 0.298 \pm 0.012$

$w_0 = -1.005 \pm 0.051$

HIIG+CMB+BAO (190)
HIIG (181)
CMB (3)
BAO (6)

$\Omega_m = 0.2940 \pm 0.0057$

$w_0 = -1.024 \pm 0.022$

SNIa+CMB+BAO (1057)
SNIa (1048)
CMB (3)
BAO (6)

(a) HIIG + CMB + BAO

(b) SNIa + CMB + BAO
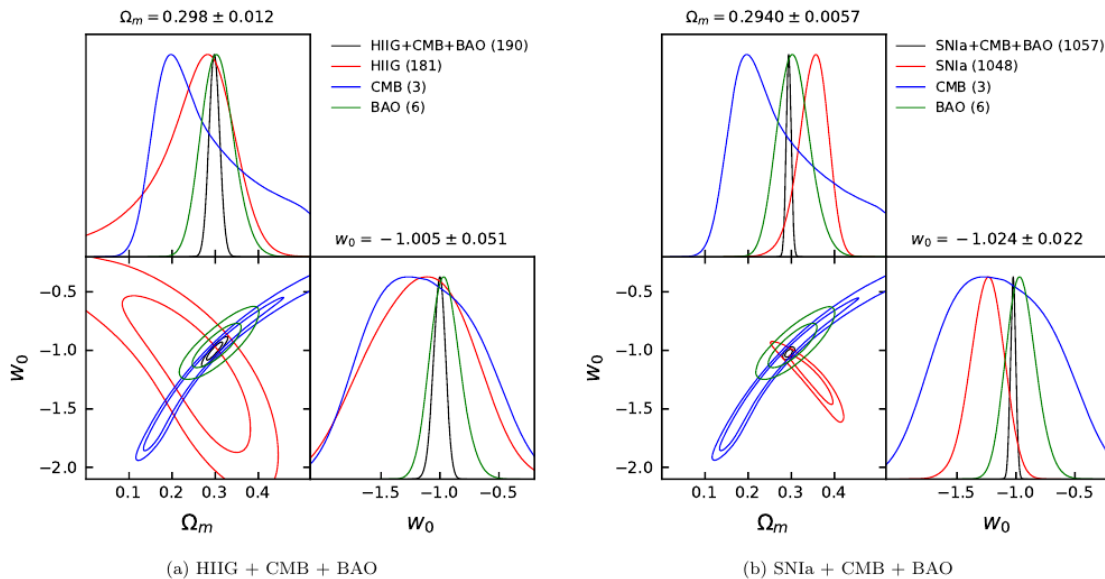
Figure 5: Likelihood contours corresponding to the 1σ and 2σ confidence levels in the $\{\Omega_m, w_0\}$ space for a) the joint sample of HIIG, CMB and BAO and b) the joint sample of SNIa, CMB and BAO. We show in the inset the sample size used in the analysis. Only statistical uncertainties are shown. Taken from [9].

- Combining HIIG, CMB and BAO yields our best estimates $\Omega_m = 0.298 \pm 0.012$ and $w_0 = -1.005 \pm 0.051$, which, although less constrained, are certainly compatible with the solution space of SNIa/CMB/BAO using the SNIa Pantheon sample.

- The HIIG results are comparable with those obtained from SNIa a decade ago when the sample of SNIa was around few hundred. This is consistent with the main conclusion of [13] that a sample of at least 500 HIIG (which we aim to procure in the forthcoming developments of the project) is needed to have errors comparable with those of the SNIa approach.

Acknowledgements

References

[1] Calzetti D., Armus L., Bohlin R. C., Kinney A. L., Koornneef J., Storchi-Bergmann T.: 2000, http://dx.doi.org/10.1086/308692, http://adsabs.harvard.edu/abs/2000ApJ...533..682C, 533, 682.

[2] Cao S., Ryan J., Ratra B., 2021, http://dx.doi.org/10.1093/mnras/stab942, https://ui.adsabs.harvard.edu/abs/2021MNRAS.504..300C, 504, 300.

[3] Cao S., Ryan J., Ratra B., 2022, http://dx.doi.org/10.1093/mnras/stab3304, https://ui.adsabs.harvard.edu/abs/2022MNRAS.509.4745C, 509, 4745.

[4] Chávez R., Terlevich E., Terlevich R., Plionis M., Bresolin F., Basilakos S., Melnick J., 2012, http://dx.doi.org/10.1111/j.1745-3933.2012.01299.x, http://adsabs.harvard.edu/abs/2012MNRAS.tmpL.484C, p. L484

[5] Chávez R., Terlevich R., Terlevich E., Bresolin F., Melnick J., Plionis M., Basilakos S., 2014, http://dx.doi.org/10.1093/mnras/stu987, http://adsabs.harvard.edu/abs/2014MNRAS.442.3565C, 442, 3565

[6] Chávez R., Plionis M., Basilakos S., Terlevich R., Terlevich E., Melnick J., Bresolin F., González-Morán A. L., 2016, http://dx.doi.org/10.1093/mnras/stw1813, http://adsabs.harvard.edu/abs/2016MNRAS.462.2431C, 462, 2431

[7] Fernández-Arenas D., et al., 2018, http://dx.doi.org/10.1093/mnras/stx2710, http://adsabs.harvard.edu/abs/2018MNRAS.474.1250F, 474, 1250

[8] González-Morán A. L., et al., 2019, http://dx.doi.org/10.1093/mnras/stz1577, https://ui.adsabs.harvard.edu/abs/2019MNRAS.487.4669G, 487, 4669

[9] González-Morán A. L., et al., 2021, http://dx.doi.org/10.1093/mnras/stab1385, https://ui.adsabs.harvard.edu/abs/2021MNRAS.505.1441G, 505, 1441

[10] Gordon K. D., Clayton G. C., Misselt K. A., Landolt A. U., Wolff M. J., 2003, http://dx.doi.org/10.1086/376774, http://adsabs.harvard.edu/abs/2003ApJ...594..279G, 594, 279

[11] Kennicutt Jr. R. C., 1979, http://dx.doi.org/10.1086/156858, http://adsabs.harvard.edu/abs/1979ApJ...228..394K, 228, 394

[12] Melnick J., et al., 2017, http://dx.doi.org/10.1051/0004-6361/201629728, http://adsabs.harvard.edu/abs/2017A%26A...599A..76M, 599, A76

[13] Plionis M., Terlevich R., Basilakos S., Bresolin F., Terlevich E., Melnick J., Chavez R., 2011, http://dx.doi.org/10.1111/j.1365-2966.2011.19247.x, http://adsabs.harvard.edu/abs/2011MNRAS.416.2981P, 416, 2981

[14] Ruan C.-Z., Melia F., Chen Y., Zhang T.-J., 2019, http://dx.doi.org/10.3847/1538-4357/ab2ed0, https://ui.adsabs.harvard.edu/abs/2019ApJ...881..137R, 881, 137

[15] Sandage A., 1962, in McVittie G. C., ed., IAU Symposium Vol. 15, Problems of Extra-Galactic Research. p. 359

[16] Sérsic J. L., 1960, http://adsabs.harvard.edu/abs/1960ZA.....50..168S, 50, 168

[17] Terlevich R., Melnick J., 1981, http://adsabs.harvard.edu/abs/1981MNRAS.195..839T, 195, 839

[18] Terlevich R., Terlevich E., Melnick J., Chávez R., Plionis M., Bresolin F., Basilakos S., 2015, http://dx.doi.org/10.1093/mnras/stv1128, http://adsabs.harvard.edu/abs/2015MNRAS.451.3001T, 451, 3001

[19] Tsiapi P., et al., 2021, http://dx.doi.org/10.1093/mnras/stab1933, https://ui.adsabs.harvard.edu/abs/2021MNRAS.506.5039T, 506, 5039

[20] Wu Y., Cao S., Zhang J., Liu T., Liu Y., Geng S., Lian Y., 2020, http://dx.doi.org/10.3847/1538-4357/ab5b94, https://ui.adsabs.harvard.edu/abs/2020ApJ...888..113W, 888, 113

[21] Yennapureddy M. K., Melia F., 2017, http://dx.doi.org/10.1088/1475-7516/2017/11/029, https://ui.adsabs.harvard.edu/abs/2017JCAP...11..029Y, 2017, 029

GAUGE CPT EXPERIMENTAL PREDICTIONS

Kurt Koltko

Denver, Colorado, USA
g8cpt@protonmail.com

Abstract: We present the weak field force law due to those components of the gauge CPT field which are a complex extension of the metric spin connection. Even though there is a resemblance to Modified Newtonian Dynamics (MOND), we point out that there is no fundamental relation between gauge CPT and MOND. However, we view MOND as an important empirical insight which allows us to determine the physical strength constant in the weak gauge CPT force law. Four simple experimental predictions are presented to validate gauge CPT. Additional speculative experimental and observational predictions are briefly discussed.

Keywords: gauge theory, CPT symmetry, experimental tests, nuclear reactors, accelerators, neutrinos

PACS: 11.15.-q, 24.80.+y, 11.30.-j, 29.20.-c, 14.60.Lm

In this paper we propose four experiments obtained from the gauge theory of CPT transformations. An introduction to gauging the CPT symmetry as well as its relation to the Baryonic Tully-Fisher Law (BTFL) - the basis for the experiments – can be found in [5]. The development of the theory can be found in [1], [2], [3], [4].

Our starting point will be the arguments found in [5] showing that the flat galactic rotation curves and the BTFL for spiral galaxies arise from the neutrinos produced by stellar fusion sourcing the gauge CPT field. The extension of general relativity (GR) from gauge CPT results in the replacement of the GR metric spin connection, $\omega_{\mu ab}$, by $\omega_{\mu ab} + 2\beta x_{\mu ab}$, where β is the coupling constant associated with the new gauge CPT field X_μ.[1] Gauge CPT results in a mass independent acceleration, a_X, sourced by fermion chirality. The point source, weak field approximation due to the fixed neutrino chirality is [5]:

$$a_X = k\frac{(I_\nu)^{\frac{1}{2}}}{r},$$

---

[1] $X_\mu = x_{\mu I}I + x_{\mu 5}\gamma^5 + x_{\mu ab}\sigma^{ab}$, where $\sigma^{ab} = \frac{1}{4}[\gamma^a, \gamma^b]$, γ^a are the familiar Dirac gamma matrices, and $x_{\mu(\dots)}$ are the dynamical field components of the new gauge field. The physical implications of the $x_{\mu I}$ and $x_{\mu 5}$ components are not discussed in this paper.

where I_ν is the total neutrino luminosity (power), r is the distance from the neutrino source, and k is the physical constant associated with gauge CPT analogous to Newton's gravitational constant, G_N. The $x_{\mu ab}$ field equation and source term, $4i\overline{\psi}\sigma_{ab}\gamma_\mu\psi$, are found in [5]. The reasons for the neutrinos produced by stellar fusion reactions being the source of a_X can be found in [1], [3]. An additional discussion regarding the appearance of $(I_\nu)^{\frac{1}{2}}$ as the source is in the appendix.

To determine the value of k, we turn to MOND by viewing it as an important, empirical insight. We first note that a_X has the same form, albeit with a different source term, as the deep MOND regime gravitational acceleration (e.g., [6]), a_m, due to a point mass, M:

$$a_m = (G_N a_0)^{\frac{1}{2}}\frac{(M)^{\frac{1}{2}}}{r},$$

where a_0 is the MOND acceleration parameter $(1.2\times 10^{-10}\,\text{m/s}^2)$, and r is the distance to the point mass. However, a_X comes from a gauge theory of a verified symmetry whereas a_m comes from a proposed change to Newton's second law at extremely low accelerations $\leq a_0$. Because of the success in predicting flat rotation curves of spiral galaxies, we view the MOND acceleration as an empirical law from which we can determine k.

We use our Sun as the physical setting for determining k because its relevant properties are known. We begin by noticing that because of the r^{-1} dependence of a_X, the strength of the gauge CPT force will always eventually overtake the r^{-2} gravitational force of a star. The distance from the Sun's center, R_s, at which the gauge CPT force equals the gravitational force will be taken as the onset of the MOND regime:

$$\frac{k\,(I_{\nu s})^{\frac{1}{2}}}{R_s} = \frac{G_N M_s}{R_s^2} = a_0,$$

where the solar values are $I_{\nu s} = (.023)\times 3.83\times 10^{26}\,\text{W}$ [7] and $M_s = 1.99\times 10^{30}\,\text{kg}$. From these two equations, we obtain k:

$$k = \left(\frac{a_0 G_N M_s}{I_{\nu s}}\right)^{\frac{1}{2}} = 4.25\times 10^{-8}\,\frac{m}{(\text{kg}\cdot\text{s})^{\frac{1}{2}}}.$$

To see if this is a reasonable value, we estimate the flat rotation curve velocity, v_c, of the Milky Way by approximating our Galaxy as a spherically symmetric system with our Sun taken as the average star. We equate the value of a_X with the centripetal acceleration:

$$k\frac{I_{\nu\text{gal}}^{\frac{1}{2}}}{r_{\text{edge}}} = \frac{v_c^2}{r_{\text{edge}}}, \quad \text{or} \quad v_c = \left(kI_{\nu\text{gal}}^{\frac{1}{2}}\right)^{\frac{1}{2}},$$

where r_{edge} is the radius of the Milky Way disc. Using the values $I_{\nu gal}\approx 0.023 L_{\text{gal}}$, and $L_{\text{gal}}\approx 3\times 10^{10}L_{\text{sun}}$ (L being the photon luminosity), we obtain $v_c\approx 148\,\text{km/s}$ which is about $\frac{2}{3}$ of the actual value. So, given the approximations, we accept the above value of k for the following experimental predictions.

The first two experimental predictions use a nuclear reactor as a tiny proxy for a galaxy. Instead of the neutrinos produced by stellar fusion, the source of the weak field gauge CPT force is the antineutrinos produced by the decay of fission fragments in the reactor core. Just like the stellar neutrinos, the reactor antineutrinos are relativistic, have negligible interaction with anything, and have fixed chirality. As with neutrinos, we assume that the force sourced by the antineutrinos is attractive. However, as suggested in [3], the possibility of a repulsive force sorced by antineutrinos must be kept in mind because a third of the $x_{\mu ab}$ source terms have opposite sign for neutrinos and antineutrinos.

The first experiment is simple – just test the value of a_X at various distances from the reactor core using precision gravimeters or accelerometers. For example, by treating a 200 MW reactor core as a point antineutrino source with 5% of the energy carried away by antineutrinos, we obtain from the above a_X equation:

$$a_{X\text{reactor}} \approx \frac{1.34 \times 10^{-4}}{r} \frac{\text{m}}{\text{s}^2}.$$

Equipment exists which can measure this. Obviously, this result is an approximation for the actual distribution of cylindrical fuel rods. Because the a_X formula was derived from a linear weak field approximation argument [5], the actual reactor $a_X(r)$ expression can be obtained by the vector addition of the $a_X(r)$ contributions of the individual pellets contained in the fuel rods.

The second experiment is conceptually simple – test the time differences on clocks placed at various distances from the reactor core. Because the effect of $x_{\mu ab}$ is to replace the GR $\omega_{\mu ab}$ by $\omega_{\mu ab} + 2\beta x_{\mu ab}$, we expect a gravitational redshift contribution due to $x_{\mu ab}$. The effective weak-field potential, Φ_X, associated with a_X is

$$\Phi_X = -kI_\nu^{\frac{1}{2}} \ln r.$$

Therefore, the associated Φ_X frequency (f) shift (at various distances from a 200 MW reactor core treated as a point antineutrino source) is taken as in GR:

$$\frac{\Delta f}{f} \approx \frac{\Delta \Phi_X}{c^2} \approx \frac{kI_\nu^{\frac{1}{2}}}{c^2} \ln\left(\frac{r_2}{r_1}\right) \approx 1.5 \times 10^{-21} \ln\left(\frac{r_2}{r_1}\right).$$

Unfortunately, this will be difficult to measure because it will require the most sensitive atomic clocks operating for a long time.

Because of the intense (anti)neutrino beams produced at some accelerators for various experiments, we derive the formulae for the above experiments to be done in the center of the beam at different distances along the beamline. The key to the simple derivation of accelerator predictions is that the (anti)neutrinos are one of only two particles produced in the decay of the pions and kaons produced by the accelerator proton beam hitting a dense target. In the rest frame of the decaying pion, the distribution of (anti)neutrinos will obviously be isotropic and monoenergetic

(treating the neutrinos as massless). Hence, the decaying pions can themselves be viewed as tiny nuclear reactors or stars as far as the production of (anti)neutrinos is concerned. Therefore, we can calculate Φ_X in the rest frame and then transform to the lab frame to find Φ_X there and subsequently calculate the acceleration and frequency shift.

Our starting point will be simple kinematical relations from special relativity. The first step is to find the neutrino energy, E_0, in the rest frame of the decaying pion, π. As routinely done, we treat the neutrino as a massless particle because it has a small mass and is relativistic. Because the overwhelmingly dominant decay channel of the pion is just a muon, μ, and neutrino, ν_μ, we immediately obtain two elementary equations using the conservation of momentum and of energy. Solving for E_0, one easily obtains

$$E_0 = \frac{\left(m_\pi^2 - m_\mu^2\right)c^2}{2m_\pi},$$

where m_π, m_μ are the masses of the pion and muon, respectively, and c is the speed of light. The measured value of the neutrino energy in the lab frame, E_ν, enables us to calculate the relative velocity, v, between the pion rest frame and lab frame by the simple transformation of the neutrino energy-momentum four vector: $E_\nu = \gamma E_0 \left(1 + \beta\right)$, where $\beta = |v|/c$, and $\gamma = \left(1 - \beta^2\right)^{-\frac{1}{2}}$. One immediately obtains

$$\beta = \frac{E_\nu^2 - E_0^2}{E_\nu^2 + E_0^2}.$$

We can now determine the transformation of the neutrino luminosity magnitude, I_ν, in the lab frame from the neutrino luminosity in the pion rest frame, I_0, where we define neutrino luminosity as the neutrino energy in a pulse divided by the pulse duration. Using the energy transformation and time dilation, we have $I_\nu = I_0(1+\beta)$.

To obtain Φ_X in the lab frame, we again identify Φ_X as an extension of the gravitational potential because of the replacement of the GR metric spin connection, $\omega_{\mu ab}$, by $\omega_{\mu ab} + 2\beta x_{\mu ab}$. This results in a modification of the metric tensor, $g_{\mu\nu}$, because of the equivalency between the metric spin connection formulation and the standard $(g_{\mu\nu})$ formulation of GR. Assuming the weak-field, stationary scenario in the accelerator neutrino beam, we have $g_{00} \approx 1 + \frac{2\Phi_X}{c^2}$ and $g_{ik} \approx -\delta_{ik}$ for i, k spatial coordinates $(+, -, -, -)$. Now, we can transform Φ_X from the rest frame of the pion to the lab frame via the Lorentz boost, $\Lambda_a^{\ b}$, connecting the two frames: $g_{00}^{lab} = \Lambda_0^{\ a}\Lambda_0^{\ b}g_{ab}^\pi$. We define the x spatial coordinate in the lab frame by the origin at the pion decay location, and the narrow neutrino beam axis defines the x-axis with the positive direction aligned with the neutrino flow. The only non-vanishing $\Lambda_a^{\ b}$ are $\Lambda_0^{\ 0} = \cosh\omega$ and $\Lambda_0^{\ 1} = -\sinh\omega$, where $\gamma = \cosh\omega$. So, $g_{00}^{lab} = \Lambda_0^{\ a}\Lambda_0^{\ b}g_{ab}^\pi = g_{00}^\pi(\cosh^2\omega) - \sinh^2\omega$. This gives us: $\Phi_X^{lab} = \frac{c^2}{2}[g_{00}^\pi(\cosh^2\omega) - \sinh^2\omega - 1] = \frac{c^2}{2}[(g_{00}^\pi - 1)\cosh^2\omega] = \Phi_X^\pi \cosh^2\omega = \gamma^2\Phi_X^\pi$. From the above reactor formula, we have $\Phi_X^\pi = k(I_0)^{\frac{1}{2}}\ln(\frac{r}{\gamma})$, where r is the lab frame distance from the origin to the point of interest. So, we

finally get

$$\Phi_X^{\text{lab}}(r) \approx k\gamma^2 \left(\frac{I_\nu}{1+\beta}\right)^{\frac{1}{2}} \ln\left(\frac{r}{\gamma}\right), \quad \text{and} \quad a_X^{\text{lab}}(r) = -\frac{\partial \Phi_X^{\text{lab}}(r)}{\partial r} \approx -\frac{k\gamma^2}{r}\left(\frac{I_\nu}{1+\beta}\right)^{\frac{1}{2}}.$$

To obtain a numerical estimation of the clock and acceleration experiments, we turn to parameters found in [8] regarding the early Fermilab LBNF and DUNE experiments. We also assume that the pions all decay at some average point. The parameters are: $E_\nu = 2.5\,\text{GeV}$, 7.5×10^{13} protons hitting a graphite target per pulse (75% of those producing desired (anti)neutrinos), and $10\mu s$ pulse duration. These numbers, along with the rest masses of the pion and muon, give from above: $\beta = 0.9997$, $\gamma = 40.8$, and $I_\nu = 2.25 \times 10^9\,J/s$ (during pulse). Finally, we obtain the following Fermilab (Fl) accelerator estimates during the pulse:

$$a_X^{Fl}(r) \approx \frac{2.37}{r}\,\text{m/s}^2, \quad \text{and} \quad \frac{\Delta f}{f} \approx 2.63 \times 10^{-17} \ln\left(\frac{r_2}{r_1}\right).$$

So, these numbers are a significant improvement over the reactor estimates, albeit only during the pulse duration. Also, because both antineutrinos or neutrinos can be produced at accelerators, the attractive or repulsive nature of the X_μ force can be experimentally determined.

The accelerator formula can be easily generalized to points outside of the neutrino beamline – even to positions *before* the proton target. Because the neutrino distribution is spherically symmetric in the pion rest frame, $r^\pi = (x^2 + y^2 + z^2)^{\frac{1}{2}}$, where y and z are the coordinates perpendicular to the neutrino beamline. When transforming to the lab frame, y and z do not change. Therefore, one immediately obtains the generalized accelerator formula

$$\Phi_X^{\text{lab}}(x, y, z) \approx \frac{k\gamma^2}{2}\left(\frac{I_\nu}{1+\beta}\right)^{\frac{1}{2}} \ln(x^2\gamma^{-2} + y^2 + z^2).$$

(Obviously, the arguments of logarithms must be dimensionless. We are using a scale factor of 1 meter in this paper.)

We now offer a couple of other conjectures similar to the comments found in [5]. First, inspired by thermal neutron experiments used to test GR, interference effect experiments can be carried out at accelerator neutrino beams by putting one path in the neutrino beamline and recombining with another path outside of the beamline. Second, we speculate that the $x_{\mu ab}$ terms may be of relevance to the disagreement of G_N measured by various experiments. Because these terms act on matter in the same manner (via the coupling to σ^{ab}) as the expected gravitational $\omega_{\mu ab}$, some experiments might be susceptible to the flux of solar neutrinos passing through them. Variations in the experimental results due to the apparatus orientation with solar neutrinos, as well as neutrino flux variations due to time of day and season, may occur. It is interesting to note that the variation of a_X at the Earth's surface from

day to night due to the flux of solar neutrinos is given by $\frac{\delta a_X}{a_X} \approx \frac{-2r_E}{R_E} \approx 8.5 \times 10^{-5}$ – about 1.8 times larger than $\frac{\delta G_N}{G_N}$, where r_E is the Earth's radius, and R_E is the Earth's distance from the Sun.

Also, galactic neutrino events should source an a_X. For example, the neutrino burst emitted at the beginning of a type II supernova will source an a_X. This should appear as a spike in gravitational wave detectors coincident with the arrival of the supernova neutrinos. Other qualitative astrophysical comments can be found in [5], however, the comment regarding GR predictions near black holes needs amending. The author has subsequently learned that non-fusion sourced neutrinos can be produced by black holes accreting significant amounts of matter via the collision of extremely high energy jet material with surrounding matter. Presumably, the neutrino emission will be narrowly confined along the jet directions (parallel and antiparallel to the black hole rotation axis) much like the neutrino distribution produced at accelerators. If there is no significant accretion disk, then no neutrinos are sourced by the black hole, hence, no X_μ modifications to GR predictions near the black hole. If one can observe stellar motion near a supermassive black hole with accretion disks and jets, then deviations from GR will occur due to the generalized accelerator formula for a_X.

Appendix

We present a brief supplementary discussion to that found in [5] regarding the form of the weak field a_X law. The r^{-1} dependence has been adequately covered in [1], [3], [5], so we present two more arguments for the $(I_\nu)^{\frac{1}{2}}$ source term. First, we examine the field equation in [5] obtained from varying the action with respect to $x_{\mu ab}$:

$$
\begin{aligned}
4\beta D_\nu (\partial^\nu x_{cd}^\mu &- \partial^\mu x_{cd}^\nu) Tr[(\sigma^{ab})^\dagger \sigma^{cd}] \\
&+ 2\beta\{(\omega_{\nu rs} + 2\beta x_{\nu rs}^*)(\partial^\nu x_{cd}^\mu - \partial^\mu x_{cd}^\nu) Tr[[\sigma^{ab}, \sigma^{rs}]^\dagger \sigma^{cd}]\} \\
&+ 2\beta D_\nu (2\beta x_{cd}^\nu x_{rs}^\mu + \omega_{cd}^\nu x_{rs}^\mu + \omega_{rs}^\mu x_{cd}^\nu) Tr[(\sigma^{ab})^\dagger [\sigma^{cd}, \sigma^{rs}]] \\
&- \{\beta(\omega_{\nu cd} + 2\beta x_{\nu cd}^*)(2\beta x_{mk}^\mu x_{rs}^\nu + \omega_{mk}^\mu x_{rs}^\nu + \omega_{rs}^\nu x_{mk}^\mu) Tr[[\sigma^{ab}, \sigma^{cd}]^\dagger [\sigma^{mk}, \sigma^{rs}]]\} \\
&+ 8\kappa\eta^{bc}(e^{a\mu}e^{n\rho} - e^{n\mu}e^{a\rho})(\omega_{\rho cn} + 2\beta x_{\rho cn}^*) \\
&+ 8\kappa\eta^{ac}(e^{b\mu}e^{n\rho} - e^{n\mu}e^{b\rho})(\omega_{\rho nc} + 2\beta x_{\rho nc}^*) \\
=& 4i\overline{\psi}\sigma^{ab}\gamma^\mu\psi + 8\kappa D_\nu(e^{a\nu}e^{b\mu} - e^{a\mu}e^{b\nu}).
\end{aligned}
$$

As discussed in [5], the terms with coefficient κ ($\kappa = (-16\pi G_N)^{-1}$) identically satisfy a new metric spin connection with $\omega_{\mu ab}$ replaced by $\omega_{\mu ab} + 2\beta x^*$, so we will ignore those and focus on the rest of the terms. We interpret these terms as the field equations for $x_{\mu ab}$ (coupled to $\omega_{\mu ab}$). In the very, very slowly changing regime with very weak gravity and very far from the neutrino source, we have the $x_{(\dots)}\partial x_{(\dots)}$ and $x_{(\dots)}x_{(\dots)}$ terms dominating over the $D_\nu \partial x^{(\dots)}$, $\omega_{(\dots)}$, and $x_{(\dots)}x_{(\dots)}x_{(\dots)}$ terms. Because the neutrino source term, $4i\overline{\psi}\sigma^{ab}\gamma^\mu\psi$, is proportional to E_ν, we will have

119

$x_{(...)} \sim (E_\nu)^{\frac{1}{2}}$, hence the $(I_\nu)^{\frac{1}{2}}$ dependence. We apply the exact same argument to the Palatini variation with respect to $\omega_{\mu ab}$ of the Lagrangian found in [5]. The Palatini variation results in:

$$
\begin{aligned}
\kappa\eta^{bc}&(e^{n\mu}e^{a\rho} - e^{a\mu}e^{n\rho})(\omega_{\rho cn} + \beta x^*_{\rho cn} + \beta x_{\rho cn}) \\
&+ \kappa\eta^{ac}(e^{n\mu}e^{b\rho} - e^{b\mu}e^{n\rho})(\omega_{\rho nc} + \beta x^*_{\rho nc} + \beta x_{\rho nc}) \\
&+ \frac{\mathrm{i}}{4}\overline{\psi}\{\sigma^{ab}, \gamma^\mu\}\psi + \frac{\beta^2}{4}\{x^*_{\nu rs}(-\partial^\nu x^\mu_{cd} + \partial^\mu x^\nu_{cd})Tr[[\sigma^{ab}, \sigma^{rs}]^\dagger\sigma^{cd}] \\
&+ x_{\nu rs}(-\partial^\nu x^{*\mu}_{cd} + \partial^\mu x^{*\nu}_{cd})Tr[[\sigma^{ab}, \sigma^{rs}](\sigma^{cd})^\dagger] + \frac{1}{2}x_{\nu rs}(2\beta x^{*\mu}_{mk}x^{*\nu}_{cd} \\
&+ \omega^\mu_{mk}x^{*\nu}_{cd} + x^{*\mu}_{mk}\omega^\nu_{cd})Tr[[\sigma^{ab}, \sigma^{rs}] \cdot [\sigma^{mk}, \sigma^{cd}]^\dagger] \\
&+ \frac{1}{2}x^*_{\nu rs}(2\beta x^\mu_{mk}x^\nu_{cd} + \omega^\mu_{mk}x^\nu_{cd} + x^\mu_{mk}\omega^\nu_{cd})Tr[[\sigma^{ab}, \sigma^{rs}]^\dagger \cdot [\sigma^{mk}, \sigma^{cd}]]\} \\
=&\kappa D_\nu(e^{a\mu}e^{b\nu} - e^{a\nu}e^{b\mu}).
\end{aligned}
$$

This paper is dedicated to the memory of the author's father.

References

[1] Koltko, K.: Attempts to find additional dynamical degrees of freedom in space-time using topological and geometric methods. Ph.D. Thesis, University of South Carolina, 2000.

[2] Koltko, K.: A Gauge theory of CPT transformations to first order. Foundations of Physics Letters 15 (2002), 299–304.

[3] Koltko, K.: Gauge CPT as a possible alternative to the dark matter hypothesis. arXiv 1308.6341 [physics.gen-ph] and cross listed as [astro-ph.GA] (2013).

[4] Koltko, K.: A free-field Lagrangian for a gauge theory of the CPT symmetry. arXiv 1703.10904v3 [physics.gen-ph] and cross listed as [astro-ph.GA], [hep-th] (2018).

[5] Koltko, K.: The baryonic Tully-Fisher law and the gauge theory of CPT transformations. Proceedings of the International Conference: Cosmology on Small Scales 2020, Excessive Extrapolations and Selected Controversies in Cosmology, Prague, September 23–26, 2020, 84–92.

[6] Sanders, Robert H.: Dark Matter – Modified Dynamics: Reaction vs. Prediction. arXiv 1912.00716v1 [astro-ph.GA] (2019).

[7] Bahcall, John N.: Neutrino Astrophysics. Cambridge University Press, 1989.

[8] Kopp, Sacha E.: Accelerator neutrino beams. arXiv physics/0609129v1 [physics.acc-ph] (2006).

HUBBLE–LEMAÎTRE DIAGRAM OF SUPERNOVAE WITHOUT DARK ENERGY

Martín López-Corredoira[1,2], José Ignacio Calvo-Torel[2]

[1] Instituto de Astrofísica de Canarias
38205 La Laguna, Tenerife, Spain
martin@lopez-corredoira.com
[2] Departamento de Astrofísica, Universidad de La Laguna
38206 La Laguna, Tenerife, Spain
alu0101251431@ull.edu.es

Abstract: We make fits to the corresponding Hubble–Lemaître diagram of supernovae Ia with various cosmological models incorporating intergalactic extinction, evolution of the luminosity of supernovae and redshift components due to partially non-cosmological factors. The data are well fitted by the standard model including dark energy, but there is a degeneracy of solutions with several other variables.

Within this degeneracy, some models (Einstein–de Sitter, static and other models), which were previously discarded with this Hubble–Lemaître diagram of supernovae Ia, can give good fits to the data if we introduce a supernova absolute magnitude evolution ~ -0.10 mag Gyr^{-1} or gray extinction $\sim 10^{-4}$ mag Mpc^{-1}. Extiction or evolution may thus mimic the effect of dark energy. A partial non-cosmological redshift component may also mimic dark energy but would require a recalibration of the absolute magnitude different from the local measurements.

(Abridged version of Ref. [1]).

Keywords: cosmology; dark energy; supernovae Ia

PACS: 98.80.Es

1. Introduction

In 1998–1999 Riess et al. [2] and Perlmutter et al. [3] published papers establishing the existence of an accelerated expansion from the analysis of type Ia supernovae (SNe Ia). Measured luminosity distance with supernovae exceeded by up to 0.25 to 0.28 magnitudes that expected in the standard model in the early 1990s (open universe with matter density $\Omega_M \sim 0.2$). This excess could be explained by adding a positive cosmological constant or quintessence. They saw that the fit determines an accelerating expanding universe with 99.5%–99.9% confidence level. With

the more recent, larger and more accurate sample of data by Ref. [4] (Pantheon data), the results of Riess et al. and Perlmutter et al., a universe with a positive cosmological constant, were confirmed with much lower error bars.

There are other ways to obtain a fit to the data of SNe Ia. We next analyze various fits, focusing on scenarios, where no Λ term is included.

2. SNe Ia data: Pantheon

The 'Pantheon' sample of SNe Ia [4] is currently one of the largest samples and with highest-redshift supernova data. Thes redshift range of the sample spans between $z = 0.001$ and $z = 2.3$, extending the range far beyond $z = 1$. We use the version of 2018 of this sample with 1048 SNe.

The function to fit is:

$$y = 10^{0.2m} = A\,D_{L70}, \tag{1}$$

$$A = \frac{70 \text{ km s}^{-1}\text{Mpc}^{-1}}{H_0} 10^{0.2M+5}, \tag{2}$$

where D_{L70} is the calculated luminosity distance (dependent on the cosmology) for $H_0 = 70\,\text{km s}^{-1}\,\text{Mpc}^{-1}$. Thus, both H_0 and M (absolute magnitude) are included in A.

3. Fits with various cosmological models

We can fit Pantheon data for either the standard cosmological ΛCDM model or alternative cosmologies [5], [6]. Results in Table 1.

Standard ΛCDM model: The fit leaves A and Ω_M as free parameters. In Fig. 1, we show the logarithm of the quantity y versus the logarithm of z.

FLRW with curvature without dark energy: We now consider a Friedman – Lemaître – Robertson – Walker (FLRW) cosmology without dark energy satisfying $\Omega_K = 1 - \Omega_M$, leaving both A and Ω_M as free parameters. In this way, we obtain a negative curvature cosmology (or a flat one if $\Omega_M = 1$). In the fit we obtain an Ω_M value of practically zero. The fit is worse than in the case of the model ΛCDM. The low value of Q almost completely rules out this model.

Einstein–de Sitter: The Einstein–de Sitter (EdS) model is equivalent to an FLRW cosmology with $\Omega_M = 1$ and $\Omega_\Lambda = 0$. There is only one free parameter: A. Such a restricted model obtains a very poor fit and is completely discarded. As we shall see later, if we add certain factors to this model (evolution, extinction or partially non-cosmological redshifts) we can obtain much better fits.

Quasi-steady state cosmology (QSSC): In this model, calling Ω_c the matter creation field we have:

$$D_L(z) = \frac{c}{H_0}(1+z)\int_0^z \frac{dz}{\sqrt{\Omega_c(1+z)^4 + \Omega_m(1+z)^3 + \Omega_\Lambda}}. \tag{3}$$

Table 1: Best fits of Pantheon data ($N = 1048$ supernovae Ia) with different cosmological models, or with extinction, or evolution or a non-cosmological LSV redshift component. Here Q is the probability associated to a χ^2 with degrees of freedom$= N - p$, where p is the number of free parameters.

Model	Free parameters	χ^2	Q
ΛCDM	$A = 13.389 \pm 0.041$ $\Omega_M = 0.287 \pm 0.012$ $\Omega_\Lambda = 1 - \Omega_M$	1024.3	0.678
FLRWcurv$\Lambda = 0$	$A = 13.909 \pm 0.039$ $\Omega_M = 0 \pm 0.024$	1147.1	0.015
EdS	$A = 14.832 \pm 0.043$	2395.4	0
QSSC	$A = 14.444 \pm 0.067$ $\Omega_M = 1.439 \pm 0.068$ $\Omega_\Lambda = 0 \pm 0.042$ $\Omega_c = 1 - \Omega_M - \Omega_\Lambda$	1635.6	0
$R_h = ct$	$A = 14.091 \pm 0.030$	1296.3	0
Milne	$A = 13.909 \pm 0.029$	1147.1	0.016
Static. lin. Hub.	$A = 14.047 \pm 0.029$	1239.1	0
Static tired light	$A = 15.559 \pm 0.061$	4374.1	0
EdS extinction	$A = 13.487 \pm 0.045$ $a_V = (1.156 \pm 0.031) \times 10^{-4}~\mathrm{Mpc}^{-1}$	1050.8	0.453
St. lin. Hub. ext.	$A = 13.566 \pm 0.045$ $a_V = (0.403 \pm 0.031) \times 10^{-4}~\mathrm{Mpc}^{-1}$	1065.2	0.333
St. tir. l. ext.	$A = 12.959 \pm 0.051$ $a_V = (2.775 \pm 0.048) \times 10^{-4}~\mathrm{Mpc}^{-1}$	1072.9	0.275
EdS evol.	$A = 13.257 \pm 0.048$ $\alpha = -0.102 \pm 0.003~\mathrm{Gyr}^{-1}$	1020.4	0.709
EdS+LSV1	$A = 31.445 \pm 0.119$ $K_1 = (-2.046 \pm 0.005) \times 10^{-4}~\mathrm{Mpc}^{-1}$	1490.7	0
EdS+LSV2	$A = 38.263 \pm 0.212$ $K_2 = (-2.113 \pm 0.003) \times 10^{-4}~\mathrm{Mpc}^{-1}$	1194.8	0.0008
FLRW curv. $\Lambda = 0$ $+LSV1$	$A = 9.479 \pm 0.712$ $\Omega_M = 0.090 \pm 0.015$ $K_1 = (0.720 \pm 0.060) \times 10^{-4}~\mathrm{Mpc}^{-1}$	1091.1	0.157
FLRW curv. $\Lambda = 0$ $+LSV2$	$A = 40.563 \pm 0.192$ $\Omega_M = 0.190 \pm 0.010$ $K_2 = (-2.220 \pm 0.010) \times 10^{-4}~\mathrm{Mpc}^{-1}$	1082.0	0.208
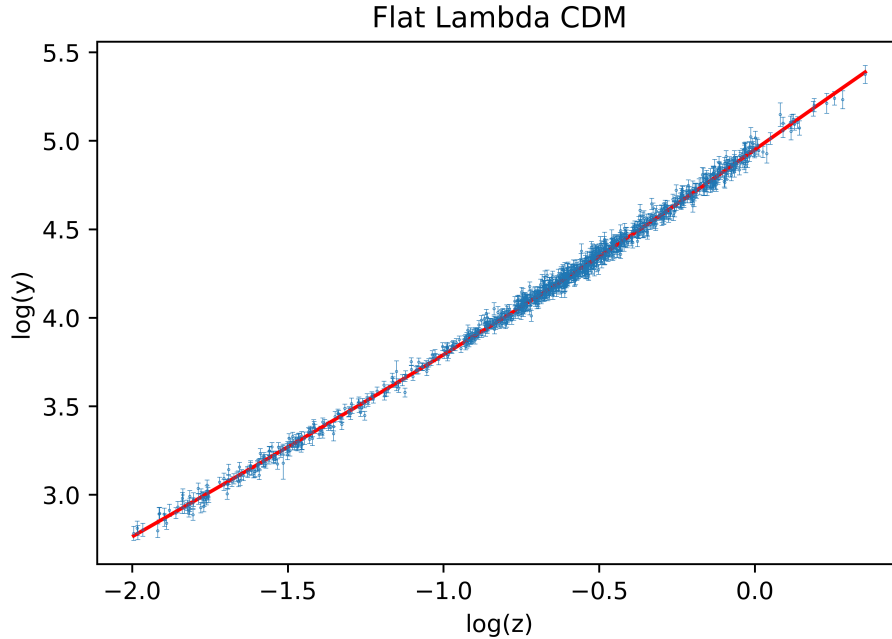
Figure 1: Fit of Pantheon data with ΛCDM, $\Omega_M = 0.287$.

We see that the term Ω_c behaves like a radiation term in FLRW, which also goes as $(1+z)^4$. With the Pantheon data and without taking into account other factors, we obtain a fit that completely rules out this model. There have been previous attempts to fit supernova Ia data with this model [8] with apparently very good results, but in that paper they also take dust extinction into account.

$\mathbf{R_h = ct}$: This is an FLRW model in which we have an equation of state: $\rho + 3p = 0$, thus leading to an expansion $R_h = ct$. The luminosity distance is:

$$D_L(z) = \frac{c}{H_0}(1 + z)\ln(1 + z). \tag{4}$$

The fit, being better than QSSC or Einstein–de Sitter is still ruled out by the Pantheon data. Other authors [9] have stated that this model fits the supernova diagram, but only after re-evaluating the calibration of their luminosities, setting their absolute magnitude as a function of several adjustable parameters instead of being constant.

Milne Universe: This model is a special case of the FLRW metric in which we consider zero density, pressure and cosmological constant. This results in a linear time dependence of the scale factor. We have the following expression for the luminosity distance:

$$D_L(z) = \frac{c}{H_0}(1 + z)\sinh[\ln(1 + z)]. \tag{5}$$

Despite being a model with very restricted parameters, the fit is better than that of other models considered.

Static Euclidean with linear Hubble–Lemaître law: In this case, we consider a static universe in which we have a redshift term due to energy loss without expansion (no time dilation), and the linear Hubble–Lemaître law $c\,z = H_0 D$ is maintained even at high redshift. The luminosity distance is:

$$D_L(z) = \frac{c}{H_0}\sqrt{(1+z)}z. \tag{6}$$

The factor $\sqrt{(1+z)}$ stems from the loss of energy of photons due to the non-cosmological redshift. We obtain a setting that rules it out. Moreover, although it is not the subject of this work, a simple static model has many other problems.

Static Euclidean with tired light: This variation considers that photons lose energy in their path by some kind of interaction, and that this energy loss is proportional to the length traveled: $\frac{dE}{dr} = -\frac{H_0}{c}E$. This modifies the luminous distance as follows:

$$D_L(z) = \frac{c}{H_0}\sqrt{(1+z)}\ln(1+z). \tag{7}$$

In view of the results, this consideration of energy loss is totally incompatible with the Pantheon data and greatly worsens the fit of the simplest linear model.

4. Fits including extinction

Introducing an extinction term will make very distant galaxies appear less luminous. This effect can counteract that of dark energy and thus obtain a good fit [5]. Assuming a constant comoving dust density term and with κ representing the absorption coefficient per unit mass, we have the following expression for luminosity:

$$L_{V,\mathrm{rest}} = 4\pi F_{V,\mathrm{rest}} D_L^2 e^{\rho_{dust}\int_0^d dr\,\kappa\left[\lambda_V \frac{1+z(d)}{1+z(r)}\right]}, \tag{8}$$

where the comoving distance d in the corresponding cosmology associated with the redshift of the supernovae. If we assume the absorption coefficient with a wavelength dependence:

$$\kappa(\lambda) = \kappa(\lambda_V)\left(\frac{\lambda}{\lambda_V}\right)^{-\beta}, \tag{9}$$

we adopt $\beta = 2$, see [5]. With this we obtain:

$$L_{V,\mathrm{rest}} = 4\pi F_{V,\mathrm{rest}} D_L^2 e^{\frac{c\,a_V}{H_0(\beta+m)}[(1+z)^m - (1+z)^{-\beta}]}, \tag{10}$$

with $a_V \equiv \kappa(\lambda_V)\rho_{\mathrm{dust}}$ the absorption in V per unit length. Together with A, the parameter a_V will be the one we shall fit. Regarding the other parameters, $m = 1$ for the Einstein de–Sitter (see best fit in Fig. 2) and Linear Static models, and $m = 0$ for the static model with tired light. The attenuations of $a_V = 0.4 - 2.8 \times 10^{-4}\,\mathrm{Mpc}^{-1}$
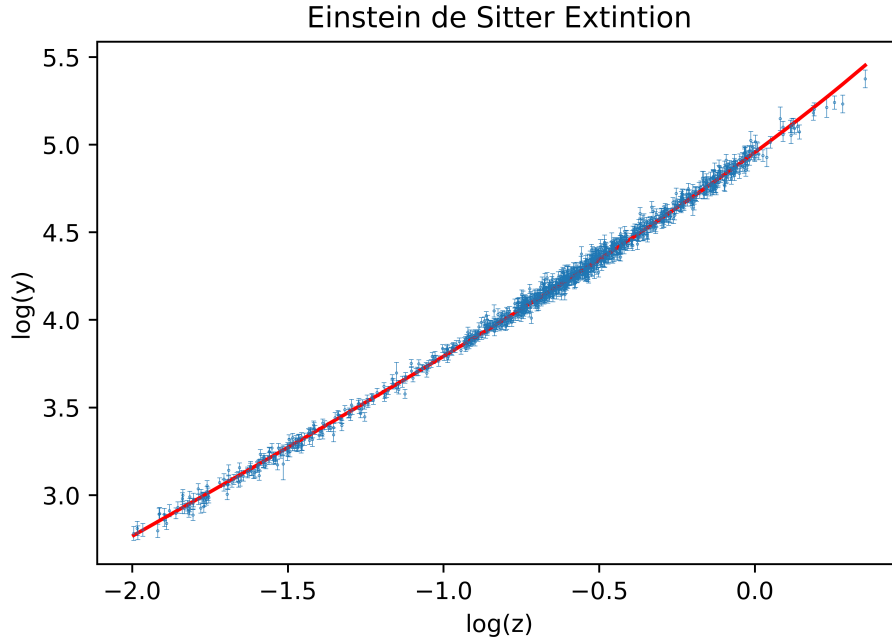
Figure 2: Fit of Pantheon data with Einstein de–Sitter including $a_V = 1.156 \times 10^{-4}\,\mathrm{Mpc}^{-1}$, respectively.

are within the range of possible values. Assuming $\kappa(\lambda_V) \sim 10^5\,\mathrm{cm}^2/\mathrm{gr}$ [10], the value for the dust density necessary to produce such an extinction would be $\rho_{\mathrm{dust}} \sim 10^{-34} - 10^{-35}\,\mathrm{g}/\mathrm{cm}^3$, which is within the range of possible values. Ref. [11] allows values as high as $\rho_{\mathrm{dust}} \sim 10^{-33}\,\mathrm{g}/\mathrm{cm}^3$ for the high z IGM within the standard concordance cosmology. For comparison, the average baryonic density of the Universe (taking $\Omega_b = 0.042$) is $\rho_b = 3.9 \times 10^{-31}\,\mathrm{g}/\mathrm{cm}^3$, so this would mean that IGM dust constitutes 0.025–0.25% of the total baryonic matter. These amounts are reasonable.

5. Fits including evolution

Several researchers (e.g., Refs. [12], [13], [14]) have pointed out that an evolution of SNe Ia luminosity can fit their Hubble–Lemaître diagram without dark energy.

In our analysis, we use a simple expression to model cosmic time-dependent evolution and a parameter α that will fit cosmological models without dark energy. We assume that the absolute magnitude of supernovae varies with cosmological time, using a simple evolution equation:

$$M = M_0 - \alpha[t(0) - t(z)], \tag{11}$$

where M_0 is the absolute magnitude without considering evolution, $t(z)$ is the age of the universe at a given z [$t(0)$ for $z = 0$]. We calculate for each given z that age and incorporate the new M into the formula for the A parameter fit:

$$A_{\mathrm{evol}} = A \times 10^{-0.2\alpha[t(0)-t(z)]}. \tag{12}$$

We fit the SNe Ia using an Einstein–de Sitter model with evolution. We obtain a very good fit. In addition, we have smaller uncertainties by fitting only two parameters (A and α). As we can see, with the Pantheon data, a model with evolution is just as valid (or better) than one with dark energy. Moreover, when trying to fit with both terms, the best value of Q is for the one that gives $\Omega_\Lambda \sim 0$. See best fit in Fig. 3.
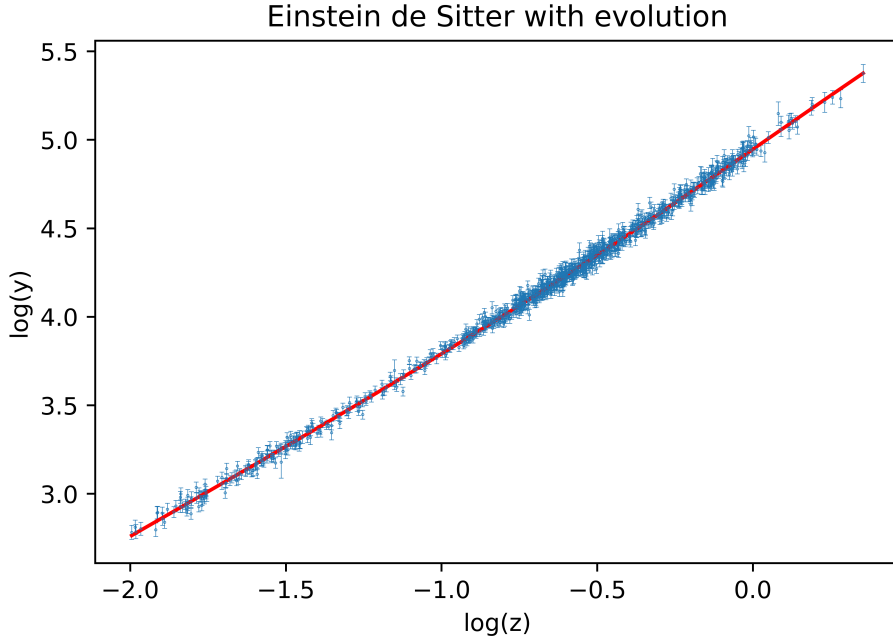
Figure 3: Einstein–de Sitter with evolution: $\Omega_M = 1$, $\Omega_\Lambda = 0$, $\alpha = -0.102$ Gyr^{-1}.

As said by Ref. [12], the result is that cosmological models and evolution are highly degenerate with one another, so that the incorporation of even very simple models for evolution makes it virtually impossible to pin down the values of Ω_M and Ω_Λ.

6. Fits including partially non-cosmological redshifts

If we add a partially non-cosmological redshift or blueshift we obtain distances for the supernovae that differ from those obtained in the standard model. The non-cosmological redshift component may be due to the non-conservation of the energy-momentum tensor of a photon propagating through electromagnetic fields [Lorentz–Poincaré Symmetry Violation (LSV)] [15] or Mach effects that relate tired light with the mass of the Universe [16], [17] or other non-standard effects. The Hubble diagram could be fitted without the need for dark energy.

We consider models in which the total redshift is the sum of the redshift due to expansion plus a static term. The excessive dimming of very distant galaxies can be attributed to this combined redshift without the need to include a dark energy term.

127

For an SN Ia we have the relation:

$$z_c = \frac{1+z}{1+z_{\mathrm{LSV}}} - 1,$$

(13)

where z_c is the cosmological redshift, z_{LSV} is the non-cosmological redshift, which depends on the model. We have two different LSV models as given in Table 2.

Table 2: Two different models of non-cosmological redshifts.

Type	1	2
d_ν	$k_1 \nu dr$	$k_2 \nu_e dr$
ν_0	$\nu_e \mathrm{e}^{k_1 r}$	$\nu_e(1 + k_2 r)$
z_{LSV}	$\mathrm{e}^{-k_1 r} - 1$	$-\frac{k_2 r}{1+k_2 r}$
r_{LSV}	$-\frac{\ln(1+z_{LSV1})}{k_1}$	$-\frac{z_{LSV2}}{k_2(1+z_{LSV2})}$

In model LSV-1, the variation in frequency is proportional to the instantaneous frequency and the distance; in model LSV-2, to the emitted frequency (ν_e) and the distance. We need an iterative function to obtain the values of z_c, r and z_{LSV}, since they depend on each other. For this we will use Eq. (13) and the relations in Table 2 with

$$r(z_c) = c[t(0) - t(z_c)],$$

(14)

where $t(z)$ is the age of the universe at redshift z. Positive values for the k indicate a blueshift with a small or even decreasing change in the amplitude A. This non-cosmological blueshift increases the magnitude of SNe Ia at high redshift. With negative values, we obtain a non-cosmological redshift that increases the value of A and a reduction in photon frequency with distance traveled. For instance, we try the fits with Einstein-de Sitter or FLRW with curvature, $\Omega_\Lambda = 0$.

In an Einstein–de Sitter universe with the LSV-1 model, by including the non-cosmological redshift we obtain a better fit than the original one, although still far from that obtained by including extinction or evolution. In view of the results, the Pantheon data would rule out this model. The negative value of k_1 indicates that we have redshift. The LSV-2 model works better than the LSV-1 model but is also practically ruled out (Q =0.0008). Similar results were obtained with the Pantheon sample by Ref. [18].

With FLRW with curvature ($\Omega_\Lambda = 0$) we obtain good fits. However, the amplitude of A is quite different from that in the standard model fit, thus implying, according to Eq. (2), an important variation in the absolute magnitude with respect to the locally calibrated one. Results with the Pantheon sample by Ref. [18] were similar, although within unclear dependence of A given that the type of fit was different.

7. Conclusions

In this work we have focused on well-known cosmologies, as well as on simple models for extinction, evolution and partial redshift not due to expansion. As expected, the standard model continues to fit the data excellently, just as it did previously the small SNe Ia samples used by Riess et al. and Perlmutter et al. It is very interesting to see, however, that other models, discarded as a basis for current cosmological study, also fit the supernova data.

Some models (Einstein–de Sitter, static models and others) have the same probability as that of the standard model or even slightly higher if we allow a supernova absolute magnitude evolution of $\sim -0.10\,\mathrm{mag\,Gyr^{-1}}$ or a gray extinction of $\sim 10^{-4}\,\mathrm{mag\,Mpc^{-1}}$. The inclusion of dark energy (and thus accelerated expansion of the universe) is not necessary in view of this analysis. There is a degeneracy of several variables: dark energy, extinction, evolution, partially non-cosmological redshifts (although requiring calibration of M far from compatibility with local SNe Ia measurements), and possibly other paramaters that we have not explored here.

References

[1] López-Corredoira, M., Calvo-Torel, J. I.: Fitting of supernovae without dark energy. Submitted (2022).

[2] Riess, A. G. R., Filippenko, A. V., Challis, P., et el.: Observational evidence from supernovae for an accelerating universe and a cosmological constant'. Astron. J. *116* (1998), 1009–1038.

[3] Perlmutter, S., Aldering, G., Goldhaber, G., et al.: Measurements of Omega and Lambda from 42 High-Redshift Supernovae. Astrophys. J. *517* (1999), 565–586.

[4] Scolnic, S. M., Jones, D. O., Rest, A., et al.: The complete light-curve sample of spectroscopically confirmed sne ia from pan-starrs1 and cosmological constraints from the combined pantheon sample'. Astrophys. J. *859* (2018), id. 101, 28 pp.

[5] López-Corredoira, M.: Angular size test on the expansion of the universe. Int. J. Mod. Phys. D *19* (2010), 245–291.

[6] López-Corredoira, M., Melia, F., Lusso, E., Risaliti, G.: Cosmological test with the QSO hubble diagram. Int. J. Mod. Phys. D *25* (2016), id. 1650060, 11 pp.

[7] Planck Collaboration: Planck 2013 results. XVI. Cosmological parameters, Astron. Astrophys. *571* (2014), id. A16, 66 pp.

[8] Banerjee, S. K., Narlikar, J. V., Wickramasinghe, N. C., Hoyle, F., Burbidge, G.: Possible interpretations of the magnitude-redshift relation for supernovae of type Ia. Astron. J. *119* (2000), 2583–2588.

[9] Melia, F.: Fitting the Union2.1 supernova sample with the $R_h = ct$ Universe. Astron. J. *144* (2012), id. 110, 7 pp.

[10] Wickramasinghe, N. C., Wallis, D. H.: Far-infrared contribution to interstellar extinction from graphite whiskers. Astrophys. Space Sci. *240* (1996) 157–160.

[11] Inoue, A. K., Kamaya K.: Amount of intergalactic dust: constraints from distant supernovae and the thermal history of the intergalactic medium. Mon. Not. Roy. Astron. Soc. *350* (2004), 729–744.

[12] Drell, P. S., Loredo, T. J., Wasserman, I.: Type Ia Supernovae, evolution, and the cosmological constant. Astrophys. J. *530* (1999), 593–617.

[13] Tutusaus, I., Lamine, B., Blanchard, A.: Model-independent cosmic acceleration and redshift-dependent intrinsic luminosity in type-Ia supernovae. Astron. Astrophys. *625* (2019), id. A15, 13 pp.

[14] Lee, Y.-W., Chung, C., Kang, Y., Jee, M. J.: Further evidence for significant luminosity evolution in supernova cosmology. Astrophys. J. *903* (2020), id. 22, 5 pp.

[15] Spallicci, A. D. A. M., Helayël-Neto, J. A., López-Corredoira, M., Capozziello, S.: Cosmology and the massive photon frequency shift in the standard-model extension. Eur. Phys. J. C *81* (2021), id. 4, 12 pp.

[16] Gupta, R.P.: Static and dynamic components of the redshift. Int. J. Astron. Astrophys. *8* (2018), 219–229.

[17] Gupta, R. P.: Weighing cosmological models with SNe Ia and Gamma ray burst redshift data. Universe *5* (2019), id. 102.

[18] Spallicci, A. D. A. M., Sarracino, G., Capozziello, S.: Investigating dark energy by electromagnetic frequency shifts. Eur. Phys. J. Plus *137* (2022), id. 253.

100 YEARS OF THE FRIEDMANN EQUATION

Michal Křížek

Institute of Mathematics, Czech Academy of Sciences
Žitná 25, 115 67 Prague 1, Czech Republic
krizek@math.cas.cz

Abstract: In 1922, Alexander Friedmann applied Einstein's equations to a three-dimensional sphere to describe the evolution of our universe. In this way he obtained a nonlinear ordinary differential equation (called after him) for the expansion function representing the radius of that sphere. At present, the standard cosmological ΛCDM model of the universe is based just on the Friedmann equation. It needs a significant amount of dark matter, about six times that of the usual baryonic matter, besides an even larger amount of dark energy to be consistent with the real universe. But to date, both dark matter and dark energy have remained without concrete evidence based on direct physical measurements. We present several arguments showing that such a claimed amount of dark matter and dark energy can only be the result of vast overestimation, incorrect extrapolations, and that it does not correspond to the real universe.

The spatial part of our universe seems to be locally flat and thus it can be locally modeled by the Euclidean space. However, Friedmann did not consider the flat space with zero curvature. Therefore, in the second part of this paper we will derive a general form of the corresponding metric tensor satisfying Einstein's equations with zero right-hand side.

Keywords: Einstein's equations, modeling error, incorrect extrapolations, dark matter, dark energy, metric tensor, Ricci tensor, Christoffel symbols, Laplace operator

PACS: 4.20.-q, 95.35.+d, 98.80.-k

1. Introduction

In 1584, Giordano Bruno wrote the treatise [2], where among other things he conjectured that the universe is infinite. From that time, opinions on the shape of the universe have often changed. Isaac Newton and many others understood the universe as the Euclidean space $\mathbb{E}^n$ for $n = 3$.

However, in 1900 the German mathematician and physicist Karl Schwarzschild proposed (see [22, p. 66]) that the universe for a fixed time might be non-Euclidean

and even bounded, i.e., having a finite volume. He envisioned it as a three-dimensional manifold. Recall that a manifold locally resembles Euclidean space near each point. More precisely, a set of points $M \subset \mathbb{E}^m$ is said to be an *n-dimensional manifold* with $n \leq m$ if each of its points has an open neighborhood in M that can be continuously mapped onto an open subset of $\mathbb{E}^n$ such that the inverse is continuous, too. An example of a manifold is the graph of a parabola, a hyperboloid of two sheets, the surface of a torus, and so on. On the other hand, the union of the hyperplane $x_1 = 0$ and axis x_1 in $\mathbb{E}^n$ is not a manifold for $n > 1$.

Note that non-Euclidean geometry arose in the first half of the 19th century during many attempts to understand the axiomatic construction of Euclidean geometry — especially in proving the independence of Euclid's fifth postulate of parallels. We include among its founders Carl Friedrich Gauss, Nikolai I. Lobachevskii, János Bolyai, Bernhard Riemann, Sophus Lie, Felix Klein, and many others. The history of the development of non-Euclidean geometries is described in detail in the review article [3].

According to *Einstein's cosmological principle*, our universe at each point in time, i.e. on each isochrone, is homogeneous (possessing translation symmetry) and isotropic (possessing rotational symmetry) on large scales, see [23, p. 409]. Roughly speaking, its curvature is constant at any point and in any direction.

According to the *Copernican principle*, humans on Earth are not privileged observers of the universe. The isotropy is thus verified by astronomers only from our Earth and its close neighborhood. For instance, it is confirmed by the cosmic microwave background radiation (CMB) which exhibits tiny fluctuations of order $10^{-4}\,\mathrm{K}$ from its mean temperature $2.7260\,\mathrm{K}$. Also the well-known γ-ray bursts show an almost uniform distribution on the celestial sphere. Pictures of the Hubble Deep Field, the Hubble Deep Field-South, the Hubble Ultra-Deep Field, the Hubble eXtreme Deep Field, etc., taken by the Hubble space telescope illustrate this isotropy on very large cosmological scales as well.

In the Hubble test of the homogeneity of the universe, one has to measure the apparent magnitude (energy flux f from the galaxy). The number of galaxies in the sky brighter than f should vary as $f^{-3/2}$, see [18], [23, Chapt. 14]. For a modification of this test to γ-ray bursts see also [15]. Note that isotropy at all points implies homogeneity at all points, see [24, Appendix].

Einstein's equations were not developed for the purpose of the dynamical evolution of the entire universe. This was done later in 1922 by Alexander Friedmann (1888–1925) who derived from Einstein's equations a nonlinear ordinary differential equation (4) for the *expansion function $a = a(t)$*, see [4]. He assumed that the universe can be described by an expanding three-dimensional sphere (hypersphere)

$$\mathbb{S}_a^3 = \{(x, y, z, w) \in \mathbb{E}^4 \,|\, x^2 + y^2 + z^2 + w^2 = a^2\} \tag{1}$$

which enabled him to avoid boundary conditions.

The present standard cosmological ΛCDM (Lambda-Cold Dark Matter) model of the evolution of our universe is based just on the Friedmann equation. However,

Friedmann's description was very brief. Therefore, in [8] we presented a detailed derivation of the Friedmann equation for an unknown expansion function $a = a(t)$ representing the radius of the universe. A natural question arises whether we can apply Einstein's equations that are tested on scales of the Solar system to the whole universe, which is a 15 orders of magnitude larger object than the astronomical unit au. We will answer this question in Sections 2 and 3.

The term *Big Bang* was first used by Fred Hoyle in 1949. Nevertheless, the idea that the universe could have "zero radius" in the very distant past was formulated by Friedmann already in 1922. In the English translation of his article [4], footnote 11 states:

The time since the creation of the world is the time that has flowed from that instant when the space was one point ($R = 0$) until the present state ($R = R_0$); this time may also be infinite.

George Lemaître came to the same conclusion five years later in his article *A homogeneous universe with constant mass and increasing radius explains the radial velocities of extragalactic nebulae*, see [14].

Now we present an important theorem which helps us to model Einstein's cosmological principle. Its proof can be found in e.g. [23, Chapt. 13].

Theorem 1. *For any dimension $n > 1$ there exist exactly three maximally symmetric manifolds, namely, the sphere $\mathbb{S}^n$, the Euclidean space $\mathbb{E}^n$, and the hyperbolic pseudosphere $\mathbb{H}^n$.*

The *curvature index* of the above three maximally symmetric manifolds is $k = 1$, $k = 0$, and $k = -1$, respectively.

Already in 1900, Karl Schwarzschild [22] speculated that the our universe could be hyperbolic. In 1924, Alexander Friedmann published another famous paper [5], where a negative curvature index $k = -1$ is considered. However, he assumed the universe has a negative mean mass density (see [5, p. 2006]) and thus it is not clear how to satisfy such a paradoxical assumption. Moreover, the manifold $\mathbb{H}^3$ cannot be isometrically imbedded to a low-dimensional Euclidean space, see [7, p. 279].

In Sections 4–8, we will apply Einstein's equations to the three-dimensional Euclidean space $\mathbb{E}^3$.

2. Friedmann equation for the three-dimensional sphere

For a given smooth positive expansion function $a = a(t)$ define the *Hubble parameter* $H = H(t)$, called also the *Hubble-Lemaître parameter*, by

$$H(t) := \frac{\dot{a}(t)}{a(t)}. \tag{2}$$

It can be thus expressed as the time derivative of the natural logarithm in the following way

$$H(t) = \frac{\mathrm{d}\left(\ln\frac{a(t)}{a_0}\right)}{\mathrm{d}t}, \tag{3}$$

where $a_0 > 0$ is an arbitrary length constant and thus the argument $a(t)/a_0$ is dimensionless.

Consider Einstein's equations with cosmological constant Λ (see [17]) on the expanding sphere (1) with radius $a = a(t)$. Due to its maximum symmetry, Einstein's equations can be largely simplified (see e.g. [8] for a detailed derivation). In this way, Friedmann arrived at the following equation

$$\frac{\dot{a}^2}{a^2} = \frac{8\pi G \rho}{3} + \frac{\Lambda c^2}{3} - \frac{kc^2}{a^2} \tag{4}$$

which is at present called the *Friedmann equation*. Here $G = 6.674 \cdot 10^{-11}\,\mathrm{m^3 kg^{-1} s^{-2}}$ is the gravitational constant, $c = 299\,792\,458\,\mathrm{m/s}$ is the speed of light in a vacuum, $\rho > 0$ is the mean mass density, and $k = 1$ is the curvature index. It is a first order nonlinear ordinary differential equation for the unknown radius $a = a(t)$. Several typical graphs of the expansion function $a = a(t)$ are given in [12, pp. 21–22].

Let us emphasize that Friedmann in [5] derived his equation also for the curvature index $k = -1$, but the case $k = 0$ was not taken into account by him. From Einstein's equations one may also derive a second order linear ordinary differential equation for $a = a(t)$ that is surprisingly independent of the curvature index k and that is also called the Friedmann equation, see [8, p. 169]. However, this equation does not appear in [4], [5], too.

Now divide the Friedmann equation (4) by the square $H^2 \geq 0$ as is usually done in the literature on cosmology, i.e., without a preliminary warning that we may possibly divide by zero, which can lead to various paradoxes (see e.g. [10], [11]). Then we get the so-called *normalized Friedmann equation*

$$1 = \Omega_{\mathrm{M}}(t) + \Omega_{\Lambda}(t) + \Omega_{\mathrm{K}}(t) \tag{5}$$

for three normalized cosmological parameters, which are defined as follows

$$\Omega_{\mathrm{M}}(t) := \frac{8\pi G \rho(t)}{3H^2(t)} > 0, \quad \Omega_{\Lambda}(t) := \frac{\Lambda c^2}{3H^2(t)}, \quad \Omega_{\mathrm{K}}(t) := -\frac{kc^2}{\dot{a}^2(t)}. \tag{6}$$

Saul Perlmutter calls the parameter Ω_{M} the *mass density* and Ω_{Λ} the *vacuum energy density* (see [19]). The parameter Ω_{K} is called the *curvature parameter* in [20]. Note that (5) is still a differential equation, since the derivative $\dot{a}$ is obviously present in the Hubble-Lemaître parameter (2) which is contained in (6).

3. Main drawbacks of the standard ΛCDM model

In this section we present several inadequate properties of the current cosmological model.

1. It is said that the gravitational constant G is the worst established constant of all fundamental physical constants, since its value is known only to 3 (or 4) significant digits. However, we do not know any significant digit of the cosmological

constant Λ, yet. We even do not know whether it exists, even though there are thousands of papers on this constant. Note that the standard cosmological model only assumes that $\Lambda \sim 10^{-52}$ m^{-2}, i.e., an extremely small number in the SI base units. From its physical dimensions it follows that Λ has nothing to do with any kind of energy.

2. The main argument against the proposed amount of vacuum (dark) energy is the 120-order-of-magnitude discrepancy between the measured and theoretically derived density of vacuum energy (see [1]). From this it is clear that the standard cosmological model, which is a direct mathematical consequence of Einstein's equations, does not approximate the real universe well [12].

3. The following approximate values

$$\Omega_M(t_0) \approx 0.3, \quad \Omega_\Lambda(t_0) \approx 0.7, \quad \Omega_K(t_0) \approx 0, \tag{7}$$

where t_0 is the age of the universe, were obtained by a combination of the methods of Baryonic Acoustic Oscillations, Cosmic Microwave Background, and Supernovae type Ia explosions. Independent fits with data for these three methods are performed and it is said that these methods are independent. However, they cannot be independent, since all of them use the cosmological parameters (6) satisfying the Friedmann equation (5).

4. For the Einstein stationary universe we have

$$\dot{a} \equiv 0. \tag{8}$$

Hence, by (2) we get $H(t) = 0$ for any time instant and the density of dark and baryonic matter $\Omega_M = \infty$ which is absurd. More precisely, Ω_M is not well defined. However, the density of baryonic matter is always a finite number in the real universe. In [6], we present ten independent arguments against the proclaimed amount of dark and baryonic matter $\Omega_M(t_0) \approx 0.3$ from (7).

For an oscillating universe we find that $\dot{a}(t_1) = 0$ for some $t_1 > 0$, where $a = a(t)$ attains its maximum. Hence, $H(t_1) = 0$ and the density of dark matter is $\Omega_\Lambda = \infty$, although the universe starts to collapse from the time instant t_1.

5. At present it is believed that $a(t) \to \infty$ for $t \to \infty$. From (5)–(6) we get $1 > \Omega_\Lambda(t)$ if $k \leq 0$, and thus $\frac{1}{3}\Lambda c^2 < H^2(t)$ for arbitrary time. From this and (2) we see that also the time derivative of the expansion function grows beyond all limits if $\Lambda > 0$. Consequently, the derivative $\dot{a}(t) \to \infty$ for $t \to \infty$, i.e., the expansion speed is much faster than the speed of light.

6. Another paradox concerns the Big Bang itself. Since $\dot{a}(0) = \infty$, we find that $\Omega_K(0) = 0$. However, a similar value of $\Omega_K(t_0) \approx 0$ is proposed by cosmologists also at present. For the time before the decoupling of the cosmic microwave background the equation (4) has to be slightly modified (see [7, p. 296]), but the unpleasant property $\dot{a}(0) = \infty$ remains.

7. For a parabolic space with $\Lambda = 0$ the first derivative of the expansion function $\dot{a}$ is decreasing, but $|\Omega_{\mathrm{K}}|$ is increasing in time. This is strange, is not it?

8. If at present the expansion of the universe accelerates, then $\dot{a} = \dot{a}(t)$ is not a monotone function. However, then the curvature parameter $\Omega_{\mathrm{K}}(t)$ is also not monotone. This is also strange, since the universe is by observations continually expanding all the time.

9. Luminosity distances of cosmological objects (including supernovae explosions) are evaluated by means of the formula

$$d_{\mathrm{L}} = \frac{c(1+z)}{H_0|\Omega_{\mathrm{K}}|^{\frac{1}{2}}} \operatorname{sinn}\left\{|\Omega_{\mathrm{K}}|^{\frac{1}{2}} \int_0^z [(1+\bar{z})^2(1+\Omega_{\mathrm{M}}\bar{z}) - \bar{z}(2+\bar{z})\Omega_{\Lambda}]^{-\frac{1}{2}}\mathrm{d}\bar{z}\right\}, \quad (9)$$

where

$$H_0 = H(t_0) \approx 70 \quad \mathrm{km\,s^{-1}Mpc^{-1}} \quad (10)$$

is the current value of the Hubble constant and

$$\operatorname{sinn} x = \begin{cases} \sin x & \text{for} \quad k = 1, \\ x & \text{for} \quad k = 0, \\ \sinh x & \text{for} \quad k = -1. \end{cases}$$

Note that formula (9) contains cosmological parameters (6). Hence, (9) approximates real distances sufficiently accurately, if the Friedmann equation describes reality well. Therefore, testing whether the expansion of the universe accelerates by means of (9) is a typical circular argument.

10. Einstein's equations are not scale invariant from several reasons. They do not describe reality well on micro-scales. They are nonlinear and fully deterministic, whereas the evolution of the universe may depend on quantum phenomena. For instance, a small quantum fluctuation in one human brain may completely destroy the Earth or change the trajectory of an asteroid. This cannot be described by Einstein's equations. Therefore, we should not make any extrapolations from local systems (such as the Solar system) to the entire universe, see [10], [11], [12]. A century of excessive extrapolations of Einstein equations yielded that the ΛCDM-model gives completely wrong results. Moreover, from a trivial ordinary differential equation (4) incorrect conclusions are made about the age of the universe, its composition (the existence of some mysterious dark matter and dark energy), its development, etc. We should avoid various "delicate" limits such as $t \to 0$, $t \to \infty$, $a \to 0$, $a \to \infty$, etc.

4. Einstein's equations for the Euclidean space

Now we shall consider Einstein's field equations of general relativity with zero right-hand side and zero cosmological constant

$$R_{\mu\nu} - \frac{1}{2}Rg_{\mu\nu} = 0, \quad \mu, \nu = 0, 1, 2, 3, \quad (11)$$

for the symmetric metric tensor

$$g_{\mu\nu} = g_{\nu\mu}, \tag{12}$$

where $R_{\mu\nu}$ is the *Ricci tensor* (defined by (30) later) which is also symmetric

$$R_{\mu\nu} = R_{\nu\mu} \tag{13}$$

and

$$R = \sum_{\mu,\nu=0}^{3} g^{\mu\nu} R_{\mu\nu} \tag{14}$$

is called the *Ricci scalar*, where $g^{\mu\nu}$ is the inverse 4×4 tensor to $g_{\mu\nu}$. We shall not use Einstein's summation rule in this paper (because of (26) below). The metric tensor $g_{\mu\nu} = g_{\mu\nu}(x^0, x^1, x^2, x^3)$ depends, in general, on time x^0 and three spatial coordinates x^1, x^2, x^3.

Multiplying (11) by $g^{\mu\nu}$ and summing over all μ and ν, we obtain by (14) that

$$0 = \sum_{\mu,\nu=0}^{3} g^{\mu\nu} R_{\mu\nu} - \frac{1}{2} R \sum_{\mu,\nu=0}^{3} g^{\mu\nu} g_{\mu\nu} = R - \frac{1}{2} R \sum_{\mu=0}^{3} \delta^{\mu}{}_{\mu} = R - \frac{1}{2} 4R,$$

where $\delta^{\mu}{}_{\nu}$ is the Kronecker delta. Thus, $R = 0$ and Einstein's equations (11) can be rewritten into a shorter classical form

$$R_{\mu\nu} = 0. \tag{15}$$

Their solution is, for instance, the well-known exterior Schwarzschild metric [13, p. 284]. In this paper, we shall look for other exact solutions, when the space component of space-time is Euclidean. To this end, we first introduce the Christoffel symbols (also called the *connection coefficients*). The reason is that all entries of the Ricci tensor (15) are defined by means of the Christoffel symbols (cf. (19), (25), and (30) bellow). Therefore, the metric tensor is supposed to be twice differentiable with respect to all four variables.

Throughout this paper we shall assume that the spatial part of the 4×4 metric tensor is the following constant 3×3 diagonal tensor associated to the three-dimensional Euclidean space

$$g^{\alpha\beta} = g_{\alpha\beta} = -\delta_{\alpha\beta} \quad \text{and let} \quad g^{\alpha 0} = g^{0\beta} = g_{\alpha 0} = g_{0\beta} = 0 \quad \text{for all } \alpha, \beta = 1, 2, 3. \tag{16}$$

That is,

$$g_{\mu\nu} = \begin{pmatrix} g_{00} & 0 & 0 & 0 \\ 0 & -1 & 0 & 0 \\ 0 & 0 & -1 & 0 \\ 0 & 0 & 0 & -1 \end{pmatrix}. \tag{17}$$

However, $g_{00} = g_{00}(x^0, x^1, x^2, x^3)$ may depend on all four coordinates x^0, x^1, x^2, x^3, in general, and for the determinant g of $g_{\mu\nu}$ we have

$$g := -g_{00}. \tag{18}$$

Theorem 2. *Assume that the metric tensor $g_{\mu\nu} = g_{\mu\nu}(x^0, x^1, x^2, x^3)$ satisfying Einstein's equations (15) is of the form (17). Then*

$$g_{00} = g_{00}(x^0),$$

i.e., it is independent of x^1, x^2, x^3.

The proof will be successively given in the next three sections.

5. Calculation of the Christoffel symbols

The *Christoffel symbols of the first kind* (in the covariant form, i.e. only with lower indices) are defined as follows

$$\Gamma_{\mu\nu\varkappa} = \frac{1}{2}(g_{\mu\nu,\varkappa} + g_{\varkappa\mu,\nu} - g_{\nu\varkappa,\mu}), \quad \mu, \nu, \varkappa = 0, 1, 2, 3, \tag{19}$$

where for simplicity we define $g_{\mu\nu,\varkappa} = \partial g_{\mu\nu}/\partial x^\varkappa$ to reduce notation. This is altogether $4 \times 4 \times 4 = 64$ entries. However, since the metric tensor is symmetric (12), we get by (19) the following symmetry in the last two indices

$$\Gamma_{\mu\nu\varkappa} = \frac{1}{2}(g_{\mu\varkappa,\nu} + g_{\nu\mu,\varkappa} - g_{\varkappa\nu,\mu}) = \Gamma_{\mu\varkappa\nu}, \tag{20}$$

i.e., there are only $4 \times 10 = 40$ independent Christoffel symbols.

First, we prove that these symbols will be zero for the case (16) if at most one index is zero. Since all nondiagonal entries of the metric tensor are zeros (17) and the time derivative of a constant is zero as well, we obtain that:

(1) There are $6 = 1 + 2 + 3$ independent components of $\Gamma_{0\alpha\beta}$ due to the symmetry (20),

$$\Gamma_{0\alpha\beta} = \frac{1}{2}(g_{0\alpha,\beta} + g_{\beta 0,\alpha} - g_{\alpha\beta,0}) = 0 \quad \text{for } \alpha, \beta = 1, 2, 3.$$

(2) There are $9 = 3 \times 3$ independent components of $\Gamma_{\alpha 0\beta}$,

$$\Gamma_{\alpha 0\beta} = \frac{1}{2}(g_{\alpha 0,\beta} + g_{\beta\alpha,0} - g_{0\beta,\alpha}) = 0 \quad \text{for } \alpha, \beta = 1, 2, 3. \tag{21}$$

(3) There are $18 = 3 \times 6$ independent components of $\Gamma_{\alpha\beta\gamma}$,

$$\Gamma_{\alpha\beta\gamma} = \frac{1}{2}(g_{\alpha\beta,\gamma} + g_{\gamma\alpha,\beta} - g_{\beta\gamma,\alpha}) = 0 \quad \text{for } \alpha, \beta, \gamma = 1, 2, 3. \tag{22}$$

Second, we prove that the Christoffel symbols will be, in general, nonzero for the case (16) if at least two indices are zero. Hence, by (12), (16), (17), and (19) we have only the following nontrivial cases:

(4) There are 4 component such that

$$\Gamma_{0\varkappa 0} = \frac{1}{2}(g_{0\varkappa,0} + g_{00,\varkappa} - g_{\varkappa 0,0}) = \frac{1}{2}g_{00,\varkappa} = -\frac{1}{2}g_{,\varkappa} \quad \text{for } \varkappa = 0, 1, 2, 3. \qquad (23)$$

(5) Finally, for the remaining 3 components we get

$$\Gamma_{\alpha 00} = \frac{1}{2}(g_{\alpha 0,0} + g_{0\alpha,0} - g_{00,\alpha}) = \frac{1}{2}(-g_{00,\alpha}) = \frac{1}{2}g_{,\alpha} \quad \text{for } \alpha = 1, 2, 3. \qquad (24)$$

So altogether we have evaluated

$$6 + 9 + 18 + 4 + 3 = 40$$

symbols $\Gamma_{\varkappa\mu\nu}$, but only 7 of them are nonzero, in general.

The *Christoffel symbols of the second kind* are defined as follows

$$\Gamma^{\mu}{}_{\nu\varkappa} = \sum_{\lambda=0}^{3} g^{\mu\lambda}\Gamma_{\lambda\nu\varkappa}. \qquad (25)$$

However, since in our case the metric tensor is diagonal (17), we find that

$$\Gamma^{\mu}{}_{\nu\varkappa} = g^{\mu\mu}\Gamma_{\mu\nu\varkappa}, \quad \mu, \nu, \varkappa = 0, 1, 2, 3. \qquad (26)$$

Thus, by (16), (18), and (23)–(25) we get

$$\Gamma^{0}{}_{\varkappa 0} = -\frac{g_{,\varkappa}}{2g} \quad \text{for } \varkappa = 0, 1, 2, 3, \qquad (27)$$

where g does not vanish, and

$$\Gamma^{\alpha}{}_{00} = -\frac{1}{2}g_{,\alpha} \quad \text{for } \alpha = 1, 2, 3. \qquad (28)$$

By (20) and (25) we obtain the symmetry in the last two indices of the Christoffel symbols of the second kind,

$$\Gamma^{\mu}{}_{\nu\varkappa} = \Gamma^{\mu}{}_{\varkappa\nu}. \qquad (29)$$

6. Calculation of the Ricci tensor

Using the definition of the Ricci tensor [13], [17], [23]

$$R_{\mu\nu} = \sum_{\varkappa=0}^{3}\left(\Gamma^{\varkappa}{}_{\mu\nu,\varkappa} - \Gamma^{\varkappa}{}_{\mu\varkappa,\nu} + \sum_{\lambda=0}^{3}\left(\Gamma^{\lambda}{}_{\mu\nu}\Gamma^{\varkappa}{}_{\lambda\varkappa} - \Gamma^{\lambda}{}_{\mu\varkappa}\Gamma^{\varkappa}{}_{\nu\lambda}\right)\right), \quad \mu, \nu = 0, 1, 2, 3, \qquad (30)$$

for the entry R_{00} we get

$$R_{00} = \sum_{\varkappa=0}^{3} \left(\Gamma^{\varkappa}{}_{00,\varkappa} - \Gamma^{\varkappa}{}_{0\varkappa,0} + \sum_{\lambda=0}^{3} \left(\Gamma^{\lambda}{}_{00} \Gamma^{\varkappa}{}_{\lambda\varkappa} - \Gamma^{\lambda}{}_{0\varkappa} \Gamma^{\varkappa}{}_{0\lambda} \right) \right). \qquad (31)$$

For the first part of (31) with derivatives we obtain by (28) that

$$\sum_{\varkappa=0}^{3} \left(\Gamma^{\varkappa}{}_{00,\varkappa} - \Gamma^{\varkappa}{}_{0\varkappa,0} \right) = \left(\Gamma^{0}{}_{00,0} - \Gamma^{0}{}_{00,0} \right) + \sum_{\alpha=1}^{3} \Gamma^{\alpha}{}_{00,\alpha} = -\frac{1}{2} \sum_{\alpha=1}^{3} g_{,\alpha\alpha}, \qquad (32)$$

since by (21), (22), and (26) we have

$$\Gamma^{\alpha}{}_{\lambda\alpha} = 0 \quad \text{for } \alpha = 1, 2, 3, \quad \lambda = 0, 1, 2, 3.$$

From this for the second part of (30) with nonlinearities we have by (18) and (27)–(29) that

$$\sum_{\varkappa=0}^{3} \sum_{\lambda=0}^{3} \left(\Gamma^{\lambda}{}_{00} \Gamma^{\varkappa}{}_{\lambda\varkappa} - \Gamma^{\lambda}{}_{0\varkappa} \Gamma^{\varkappa}{}_{0\lambda} \right) = \sum_{\lambda=0}^{3} \Gamma^{\lambda}{}_{00} \Gamma^{0}{}_{\lambda 0} - \sum_{\lambda=0}^{3} \Gamma^{\lambda}{}_{00} \Gamma^{0}{}_{0\lambda} - \sum_{\alpha=1}^{3} \Gamma^{0}{}_{0\alpha} \Gamma^{\alpha}{}_{00} = \frac{1}{4} \sum_{\alpha=1}^{3} \frac{g_{,\alpha}}{g} g_{,\alpha}.$$

Substituting this and (32) into (31), we obtain by (15) the following second order partial differential equation for the unknown function, see (18),

$$g = g(x^0, x^1, x^2, x^3),$$

namely,

$$R_{00} = \sum_{\alpha=1}^{3} \left(g_{,\alpha\alpha} - \frac{(g_{,\alpha})^2}{2g} \right) = 0 \qquad (33)$$

with the standard Laplace operator and the squared gradient.

Now, we show that for the metric tensor (17) the entries $R_{0\beta}$ of the corresponding Ricci tensor are identically zeros without using (15). This means that we do not get any further condition on g. By (30), (29), (27), and the equality $\Gamma^{\mu}{}_{\nu\varkappa} = 0$ if at most one index is zero we obtain that

$$R_{0\beta} = \sum_{\varkappa=0}^{3} \left(\Gamma^{\varkappa}{}_{0\beta,\varkappa} - \Gamma^{\varkappa}{}_{0\varkappa,\beta} + \sum_{\lambda=0}^{3} \left(\Gamma^{\lambda}{}_{0\beta} \Gamma^{\varkappa}{}_{\lambda\varkappa} - \Gamma^{\lambda}{}_{0\varkappa} \Gamma^{\varkappa}{}_{\beta\lambda} \right) \right)$$

$$= \Gamma^{0}{}_{0\beta,0} - \Gamma^{0}{}_{00,\beta} + \Gamma^{0}{}_{0\beta} \Gamma^{0}{}_{00} - \Gamma^{0}{}_{00} \Gamma^{0}{}_{\beta 0} = \Gamma^{0}{}_{0\beta,0} - \Gamma^{0}{}_{00,\beta}$$

$$= -\frac{1}{2} \left(\frac{g_{,\beta}}{g} \right)_{,0} + \frac{1}{2} \left(\frac{g_{,0}}{g} \right)_{,\beta} = -\frac{1}{2} \frac{g_{,\beta 0} \, g - g_{,\beta} \, g_{,0} - g_{,0\beta} \, g + g_{,0} \, g_{,\beta}}{g^2} = 0, \quad \beta = 1, 2, 3.$$

Finally, we find that

$$R_{\alpha\beta} = \sum_{\varkappa=0}^{3} \left(\Gamma^{\varkappa}{}_{\alpha\beta,\varkappa} - \Gamma^{\varkappa}{}_{\alpha\varkappa,\beta} + \sum_{\lambda=0}^{3} \left(\Gamma^{\lambda}{}_{\alpha\beta}\Gamma^{\varkappa}{}_{\lambda\varkappa} - \Gamma^{\lambda}{}_{\alpha\varkappa}\Gamma^{\varkappa}{}_{\beta\lambda} \right) \right)$$

$$= \Gamma^{0}{}_{\alpha\beta,0} - \Gamma^{0}{}_{\alpha 0,\beta} + \Gamma^{0}{}_{\alpha\beta}\Gamma^{0}{}_{00} - \Gamma^{0}{}_{\alpha 0}\Gamma^{0}{}_{\beta 0} = -\Gamma^{0}{}_{\alpha 0,\beta} - \Gamma^{0}{}_{\alpha 0}\Gamma^{0}{}_{\beta 0}$$

$$= \left(\frac{g_{,\alpha}}{2g} \right)_{,\beta} - \frac{1}{4} \frac{g_{,\alpha}}{g} \frac{g_{,\beta}}{g} = \frac{g_{,\alpha\beta}\, g - g_{,\alpha}\, g_{,\beta}}{2g^2} - \frac{g_{,\alpha}\, g_{,\beta}}{4g^2}$$

$$= \frac{g_{,\alpha\beta}}{2g} - \frac{3g_{,\alpha}\, g_{,\beta}}{4g^2}, \quad \alpha, \beta = 1, 2, 3.$$

From this and (15) we obtain 6 partial differential equations different than those in (33), namely,

$$g_{,\alpha\beta} - \frac{3g_{,\alpha}\, g_{,\beta}}{2g} = 0, \quad \alpha, \beta = 1, 2, 3. \tag{34}$$

7. Establishing the metric tensor

Proof of Theorem 2. First, we show that a general solution of the system (33)–(34) is independent of the space variables x^1, x^2, x^3. Setting $\beta := \alpha$ and summing (34) over all α, we obtain

$$\sum_{\alpha=1}^{3} \left(g_{,\alpha\alpha} - \frac{3(g_{,\alpha})^2}{2g} \right) = 0. \tag{35}$$

Subtracting this from (33) and multiplying by g gives

$$\sum_{\alpha=1}^{3} (g_{,\alpha})^2 = 0$$

which yields

$$g_{,1} = g_{,2} = g_{,3} = 0. \tag{36}$$

Hence, a general solution is of the form

$$g = g(x^0), \text{ i.e. } g_{00} = g_{00}(x^0).$$

The proof is completed. $\qquad\square$

So we see that the potential g_{00} may depend on time. This result may have applications in cosmology, see e.g. [16].

The class of all solutions of (33)–(34) is therefore not too rich when compared with (37) below and (18).

According to [23, p. 403], it is convenient to define a new coordinate

$$t := \int \sqrt{-g(x^0)}\mathrm{d}x^0.$$

141

Then $(\mathrm{d}t)^2 = -g(x^0)(\mathrm{d}x^0)^2$ and

$$g = g(t, x^1, x^2, x^3) \equiv -1 \tag{37}$$

solves all partial differential equations (33)–(34). This solution leads to the Minkowski metric known from the Special Theory of Relativity [17], [23].

8. Final remark

From (35) and (36) we observe that g satisfies the Laplace equation. Let us employ the standard spherical coordinates (r, θ, φ), $\varphi \in [0, 2\pi)$, $\theta \in [0, \pi]$, i.e., $x^1 = r \sin\theta \cos\varphi$, $x^2 = r \sin\theta \sin\varphi$, $x^3 = r \cos\theta$. The Laplace operator in the these coordinates reads (see [21, Sect. 7.2])

$$\Delta g = \frac{\partial^2 g}{\partial r^2} + \frac{2}{r}\frac{\partial g}{\partial r} + \frac{1}{r^2}\Big(\frac{\partial^2 g}{\partial \theta^2} + \cotan\theta\frac{\partial g}{\partial \theta} + \frac{1}{\sin^2\theta}\frac{\partial^2 g}{\partial \varphi^2}\Big).$$

The sum in parenthesis on the right-hand side is zero for the spherically symmetric case. The coordinates of $\operatorname{grad} g$ in directions r, θ, φ are

$$\frac{\partial g}{\partial r}, \qquad \frac{1}{r}\frac{\partial g}{\partial \theta}, \qquad \frac{1}{r\sin\theta}\frac{\partial g}{\partial \varphi}$$

and thus the second and third terms also vanish. Substituting this into (33), we get the following homogeneous nonlinear ordinary differential equation

$$g'' + \frac{2}{r}g' - \frac{(g')^2}{2g} = 0, \tag{38}$$

where prime denotes the differentiation of g with respect to r. Note that solutions of (38) are denoted by the same symbol g as in (33), since no ambiguity can arise.

The natural initial conditions

$$g(0) = 1 \quad \text{and} \quad g'(0) = 0$$

yield again the Minkowski metric. But since coefficients in (38) are not Lipschitz continuous, no uniqueness is guaranteed. For instance, the problem $y' - \sqrt{y} = 0$, $y(0) = 0$, has the trivial solution $y \equiv 0$ and also another solution $y(x) = \frac{1}{4}x^2$.

References

[1] Adler, J. R., Casey, B., Jacob, O. C.: Vacuum catastrophe: An elementary exposition of the cosmological constant problem. Amer. J. Phys. 63 (1995), 620–626.

[2] Bruno, G.: De l'Infinito, Universo e Mondi. Venezia, 1584.

[3] Cannon, J. W., Floyd, W. J., Kenyon, R., Parry, W. R.: Hyperbolic geometry. In: Flavors of Geometry, Math. Sci. Res. Inst. Publ. 31, Cambridge Univ. Press, 1997, 59–115.

[4] Friedman, A.: Über die Krümmung des Raumes. Z. Phys. 10 (1922), 377–386; English translation: On the curvature of space. General Relativity and Gravitation 31 (1999), 1991–2000.

[5] Friedmann, A.: Über die Möglichkeit einer Welt mit konstanter negativer Krümmung des Raumes. Z. Phys. 21 (1924), 326–332; English translation: On the possibility of a world with constant negative curvature of space. General Relativity and Gravitation 31 (1999), 2001–2008.

[6] Křížek, M.: Ten arguments against the proclaimed amount of dark matter. Gravit. Cosmol. 24 (2018), 350–359.

[7] Křížek, M., Křížek, F., Somer, L.: Antigravity — its origin and manifestations. Lambert Acad. Publ., Saarbrücken, 2015.

[8] Křížek, M., Mészáros, A.: On the Friedmann equation for the three-dimensional hypersphere, Proc. Conf. Cosmology on Small Scales 2016, Local Hubble Expansion and Selected Controversies in Cosmology (eds. M. Křížek, Y. V. Dumin), Inst. of Math., Prague, 2016, 159–178.

[9] Křížek, M., Mészáros, A.: Classification of distances in cosmology, Proc. Conf. Cosmology on Small Scales 2018, Dark Matter Problem and Selected Controversies in Cosmology (eds. M. Křížek, Y. V. Dumin), Inst. of Math., Prague, 2018, 92–118.

[10] Křížek, M., Somer, L.: A critique of the standard cosmological model. Neural Netw. World 24 (2014), 435–461.

[11] Křížek, M., Somer, L.: Excessive extrapolations in cosmology. Gravit. Cosmol. 22 (2016), 270–280.

[12] Křížek, M., Somer, L.: Excessive extrapolations of Einstein's equations. Proc. Conf. Cosmology on Small Scales 2020, Excessive Extrapolations and Selected Controversies in Cosmology (eds. M. Křížek, Y. V. Dumin), Inst. of Math., Prague, 2020, 9–34.

[13] Landau, L. D., Lifshitz, E. M.: The classical theory of fields (4th revised edition). Pergamon Press Ltd., 1975.

[14] Lemaître, G. E.: Un Univers homogène de masse constante et de rayon croissant rendant compte de la vitesse radiale des nébuleuses extragalactiques. Ann. Soc. Sci. de Bruxelles (1927), April, 49–59.

[15] Li, M.-H., Liu, H.-N.: Testing the homogeneity of the Universe using gamma-ray bursts. Astron. Astrophys. 582 (2015), A111, 1–7.

[16] Mészáros, A.: A possible fast growth of adiabatic cosmological perturbations. Astron. Astrophys. 278 (1993), 1–5.

[17] Misner, C. W., Thorne, K. S., Wheller, J. A.: Gravitation, 20th edition. New York, W. H. Freeman, 1997.

[18] Peebles, P. J. E.: Principles of physical cosmology. Princeton Univ. Press, New Jersey, 1993.

[19] Perlmutter, S.: Supernovae, dark energy, and the accelerating universe. Physics Today 56 (2003), April, 53–60.

[20] Planck Collaboration: Planck 2013 results, I. Overview of products and scientific results. Astron. Astrophys. 571 (2014), A1, 48 pp.

[21] Rektorys, K. et al.: Survey of applicable mathematics I. Kluwer Acad. Publ., Dordrecht, 1994.

[22] Schwarzschild, K.: Über das zulässige Krümmungsmaaß des Raumes. Vierteljahrsschift der Astronomischen Gesellschaft 35 (1900), 337–347; English translation: On the permissible numerical value of the curvature of space. Abraham Zelmanov J. 1 (2008), 64–73.

[23] Weinberg, S.: Gravitation and cosmology: principles and applications of the general theory of relativity. John Wiley & Sons, Inc., New York, London, 1972.

[24] Weinberg, S.: The first three minutes, 2nd edition. Basic Books, 1993.

ALBERT EINSTEIN AND GUSTAV JAUMANN ON THE BALANCE (NEGOTIATIONS FOR THE PROFESSORSHIP OF THEORETICAL PHYSICS AT THE GERMAN UNIVERSITY IN PRAGUE IN 1910–1911)

Emilie Těšínská

Institute of Contemporary History, Czech Academy of Sciences, Prague, Czech Republic
tesinska@cesnet.cz

Abstract: This paper presents some archive documents illustrating the negotiations for the professorship of theoretical physics at the former German Karl-Ferdinand University in Prague (GU), which became vacant with the retirement of Ferdinand Lippich (1838–1913) on 30 September 1910. Three candidates were nominated for the vacant professorship by the professorial board of the Faculty of Philosophy of GU: in first place Albert Einstein (extraordinary professor of theoretical physics at the University of Zurich), in second place Gustav Jaumann (ordinary professor of general and technical physics at the German Technical University in Brno) and in third place Emil Kohl (private docent of physics at the University of Vienna and actuary of the Vienna Academy of Sciences).

The proposal was sent to the Ministry of Culture and Education in Vienna (as the Czech lands, with their capital Prague, were part of the Austro-Hungarian Monarchy at that time). The Ministry asked for a confidential comment on the proposal from Ernst Mach, at that time professor of philosophy at the University of Vienna, who had been professor of experimental physics in Prague in 1867–1895. E. Mach supported the selection and order of the nominated candidates. So did F. Lippich in a personal letter to the Ministry. However the Ministry decided to offer the professorship first to an inland candidate, G. Jaumann, which was not an unusual procedure. Jaumann initially welcomed the offer as merited appreciation of his talents and specialization, but eventually refused it because his claim for a higher salary was not met. Only then did the Ministry offer the professorship to A. Einstein, who accepted the offer without any extraordinary demands and was appointed ordinary (full) professor (and head of the Institute) of theoretical physics at GU by a decision of the Emperor Franz Joseph of 6 January 1911, effective from 1st April 1911.

Keywords: German University in Prague, Albert Einstein, Gustav Jaumann

PACS: 01.65.+g

1. Introduction

In this article, we will focus on the negotiations for a new professorship of theoretical physics at the German Karl-Ferdinand University in Prague (*k. k. deutsche Karl-Ferdinands Universität in Prag*, hereinafter abbreviated as German University, GU), which became vacant with the retirement of professor Ferdinand Lippich on 30 September 1910. To supplement the already existing historical literature (or to recall lesser-known circumstances of this history), we will present the statements of Ernst Mach and Ferdinand Lippich on the proposal for the new professorship drawn up by the professorial board of the Faculty of Philosophy of GU and submitted to the Ministry of Culture and Education in Vienna (*k. k. Ministerium für Cultus und Unterricht*), in which Albert Einstein was strongly proposed as the first candidate. We will also document the position of Gustav Jaumann, the inland candidate proposed by the professorial board for the professorship *in secundo loco*, who was offered the professorship by the Ministry as the first, who, however, eventually declined the offer.

The article is based mostly on written documents preserved in the collection of the Vienna Ministry of Culture and Education in the National Archives in Prague. Quoted are also three items of Ernst Mach's correspondence held in the Archives of the *Deutsches Museum* in Munich. The broader context of the topic (and references to other historical sources and literature) can be found e.g. in articles [1], [2] or in publication [3]. A. Einstein, his stay and work in Prague (Bohemia), is the subject e.g. of a new monograph [4].

The historical documents are quoted in their German original with the preservation of the period German spelling.

2. Vacancy of the professorship of mathematical physics at GU and the proposal of the Faculty of Philosophy for its new filling

2.1. Announced retirement of Ferdinand Lippich

On 4 October 1908, Ferdinand Lippich (1838–1913), professor of mathematical physics at the Faculty of Philosophy of GU, reached the age of 70, which was the legal limit for university professors in the Austro-Hungarian Monarchy to retire permanently (after the completion of the school year). In recognition of F. Lippich's merits, he was extended by one "honorary year" by a decree of the Ministry of Culture and Education of 22 January 1909. By the same decree, the Ministry invited the Faculty of Philosophy of GU to propose a trienium of candidates for the professorship of mathematical physics, which would become vacant on 1st October 1910.

F. Lippich had held the professorship from its establishment in 1872. It was an ordinary (full) professorship. It already had at its disposal a modest Institute (*k. k. mathematisch-physikalisches Cabinet*) with one auxiliary assistant (wissenschaftliche Hilfskraft, a post held by Emil Nohel from 1st October 1910) and a Seminar, which was shared with the professorship of mathematics (at that time held by George Pick). The Institute and the Seminar were located in the building

of the Natural Science Institutes of GU in Prague, Viničná Street *(Weinberggasse)*; the teaching, however, was still partly carried out in premises of GU in the Prague Clementinum (the former Jesuit college).

2.2. Proposal of the professorial board

At the meeting on 27 January 1910, the professorial board of the Faculty of Philosophy of GU appointed a three-member committee to prepare a proposal of suitable candidates for the professorship of mathematical physics. Members of the committee were Anton Lampa (ordinary professor of experimental physics), Georg Pick (ordinary professor of mathematics), and Viktor Rothmund (extraordinary professor of physical chemistry). Ferdinand Lippich decided to refrain from the negotiations of his successor. The main responsibility for the proposal thus shouldered A. Lampa who was appointed professor at GU only a year before that, in 1909 when he succeeded Mach's successor at the professorship of (experimental) physics at GU Ernst Lecher.

In the proposal submitted by the committee to the professorial board, dated April 1910, the following physicists were nominated for the professorship (with a newly proposed title) of theoretical physics: Albert Einstein, a 31-year-old extraordinary professor of theoretical physics at the University of Zurich, in first place; Gustav Jaumann, a 47 year-old ordinary professor of general and technical physics at the German Technical University in Brno, in second place; and Emil Kohl, a 48-year-old private docent of physics at the University of Vienna and actuary of the Vienna (Imperial) Academy of Sciences, in third place. The main criterion on which the candidates were selected was their scientific contribution to the modern theoretical physics, i.e. to the field of electromagnetism. In the proposal of the committee it was worded as follows:

> *Die moderne theoretische Physik hat die kräftigen Impulse aus der Elektrizitätslehre empfangen. Durch Maxwell ist die Optik als ein Spezialkapitel in die Elektrizitätslehre eingegliedert worden. Glänzende Experimentaluntersuchungen von Boltzmann, Hertz und anderen haben gezeigt, welche Fruchtbarkeit den kühnen theoretischen Spekulationen Maxwells innewohnt, und die Berechtigung des Gedankens erwiesen, die optischen Erscheinungen, die bis dahin mechanisch gedeutet wurden, als elektromagnetische Vorgänge aufzufassen. Dieser erfolgreiche Schritt legte in weiterer Konsequenz das allgemeinere Problem des Verhältnisses der Mechanik zur Elektrizitätslehre nahe. Dieses Problem nimmt in der neuesten Zeit die Aufmerksamkeit der theoretischen Physik in gleich hohem Masse in Anspruch, wie zu Beginn der Maxwell'schen Gedankenbildungen. Während aber damals die Mechanik das Fundament bildete, von welchem aus man in das fremdartige Gebiet der Elektrizität einzudringen bemüht war, ist nun, am Ende einer langen und an weittragenden Entdeckungen reichen Entwicklung der Standpunkt verschoben: jetzt bildet die Elektrizitätslehre den Ausgangspunkt für alle das genannte Problem betref-*

fenden Ueberlegungen. Dieses Problem ist das centrale Problem der modernen theoretischen Physik und wird es auf lange hinaus bleiben. Jeder Versuch, dieses Problem seiner Lösung näher zu bringen, muss von Fragen der elektromagnetischen Theorie ausgehen; jeder solche Versuch hat die weitgehendsten, das gesamte System der theoretischen Physik berührenden Konsequenzen, so dass man wohl, ohne sich einer Uebertreibung schuldig zu machen, sagen darf, dass die weitere Entwicklung der theoretischen Physik durchaus an die Bearbeitung des hier berührten Problems gebunden ist.

In Berücksichtigung dieser Sachlage ist die Kommission zu der Ansicht gelangt, der Fakultät zu empfehlen, nur solche Forscher in den Besetzungsvorschlag aufzunehmen, welche in ihren Arbeiten zu diesem wichtigsten Problem der modernen theoretischen Physik Stellung genommen haben und daher die Gewähr bieten, dass unserer Universität ein ihrer Tradition entsprechender Anteil an der Weiterentwicklung der theoretischen Physik gesichert bleibt.[1]

The nomination of A. Einstein (a foreigner and the youngest of the three) for the professorship in the first place was justified in the proposal by his outstanding scientific achievements and his leadership in the field of modern theoretical physics. It was emphasized that his appointment would contribute significantly to the prestige of GU in the field of science.

The committee's proposal was unanimously approved by the professorial board and in a copy forwarded to the Ministry of Culture and Education in Vienna through the Dean's Office of the Faculty, with a covering letter of 23 April 1910.[2]

2.3. Decision to ask three external scholars for their opinions

The three candidates for the professorship of theoretical physics at GU were presented and compared without a sign of doubt in the proposal that the committee tabled to the professorial board. The way to that proposal, however, was not an easy one. Opinions of the committee members on Gustav Jaumann and his convoluted work diverged. It was at the instance of Viktor Rothmund (who was Jaumann's successor at the professorship of physical chemistry at GU and his younger by seven years) that the committee decided to ask three external scholars for their expert opinion on Jaumann, namely Ernst Mach (professor of philosophy at the University in Vienna), Max Planck (professor of theoretical physics at the University in Berlin) and Woldemar Voigt (professor of theoretical physics at the University in Göttingen). Anton Lampa was entrusted to address Ernst Mach (who was his former teacher and colleague at the University in Vienna) in the matter. Mach was professor of (experimental) physics in Prague in 1867–1895, and Jaumann was one of his students and assistants at GU; it was also Mach who presented (and recommended for publication) most of Jaumann's papers to the Vienna Academy of Sciences (before Jaumann's election inland corresponding member of the Academy in 1905).

Lampa outlined the task and work of the committee to Mach in a personal letter of 9 February 1910. He did not contest Jaumann's talent, and confessed a sort of support to his way of thinking, but expressed some scepticism towards Jaumann's theoretical physical constructs. Mach's expert view of Jaumann and his work was to help Lampa (and the whole committee) assess Jaumann's achievements in the field of modern physics correctly. Lampa's handwritten letter to Mach reads as follows:

Prag II 1594, Weinbergasse 3,
am 9. Februar 1910.
Hochgeehrter Herr Professor!
Die Frage der Wiederbesetzung der Lehrkanzel von Hofrat Lippich ist nun aktuell geworden. Lippich hat es abgelehnt in die Kommission einzutreten, so dass ich nun der einzige Physiker in dieser Kommission bin. Außer mir gehören ihr an Pick und Rothmund (physik. Chemie). Die Verantwortung, welche auf mir liegt, ist durch die Resignation von Lippich doppelt so groß als sie es sonst wäre. Ich habe es daher mit Freude begrüßt, als von Rothmund der Antrag gestellt wurde, bezüglich Jaumanns Äußerungen fremder Gelehrter einzuholen; wir haben uns geeinigt, Sie, Planck und Voigt zu bitten, uns Ihre Ansichten mitzuteilen. Im Einverständnis mit der Kommission darf ich dem Schreiben an Sie mehr persönlichen Charakter verleihen, indem ich Ihnen gegenüber die speziellen Fragen zur Besprechung bringe, welche mir für die Beurteilung von Jaumanns Leistungen von besonderer Wichtigkeit erscheinen. Ich brauche nicht zu versichern, dass mir die hohe Begabung Jaumanns außer Zweifel scheint und dass mir seine ganze Denkart sympathisch ist. Ich betrachte als Ideal der theoretischen Physik die rein phänomenologische Darstellung, wie sie etwa in der Thermodynamik vorliegt. Jaumann geht von dem Wunsche aus, eine solche phänomenologische Darstellung für die Elektrizitätslehre und was sich mit ihr in Zusammenhang bringen lässt, aufzubauen. Er verwirft also Atomtheorie und Elektronik und sucht die Feldgleichungen Maxwell's zu erweitern, so dass sie auch zur Beschreibung nicht superpositorischer Vorgänge ausreichen. Nun beginnt aber, wie es ja auch nicht anders sein kann, die Bildung von Hypothesen zur Erreichung dieses Zieles. Gegen diese Hypothesen, die schrittweise einer immer weiter gehende Vervollständigung und Ergänzung erfahren, habe ich nun zweierlei einzuwenden.
1. Erkenntnistheoretisch sehe ich keinen Unterschied gegen das Verfahren der Elektronentheorie. Hier werden Körperchen eingeführt, die sich der Erfahrung entziehen, bei Jaumann Zustandsveränderungen, die sich gleichfalls der Erfahrung entziehen. Welches Verfahren man einschlagen will, ist mehr Geschmackssache. Die Rechtfertigung liegt im Erfolg. Und da scheint mir bei aller Abneigung gegen die Elektronik vorderhand diese überlegen.

2. Vom physikalischen Standpunkt habe ich gegen Jaumanns Hypothesen den Einwand zu erheben, dass zu ihrer Stütze keine anderen Erfahrungen angeführt werden können, als eben diejenigen, zu deren Interpretation sie dienen sollen. Die erste Hypothese Jaumanns war die Veränderlichkeit der Dielektrizitätskonstante durch die elektrischen Kräfte selbst. Diese Hypothese schiene mir sehr berechtigt, wenn man jemals die Kapazität eines Kondensators von der Potentialdifferenz seiner Belegungen abhängig gefunden hätte. Die dielektrische Hysteresis kann hier nicht herangezogen werden, denn bei sehr raschen Schwankungen der elektrischen Kraft wird sie Null. Mit dieser Hypothese findet aber Jaumann nicht sein Auslangen. Es muss zwei neue Energiearten potentieller und lebendiger Art (ich will das Wort kinetisch vermeiden) einführen, neben dem Leitungs- und Verschiebungsstrom erscheint ein sogenannter chemischer Strom zur Vervollständigung der Feldgleichungen Erst jetzt gelingt es, das Wesentliche der Erscheinungen wiederzugeben.

Eine Rechtfertigung dieser Hypothesen ist, glaube ich, nur durch einen quantitativen Vergleich seiner theoretischen Resultate mit der Erfahrung zu liefern und durch die Vorhersage neuer Erscheinungen. Den Vergleich hat Jaumann ganz unzureichend geführt, Erscheinungen in genügend großer Zahl vorhergesagt, aber leider nicht eine einzige aufgesucht.

Ich befinde mich daher in der unangenehmen Situation, die Intentionen Jaumans zu billigen, seine wissenschaftliche Phantasie und sein architektonisches Talent bewundern zu müssen, ohne einen Anhaltspunkt für ein gerechtes Urteil zu haben. Ich habe es mir sauer genug werden lassen, in seine Gedanken trotz des mathematischen Gestrüppes, das übrigens nicht gar so arg ist, einzudringen. Ich fürchte aber sehr, dass es mir nicht in zureichendem Maß gelungen ist. Und so habe ich das Bedenken, einerseits die Jaumann'sche Theorie aus prinzipiellen Gründen zu überschätzen, anderseits wegen Mangels einer erfahrungsmäßigen Rechtsfertigung ihr mehr den Charakter einer geistreichen naturphilosophischen Konstruktion beizulegen. Aus diesem Grunde wäre ich Ihnen für ein aufklärendes Wort sehr dankbar.

Ihre Antwort ist zunächst nur für den Gebrauch in der Kommission bestimmt. Doch erbitte ich mir die Ermächtigung, gegebenenfalls in der Fakultät von ihr Gebrauch machen zu dürfen.

Für Ihren freundlichen Gruß durch Marty herzlichen Dank. Ich hoffe, dass Sie Sich recht wol befinden und dass Sie die Mühe, die ich Ihnen mit dieser Anfrage mache, nicht allzu lästig empfinden werden. Ich freue mich schon sehr, Sie in einigen Wochen persönlich begrüßen zu können und Ihnen dann von dem weiteren Fortgang der Angelegenheit zu berichten.

Mit herzlichsten Grüßen bleibe ich Ihr in ausgezeichnetster Hochachtung ergebener   A Lampa[3)]

Next letter of A. Lampa to E. Mach, dated 18 February 1910, documents that Mach granted Lampa's request. Mach's opinion, as well as the opinions of Voigt and Planck influenced then the final proposal of the committee. It seems that there was a general agreement on Jaumann's talent, reproached to him was a lack of his own criticality (noticeable namely in his latest work). Interesting is Lampa's note of professor Pick and his attitude towards (support to) Jaumann's candidacy to the professorship. Lampa also mentioned that the committee had agreed to approach Jaumann and ask him if he would possibly accept the professorship in Prague.

Prag, am 18 Februar 1910.

Hochgeehrter Herr Professor!
Ich danke Ihnen sehr für das ausführliche Schreiben, welches Sie mir in der Angelegenheit Jaumann zu senden so gütig waren. Planck und Voigt haben auch geschrieben. Beide sprechen mit Anerkennung von J.'s Begabung, beide tadeln den Mangel an Selbstkritik, der namentlich in den letzten Arbeiten zutage tritt. So nähern sich diese Urteile in gewissem Sinne meinem Eindruck, dass sich J. die Vergleichung mit der Erfahrung sehr leicht macht. Ihre Auseinandersetzungen haben mich bezüglich der Methodik Jaumanns beruhigt und so konnte ich in der Kommission wärmer für J. eintreten, als mir dies sonst möglich gewesen wäre. Einen besonders warmen Anwalt hat J. in Pick, der zwar manchen Seiten von J.'s Persönlichkeit recht kritisch gegenübersteht, sich aber mit Nachdruck für ihn einsetzt. So haben wir denn in der letzten Kommissionssitzung einstimmig beschlossen, an J. mit der Frage heranzutreten, ob er einem Rufe nach Prag Folge leisten würde.
Indem ich Sie bitte, diese Mitteilungen als vertrauliche anzusehen, bleibe ich, nochmals herzlich dankend, Ihr Sie aufrichtigst hochschätzender und Ihnen treu ergebener
A Lampa[4]

3. Position of the Vienna Ministry on the proposal of the GU Faculty of Philosophy

3.1. The Ministry's preference for an inland candidate

The Ministry of Culture and Education in Vienna decided to offer the professorship of theoretical physics at GU first to the inland candidate G. Jaumann. His scientific achievements appeared to the Ministry to be significant, and his academic positions (Dean of the General Department in 1903–1905 and of the Department for Technical Chemistry in 1908–1910 at the German Technical University in Brno) and membership in scientific academies (member of the *Kaiserliche Leopoldinisch-Carolinische deutsche Akademie der Naturforscher* since 1891 and corresponding inland member of the Vienna Academy of Sciences, its Mathematical and Science

Department, since 1905) also played in his favour. In addition, Jaumann's appointment at GU would have opened up a post at the German Technical University in Brno for one of the young Viennese physicists.

This way of thinking by the Ministry was not exceptional; the Ministry also gave preference to inland candidates when filling other teaching positions at the Austro-Hungarian universities, for example when appointing A. Lampa as professor of experimental physics at GU in 1909 (when the candidate nominated at the first place by the professorial board of the Faculty of Philosophy was German physicist Johannes Stark) [5].

3.2. Statement of Ernst Mach for the Ministry

Before the Ministry of Culture and Education approached G. Jaumann to offer him the Prague professorship, it also asked for an opinion on the proposal of the GU Faculty of Philosophy from Professor Ernst Mach. As it was already mentioned, Mach had been a professor of (experimental) physics in Prague for 28 years and Jaumann was one of his students and assistants at the Institute of Physics at GU. In a letter dated 18 May 1910, the Minister of Culture and Education Karl Stürgkh briefly informed Mach about the proposal of the GU Faculty of Philosophy for a new professorship after F. Lippich and asked for his personal, confidential opinion on the proposal. Specifically, he asked Mach to comment on whether the scientific results of the first-place foreign nominee, Dr. Einstein, could be considered so outstanding in comparison with the scientific results of Professor Jaumann that the acquisition of Einstein for the GU would be particularly desirable. In the draft letter noted on the ministerial file, this was phrased in words:

> *Ich ersuche Eure // sich über diesen Personalvorschlag vertraulich außern und sich hiebei namentlich darüber aussprechen zu wollen, ob die wissenschaftlichen Leistungen des an erster Stelle genannten Ausländers Dr Einstein gegenüber jenen des Professors Jaumann als derart hervorragend erachtet werden können, daß die Gewinnung des Ersteren für die Deutsche Universität in Prag als empfehlenswert besonders wünschenswert darstellen würde.*[5)]

Ernst Mach replied by letter of 22 May 1910. He described the proposal for the professorship – the selection and order of the proposed candidates – as economical, fair and hardly contestable. He stated that A. Einstein undoubtedly stood in the first rank among the younger physicists of mathematical orientation. He praised Einstein's formulation of the principle of relativity, saying that it had been received with the greatest interest by physicists and had also found a supporter in the leading mathematician Hermann Minkowski. He added that, given the small number of mathematical physicists in the Austro-Hungarian Monarchy, Einstein's nomination for the professorship in question was no surprise. In experimental physics however, he continued, the situation was different; the Monarchy had no shortage of excellent

experimental physicists and calling upon a foreigner to fill such a vacant professorship would be discouraging and would weigh heavily on the younger generation in particular. Mach also expressed his appreciation of G. Jaumann. He described him as one of the very talented young Austrian physicists. Even if Einstein's reputation was greater than Jaumann's at that time, he added, this could be reversed in the future. He remarked that Jaumann had adversely affected his professional career by taking a stern stand against the prevailing theories, "which is always dangerous for a young person"; Einstein cleverly managed to avoid this. At the same time, Mach expressed surprise that Jaumann aspired to a poorly endowed teaching chair of mathematical physics in Prague, while at the Technical University in Brno he had a richly equipped collection of instruments for experimentation. He tried to explain this by saying that Jaumann probably did not see the right response in his Brno audience, or that he wanted to switch to mathematical physics, "which he is no stranger to", and spend more time on his own research. Mach concluded by expressing his great pleasure that the proposal in question did not omit the Viennese physicist Emil Kohl, a quiet and solid worker in mathematical physics. The full text of Mach's typed statement was as follows (the underlining of words in the text is original).

Hohes Ministerium f C u U!
In Beantwortung der h Zuschrift vom 18/V '10 ad Z 17.589 ex 1910 beeile
ich mich ergebenst mitzuteilen:
Der Vorschlag Io A Einstein
    IIo G Jaumann
    IIIo E Kohl
scheint mir sehr billig, gerecht und kaum angreifbar.
Unter den jüngeren Physikern mathematischer Richtung steht <u>*Einstein*</u>
zweifellos in <u>*erster*</u> *Reihe durch Aufstellung des fruchtbaren Relativitäts-*
prinzipes, welches auch von der Gesammtheit der Physiker mit dem gröss-
ten Interesse aufgenommen wurde. Dieses Prinzip hat auch das Glück
gehabt in einem so hervorragenden Mathematiker, wie <u>*H Minkowski*</u>*, einen*
eifrigen Vertreter zu finden. Nimmt man hinzu, dass die Zahl der <u>*mathe-*</u>
<u>*matischen*</u> *Physiker in Oesterreich nicht sehr gross ist, so könnte die*
Berufung <u>*Einsteins*</u> *kaum Befremden erregen.*
Etwas anders verhält es sich in Bezug auf die Physiker <u>*experimenteller*</u>
Richtung. Oesterreich ist nicht arm an ausgezeichneten Leuten dieser
Art, so dass die Berufung eines Fremden beinahe notwendig als eine
Entmutigung unserer Landsleute empfunden werden müsste, welche bei
den geringen Aussichten unserer jungen Collegen besonders schwer ins
Gewicht fallen würde. Zu diesen jüngeren, nach meiner Meinung hochbe-
gabten Leuten, gehört <u>*G Jaumann*</u>*. Wenn heute auch der Ruf* <u>*Einsteins*</u>
grösser ist, so kann sich dieses Verhältnis doch umkehren. <u>*Jaumann*</u>
hat seine Laufbahn dadurch nicht gerade günstig beeinflusst, als er seine
Opposition gegen herrschende Theorien ziemlich schroff hervorgekehrt

hat, was namentlich für einen jungen Mann immer etwas gefährlich ist. <u>Einstein</u>, ebenfalls in der Opposition, wusste das klug zu vermeiden. Befremdlich ist mir bei <u>Jaumann</u>, dass er die karg dotirte Lehrkanzel der mathematischen Physik in Prag anstrebt, während ihm in Brünn eine reich ausgestattete Instrumentensammlung für Experimente zur Verfügung steht. Vielleicht findet er in seinem Brünner Auditorium nicht die richtige Resonanz; oder vielleicht wünscht er zur mathematischen Physik überzugehen, die ihm ja nicht fremd ist, um mehr Arbeitszeit für eigene Untersuchungen zu gewinnen.

Sehr erfreut hat mich, dass man <u>Emil Kohl</u> nicht vergessen hat, einen stillen soliden Arbeiter auf dem Gebiete der mathematischen Physik, der einstweilen den Dienst als Aktuar der Akademie der Wissenschaften übernommen hat.

Hiermit glaube ich dem h Ministerium alle Anhaltspunkte zu Beurteilung der Situation gegeben zu haben, die ich liefern kann.

Wien am 22. Mai 1910   *Ehrerbietigst*

[stamped signature] *Dr Ernst Mach*[6]

Let us add that E. Mach and A. Einstein had exchanged a pair of letters and publications in 1909. Under the term of that correspondence Einstein expressed his deep respect for Mach. Specifically, in the letter of 9 August 1909 Einstein wrote to Mach:

> *Sie haben auf die erkenntnistheoretischen Auffassungen der jüngeren Physiker-Generation einen solchen Einfluß gehabt, daß sogar Ihre heutigen Gegner, wie z. B. Herr Planck, von einem der Physiker, wie sie vor einigen Jahrzehnten im Ganzen waren, ohne Zweifel für "Machianer" erklärt würden.*[7]

3.3. Position of Ferdinand Lippich (a supplementary explanation)

F. Lippich explained his refusal to participate in the negotiations of his successor at GU in a letter of 19 May 1910; the letter was intended to prevent the possible misunderstanding of his position in Vienna (the addressee of the letter is not specified). Lippich stated that he had not wanted to influence his colleagues in the selection of his successor. He approved of the nomination of A. Einstein as a candidate for the professorship in first place, adding that Einstein would be a great asset to GU in scientific terms. The full text of Lippich's typewritten letter was as follows.

Prag den 19. Mai 1910.

Hochverehrter Herr Hofrat!

Es ist Ihnen vielleicht aufgefallen, dass unter den Namen der Mitglieder der Kommission, welche den Besetzungsvorschlag für die nach mir erledigte Lehrkanzel erstattet hat, mein Name fehlt. Es liegt mir nun sehr viel

154

daran, dass dieser Umstand an massgebender Stelle nicht falsch beurteilt werde und ich bitte Sie daher mir zu gestatten, dass ich Ihnen den von mir eingenommenen Standpunkt darlegte.

Als ich erklärte die Wahl in die Besetzungskommission nicht annehmen zu können und das Kollegium bat, von meiner Wahl absehen zu wollen, geschah das einzig und allein nur deshalb, weil ich es vermeiden wollte, den Besetzungsvorschlag möglicherweise in einer Weise beeinflusst zu haben, dass er die Meinung meiner engeren Fachkollegen nicht mehr ganz zum Ausdruck bringt. Ein Kompromiss ist ja bei geteilten Ansichten das gewöhnliche Resultat und ich wollte nicht mit dem Gefühle scheiden, dass durch ein solches mein Nachfolger nicht jene Persönlichkeit wäre, die das Kollegium vor Allen anderen gewünscht hat.

Nun ist der Besetzungsvorschlag so ausgefallen, dass ich demselben zustimmen konnte und ganz besonders mit Rücksicht auf den primo loco vorgeschlagenen Prof. Dr. Einstein, der, wie sich in der Sitzung erklärte und wie ich auch zur wärmsten Unterstützung dieses Vorschlages Ihnen gegenüber hervorhe[be]n möchte, eine glänzende Errungenschaft in wissenschaftlicher Beziehung für die hiesige Universität sein würde.

Genehmigen Sie, verehrter Herr Hofrat die Versicherung meiner vorzüglichsten Hochachtung mit der ich bin

      Ihr ganz ergebener

        [signature] *F. Lippich*[8]

4. The Ministry's negotiations with Gustav Jaumann

4.1. Offering the professorship to G. Jaumann

Although E. Mach fully supported the proposal of the professorial board of the GU Faculty of Philosophy, his statement about Jaumann confirmed the Ministry of Culture and Education in the conviction that the most (or sufficiently) suitable candidate for the professorship in question was G. Jaumann. In a letter dated 28 May 1910, the Ministry addressed G. Jaumann. The letter informed Jaumann that the Minister, Count Karl von Stürgkh, had given his preliminary consent to the proposal to appoint him professor of theoretical physics in Prague as of 1st October 1910, as successor to F. Lippich, and asked whether and under what conditions Jaumann would accept the professorship. The draft letter was originally dated 10 April 1910, but its dispatch was delayed pending the statement of E. Mach. Simultaneously then, in a letter dated 28 May 1910, the Ministry addressed the Moravian Governorate in Brno with a request for information about Jaumann's general behaviour.[9] The Governor's statement about Jaumann, dated 7 June of that year, was complimentary and without reservation:

Gegen den Obgenannten [Jaumann Dr. Gustav, Hochschulprofessor in Brünn] ist während seines Aufenthaltes in Brünn weder in moralischer

155

noch in staatsbürgerlicher Beziehung etwas Nachteiliges vorgekommen. Er ist politisch nie hervorgetreten, lebt in geordneten Vermögensverhält-nissen und geniesst sowohl unter seinen Berufskollegen als auch in bür-gerlichen Kreisen das grösste Ansehen und den besten Ruf.[10)]

4.2. Professional profile of G. Jaumann

Gustav Jaumann was born in 1863 in Karánsebes in what was then Bukovina (now Rumania) to the family of an Austro-Hungarian military official. After finishing in 1880 a secondary school (*die erste deutsche Staats-Oberrealschule*) in Prag (where the family had moved), he first studied chemistry for three years at the German Technical University in Prague and the Technical University in Vienna. From the school year 1883/84 he continued his studies at the Faculty of Philosophy of GU, where he soon captured attention of professor E. Mach. From 1st January 1885, he was appointed as an auxiliary assistant to E. Mach at the Institute of Physics (for a remuneration of 400 guldens per year); there he began his own experimental work in physics. In April 1890, pushed to it by professor Mach, he graduated as Doctor of Philosophy, and within three months of the same year he also habilitated for experimental physics and physical chemistry; both his doctoral dissertation and his habilitation work dealt with electrical discharges in gases and were already published in the Proceedings of the Vienna Academy of Sciences in 1888.[11)] From 1st October 1890, Jaumann was promoted to full assistant at the Institute of Physics (with a remuneration of 600 guldens per year). As Mach's full assistant, from the school year 1890/91 he conducted practical exercises in experimental physics for teacher candidates and medical students. He also collaborated with professor Mach on a secondary school textbook of natural history (*Grundriss der Naturlehre für die oberen Classen der Mittelschulen*, first edition in 1890); Jaumann wrote chapters on electricity, magnetism, atmospheric and celestial phenomena. By a Supreme Decision of 14 June 1893, effective from 1st October of that year, Jaumann was appointed as unpaid extraordinary professor of experimental physics and physical chemistry at GU. In 1896, he also became head of a newly established Institute of Physical Chemistry at GU, and from the school year 1896/97 he took over lectures on experimental physics for students of pharmaceutical courses at the Faculty of Philosophy (instead of Professor Ernst Lecher, Mach's successor in Prague, and for an extra remuneration). From 1st January 1901, Jaumann was assigned a pay of an extraordinary professor (in the amount of 3600 K plus a performance bonus of 840 K per year, as calculated in the new Austro-Hungarian currency – the crowns). Half a year later, by a Supreme Decision of 19 July 1901 (effective from 1st August of that year), Jaumann was appointed as ordinary (full) professor of general and technical physics at the German Technical University in Brno (Brünn, the administrative city of Moravia); his starting salary there was set at 6400 K plus a performance bonus of 960 K per year. Shortly before this appointment, in April 1901, he got married to Augustine Alix (born in 1873 in Hermeray, France); two sons were then born from the marriage.[12)]

Let us note that in 1901, A. Lampa (at that time still a private docent and assistant of the Institute of Physics at the University of Vienna) was also a candidate for the professorship of general and technical physics at the German Technical University in Brno; he was nominated in third place *ex aequo* with Josef von Geitler (private docent and since October 1893 Jaumann's successor at the post of assistant at the Institute of Physics at GU). Only Austrian candidates were considered for this professorship, which corresponds well with the above-quoted statement of E. Mach of the Austro-Hungarian experimental physics as a field not suffering from a lack of excellent people. In the selection and assessment of candidates for the professorship at the German Technical University in Brno in 1901, the decisive criteria were scientific competence in experimental physics and links to technical fields; for this reason, e.g. 36-year-old physicist Gustav Jäger, native from Bohemia and extraordinary professor at the University of Vienna, whose scientific work was mainly theoretical, was not included among the candidates. In contrast, G. Jaumann fulfilled the criteria for that professorship very well at that time.[13]

Jaumann's physics papers from his time at GU were mostly experimental, in the fields of electricity, optics and mechanics. In these works he dealt with improvements of physical precision instruments (W. Thomson's absolute electrometer, a regulator for an automatic mercury vacuum pump and others), studied discharges in gases, interference and diversion of cathode rays in electrical field, fading of light emission of radiating bodies, suggested a modification of Foucault's and Fizeau's methods of determination of speed of light. From Prague, he also published a theoretical work "on longitudinal light" (with a concept of light and cathode rays which was contrary to the common views of that time)[14] and two theoretical works on physical chemistry – an attempt on building a chemical theory on physical foundations[15] and a contribution to the theory of solutions.[16] After moving to Brno, Jaumann's publications were dominated by theoretical issues, he dealt with the heat production in flowing viscous liquids, theory of electromagnetic phenomena in moving media[17] and of radiation in strong electromagnetic fields,[18] he was also one of the first to use tensor calculus in his theoretical work.[19]

Jaumann was influenced in his work by E. Mach, references to Mach can be found in most of his publications. He nevertheless tried to find and make his own way in physics. For his work, he was granted subsidies of the local *Gesellschaft zur Förderung deutscher Wissenschaft, Kunst und Literatur in Böhmen* (of its Science Department), as well as of the Mathematical and Science Department of the Vienna Academy of Sciences.

In the proposal for the new professorship of theoretical physics at GU of April 1910, worked out by professors Lampa, Pick and Rothmund, the scientific activities of G. Jaumann were assessed just briefly and in more or less neutral way.

Jaumann hat auch eine Reihe experimenteller Arbeiten ausgeführt, von welchen die Konstruktion eines Elektrometers und einer Quecksilberluftpumpe hervorgehoben seien. Seine Experimentaluntersuchungen über den

*Einfluss rascher Potentialschwankungen auf den Entladungsvorgang, ferner
die elektrostatische Ablenkung und die Interferenz der Kathodenstrahlen
waren von Bedeutung für seine theoretischen Ansichten, seien daher eben-
falls besonders angeführt. Endlich sei auf sein Werk: 'Die Grundlagen
der Bewegungslehre' Leipzig 1905, hingewiesen.*[20)]

4.3. Jaumann's response to the Ministry's offer and his request

Gustav Jaumann replied to the Ministry's offer of the Prague professorship of
theoretical physics by letter of 3 June 1910. First, he thanked the Ministry for
the confidence they had shown in him. He stated that the offer was a great sat-
isfaction for him, as it would be the first time that he would take up a teaching
post corresponding to his talents and specialization. For all that, he conditioned his
acceptance of the proffered post in Prague on the request that he be granted a per-
sonal allowance of 2000 K per year. He justified this on the grounds of the higher
workload and strain placed on a professor of theoretical physics in terms of training
if he wanted to keep up with the field, as opposed to teaching practically-oriented
physics at a technical university. The moral recognition he was offered should there-
fore also take a material form. He stated that it was also the last opportunity to
make amends for him for the sacrifices he had made for science during his early
career in Prague. In addition, he knew the higher cost of living there. Finally he
remarked that, in general, a professor who had another scientific career ahead of
him would gladly accept a call to the Prague professorship even at some material
sacrifice. In his (Jaumann's) case, however, the Ministry could offer him no further
career promotion, because the professorship of theoretical physics at the (central)
University of Vienna was occupied by young talent. He concluded that he could
not therefore accept the increased workload associated with the Prague professor-
ship without material compensation. Last but not least, he also had to take into
account the welfare of his family. The Jaumann's letter was typed on the letterhead
of his Chair of General and Technical Physics at the German Technical University
in Brno; the letter was obviously preceded by a personal meeting at the Ministry in
Vienna.

*Lehrkanzel für Physik
der k. k. deutschen technischen Hochschule.*

Brünn, 3. Juni 1910.

*Hochgeehrter Herr Ministerialrat.
In höflichster Erwiederung Ihres geehrten Schreibens vom 28. Mai 1910
und in Zusammenfassung der Unterredung, welche ich am 1. Juli mit
dem Herrn Sektionschef und mit Ihnen, hochgeehrter Herr Ministerial-
rat, zu führen die Ehre hatte, möchte ich zunächst aufrichtig danken für
das Vertrauen, welches das hohe Ministerium mir entgegenbringt, indem
dasselbe meine Ernennung zum ordentlichen Professor für theoretische
Physik an der deutschen Universität in Prag in Aussicht nimmt. Ich*

werde nicht versäumen, diesen Dank Seiner Exzellenz dem Herrn Minister für Kultus und Unterricht, Grafen Stürgkh in einer anzustrebenden Audienz persönlich zum Ausdruck zu bringen.

Diese ehrenvolle Berufung erfüllt mich mit hoher Genugthuung, da ich damit zum erstenmale in eine Lehrstellung käme, welche meiner speziellen Begabung und Arbeitsrichtung ganz angemessen ist.

Dennoch muss ich nach reiflicher Uiberlegung meine Zusage davon abhängig machen, dass das hohe k. k. Ministerium mich durch die Gewährung einer Personalzulage jährlicher 2000 Kronen auszeichnet und fördert.

Ich will mir erlauben, die Motive, welche mich zu diesem Entschlusse führen, nachfolgend aufzuzählen:

1. Die Arbeitslast und geistige Anspannung, welche ein Professor für theoretische Physik an einer Universität übernimmt, wenn er auf der Höhe seines Spezialfaches bleiben will, ist wegen der unbedingt nötigen Vertiefung in der Behandlung des Lehrstoffes weitaus grösser, als die durch die mehr auf die grundlegenden technisch wichtigen Tatsachen aufgebaute Lehrtätigkeit eines Physikers an einer technischen Hochschule. Der hingegen an der Technik hinzukommende intensive experimentelle Unterricht wird mir an der hiesigen Hochschule durch vorzügliche Hilfskräfte sehr erleichtert, so dass mir mehr Kraft und Zeit für wissenschaftliche Arbeit übrigbleibt.

2. Der Wunsch, dass der Anerkennung, welche in diesem Rufe liegt, auch eine materielle Förderung folge, ist ein wohlberechtigter. Es ist diese Berufung vielleicht die letzte Gelegenheit, bei welcher ich eine Entschädigung für die grossen materiellen Opfer, welche ich bis zu meinem 38. Lebensjahre meiner wissenschaftlichen Karriere bringen musste, erhoffen kann.

3. In letzter Linie wären die mir aus früherer Zeit wohlbekannten ungünstigen Lebensverhältnisse in Prag zu berücksichtigen.

Ich gebe gern zu, dass ein Professor, welcher an eine weitere wissenschaftliche Karriere denkt, im allgemeinen einen Ruf an die Universität Prag selbst unter materiellen Opfern annehmen wird. In meinem Falle kann mir aber das hohe Ministerium eine weitere Karriere überhaupt nicht in Aussicht stellen, weil das gleiche Fach an der Wiener Universität durch eine junge Kraft besetzt ist.

Ich kann also mich nicht entschliessen, diese bedeutende Mehrbelastung ohne ganz entsprechende materielle Kompensation zu übernehmen.

Ich erlaube mir schliesslich darauf aufmerksam zu machen, dass ich meine materiellen Wünsche von Anfang an auf das mir mit Rücksicht auf das Wohl meiner Familie unumgänglich Notwendige beschränken zu müssen glaubte.

Indem ich Sie, hochgeehrter Herr Ministerialrat, bitte, diese Erklärung wohlwollend zur Kenntnis zu nehmen und meine Bitte dem Herrn Sek-

tionschef vorzulegen und Seiner Exzellenz dem Herrn Minister zu über-
mitteln,

> *zeichne ich*
> *mit dem Ausdrucke vorzüglichster Hochachtung*
> *Eurer Hochwohlgeborenen*
> [signed by hand] *ergebenster Prof Dr G. Jaumann*[21)]

4.4. Rejection of Jaumann's request and complaint by the Treasury Department

The Ministry of Culture and Education considered Jaumann's request and consulted it with the Treasury Department, which however took a negative stand on the issue. The Department refused to grant a personal allowance to Jaumann just because of his transfer to a professorship in Prague, not only for restricted budgetary reasons but also as an undesirable precedent. The Department also contradicted Jaumann's claims about the unfavourable circumstances of his academic career. It stated that, as an unpaid extraordinary professor in Prague, from 1894 Jaumann received a remuneration for conducting physics practical exercises for philosophers (i.e., teacher candidates) and students of medicine and, from 1896, for giving lectures on experimental physics for pharmacists (i.e., he had received a yearly remuneration of 1000 guldens, increased to 1500 guldens in 1899; converted into the new Austrian currency, this corresponded to 2000 K and 3000 K, respectively). From 1st January 1901, at the age of 37, he was awarded the salary of an extraordinary professor (3600 K plus an performance bonus of 840 K per year) and six months later, from 1st August 1901, that of an ordinary professor (6400 K plus an performance bonus of 960 K). After next five years he received his first statutory salary increase (800 K) and from 1st August 1911 he would be entitled to a second increase (another 800 K); the upper limit of the basic salary of an ordinary professor 11 200 K was to be reached by him on 1st August 1921. Jaumann was therefore not disadvantaged in any way compared with his peers in academia, wrote the Treasure Department in its statement of 9 August 1910, and added:

> *Uebrigens würde Jaumann durch seine Berufung nach Prag nicht nur in honorifico sondern durch die ihm daselbst zukommende Jahresremuneration für das Seminar per 800 K auch in utili gewissen.*[22)]

By letter of the Ministry of Culture and Education dated 23 August 1910, G. Jaumann was informed that Minister Stürgkh could not grant his request for the personal allowance on the grounds of principle, as had already been indicated to him in earlier discussions. However, he would be granted an annual remuneration of 800 K for the direction of the Seminar at the Prague professorship (this however was not an income counted in the old-age pension). Referring to Jaumann's own words about what the offer of the professorship meant to him, the letter stated that the Minister expected Jaumann to accept the offer, adding that Jaumann had been regarded by

the Ministry as the most competent representative from the beginning. The letter concluded by urging Jaumann to reconsider carefully this important issue for his academic career and to communicate his final decision to the Ministry.[23]

4.5. Jaumann's final refusal of the offered professorship in Prague

In a handwritten letter of 28 August 1910 (sent from a summer holiday stay), G. Jaumann definitively refused the offer of the professorship of theoretical physics at GU as his financial requirement had not been met. He probably also thought of the reception he would meet with the colleagues in the professorial board in Prague, who had so vehemently sought to attract the young A. Einstein to their ranks. Jaumann's final reply to the Ministry in Vienna was respectful but it showed his disappointment.

Hochgeehrter Herr Ministerialrath!

Ihrem geschätzten Schreiben vom 23. August l. J. habe ich mit Genugtuung entnommen, dass das hohe Ministerium mich gleich anfangs als den berufensten Vertreter für die Prager Lehrkanzel erachtet hat, ein Vertrauen, welches weit grösser als jenes ist, welches mir von Seite der Prager Fakultät entgegengebracht worden ist, und für welches ich nochmals meinen ganz ergebensten Dank sage.

Hingegen bedauere ich sehr, dass prinzipielle Bedenken bestehen, einem inländischen Gelehrten im Bedarfsfalle den Wechsel der Lehrkanzel durch eine materielle Förderung zu erleichtern. Jedenfalls gereicht es mir aber zu grosser Beruhigung, dass Seine Exzellenz der Herr Minister für Kultus und Unterricht Graf Stürgkh den in meinem Schreiben vom 3. Juni l. J. angeführten Gründen, welche mir den Wechsel der Lehrkanzel erschweren, alle Würdigung angedeihen lässt.

Da diese Gründe unverändert fortbestehen, so sehe ich mich, insbesondere mit Rücksicht auf das Wohl meiner Familie, zu meinem grossen Bedauern genötigt, unter solchen Umständen den ehrenvollen Ruf an die Prager Universität definitiv abzulehnen.

Mit dem Ausdrucke vorzüglichster Hochachtung

<div align="center">

Ihr ergebener

</div>

Neuhaus i. Ww., 28. Aug. 1910.   Dr Gustav Jaumann,

<div align="right">

o. ö. Professor an der deutschen
technischen Hochschule in Brünn.[24]

</div>

5. The Ministry's meeting with Albert Einstein

5.1. Offering the professorship to A. Einstein

After Jaumann's final refusal of the Prague professorship, the Vienna Ministry of Culture and Education negotiated with Albert Einstein. In a letter dated 17 September 1910, the Ministerial Section Head Max Husarek informed Einstein confidentially that he had been nominated for a professorship of theoretical physics at GU, and

asked him to state whether he was willing to accept the appointment (and assume the position right from the beginning winter semester or from the next summer semester 1911). He indicated preliminary that the salary of an ordinary professor was 6400 K per year (which sum was increased by 800 K after the fifth and the tenth year, by 1000 K after the fifteenth and the twentieth year, and by 1200 K after the twenty-fifth year) plus an yearly performance bonus of 1472 K. On top of that, there was a remuneration of 800 K per year for the direction of the Seminar.[25]

In the statement dated in Vienna on 27 September 1910, Einstein accepted the offer, with a possible start in April 1911. In the event of his appointment, he asked only for a contribution to at least partly cover his service fees and the cost of moving from Zurich to Prague. The text of Einstein's statement was as follows; Einstein signed a typewritten text and added the day in the date; he also made the partial wording changes in pen to the typescript which are indicated in the citation in pointed brackets.

> *Ich erkläre mich bereit einer Berufung für die an der deutschen Univer-sität in Prag erledigte ordentliche Lehrkanzel der theoretischen Physik unter den in dem Schreiben vom 17. September 1910 mir bekanntgegebe-nen Modalitäten zum Apriltermine 1911 Folge zu leisten.*
> *Gleichzeitig möchte ich aber die Bitte stellen, mir im Falle meiner Ernen-nung einen angemessenen Beitrag <wenigstens> zur <teilweisen> Be-streitung der Diensttaxen und Uebersiedlungskosten bewilligen zu wollen.*
> *Wien, am 27 September 1910.*
> [signature] *A. Einstein.*[26]

After that, by letter dated 18 October 1910, the Ministry of Culture and Edu-cation requested information from the Ministry of Foreign Affairs in Vienna about Einstein's general behaviour during the years of his stay in Switzerland; no obstacles to Einstein's appointment as professor in Prague were found in this respect.[27]

In mid-December 1910 the appointment of A. Einstein was still "in process". However, in a letter to E. Mach of 18 December 1910, A. Lampa commented on the situation optimistically, based on an inquiry made in the Ministry in Vienna.

> *Die Ernennung Einsteins ist, wie Hofrat Kelle kürzlich auf eine dies-bezügliche Anfrage erklärte, 'bereits im Zuge'. Nach dieser und früheren analogen Erklärungen zweifle ich nicht mehr an der Richtigkeit der in verschiedenen Zeitschriften vorweggenommenen Berufung Einsteins.*[28]

5.2. The appointment of A. Einstein

Albert Einstein was appointed professor of theoretical physics and head of the Institute of Theoretical Physics (*k. k. Institut für theoretische Physik*) at GU by the Supreme Decision of 6 January 1911, effective from 1st April 1911. He was informed of the appointment by the minister Stürgkh in a letter of 13 January 1911. He was to

take up his teaching duties from the summer semester of 1911. From 1st April 1911 he was awarded an annual salary of 6400 K plus an annual performance bonus of 1472 K. At the same time, he was put in charge of an independent Seminar for Theoretical Physics at GU, for which he was allowed a remuneration of 800 K per year (paid in two equal instalments, each at the end of the semester). He was allowed 2000 K to cover the service tax he had to pay and as a contribution to his expenses for moving from Zurich to Prague; half of the sum was to be paid upon the assumption of his teaching duties and the other half at the beginning of the year 1912. Finally the letter noted that the appointment was contingent on the acquisition of Austrian citizenship.[29]

Professor Lippich retired at the end of the school year 1909/10. His existing salary was cease on 30 September 1910 and from 1st October 1910 he was awarded a pension of 11 840 K (i.e. the amount of his active salary of 11 200 K plus 640 K as an aliquot of his existing performance bonus of 1472 K). The professorship of theoretical physics at GU remained vacant in the winter semester 1910/11. Professor Lippich reduced his teaching in the summer semester of 1910 already; on the grounds that he had to finish his experimental work before leaving his teaching post, he asked to be excused from holding a colloquium on the theory of potential.[30]

6. Addendum

Albert Einstein served as the professor of theoretical physics at GU for only three semesters. On 29 January 1912, he asked the Vienna Ministry of Culture and Education to release him from his teaching post in Prague on 30 September 1912, stating that he intended to accept an extraordinary offer made to him by the *Eidgenössische technische Hochschule* in Zurich. At the same time he thanked the Ministry for the kindness with which they had accepted him into the Austrian civil service. The handwritten letter read as follows.

> *An das k. k. Ministerium für Kultus und Unterricht.*
> *Der Unterzeichnete bittet um seine Entlassung aus dem österreichischen Staatsdienst mit 30. September 1912. Er beabsichtigt, einem Rufe an die eidgenössische technische Hochschule Folge zu leisten, der ihm die Rückkehr zu seine Heimat unter günstigen Umständen ermöglicht, eine Chance, die sich ihm voraussichtlich nie wieder bieten würde. Er empfindet es als Bedürfnis, bei diesem Anlass seinen Dank zum Ausdruck zu bringen für das Entgegenkommen der hohen Unterrichtsverwaltung bei seinem Eintritt in den österreichischen Staatsdienst, und zu bitten, das die oben angeführten besonderen Umstände als Motiv für sein rasches Ausscheiden Billigung finden.*
> *Mit ausgezeichneter Hochachtung*
> *Albert Einstein*
> *o. Professor der theoretischen Physik*
> *an der k. k. Deutschen Universität in Prag.*
> *Prag, den 29. Januar 1912.*[31]

Einstein's request was granted. A new proposal for the professorship of theoretical physics at GU was prepared by A. Einstein, A. Lampa and V. Rothmund. They were charged with the task at the meeting of the professorial board on 14 March 1912 and their proposal was presented to (and agreed by) the professorial board at the meeting on 23 May 1912. The nominated candidates this time were three "Viennese" physicists: in first place Philipp Frank, in second place Paul Ehrenfest (at that time working as a private researcher and teacher in St. Petersburg, Russia) and in third place again Emil Kohl. G. Jaumnann was no longer considered as a candidate. The selection of candidates took into account, this time, their research work as well as their teaching ability.

> *Die Kommission hat nur solche theoretische Physiker in Betracht gezogen, die durch ihre Publikationen bewiesen haben, dass sie die neueren Zweige ihrer Wissenschaft derart beherrschen, dass sie diese nicht nur durch Vorlesungen den Studenten mitzuteilen vermögen, sondern dass sie auch imstande sind, die jungen Leute zum selbständigen wissenschaftlichen Arbeiten anzuregen. Bei ihrer Umschau ist die Kommission zu der Ansicht gelangt, dass sich unter den theoretischen Physikern des Inlandes einige von solcher Tüchtigkeit befinden, dass es natürlich erschien, in den Vorschlag nur Oesterreicher aufzunehmen.*[32]

By a Supreme Decision of 7 September 1912, Philipp Frank, a 28-year-old private docent at the University of Vienna, was appointed extraordinary professor of theoretical physics at GU; his starting salary was 3600 K plus a performance bonus of 1288 K per year, and a remuneration of 800 K per year for direction of (at first just) a Proseminar (i.e. a Preliminary seminar) for Theoretical Physics.[33] Ph. Frank held this post for 26 years (from November 1917 as full professor). In the autumn of 1938 he set off for a lecture tour in the USA. To Europe, which was then on the brink of the Second World War, he did not return.

Gustav Jaumann continued his professional career at the German Technical University in Brno where he was elected Rector for the school year 1912/13. In 1911, he was awarded the prestigious Haitinger Prize by the Vienna Academy of Sciences for his theoretical work. Jaumann's pay of an ordinary professor raised to 8000 K from 1st August 1911 and to 9000 K from the end of July 1916 (plus the adequate efficiency bonuses). From 1st September 1919 his pay reached 18 408 K plus a local bonus of 5400 K per year. On top of this regular pay he was occasionally conferred a remuneration for parallel lectures and exercises on physics or for substituting some other lectures, e.g. on mechanics in the school year 1918/19.

On 21 July 1924, at the age of 61 Jaumann died of heart failure while hiking in the Oetztal Alps. In his written legacy there remained a manuscript of a textbook *Einführung in die reine theoretische Physik* of about 2000 typed pages; it was never published, and got probably lost.[35]

References

[1] Havránek, J.: Materiály k Einsteinovu pražskému působení z Archivu Univerzity Karlovy [Historical documents on the stay of A. Einstein in Prague held in the Archives of Charles University, in Czech]. Acta Universitatis Carolinae – Historia Universitatis Carolinae Pragensis *20* (1980), 109–134.

[2] Těšínská, E.: Profilování teoretické fyziky na pražské univerzitě a vazby s pražským působením A. Einsteina před 100 lety [Professorship of theoretical physics at GU in Prague and Albert Einstein, in Czech]. Pokroky mat., fyz., astronom. *57* (2012), 146–168.

[3] Klein, M. J., Kox, A. J., and Schulmann, R. (eds.): The collected papers of Albert Einstein. Vol. 5: The Swiss Years: Correspondence, 1902–1914. Princeton University Press, 1993.

[4] Gordin, M. D.: Einstein in Bohemia. Princeton University Press, 2020.

[5] Kleinert, A.: Anton Lampa und Albert Einstein. Die Neubesetzung der physikalischen Lehrstühle an der deutschen Universität Prag 1909 und 1910. Gesnerus *32* (1975), 285–292.

[6] Bednarczyk, H.: Josef Finger und Gustav Jaumann, zwei Pioniere der heutigen Kontinuumsmechanik. österreichische Ingenieur- und Architekten Zeitschrift 135 (1990), 538–545.

Footnotes

1) NA (National Archives, Prague), collection MKV/R (Ministry of Culture and Education, Vienna), sign. 5 Prag Philosophie Professoren, box 111, Einstein Albert (personal file), Nr. 842/1911 (the committee's proposal, a typed copy, 10 p.)

2) NA, MKV/R, sign. 5 C1 Prag, b. 198, Nr. 26 833/1912.

3) Deutsches Museum, München, Archiv, Nachlass Ernst Mach, Korrespondenz, catalogue number NL 174/1877.

4) Ibd., NL 174/1878.

5) NA, MKV/R, sign. 5 C1 Prag, b. 197, Nr.17 589/1910 (letter drafted in the file, editorial changes are retained in the quotation; the appropriate title of the addressee was completed in the final letter instead of "//" in the draft).

6) NA, MKV/R, sign. 5 C1, b. 197, Nr. 26 566/1910 (reply to Z. 17 589/1910).

7) Cf. [3], p. 204, letter No. 174 (A. Einstein to E. Mach, Bern, 9 August 1909). The full text of the letter is accessible at https://einsteinpapers.press.princeton.edu/vol5-doc/254.

8) NA, MKV/R, sign, 5 C1 Prag, b. 197, Nr. 26 566/1910, (ad Z. 17 589/1910).

9) Ibd., Nr. 17 589/1910 (draft of both letters in the file).

10) Ibd. (k. k. Statthalterei für Mähren, Zl. 4487 Präs., Brno (Brünn), 7 June 1910).

11) Cf. Jaumann, G.: Einfluss rascher Potentialänderungen auf den Entladungsvorgang. Sitzungsberichte der kaiserlichen Akademie der Wissenschaften, math.-naturwis. Klasse, Abteilung II a, 97 (1888), 765–805; Jaumann, G.: Glimmentladungen in Luft von normalem Druck. Ibd. 1587–1626. Both the publications were sent to the Mathematics and Science Department of the Vienna Academy of Sciences by professor E. Mach as works carried out in the Institute of Physics of GU in Prague.

12) NA, MKV/R, sign. 5 Prag Philosophie Professoren, b. 113, Jaumann Gustav (personal file).

13) Ibd. Nr. 22 491/1901 (proposal for the professorship of physics at the German Technical University in Brno ad Z. 246, dated 22 May 1901, written by professor K. Zickler).

14) Jaumann, G.: Longitudinales Licht. Sitzungsberichte, Abt. II a, 104 (1896), 747–792. Sent for publication by E. Mach. The work was subsidized by the Gesellschaft zur Förderung deutscher Wissenschaft, Kunst und Literatur in Böhmen.

15) Jaumann, G.: Versuch einer chemischen Theorie auf vergleichend-physikalischer Grundlage. Sitzungsberichte, Abt. II a, 101 (1892), 487–530. Presented for publication by E. Mach. In the introduction Jaumann stated: "Im Folgenden findet man die Darstellung einer Theorie, welche vielleicht mit Vortheil an Stelle der Atomlehre verwendet werden kann ..."

16) Jaumann, G.: Zur Theorie der Lösungen. Annalen der Physik 308 (1900), 578–617. Sent for publication by F. Lippich. The aim of the work, as outlined in its first paragraph, was as follows: "Die Ziel der folgenden Betrachtungen ist die Theorie der Lösungen von der Arrhenius'schen Ionenhypothese unabhängig zu machen und sie hingegen an die Faraday-Maxwell'sche Theorie anzuschliessen."

17) Jaumann, G.: Electromagnetische Vorgänge in bewegten Medien. Sitzungsberichte, Abt. II a, 114 (1905), 1635–1684. Presented for publication by G. Jaumann (who was elected inland corresponding member of the Mathematics and Science Department of the Vienna Academy of Sciences half a year before that). The work was also briefly reported by Czech theoretical physicist František Záviška in an overview of publications in physics in the year 1906. Cf. Věstník České akademie císaře Františka Josefa pro vědu, slovesnost a umění 17 (1908), p. 263.

18) Jaumann, G.: Strahlungen in starken elektromagnetischen Feldern. Sitzungsberichte, Abt. II a, 116 (1907), 389–508. The work was presented in the meeting of the Matematical and Science Department of the Vienna Academy of Sciences on 28 February 1907 and was summarized by words: "Die vorliegende Mitteilung behandelt die Strahlungen in Medien allgemeinen Verhaltens, und zwar die Kathodenstrahlen und Kanalstrahlen, ihre ladende Wirkung, ihre elektrostatische und magnetische Ablenkung, die elektrische Doppelbrechung des Lichtes, die magnetische Drehung der Polarisationsebene und das Zeeman'sche Phänomen. Die diesem Teile der Theorie zu Grunde liegende Idee ist, daß

alle elektromagnetischen Strahlen von chemischen Schwingungen begleitet werden. Damit soll nichts anderes ausgesagt werden, als daß die stofflichen Eigenschaften des Mediums, insbesondere der dielektrische Koeffizient und das Leitungsvermögen desselben, in einem durchstrahlten Medium sehr kleine aber rasche periodische Änderungen erleiden. Der Verfasser hat sich bemüht, seine Theorie in nüchterner Art auf ein System sehr einfacher Differentialgleichungen zu gründen, und hält sie dadurch der Lorentz'schen Theorie für überlegen, umsomehr als seine Theorie eine weit größere Zahl fundamentaler Beobachtungen ungezwungen darstellt. Als ein Experiment, welches geeignet ist, zwischen beiden Theorien zu entscheiden, führt der Verfasser seine Versuche über die elektrostatische Ablenkung der Kathodenstrahlen an." Cf. Anzeiger der kaiserlichen Akademie der Wissenschaften, mathematisch-naturwissenschaftliche Klasse, 44 (1907), 78–79.

19) Cf. Jaumann, G.: Die Grundlagen der Bewegungslehre. (Von einem modernen Standpunkte aus dargestellt). Verlag von Johann Ambrosius Barth, Leipzig 1905.

20) NA, MKV/R, sign. 5 Prag Philosophie Professoren, b. 111, Einstein A., Nr. 842/1911, l.c.

21) NA, MKV/R, sign. 5 C1 Prag, b. 197, Nr. 26 566/1910.

22) Ibd.

23) Ibd. (letter to G. Jaumann drafted in the file, dated 23 August 1910).

24) Ibd., Nr. 25 526/1910.

25) Ibd. (letter to A. Einstein drafted in the file, dated 17 September 1910 and signed by Minister Stürgkh). See also [3], pp. 255–256, letter No. 225 (Max Hussarek von Heinlein, section head in the Ministry of Culture and Education in Vienna, to A. Einstein, Vienna 17 September 1910).

26) NA, MKV/R, sign. 5 C1 Prag, b. 197, Nr. 44 334/1910.

27) NA, MKV/R, sign. 5 C1 Prag, b. 197, Nr. 25 526/1910.

28) Deutsches Museum, München, Archiv, Nachlass Ernst Mach, NL 174/1881.

29) Cf. [3], pp. 172–173, letter No. 245 (Count Karl von Stürgkh to extraordinary professor at the University in Zurich Dr. Albert Einstein, Vienna 13 January 1911).

30) NA, MKV/R, sign. 5 Prag Philosophie Professoren, b. 115, Lippich Ferdinand (personal file), Nr. 39 677/1910. Let us note that biochemist Carl Ferdinand Cori (1896–1984), Nobel Prize winner for medicine and physiology in 1947 (together with his wife Gerty Therese born Radnitz, and physiologist Bernardo Houssay), was Ferdinand Lippich's grandson, born in Prague from the marriage of Lippich's daughter Maria Luisa and professor of zoology at GU Carl Isidor Cori.

31) NA, MKV/R, sign. 5 C1 Prag, b. 198, Nr. 26 833/1912.

32) Ibd., Nr. 5925 (a copy of the committee's proposal presented to the professorial board of the Faculty of Philosophy, s. d., enclosed to the Dean's letter to the Ministry of 24 May 1912, Z.1577).

34) NA, MKV/R, sign. 5 Prag Philosophie Professoren, b. 101, Frank Philipp (personal file), Nr. 42 446/1912 (Ministry of Culture and Education to Philipp Frank, 17 September 1912).

35) Moravský zemský archiv v Brně (Moravian Land Archives in Brno), collection B 34 (Deutsche technische Hochschule in Brünn, 1849–1945), Jaumann Gustav, (personal file). On G. Jaumann as a pioneer in the field of (modern) mechanics of continuum, see [6].

A FEW PERSONAL REMARKS ABOUT OUR ANNIVERSARIANS – PROFS. MICHAL KŘÍŽEK AND ANDRÉ MAEDER

Yurii V. Dumin

Sternberg Astronomical Institute (GAISh) of Lomonosov Moscow State University,
Universitetskii prosp. 13, Moscow, 119234 Russia

Space Research Institute (IKI) of Russian Academy of Sciences,
Profsoyuznaya str. 84/32, Moscow, 117997 Russia

dumin@yahoo.com, dumin@sai.msu.ru

Abstract: I present my personal memories of two active participants of the conference series "Cosmology on Small Scales" – Profs. Michal Křížek and André Maeder. Both our scientific discussions of the issues of the small-scale cosmological effects and our joint work on the organization of the above-mentioned conferences are addressed.

Keywords: Cosmology on small scales, local Hubble expansion, Dark energy

PACS: 01.60.+q, 01.65.+g, 95.36.+x, 98.80.Bp, 98.80.Cq, 98.80.Es

In this year, we are celebrating the 70th anniversary of Prof. Michal Křížek from the Institute of Mathematics of the Czech Academy of Sciences (Prague, Czech Republic) and the 80th anniversary of Prof. André Maeder from the Geneva Observatory (Switzerland). Both of them are actively involved in the study of small-scale cosmological effects (particularly, the local Hubble expansion) as well as in the organization of the conferences "Cosmology on Small Scales" (CSS), which were held in Prague every two years, starting from 2016. So, it is a great pleasure for me to share memories of my contacts with these two eminent persons.

Prof. Michal KŘÍŽEK (born on March 8, 1952)

The first time I heard about Michal Křížek in 2005 occurred when I spent a few months in Los Angeles (USA) in the framework of the research program "Grand Challenge Problems in Computational Astrophysics" organized by Prof. Mark Morris in the University of California (UCLA). This program was concluded by the conference at Lake Arrowhead, in the vicinity of Los Angeles, where I presented a report about the local Hubble expansion, with special emphasis on the effect of the Earth–Moon recession. After my report, some young Czech participant came to me and asked,

Figure 1: Prof. M. Křížek giving a talk at the 1st Conference "Cosmology on Small Scales" in 2016.

"Do you know that there is a guy in Prague who works on the similar topics?" I answered that I did not know anything about that scientist, and he promised to give me his contact details. Unfortunately, he could not find his address, and our contact with Michal Křížek at that time did not occur.

Digressing a little from the main narrative, I would like to mention that the main topic on which I worked in UCLA was a more accurate analysis of the primary astrometric data on the deceleration of the proper rotation of the Earth due to its tidal interaction with the Moon $\dot{T}_{\text{tid}}$ (where T is the length of day). The exact value of this effect is very important, because it can be recalculated to the linear rate of recession of the Moon from the Earth $\dot{R}_{\text{tid}}$, and its subsequent comparison with the recession rate directly measured by the lunar laser ranging (LLR) $\dot{R}_{\text{LLR}}$ should give us information about a probable presence of the local Hubble expansion in the Earth–Moon system (for more details, see [1], [2]). Unfortunately, while the value of $\dot{R}_{\text{LLR}}$ is sufficiently accurate, the data on $\dot{T}_{\text{tid}}$ — collected from the astrometric observations during the last three and half centuries — are very "noisy". The value most commonly cited in the literature is 1.4 ms/cyr (millisecond per centiyear), e.g. [3]. This leads to the conclusion that the local Hubble expansion, in principle, can exist, but its rate should be about 33 km/s/Mps, i.e., only about a half of the standard value of the Hubble constant (at the intergalactic scale), which is a bit strange.

Surprisingly, when I began to process the original astrometric data — collected since the Galilean times and presented, e.g., in the book [4], — I suddenly found that they gave a considerably smaller value of the secular deceleration of the Earth's

Figure 2: Prof. A. Maeder giving a talk at the 1st Conference "Cosmology on Small Scales" in 2016.

rotation, about only $0.9\,\mathrm{ms/cyr}$. The larger values, often cited in the literature, were actually derived by taking into account the observations of ancient solar eclipses. Unfortunately, such ancient data are very unreliable: they lead to a huge scatter in the average deceleration rates and, therefore, should hardly be taken into account at all. On the other hand, the value $\dot{T}_{\mathrm{tid}} = 0.9\,\mathrm{ms/cyr}$ leads to approximately the same local Hubble constant as at the global scale.

As a result of my work in UCLA, I published a short paper [5], where I outlined a way to generalize the so-called Kottler metric for a point-like mass in the Λ-dominated universe to the case of nonstationary Robertson–Walker cosmological asymptotics. On the other hand, a much more time-consuming work on the secular deceleration of Earth's rotation remained unpublished: this was because in the subsequent years I tried to include more and more contradictory data in the analysis, so that this work became endless... Fortunately, a year ago Prof. André Maeder with his young colleague Dr. Vesselin Gueorguiev published an exhaustive report on that topic [6], and I was very proud to be its reviewer.

Returning to our contacts with Prof. Křížek, the next important step occurred in the beginning of 2013, when I received from the journal "Earth, Moon, and Planets" a request to review the manuscript by M. Křížek and L. Somer entitled "Manifestations and the origin of dark energy". My impression of the manuscript was twofold: on the one hand, there were some problems in the accurate mathematical treatment of

the relevant issues in the framework of General Relativity; but on the other hand, I was delighted with the deep physical intuition of the authors and the originality of their ideas.

Especially interesting was their suggestion that the so-called "faint young Sun" paradox could be well resolved just by taking into account the local Hubble expansion: Really, the lower luminosity of the Sun a few billion years ago should be well compensated by a closer location of the Earth to the Sun and, thereby, conditions of life on the Earth (particularly, existence of the liquid water) could persist at that time. In fact, this is an extension of the so-called "anthropic principle", i.e., a set of the physical laws and parameters that would be absolutely necessary for the life on the Earth to emerge and survive. Therefore, the local Hubble expansion turns out to be one of such laws.

The above-mentioned manuscript contained also a number of other examples of probable manifestations of the local Hubble expansion in the dynamics of solar-system bodies, which were unknown to me before. So, I had prepared a quite long review with suggestions how to correct the mathematical problems and emphasized to the editorial board that, in general, my opinion is very positive. A few months later, I received a revised version of this manuscript, where all the major drawbacks were perfectly corrected. Therefore, in my reply letter to the journal, I strongly recommended to accept this manuscript and assumed that its publication might be a good starting point for further discussion of the problem of small-scale cosmological effects by a wider scientific community. Unfortunately, as far as I understand, the opinion by the other referee(s) was negative, and this beautiful manuscript was rejected. Anyway, as a reward for my peer-review work, I received from Springer publishing house a couple of valuable books.

Fortunately, in the beginning of 2014 M. Křížek and L. Somer resubmitted their manuscript under the more accurate title "Manifestations of dark energy in the Solar system" to the journal "Gravitation and Cosmology". Surprisingly, I was again appointed as a reviewer of this manuscript and, of course, my opinion was very positive, apart from listing a few technical drawbacks. Finally, this paper was published [7]. (It is interesting that in the early 2000's, when I submitted my manuscripts on the local Hubble expansion to a number of journals, most of them were rejected. However, the editors probably remembered my name; and in the subsequent years I often received requests to review the papers on this topic by other authors.)

Meanwhile, even before a release of the above-mentioned article from the press, I sent a letter to M. Křížek, where I wrote that I was very interested in his research and also informed him that I regularly attend as a guest scientist the Max Planck Institute for the Physics of Complex Systems in Dresden, which is located not far from Prague; so that we could contact more closely. Michal showed great interest in my proposal, and since that time we regularly meet each other in Prague or Dresden. These visits were typically each autumn, when I worked in the Max Planck Institute. Additionally, Michal organized my lecture "On the Problem of Hubble Expansion at

Figure 3: Opening of the 1st Conference "Cosmology on Small Scales" in 2016 by M. Křížek (standing on the podium).

Small Scales" in the Astronomical Institute of Charles University in Prague, which took place on October 29, 2014, as well as a visit to Ondřejov Observatory near Prague, where I was able to look at the well-known 2-meter telescope and some other astronomical equipment (including a beautiful collection of old astronomical instruments).

In the course of our conversations, Michal introduced me to yet another fascinating concept — the so-called "gravitational aberration" [8]. Frankly speaking, I am not sure that this term was well-chosen; but the idea is as follows: Let us consider a binary gravitational system, e.g., a pair of equal point-like masses rotating about its common center of inertia, for simplicity, in a circular orbit. Then, if a retardation of the gravitational interaction is taken into account, the forces of mutual attraction between the two bodies will not be aligned strictly along the diameter but be slightly deviated. The corresponding tiny force components along the direction of motion (i.e., perpendicular to the diameter) will accelerate the bodies, thereby leading to the expansion of their orbits. So, such an effect can mimic the local Hubble expansion of the binary system, although its physical nature is absolutely different from the commonly-accepted paradigm of expanding space–time.

More details about "gravitational aberration" can be found in the book "Anti-gravity – Its Origin and Manifestations" written by M. Křížek in cooperation with F. Křížek and L. Somer [9]. Moreover, one can find there a number of other astrophysical and cosmological phenomena unfamiliar to a wide range of astronomers. A specific feature of this book is that the entire presentation — even of the advanced topics — is done at a sufficiently simple level, e.g., comprehensible to any student specialized in physics.

During one of our first meetings in Dresden in 2014 or 2015, I said to Michal that it would be nice to organize a special conference devoted to the local Hubble expansion and other controversial issues of cosmology, because these topics were underrepresented at other cosmological conferences. In fact, this was not my first attempt to organize such a meeting. During the previous decade or so, I had already tried to suggest the idea of the organization of such a session at some other conference; but my suggestions were rejected either immediately or after some negotiations with chairmen of these conferences. Fortunately, this was not the case with Prof. Křížek. He accepted the idea with great enthusiasm, and — which is even more important — he had already a large experience of organization of other conferences on applied mathematics. So, approximately two years later, in 2016, the 1st Conference "Cosmology on Small Scales" was successfully conducted in Prague, in the Institute of Mathematics of the Czech Academy of Sciences; and since that time they repeated regularly every two years. (Even in the very hard pandemic year 2020, Michal managed to organize a small meeting in Prague.)

When we were preparing the first conference, we tried to hold it in the spirit of the conference "Problems of Practical Cosmology", which was organized by Prof. Yurii Baryshev in Saint-Petersburg in 2008. I remembered that conference for the breadth of coverage of various topics, including the controversial ones, and by the open-minded exchange of ideas. We expected very much that Yu. Baryshev would also participate in the organization of our conference and invited him to join us. Unfortunately, after the conference in Saint-Petersburg he had some health problems, which precluded him from participating in other meetings. Nevertheless, he conveyed his warm wishes to us and sent a written text of his report, which I read at the first our conference.

As regards the logo for the conference "Cosmology on Small Scales", Michal suggested initially the picture of a binary system experiencing the "gravitational aberration" and, thereby, forming the unwinding spiral (the same as placed on the title page of his book [9]). But after some discussions we decided to prepare a new logo, more clearly reflecting the problem of small-scale cosmological effects. So, I had drawn a picture placed subsequently in all the books of proceedings: This is a sphere, representing a 2D model of the expanding Universe, with planetary systems on its surface; and a huge question mark in its center implying the main question of all our conferences, "Does the local Hubble expansion exist or not?"

Our preparation for each conference usually began a year before the event, during the autumn or winter of the previous year, when I visited the Max Planck Institute in Dresden. During this time, we met each other in Prague or Dresden and discussed a general concept of the forthcoming conference. Next, after my departure to Moscow, the majority of the organizational work was conducted just by Michal. My role was of secondary importance, but I was permanently in contact with Michal by e-mail. I believe that all these conferences were quite successful.

Additionally, I should mention the excellent excursions to the physical and astronomical sites of Prague (related to the work and life of A. Einstein, J. Kepler,

Figure 4: Discussion between M. Křížek (standing on the left) and A. Maeder (sitting on the right) at the 1st Conference "Cosmology on Small Scales" in 2016. A future director of the Institute of Mathematics CAS T. Vejchodský is sitting in the center.

T. Brahe, E. Mach, C. Doppler, and other prominent scientists), which were organized and guided by Michal after the conferences. I think that no professional guide is such a good expert in these matters as Michal.

During my visits to Prague, I learned that Michal also organized and actively led the work of Cosmological Section of the Czech Astronomical Society. I was fortunate a few times to attend the corresponding sessions, which were conducted in the same hall as the conferences. Surprisingly, while all the reports were presented in the Czech language (which I do not know), I understood their contents almost without problems, because all material was selected very carefully and presented very pictorially.

Finally, I should mention that Michal Křížek is well recognized also by the mathematicians. It is interesting that — although Michal worked for a long time as a head of the Department of applied mathematics — when I asked Russian mathematicians about Křížek, they usually remembered his works on the Fibonacci numbers (which are not immediately related to applied mathematics).

Prof. André MAEDER (born on January 10, 1942)

The history of my acquaintance with Prof. André Maeder is much shorter but also quite interesting. As I have mentioned in the previous section, in 2002 I wrote a short article about a probable manifestation of the local Hubble expansion in the

Figure 5: Excursion to the physical and astronomical sites of Prague for the participants of the 1st Conference "Cosmology on Small Scales" in 2016, guided by M. Křížek (standing in the center with outstretched hand).

dynamics of the Earth–Moon system [1] and submitted it to the journal "Astronomy & Astrophysics". Just in the next day it was rejected: there were no any explanations but only a short phrase from one of the editors that "the paper is not suitable for this journal". Later, I deposited this article in the electronic archive, but it was never published in a peer-reviewed journal. (However, it became by now the most frequently read of my publication.)

So, in the beginning of 2015 I received a letter from André Maeder, who introduced himself as Professor of theoretical astrophysics at the Geneva University and former director of the Geneva Observatory, specialising mostly in stellar evolution and nucleosynthesis. (Unfortunately, I did not hear this name before, because I was not interested in the above-mentioned branches of astrophysics.) He wrote that he was very interested in my "excellent 2008 paper on the influence of the Lambda term on the parameters of the Earth–Moon system," as well as by my reports at some meetings. Besides, he informed me about his previous publications at the end of the 1970's on the so-called scale-invariant theory of gravitation (generalization of General Relativity), which also led to the cosmological expansion on small scales. So, he asked if I have any further results and papers on this matter. Frankly speaking, I was not sure which of my "2008 papers" he had in mind. Anyway, I sent him a few recent publications and especially emphasized that the value of the local Hubble parameter of about 33 km/s/Mps, which was presented in my first publications, might be strongly underestimated because of the large uncertainty in the published

Figure 6: Prof. M. Křížek (on the left) introduces Prof. A. Maeder (on the right) before his public lecture at the 2nd Conference "Cosmology on Small Scales" in 2018.

values of the Earth rotation deceleration. I can assume that just this remark by me, done many years ago, stimulated him in collaboration with V. Gueorguiev to perform a much more careful analysis of the available data, resulting in publication of the exhaustive recent review [6].

Besides, in my first letter I had drawn the attention by A. Maeder to the work by M. Křížek [10] on the faint young Sun paradox in the context of local Hubble expansion. (I assumed that it should be especially interesting for him as a specialist in stellar evolution.) I emphasized also that, according to this paper, "a quite large number of problems in the evolution of the Solar system can be reasonably resolved just due to the local Hubble expansion". In response, I received from Prof. A. Maeder a very warm letter, in which he thanked me for the papers and wrote, "I think and hope that the research line you have been pursuing for many years may be succeeding in the future".

As a result of these contacts, Prof. A. Maeder became a member of the Scientific Committee of the conferences "Cosmology on Small Scales," as well as an active participant and speaker of our meetings. The main topic of his presentations was the scale-invariant theory of gravitation [11]. I refrain from detailed comments on this concept, because I am not an expert in this matter. However, I believe that — although the small-scale cosmological effects emerge most naturally in the scale-invariant theory — in principle, they are well admitted even in the standard General Relativity.

Besides, being a specialist of a very wide profile, in the framework of the 2nd CSS conference in 2018 Prof. A. Maeder presented a public lecture on a much more empirical topic "Glaciers, geysers, dry rivers and volcanoes on Mars. Was there

a beginning of life?" However, this subject is also closely related to the problem of small-scale cosmological effects: Really, the recent evidence for the existence of liquid water on Mars in the past might be an important argument that changing luminosity of the Sun should be corrected by the local Hubble expansion, as was already suggested by M. Křížek in the case of Earth [7], [10].

References

[1] Dumin, Yu.V.: *On a probable manifestation of Hubble expansion at the local scales, as inferred from LLR data.* Preprint arXiv:astro-ph/0203151, 2002.

[2] Dumin, Yu.V.: A new application of the lunar laser retroreflectors: Searching for the local Hubble expansion. Adv. Space Res. **31** (2003), 2461.

[3] Stephenson, F.R., Morrison, L.V.: Long-term changes in the rotation of the Earth: 700 B. C. to A. D. 1980. Phil. Trans. Royal Soc. London, Ser. A **313** (1984), 47.

[4] Sidorenkov, N.S.: *Physics of the Earth's Rotation Instabilities.* Nauka-Fizmatlit, Moscow, 2002. (In Russian)

[5] Dumin, Yu.V.: Comment on Progress in lunar laser ranging tests of relativistic gravity. Phys. Rev. Lett. **98** (2007), 059001.

[6] Maeder, A.M., Gueorguiev, V.G.: On the relation of the lunar recession and the length-of-the-day. Astrophys. Space Sci. **366** (2021), 101.

[7] Křížek, M., Somer, L.: Manifestations of dark energy in the Solar system. Grav. Cosmol. **21** (2015), 59.

[8] Křížek, M.: Does a gravitational aberration contribute to the accelerated expansion of the Universe? Commun. Comput. Phys. **5** (2009), 1030.

[9] Křížek, M., Křížek, F., Somer, L.: *Antigravity – Its Origin and Manifestations.* Lambert Acad. Publ., Saarbrücken, 2015.

[10] Křížek, M.: Dark energy and the anthropic principle. New Astron. **17** (2012), 1.

[11] Maeder, A.: An alternative to the ΛCDM model: The case of scale invariance. Astrophys. J. **834** (2017), 194.

ALTERNATIVE COSMOLOGICAL THEORIES

A DIFFERENT COSMOLOGY

John C. Botke

Nogales, Arizona, USA
jcbotke@gmail.com

Abstract: This paper summarizes a new model of cosmology based on the idea of a universe in which the curvature varies with time and that vacuum energy acts as its own source. In this model, the universe began with an exponential Plank era inflation before transitioning to a spacetime described by Einstein's equations. A solution of Einstein's equations predicts a present-day exponential acceleration of the expansion of the universe. A new model of nucleosynthesis provides a solution to the matter/antimatter asymmetry problem and a non-standard origin of the CMB. It is shown that a vacuum imprint came into existence during the inflation that was responsible for the existence of all cosmic structures. We model the evolution of all cosmic structures beginning with their definition by the vacuum imprint and ending at the time conventionally associated with galaxy formation. We then explain the stability of galaxy clusters and show that galactic supermassive black holes came into existence during the initial free-fall collapse of all galaxies. The large peaks of the CMB power spectrum are shown to be a consequence of the superclusters and through the use of Einstein's equations, we show that so-called dark matter is, in fact, vacuum energy.

Keywords: evolution of the universe, inflation, Big Bang nucleosynthesis, cosmic microwave background, origin of cosmic structures, dark matter, supermassive black holes

PACS: 98.80.-k, 98.80.Bp, 98.65.Cw, 98.65.-r, 98.35.Gi, 98.54.Aj, 95.36.+x, 95.35.+d, 26.35.+c, 97.10.B+, 04.20.Jb, 04.20.-q

1. Introduction

In these notes, we summarize a new model of cosmology that represents a major departure from the standard model. It makes a significant number of predictions that agree with observations and does so without any parameter adjusting or curve fitting. It predicts the present-day accelerated expansion of the universe and explains the origin of all cosmic structures, the origin of galactic supermassive black holes, and the source of the energy that heated the gas of galaxy clusters. We show that vacuum energy is the reality of dark matter and predict a present-day value of the

vacuum energy that is within a factor of 3 of that of so-called dark energy. The model details are available in the papers listed in the References section.

Observation tells us that the universe is highly organized on scales ranging from the size of stars to superclusters and it should be clear that no sequence of random events could ever result in such colossal organization. The conclusion is that some organizing principle must have been in play from the very beginning.

2. Plank era

In [1], we proved that superclusters are responsible for the large peaks of the CMB spectrum. We will have more to say about this later but the point here is that it follows that superclusters in some form must have been in existence at that time. We also know that at the time of recombination, superclusters, and hence the CMB spectrum peaks, were vastly too large to be explained by any causal process. (It is this consideration that proves that the acoustic oscillation model of the CMB peaks is just nonsense.) And yet, superclusters exist, so the only possible conclusion is that, even though causality is a cornerstone of the physics that applies for most of the history of the universe, there must have been an epoch at the beginning during which it had no meaning. Moving backward in time, since nothing much happened between the time of recombination and nucleosynthesis, it is natural to suppose that superclusters originated during nucleosynthesis and, indeed, their material manifestation did originate at that time. Because of causality, however, the blueprint that regulated their creation must have come into existence even earlier. The final jump backward is to a Plank era inflation.

A critical attribute of the vacuum during the Plank era was that time, distance, and energy were uncertain. To see this, imagine that we are interested in measuring the duration of some event. To do so, we need a clock whose ticks are of a shorter duration than that of the event so to measure events of shorter and shorter duration, we must keep subdividing the ticks. We eventually come to the point at which our tick is on the order of the Plank time. We now assert that the Plank tick cannot be subdivided and as a result, time becomes uncertain. The same idea holds for distance and energy as well. Because there is an inverse relationship between the radius of curvature and the vacuum energy density, it follows too that there is a maximum possible energy density because a minimum realizable length places a lower limit on the radius of curvature.

Since neither time nor distance had any exact meaning, it follows that causality had no meaning so it is only here during the Plank inflation that we are finally able to escape the constraints imposed by causality (and entropy.) (In different contexts, many people have developed models based on these ideas in attempts to tame the infinities of field theory so the idea of a Plank limit is not new although the importance of the lack of causality was not considered.) In [1], we developed a simple model that predicts an initial exponential expansion of the universe. This inflation lasted until the age of the universe became large compared to the Plank

time uncertainty. From that point onwards, the evolution of the universe could be described by Einstein's equations with the understanding that Einstein's equations have validity only for dimensions large compared to Plank dimensions. Such an inflation by itself, however, does not explain superclusters or anything else.

To make the final step, structure is needed and we conclude that large smooth acausal vacuum structures or imprints came into existence during the inflation with relative dimensions ranging from that of stars up to that of superclusters and beyond. The import of these structures will become manifest when we describe our new model of nucleosynthesis. Normally, systems do not spontaneously evolve into a highly organized state starting from a highly disorganized state but this is what happened and for it to have happened, there must have been an absence of causality.

We emphasize that there was no existence other than the vacuum during that epoch and that remained true until the time of nucleosynthesis. According to this new model, the idea that the universe began with very energetic radiation is simply wrong.

The following Fig. 1 summarizes the situation. We define $\alpha(t)$ and τ by $a(t) = a_P\,e^{\alpha(t)}$ and $t = t_P\,e^\tau$. The exponential expansion ended when the age of the universe became large compared to the Plank time. Following that expansion, a transition period occurred that carried the evolution into the Einstein era. In the next section, we will find that the value of the scaling at the end of the transition is *fixed*.
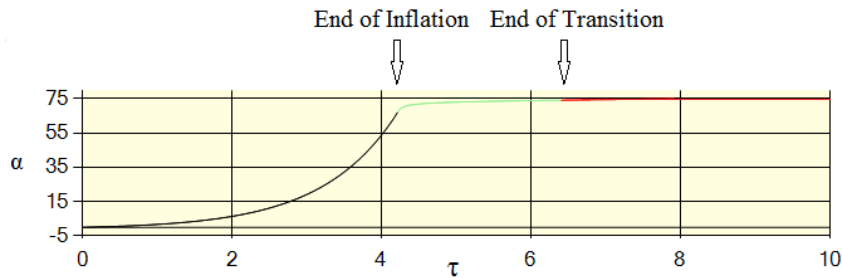
Figure 1: Initial evolution of the universe.

We recognize that there is no direct observational evidence that the inflation existed and, in fact, there never can be for the simple reason that there was nothing to observe before nucleosynthesis. The indirect evidence for an inflation, on the other hand, is overwhelming given the assumtion that the Big Bang expansion began from a Plank-sized beginning. The fact that the new model solution must join onto the scaling at the end of the transition not only constrains the magnitude of the inflation, it also forces the conclusion that it did exist. Also, a fun fact: without the inflation, the present-day size of the universe would be a small fraction of a meter.

3. New model of the Einstein era

By the end of the transition period, the uncertainties would have become negligible and normal causality would have come into play. The development of the new

model begins with the idea that the universe consists of a sequence of hyperspheres that are homogeneous and isotropic. These have no preferred origin and all their properties are dependent only on time. Our perception of the universe is concerned with signals, causality, and so on and these are dependent on both time and distance and are described by Einstein's equations. The question, then, is how do we reconcile the equations that describe our perception with a sequence of hyperspheres that have no notion of an origin or distance? The answer is that Einstein's equations describe the universe as viewed by each observer from the viewpoint of an origin at the observer's location. But a hypersphere is simply the collection of all possible observer origins so Einstein's equations become the equations that describe the hypersphere when evaluated at any observer's origin.

In the standard model, the assumption is made that not only are the hyperspheres homogeneous and isotropic but, in addition, that the universe must *appear* homogeneous and isotropic. We established that the curvature must have varied with time during the Plank era and now assert that it continued to vary afterward. Although, as we will show, the observational differences are not large for moderate redshifts, with time-varying curvature, the universe will not appear homogeneous. Putting these ideas together, the metric becomes,

$$ds^2 = \left(-1 + \frac{r^2 h(ct,r)^2}{a(ct)^2}\left(1 - k(ct)r^2\right) \right)(cdt)^2$$
$$+ 2h(ct,r)(cdt)rdr + a^2(ct)\left(\frac{dr^2}{(1 - k(ct)r^2)} + r^2 d\Omega^2 \right). \tag{1}$$

The second part of the new model concerns the vacuum energy density. Instead of the standard model concept of the vacuum described by

$$\mathbf{T}^{\mu\nu} = 0, \tag{2}$$

the new model vacuum acts as its own source so that we have

$$\mathbf{T}^{\mu\nu} = (\rho_{vac}c^2(ct,r) + p_{vac}(ct,r))\delta_0^\mu \delta_0^\nu + p_{vac}(ct,r)\, g^{\mu\nu}. \tag{3}$$

After working out Einstein's equations and taking the limit as $r \to 0$, the resulting equations can be solved in closed form. The scaling is given by,

$$a(ct) = a_* \left(\frac{ct}{ct_0} \right)^{\gamma_*} \mathrm{e}^{\frac{ct}{ct_0}c_1}, \tag{4}$$

where

$$\gamma_* = \gamma_h + \bar{k}_0 \frac{(1 - \gamma_h)^2}{\gamma_h}, \tag{5a}$$

$$a_* = a_0\, \mathrm{e}^{-c_1}. \tag{5b}$$

We see that the scaling is power-law for $ct/ct_0 \ll 1$ and exponential for $ct/ct_0 \geq 1$. The curvature is given by

$$k(ct) = \bar{k}_0 \left(\frac{a(ct)}{ct} \right)^2 \tag{6}$$

which is related to the vacuum energy density and pressure by

$$k(ct) = \frac{1}{2}\gamma_h \, a(ct)^2 \kappa \left(\rho_{vac}c^2(ct,0) + p_{vac}(ct,0) \right). \tag{7}$$

The sum is thus a fixed function of time,

$$\rho_{vac}c^2(ct,0) + p_{vac}(ct,0) = \frac{2\bar{k}_0}{\kappa(ct_0)^2\gamma_h} \frac{(ct_0)^2}{(ct)^2}. \tag{8}$$

Physical quantities, not just the curvature, are functions of this sum rather than either individually.

Aside from the present-day size and age of the universe, we need the value of the scaling at two different times to fix the parameters of the model. For one, we use a present-day value of the Hubble constant. There is some uncertainty about its value but a value of $H_0 = 70.0$ km/(s Mpc) gives a good fit to the luminosity distance data. (In [1], we used a value of 67.3 but the value of 70 gives a better fit.) For the other, we used the present-day temperature of the CMB. (Some further development which we will get to in a later section is needed to understand the connection.) The remaining parameter is $\bar{k}_0$. Recall that during and shortly after the inflation, the curvature was maximal. This motivates an additional principle which states that the *curvature must always be as large as possible* or equivalently, that the vacuum energy density *must always be as large as possible*. From the solution, it then follows that $\bar{k}_0 = 1/8$ and $k_0 = 1.414$. The derived parameters have the values $\gamma_h = 1/3$, $\gamma_* = 0.5$, and $c_1 = 0.49$. Note that there is no direct relationship between the scaling and the energy density or pressure so that the present-day acceleration of the scaling follows directly from the time variation of the curvature and has nothing to do with a cosmological constant.

Everything is now fixed and unambiguous predictions can be made. This situation is completely different from that of the standard model which is based on the FRW solution of Einstein's equations for a universe in which the curvature is assumed to be constant. The latter does not, in fact, predict anything solely on the basis of being a solution of the equations. By making choices about various parameters, it is possible to predict any sort of evolution one cares to see. In the new model that is not the case. There is one solution, there are no free parameters, and *only one evolution is possible*.

We define the effective scaling parameter $\gamma_{eff}(t)$ by $a(t) = a_0(t/t_0)^{\gamma_{eff}(t)}$. In Fig. 2, we show this parameter and the scaling as functions of time. The exponential acceleration of the scaling is clearly visible.
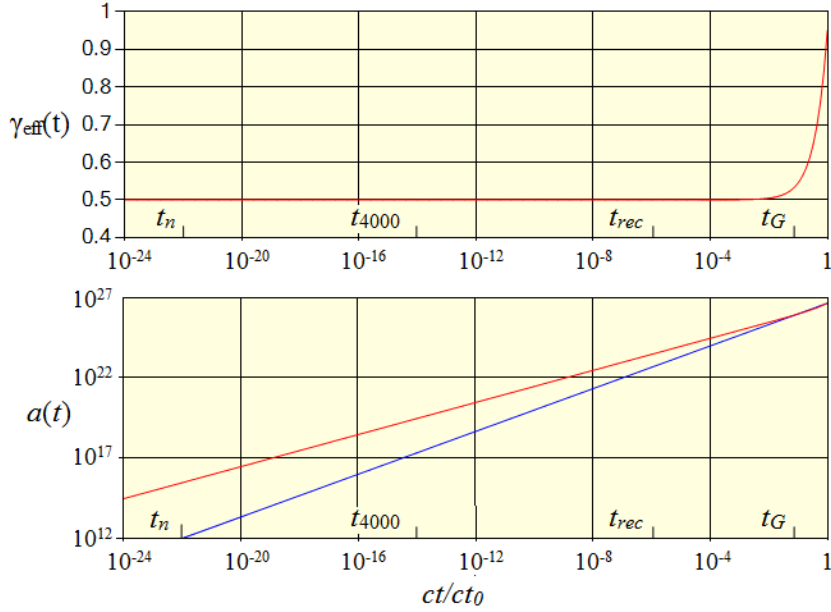
185

Figure 2: Time-varying curvature predictions in red. For comparison, the curve for $2/3^{rds}$ scaling is shown in blue. The indicated times are t_n = time of neutron formation to be explained below, t_{4000} = end of nucleosynthesis, t_{rec} = recombination, and t_G = galaxy formation.
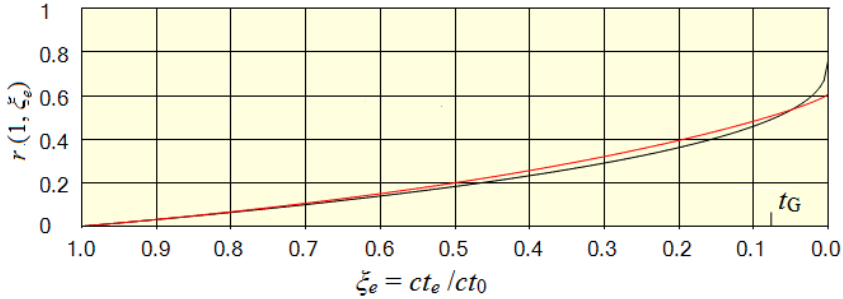

Figure 3: $r(1, \xi_e)$ vs ξ_e. The red curve is the time-varying curvature result. For comparison, we also show in black the result computed assuming a constant value of $k = 1$.

In Fig. 3, we show the coordinate distance of sources whose signals are received at the present plotted as a function of the lookback time. Both time-varying and constant curvature cases are shown. The two curves are similar for small values of look-back time but they differ considerably for large redshifts. In particular, with time-varying curvature, there is a fundamental limitation on our ability to detect distance sources. No matter how far back in time we look, we cannot see sources with coordinate distances greater than about $r = 0.6$. This is in direct contrast to the standard model where no such limitation exists.
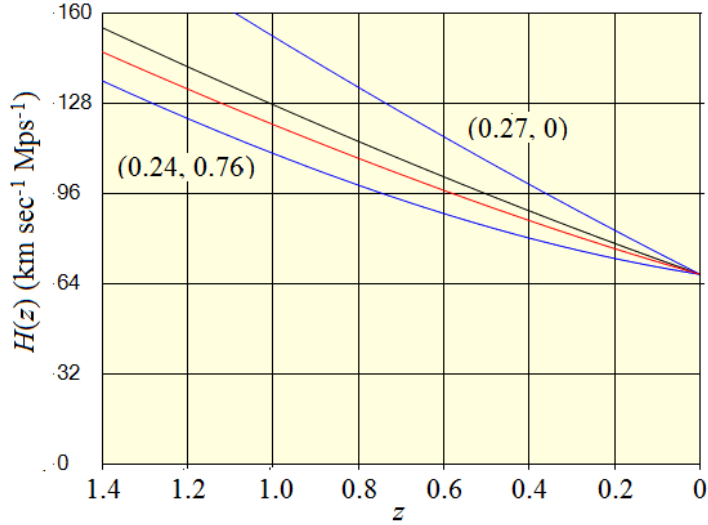
Figure 4: Hubble parameter vs redshift. Time-varying curvature in red, constant curvature in black, and the FRW results for two values of the densities in blue. The FRW curves were normalized to the value of the model curves at $z = 0$.

The redshift dependence of the Hubble parameter, $H(t) \equiv \dot{a}(t)/a(t)$, is shown in Fig. 4.

From (8), we find that the present-day vacuum energy density sum is

$$\rho c^2(ct_0, 0) + p(ct_0, 0) = 2.1 \times 10^{-10} \, \text{J m}^{-3} \tag{9}$$

which differs from the value of the so-called dark energy density $(6.3 \times 10^{-10} \, \text{J m}^{-3})$ by no more than a factor of 3. Note, however, that even though the magnitudes are similar, these are in no way equivalent. The notion of dark energy driving the acceleration of the scaling just does not exist in the new model.

Finally, we show the model prediction for the luminosity distance in Fig. 5. We emphasize that this is a prediction by a model with no free parameters. Given that the new model fits the data, we find that luminosity distance data does not provide any evidence for a cosmological constant. It only appears in the context of the standard model which we claim is wrong.

Up to this point, we have only considered the vacuum but eventually, particles permeated space so we need to consider their interaction with the vacuum energy density. For a particle with 4-velocity $u^\mu = (u^t, u^r, u^\theta, u^\varphi)$, the geodetic equations are

$$\frac{du^\mu}{d\tau} + \Gamma^\mu_{\ \nu\sigma} u^\nu u^\sigma = 0. \tag{10}$$

The important point is that the connection coefficients depend only on the metric components and these have no dependence on either the vacuum energy density or the pressure. On the RHS, the particle density is simply added to the vacuum

187
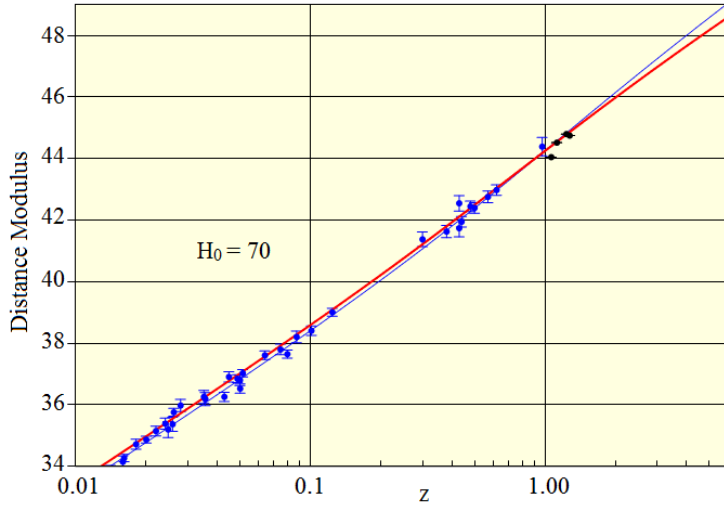
Figure 5: Time-varying curvature prediction of the luminosity distance in red. The standard (0.24, 0.76) model is shown in blue.

energy density. Ordinarily, after including a new term, we would need to re-solve the equations but, in fact, the equations have not changed since the particle density just becomes part of the sum so the original solution still holds. This means that any small variation in the particle density will be immediately canceled by a corresponding variation in the vacuum needed to keep the sum equal to the RHS of (8). This leads us immediately to the conclusion that accretion initiated by small particle density fluctuations is impossible.

4. Dark matter

Shortly, we will show that the basis of nucleosynthesis was a conversion of a small percentage of the vacuum energy into neutron/antineutron pairs. More than 99 % of this energy remained in the vacuum, however, and that energy has important consequences for cosmology. Its existence means that it must appear in any expression of Einstein's equations as a contribution to the energy-momentum tensor and it is this contribution that is responsible for the phenomena attributed to dark matter.

One of the manifestations of dark matter concerns the velocity distribution of stars in spiral galaxies and the gas making up HI rings. The spiral galaxy problem is illustrated by the curves in Fig. 6. Curve A is the calculated velocity distribution of the stars based on the visible matter. Curve B is the observed distribution. The generally accepted solution for this problem is to suppose there is a halo of dark *matter* surrounding the galaxy that provides the gravitation needed to match the observed velocity distribution. There are several problems with this proposal, however, not the least of which is the fact that a dark *matter* halo should act as a halo of stars with the lights turned off so its velocity distribution should match curve A instead of B. A different solution is needed. We get a hint if we subtract
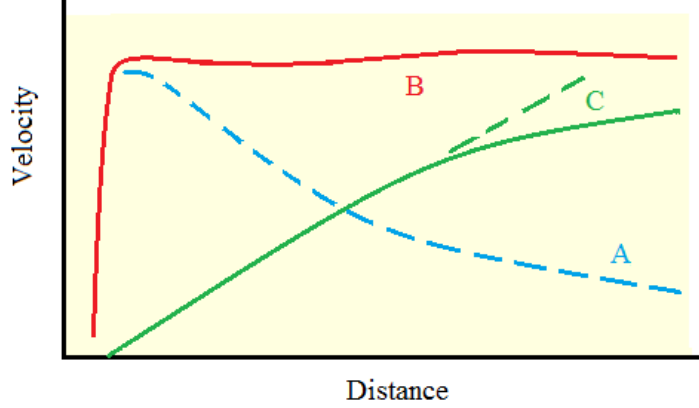
Figure 6: Typical spiral galactic velocity distribution.

the two curves to obtain curve C. This suggests that observed distribution can be understood in terms of normal gravitational interaction being carried along by a rotating spacetime. There are two issues to be addressed; namely to explain first the spacetime rotation and second, the stability of the motion within the rotating spacetime. Turning to Einstein's equations, it is reasonable to model such galaxies using a stationary axisymmetric metric,

$$
\begin{aligned}
ds^2 = & - A(cdt)^2 + B(d\phi - \omega dt)^2 + Cdr^2 + Dd\psi^2 \\
= & - (A - \frac{B\omega^2}{c^2})(cdt)^2 - 2\frac{B\omega}{c}d\psi(cdt) + Bd\phi^2 + Cdr^2 + Dd\psi^2
\end{aligned}
\tag{11}
$$

with an energy-momentum tensor of the form

$$
\mathbf{T}^{\mu\nu} = (\rho_{vac}c^2 + p_{vac})\frac{u^\mu u^\nu}{c^2} + p_{vac}\mathbf{g}^{\mu\nu} + \rho_m c^2\frac{v^\mu v^\nu}{c^2}.
\tag{12}
$$

Any small volume of the vacuum will respond to the total gravitation field in the same way as does a material particle which means that we can analyze its motion using the usual geodesic equations. Two of these are satisfied identically as a consequence of our assumption of a stationary metric. The remaining two have the solution

$$
\dot{\varphi}_{vac}(r, \psi) = \omega(r, \psi),
\tag{13}
$$

where $\omega(r, \psi)$ represents the rotation of the galaxy. What we find is that the curvature of the vacuum must rotate and it is doing so with zero angular momentum. We now consider the stars whose velocity must also satisfy the same geodetic equations. In this case, we separated their angular velocity into a component with vanishing angular momentum and a residual with non-vanishing angular momentum,

$$
\dot{\phi}_m(r, \psi) = \dot{\phi}_{m,r}(r, \psi) + \omega(r, \psi).
\tag{14}
$$

189

The residual angular velocity is then,

$$\dot{\phi}_{m,r}(l, \ z) \ = \frac{v}{l} - \omega(l, \ z).$$ (15)

The next step would normally be to solve Einstein's equations with the above metric but, unfortunately, we have not been able to do so because of the lack of sufficient computer power. Taking a Newtonian approach instead, in [1], we considered the balance of forces acting on a star at rest in the plane of the galaxy with a torus of vacuum energy lying at its outer edge co-planer with the galaxy. The result was that the required energy density of the vacuum is only about 1% of the energy density of the mass of the galaxy.

What this shows is that the vacuum energy density near large structures must be considerably larger than it is far from matter which is consistent with the notion that dark matter always seems to hover close to ordinary matter. The vacuum energy density model solves the problem of explaining why just the right amount of dark matter always manages to accumulate just outside every galaxy and why we do not find the odd galaxy here and there that is missing its dark matter halo.

In [2] and [3], we discuss other cases in which vacuum energy is shown to account for phenomena attributed to dark matter. Summing up, when vacuum energy is included in the energy-momentum tensor, the mystery of dark matter disappears.

5. Asymmetry, radiation, and nucleosynthesis

Initially, the only existence was the vacuum so the next step is to account for the creation of ordinary matter. We begin by separating what is known from what is conjecture. Observations of galaxies allow the relative abundances of the light elements to be measured. Working backward in time, the abundances at the end of nucleosynthesis can then be estimated with some confidence, because the processes that occurred during the intervening period are known. Similarly, the nucleosynthesis reactions are also known so one can work backward again to discover the relative abundances of the protons and neutrons that initiated the nucleosynthesis. We can also establish that the process began at a time of about 10^{-5} s. That, however, is as far as one can go. Whatever happened before a time of 10^{-5} s is beyond the reach of even extrapolations of observations. This means, for example, that there is no evidence to support the standard model's field theory beginning. Here, we will propose an alternate beginning that leads to the same nucleosynthesis starting point but which also accounts for the matter/antimatter asymmetry of the universe.

At this point, we wish to establish the connection between the CMB and the scaling that we referred to earlier. The temperature of the CMB at the time of the initial particle creation is given by

$$T(t_n) = T(t_0)\frac{a_0}{a(t_n)}$$ (16)

190

and, assuming a black-body spectrum, the corresponding energy density was

$$\rho_\gamma c^2(t_n) = a_B T^4(t_n). \tag{17}$$

Clearly, the vacuum energy density at $t = t_n$ is fixed once the effective scaling is known. If we now assume a trial value of $\gamma_{eff}(t_{rec}) = 0.6$, say, we find that $t_n = 5.2 \times 10^{-5}$s and $\rho_\gamma c^2(t_n) = 6.9 \times 10^{39}$J m^{-3} but we also have $\rho_{vac} c^2(t_n) = 2.1 \times 10^{34}$J m^{-3} which would imply a CMB energy density vastly larger than the total energy of the universe. If we turn the problem around and set the CMB energy density to equal the vacuum energy density, we find a value of $\gamma_{eff}(t_{rec})$ a little bit larger than 0.5. The actual value, however, must be less than that because the CMB does not contain all the energy. A value of $1/2$ is a nice round number so from here on out, we will assume that $\gamma_{eff}(t_{rec}) = 0.5$ with the understanding that it may need a small adjustment in the future. The corresponding time is $t_n = 4.3 \times 10^{-5}$ s.

This now fixes the scaling so we can determine the absolute initial abundances of the initial protons and neutrons by working backward from the present-day abundances of ordinary matter. The present-day average density of baryons is on the order of $n_{Ave}(t_0) = 1$ m^{-3} but in the subregions where most of the nucleosynthesis took place, the density was many times larger, and in the large voids, it was considerably smaller. Starting with an average value of 2 m^{-3}, we find a baryon density of $n_B(t_n) = 7.7 \times 10^{33}$ m^{-3} and a photon density of $n_P(t_n) = 1.5 \times 10^{42}$ m^{-3}. With these values, the radiation energy was about 0.1% of the vacuum energy density and that of the particles was vastly smaller even when their rest masses are included. Finally, the temperature $T(t_n) = 4.2 \times 10^{11}$ K was about a factor of 10 smaller than the standard model value at that time. With these values, we have set the basic boundaries so the next step is to establish the sequence of events that lead to nucleosynthesis while at the same time accounting for the matter/antimatter asymmetry of the universe.

In [1], we considered several possible scenarios. We concluded that nucleosynthesis began with neutron/antineutron pair production with a very small bias towards neutrons. A bias of 2-4 extra neutrons for every 10^8 neutron/antineutron pairs is sufficient to explain the matter/antimatter asymmetry as well as the present-day matter density of the universe. We also concluded that there is no other mechanism that can explain the asymmetry. This bias must have been the same, or nearly the same, everywhere which points us back to the initial inflation, because that was the only era during which normal causality did not hold.

With the origin of the CMB accounted for and a plausible explanation of the asymmetry given, we now need to account for the transition from neutrons and antineutrons to a mix of neutrons and protons that will finally get us to the beginning of nucleosynthesis proper. A long list of reactions contributed to the final outcome but
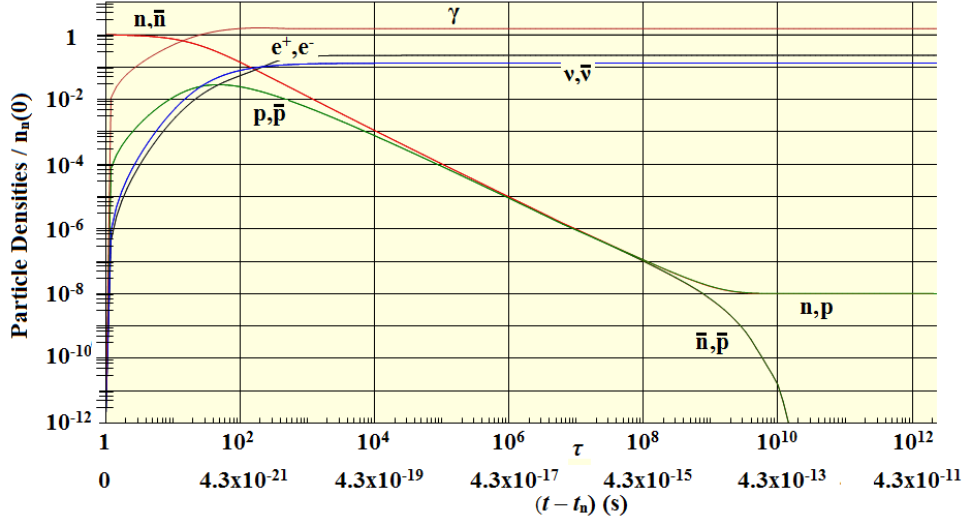
Figure 7: Evolution of the baryon annihilation and charge exchange reactions.

the principal reactions were the baryon annihilation and charge exchange reactions,

$$n + \bar{n} \rightarrow \gamma s + \text{leptons}$$
$$p + \bar{p} \rightarrow \gamma s + \text{leptons}$$
$$n + \bar{p} \rightarrow \gamma s + \text{leptons} \tag{18}$$
$$\bar{n} + p \rightarrow \gamma s + \text{leptons}$$
$$p + \bar{p} \rightleftharpoons n + \bar{n}.$$

The annihilation process was very fast. By a time of 10^{-12}s after it began, it was essentially complete. In Fig. 7 we show the evolution. See [5] for the details. (Our original idea was that weak interactions were responsible for the creation of the protons but that idea turned out to be wrong.) Following the phase shown, there was a period during which the particles thermalized and the p/n ratio reached a value of 7.4. From that point onward, nucleosyntheses proceeded in the usual manner. The details concerning the equations and reactions are given in [1].

6. The origin of cosmic structures

In the previous section, we talked about nucleosynthesis in a general way, and much earlier, we asserted that the vacuum imprint regulated the creation of neutrons and antineutrons at the time, t_n in such a manner as to account for all cosmic structures.

The filament structure that defines superclusters was fixed by this process and because they are vastly too large to undergo gravitational evolution, they are much the same today as they were initially. To study the initial evolution of all smaller cosmic structures, we consider the motion of a particle lying at the outer edge of

192

a volume containing the mass that eventually became the structure in question, see [2]. The only accelerations acting on the particles were gravitation and the acceleration due to the expansion of the universe so the equation of motion becomes

$$\ddot{R}(t) = -\frac{GM_{\text{eff}}(t)}{R(t)^2} + R_0 f_s \frac{\ddot{a}(t)}{a_0}$$

$$= -\frac{GM_{\text{eff}}(t)}{R(t)^2} + R_0 f_s \left(-\gamma_* + \left(\gamma_* + c_1 \frac{t}{t_0} \right)^2 \right) \frac{a(t)}{a_0} \frac{1}{t^2}. \tag{19}$$

The coordinate $R(t)$ is the distance from the particle to the center of the structure and

$$M_{\text{eff}}(t) = M_{\text{Struct}} \left(1 - \left(\frac{R(t)}{R_{\text{sur},s}(t)} \right)^3 \right) \tag{20}$$

is the effective mass of the structure adjusted for the presence of the background vacuum energy.

If we consider a particle located at the radius of the volume needed to form any structure from the background vacuum, nothing would happen, because the density would be the same everywhere. To get things going, we define a parameter, f_s, that fixes the starting radius of the structure at a value less than the value corresponding to the background vacuum density. The latter is denoted by f_{sur}. Also, we imagine that the particles were created at rest (no bulk motion), so their initial velocity was fixed by the expansion.

We will first consider the evolution of a galaxy cluster. Using the Virgo cluster as an example, we have $f_{sur} = 10$. According to the accretion model of structure formation, structures could not come into existence until there was something to accrete which we take to mean that the starting time would be the generally accepted time of galaxy formation. In Fig. 8, we show the model results for several values of initial over-density. The blue line is the solution for $f_s = f_{\text{sur}}$ and since in that case there was no gravitational acceleration, the size would follow the expansion of the universe. The lower black line indicates the size that would have evolved into the present-day size in the absence of gravitational acceleration (the value at $t = 0$ is its present-day size.) From the results, it is apparent that a value of $f_s < 7$ is necessary for the cluster to have any chance of forming and a value closer to 4 would be necessary to account for the present-day size. The point at which the structure ceases to expand we call the zero-velocity point (ZVP) which for $f_s = 4$ occurs at a log time coordinate of about -0.8. What we have learned is that the cluster must have already been a well-defined structure long before the time of galaxy formation.

Since we have argued that all structures came into existence at the time of nucleosynthesis, we recalculate the evolution beginning at a time of $t = t_{4000}$. The result is shown in Figs. 9 and 10. The red line shows the evolution of the cluster and we see that it reaches its ZVP at $t = t_G$ and with its present-day size. The curves show the paths of a few internal and external galaxies and the curve labeled f_{LG}
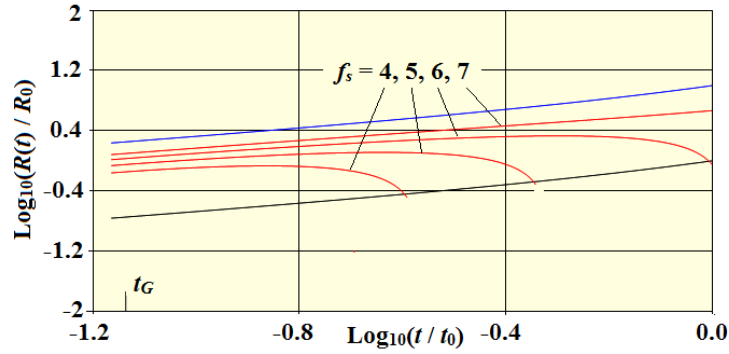
Figure 8: Solution for 4 values of the starting position with $t_s = t_G = 3 \times 10^{16}$ s and a cluster mass of $M_c = 10^{45}$ kg.
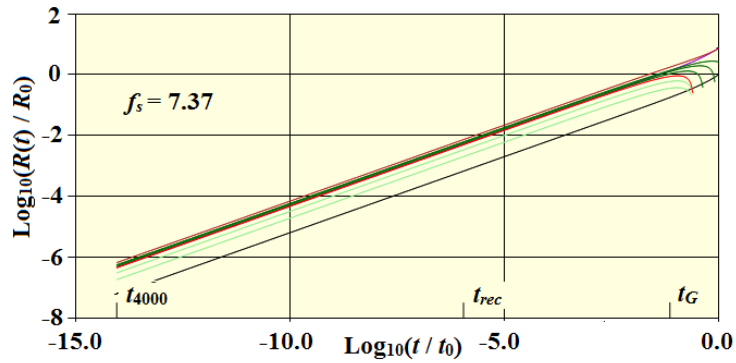

Figure 9: Solution with $t_s = 4000\,s$ and $f_s = 7.37$.
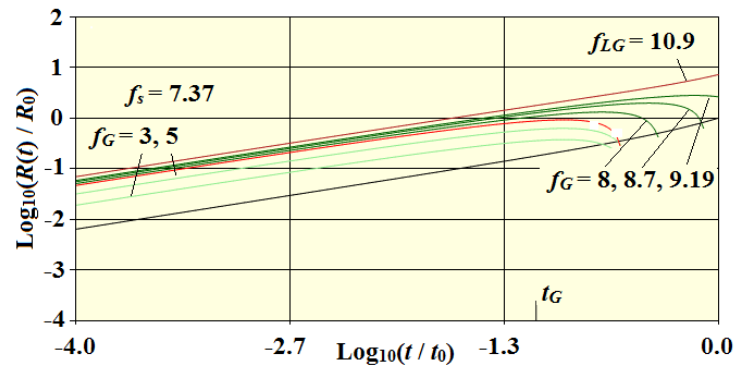

Figure 10: Detail view of Fig. 9.

represents the Local Group. An interesting point about clusters is that the evolution shown for the Virgo cluster seems to apply generally to all clusters regardless of their mass. The value $f_s = 7.37$ corresponds to an initial compaction ratio of 1.35 or an initial density of $2.5\,\mathrm{m}^{-3}$ in present-day terms. What is apparent is that the motion of the surface was completely dominated by the expansion up until a time fairly close
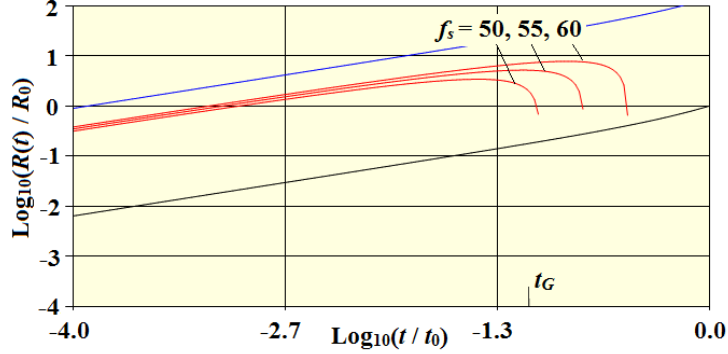
Figure 11: Galaxy evolution for three values of f_s and a mass of $M_G = 1.3 \times 10^{41}$kg.

to $t = t_G$. Up until then, the particles were moving away from each other far too rapidly for gravitation to have any effect on their evolution.

We will now apply the same model to galaxies taking the Milky Way as our example. In this case, the outer surface parameter is $f_{sur} = 140$. The result for three values of f_s is shown in Fig. 11. A value of $f_s = 55$ results in a ZVP close to $t = t_G$ and corresponds to an initial proton density of about $17\,\mathrm{m}^{-3}$ in present-day terms. The really interesting prediction of the model, however, is that galaxies reached their ZVPs with sizes many times larger than their present-day sizes. This fact turns out to be of critical importance. It is responsible for the existence of the observed large HI rings, [3] and as will show below, it is responsible for the existence of supermassive black holes which, in turn, were responsible for the radiation that stabilized those same galaxies as well as galaxy clusters.

We will next move on to the stars. Although stars are extremely dense compared to everything else, that density is a consequence of their collapse. At the time of nucleosynthesis, their density was essentially the same as that of their host galaxies. To model the stars, we considered the evolution of a gas cloud with a nominal dimension of $1\,\mathrm{ly}$ which happens to be the size of the Oort cloud. What we found was that depending on the initial value of f_s, stars could reach their ZVP at times even earlier than $t = t_{\mathrm{rec}}$. The fact that they did not undergo early collapse is a consequence of the temperature of the gas. Jean's model of collapse states that $PE + KE < 0$ which results in a critical temperature of

$$T_c = \frac{0.683}{R(\mathrm{ly})}\mathrm{K}, \tag{21}$$

where R is the radius of the cloud at the ZVP. The gas, on the other hand, had a temperature of about 4000 K at t_{rec} and its temperature decreased thereafter proportional to $a(t)^{-2}$. Comparing, we find that the temperature did not reach the critical value until $t = t_G$ when it had a value very close to $1\,\mathrm{K}$.

We have not mentioned rotation up to this point, but we present arguments in [2] indicating that each region of the vacuum imprint that defined a structure also

195

established its rotation and that on the larger scales, the rotation is not a matter of particle motion but of vacuum rotation.

Summing up, we find that all structures other than superclusters reached the ZVP of their evolution at approximately the same time. (We note that recent observations place the origins of the oldest galaxies and stars in agreement with this model.) Based on the expansion model we have used, after the ZVP, all structures would have rapidly undergone gravitational free-fall collapse. In the next section, we will explain why that did not happen.

7. Post ZVP structure evolution

The reason that galaxies and clusters did not collapse was that their constituent gas was rapidly heated very soon after they reached their ZVPs. We will first consider the evolution of clusters. To model the dynamics, we use the following hydrodynamic equations derived in [4]. We assume spherical symmetry and adopt the Lagrangian viewpoint. The final equations in terms of dimensionless coordinates are as follows;

$$\frac{\partial \bar{r}}{\partial \bar{t}} = \bar{v}, \tag{22a}$$

$$\frac{\partial \bar{v}}{\partial \bar{t}} = -\frac{\bar{m}}{\bar{r}^2} - 4\pi \frac{\tilde{\rho}^{5/3}}{\bar{r}^{4/3}} \left(\frac{\partial \bar{\psi}}{\partial \bar{m}} + \frac{5}{3} \frac{\bar{\psi}}{\tilde{\rho}} \frac{\partial \tilde{\rho}}{\partial \bar{m}} \right)$$

$$+ \frac{10}{3} \frac{\tilde{\rho}^{2/3} \bar{\psi}}{\bar{r}^{7/3}} + \frac{\bar{r}}{\bar{t}^2} \left(-\gamma_* + \left(\gamma_* + c_1 \frac{\bar{t}}{t_0} \right)^2 \right) a_*, \tag{22b}$$

$$\frac{\partial \tilde{\rho}}{\partial \bar{t}} = -4\pi \, \tilde{\rho}^2 \frac{\partial \bar{v}}{\partial \bar{m}}, \tag{22c}$$

$$\frac{\partial \bar{\psi}}{\partial \bar{t}} = \frac{2}{3} \left(\frac{\bar{r}^2}{\tilde{\rho}} \right)^{2/3} \bar{q}. \tag{22d}$$

We have defined a dimensionless time, $\bar{t}$, by $t = t_s(0.469 + \bar{t})$, where $t_s = \sqrt{R_c^3/GM_C} = 6.8 \times 10^{16}\,\mathrm{s}$ so $\bar{t}$ ranges from 0 to 5.91 as t ranges from t_G to t_0. In terms of this dimensionless time, the free-fall time is $\bar{t} = 1.1$ which sets the time frame within which the cluster must be stabilized. In these equations, we have eliminated the pressure in favor of an entropy function,

$$\bar{\psi}(\bar{t}, \bar{m}) = \frac{p(\bar{t}, \bar{m})}{\rho(\bar{t}, \bar{m})^{5/3}} \tag{23}$$

and have defined an adjusted density by

$$\tilde{\rho}(\bar{t}, \bar{m}) \equiv \bar{\rho}(\bar{t}, \bar{m}) \, \bar{r}^2. \tag{24}$$

The Lagrangian independent spatial coordinate, $\bar{m}$, is related to the radial coordinate by

$$\bar{m} = 4\pi \int_0^{\bar{r}} \tilde{\rho}(\bar{t}, \bar{r}')d\bar{r}'. \tag{25}$$

196

We note that these equations do not contain any dimensionless cluster-dependent parameters so the solutions apply to any cluster. Initially, the gas had a temperature of at most a few K and because we are starting at the ZVP, $\bar{v}(\bar{t}, \bar{m}) = 0$. We have seen that clusters reached their ZVPs with present-day size so their average density and total mass are known as well. We have two problems to solve. The first is to determine what combinations of the initial density and radiation result in a cluster that neither collapses nor evaporates. The second problem is to identify the source of the radiation.

We will now just state some results. First, it immediately becomes clear that compressive heating alone develops far too slowly to prevent a collapse. Next, we discovered that with a uniform initial density profile, a collapse will happen no matter what temperature profile is assumed. The same is also true of an initial density profile that is strongly peaked at the origin. That being the case, we considered the linear profile with a moderate negative slope shown in Fig. 12. We next need to assume a radiation profile. We first tried the relatively broad profile shown in Fig. 13. The sample profiles have a maximum value of unity which is then scaled by a multiplier in the simulation code. In Fig. 14, we show the result for a multiplier
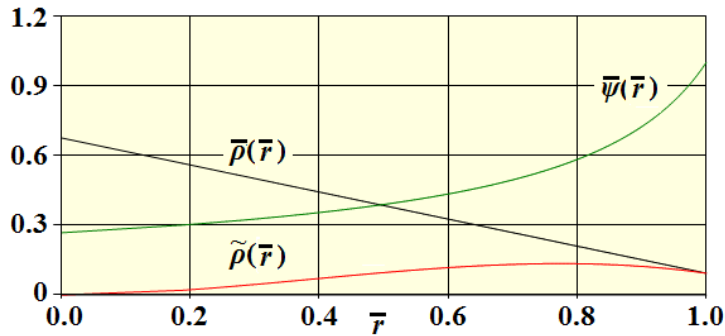
Figure 12: Linear density profile.
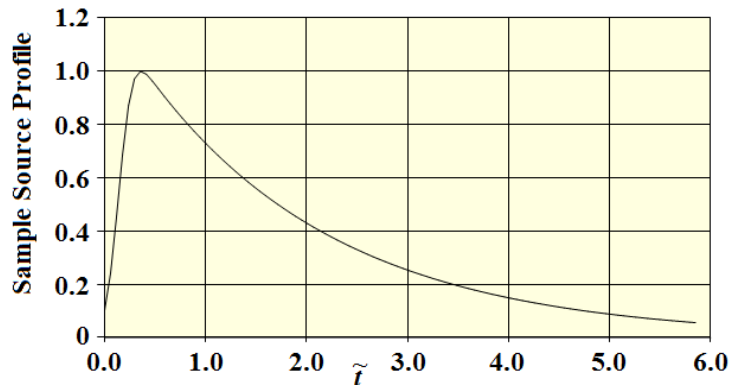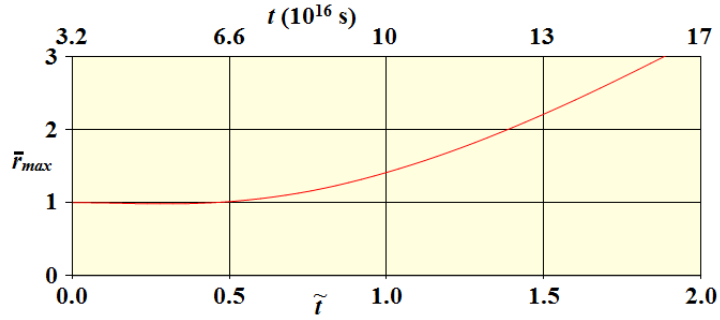

Figure 13: Broad radiation profile.

Figure 14: Solution with the density and radiation profiles of Figs. 12 and 13.
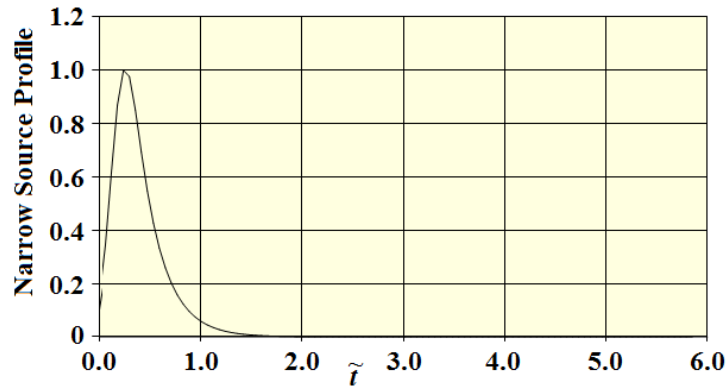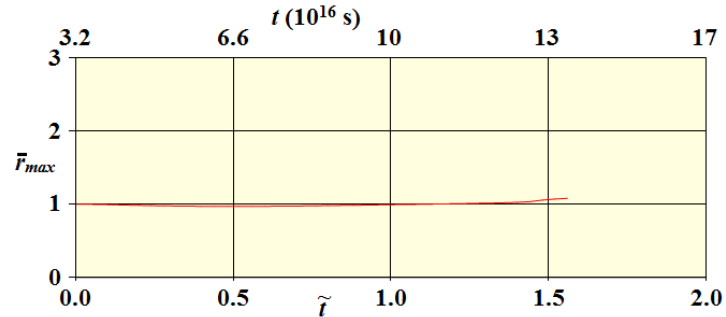

Figure 15: Narrow radiation profile.

Figure 16: Solution with narrow radiation profile and a multiplier of 6.

of 5, and find that the cluster undergoes a significant expansion with no sign of a slowing within the range shown. This is telling us that while a significant amount of radiation immediately after the ZVP is necessary, it must also be short-lived. A much narrower profile is shown in Fig. 15. (Narrow is a relative term, the width of the peak still amounts to $\approx 10^9$ yr.) Fig. 16 shows the resulting evolution. We have thus found a solution that neither collapses nor exhibits undue expansion. The necessary conditions are that the density profile must have a modest negative slope

198
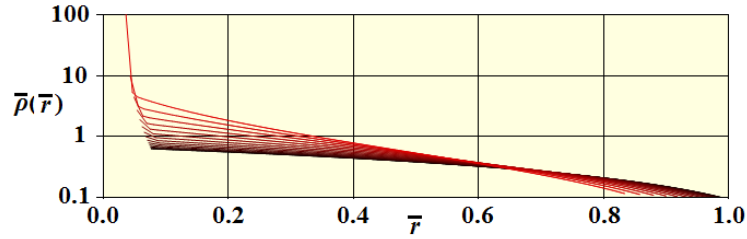
Figure 17: Density profiles of a galaxy undergoing free-fall collapse.

and that the radiation profile must rise sharply after the ZVP and then, just as quickly it must cease or nearly cease. The actual peak radiation intensity is given by $q_{\text{peak}} = f\, 1.4 \times 10^{-5}\,\text{J kg}^{-1}\,\text{s}^{-1}$, where f is on the order of 5 or 6. Multiplying by the mass of the cluster, the total absorbed radiation works out to be on the order of $f\, 10^{40}\,\text{W}$ or $f\, 2.5\, M_\odot c^2\,\text{yr}^{-1}$.

The final problem is to identify the source of this radiation. We need a huge power output and even more importantly, a long lifespan and active galactic cores, or, in other words, quasars are the only real possibility. A necessary condition for a quasar to form is that the host galaxy must contain a supermassive black hole. You will recall from the previous section that galaxies reached their ZVP with sizes many times larger than their present-day size. Immediately afterward, they began to free-fall. Initially, the gas making up the galaxy was cold so there was no pressure gradient to slow the collapse. Fig. 17 shows a sequence of density curves of a collapsing galaxy. We find that the center density increases extremely rapidly and does so long before there is any significant reduction in the radius of the galaxy.

We can now understand the sequence of events. The rapid increase in the center density resulted in the formation of a supermassive black hole. As the collapse continued, the infalling material formed an accretion disk. The resulting radiation heated the intergalactic gas which eventually stopped the collapse of the galaxy. The key point is that the supermassive black holes came first and that all galaxies must have formed such black holes, because they would have otherwise collapsed.

Much of that radiation would have escaped the galaxy and in the cases in which the galaxy was located in a cluster, it would have heated the cluster gas. The Virgo cluster contains a large number of galaxies, most of which are dwarf ellipticals. References in [4] found that quasar host galaxies are all ETGs with the bulk being ellipticals and that dwarf ellipticals do have active nuclei. The Virgo cluster does not contain a quasar at present but it is a characteristic of active nuclei that they radiate huge amounts of energy up until their supply of accretion material runs out. After that, they become normal galaxies. The conclusion is that clusters were heated from within by a large number of mini-quasars that collectively used up their accretion supplies within the time scale indicated in Fig. 15.
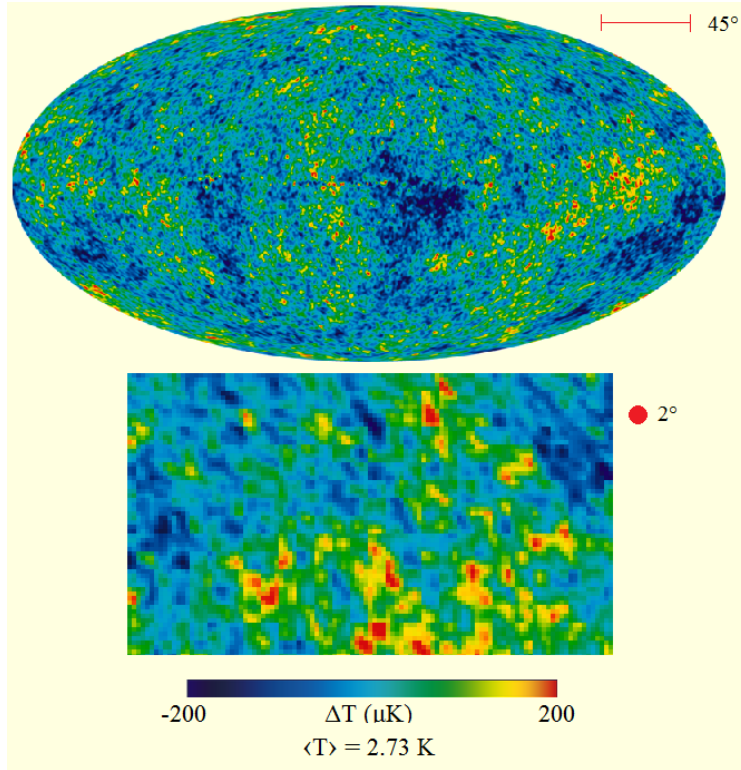
Figure 18: CMB anisotropy.

8. CMB spectrum

We began our discussion with the statement that superclusters were responsible for the peaks in the CMB spectrum. We will now justify that statement. Fig. 18 shows the well-known CMB anisotropy map. A portion of the map has been enlarged in the lower rectangle and two angular size references are also included. The CMB we receive was emitted by a spherical shell whose radius is fixed by the coordinate distance of Fig. 3 when evaluated at the time of recombination. Thus, $S(t_{\text{rec}}) = 0.6\, a(t_{\text{rec}})$. For a structure of size, $D(t_{\text{rec}})$, the subtended angle would then be

$$\theta = \frac{D(t_{\text{rec}})}{S(t_{\text{rec}})}\frac{360}{2\pi} \tag{26}$$

which becomes

$$\theta = \frac{D(t_0)}{0.6a(t_{\text{rec}})}\frac{a(t_{\text{rec}})}{a(t_0)}\frac{360}{2\pi} = 95.5\frac{D(t_0)}{a(t_0)}\text{ deg}. \tag{27}$$

An important fact is that light travels alone lines of constant angle so the subtended angle is independent of time. Plugging in the size range of superclusters, we find that their angular size lies in the range $0.2° < \theta < 2.0°$ so superclusters and voids are large enough to account for the peaks and in fact, these are the only structures that are large enough. (We note that at the time of recombination, the maximum
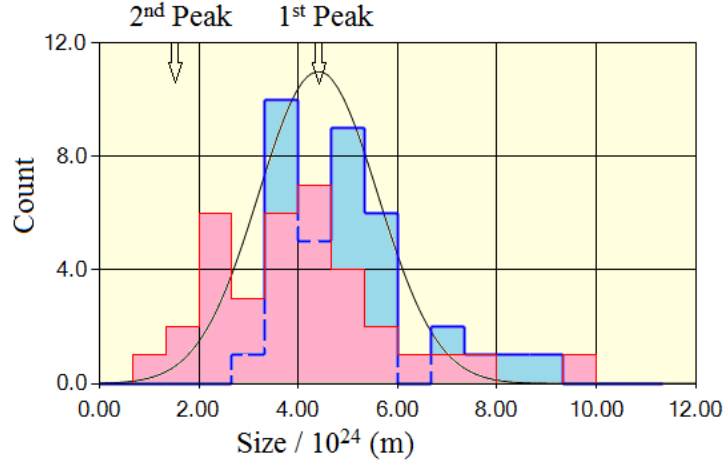
200

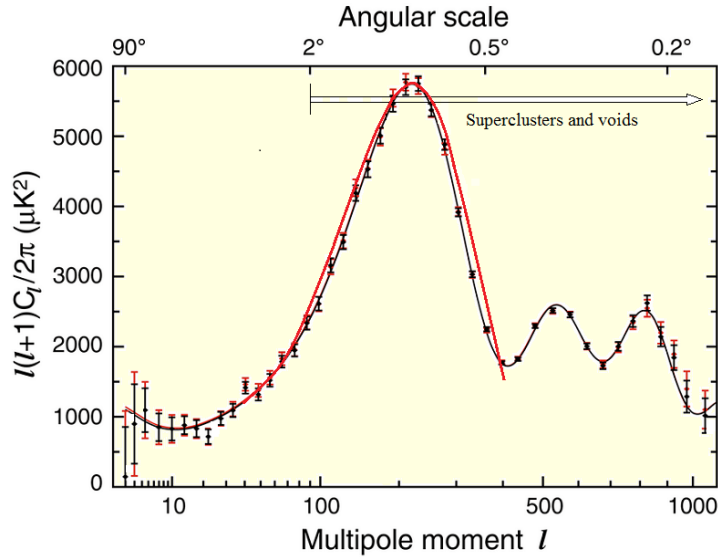Figure 19: Count of observed superclusters (red) and voids (blue).

Figure 20: Ensemble average supercluster/void CMB spectrum. Angles are related to the moment by $l = \pi/\theta_{\mathrm{rad}} = 180/\theta_{\mathrm{deg}}$.

angular distance a signal could have traveled was $0.05°$ which rules out the acoustic oscillation theory.) In Fig. 19, we show a plot of 71 known superclusters and voids. Using the Gaussian distribution shown, we obtain the spectrum shown in Fig. 20, We find that the position of the peak is correct. The shape of the predicted peak is slightly broader than the observed peak but that is quite likely because we assumed that the superclusters were spherical which is certainly not the case. The magnitude of the peak was adjusted to match the observed peak and is not a prediction. We note too that the 2nd peak does not correlate with the size of any structure which is
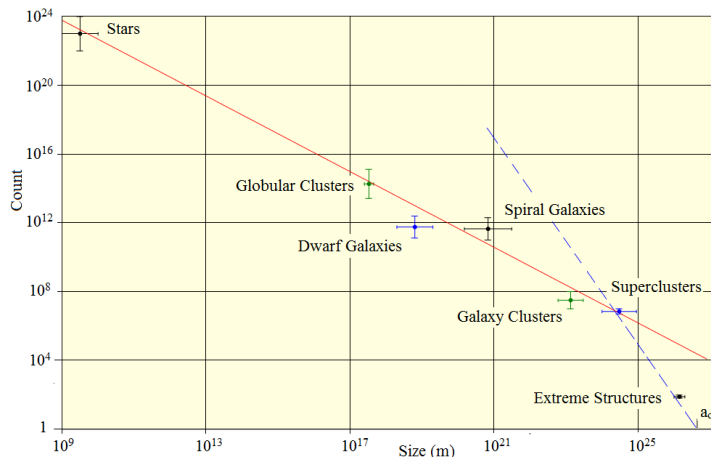
Figure 21: Count of structures vs size.

strong evidence that it results from multipole distributions within the superclusters and voids. Referring back to Fig. 18, we see that the supercluster-sized structures have a range of temperatures which supports that idea.

9. Tying things together

We showed earlier that accretion initiated by small fluctuations in an otherwise uniform distribution of ordinary matter is impossible. We also showed that gravitation was ineffective until shortly before t_G so the idea that accretion is the primary source of cosmic structures is wrong. Another insurmountable problem with accretion is that no process that involves communication could account for structures as large as superclusters. The conclusion we reached was that the existence of structures is a consequence of an imprint established during the initial inflation which regulated the material manifestation of the structures at the time of nucleosynthesis. Fig. 18 is not just a map of the CMB anisotropy but is also a photograph of the vacuum as it existed at the end of the inflation.

Given this high degree of organization, there must have been some rule that regulated the pattern embedded in the imprint. In Fig. 21, we show a plot of the count of cosmic structures versus their size. The dashed line shows the count of structures of a given size that would fill the universe. The extreme structures (size > 45°) fall below this line but this is simply a consequence of the finite size of the universe. What is remarkable is that aside from the extreme structures, all cosmic structures with their vast differences in size and numbers lie on a power-law curve and this holds all the way down to the stars. We see that superclusters fall on both lines so, in an order of magnitude sense, they fill all space. Another point to notice is that the structures have distinct sizes with no overlap. If accretion was the process by which the structures were formed, one would expect a continuum of sizes instead.
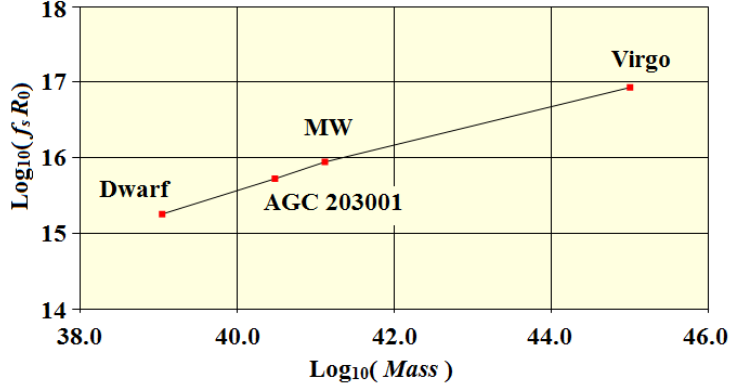
202

Figure 22: Count of structures vs size.

A fit to the curve has the following result,

$$C(s) = 5.7 \times 10^6 (s_{Sc}/s)^{1.1}, \tag{28}$$

where we have scaled by the average size of a supercluster.

The formula for the dashed line is

$$C_{\text{filled}}(s) = (a_0/s)^3. \tag{29}$$

The significant factor here is the power of 3. The idea of a fractal dimension extends this concept to situations in which the power can have any value, not just an integer but this is exactly the form of (28) so we find that the structure imprint had a fractal dimension of 1.1. It is generally true that the fractal dimension of any system is larger than the geometric dimension of that same structure so it follows that the cosmic structure must be 1-dimensional or in other words, it must consist of filaments or, to use the common term, the cosmic web. A defining property of fractal structures is self-similarity so that seems to be the underlying guiding principle that regulated the formation of the imprint.

In Section 6, we developed a model to show how nucleosynthesis regulated by the imprint formed the structures. In each case, we adjusted the f_s parameter so that the ZVP times occurred at $t = t_G$. The imprint, however, could not look ahead to make such adjustments so again, there must have been some guiding principle. In Fig. 22, we show a plot of the initial sizes of the structures versus their mass. The formula is

$$f_s R_0 = 2.06 \times 10^4 m^{0.28} \tag{30}$$

so again we have a power-law relationship between structures of vastly different sizes and masses.

Here at the end, we are back at the beginning. The big mystery is the Plank era inflation. We have no clear idea of how it worked but we have demonstrated that it was responsible for the universe we observe.

References

[1] J. C. Botke, A Different Cosmology – Thoughts from Outside the Box, Journal of High Energy Physics, Gravitation and Cosmology, Vol. 6, No. 3, July 2020.

[2] J. C. Botke, The Origin of Cosmic Structures, Part 1 – Stars to Superclusters, Journal of High Energy Physics, Gravitation and Cosmology, Vol. 7, No. 4, Oct 2021.

[3] J. C. Botke, The Origin of Cosmic Structures, Part 2 – HI Rings, Journal of High Energy Physics, Gravitation and Cosmology, Vol. 7, No. 4, Oct 2021.

[4] J. C. Botke, The Origin of Cosmic Structures, Part 3 – Supermassive Black Holes and Galaxy Cluster Evolution, Journal of High Energy Physics, Gravitation and Cosmology, Vol. 8, No. 2, April 2022.

[5] J. C. Botke, The Origin of Cosmic Structures, Part 4 – Nucleosynthesis, Preprint, Submitted for publication, 2022.

COSMOLOGY MODEL WITH POSITIVE GRAVITATIONAL POTENTIAL ENERGY

Čestmír Hradečný

IQS Group, s.r.o., Hlavní 130, Řež 250 68, Czech Republic
hradecnyc@seznam.cz

Abstract: We claim that gravitational potential energy (GPE) should be considered positive with zero in the bottoms of gravitational potentials, GPE has physical importance, and it is stored in space-time. Analysis of a toy-model example of sequential mergers of a system of N black holes (BHs) which are hierarchically structured is presented. For large N, the GPE becomes considerably larger than the total mass of the standard matter in the system. We prove that the GPE quantity of two gravitationally bound bodies is the same at both bodies independently of their masses. It explains the higher velocity of galaxy rotations in their peripheral parts than it corresponds to standard mass distributions in the galaxies. We show that the largest density of GPE is in the nearest vicinity of the connecting line of gravitationally bound bodies or systems. It explains the fibers and walls of a gravitational lensing dark matter (DM) between galaxies, galactic clusters, and super clusters. We argue that the GPE of a large number of BHs can explain both the quantity and the spatial distribution of both DM and dark energy (DE) in the observable universe.

Keywords: Gravitational potential energy, dark matter, dark energy, cosmology, black holes, spacetime

PACS: 04.70.Bw, 95.10.-a, 95.35.+d, 98.35.Hj, 98.65.-r, 98.80.-k

1. Introduction

The concept and properties of DM [1], [2] and DE [3] belongs to the greatest mysteries in physics for several decades. The goal of this paper is to analyze this concept in its relation to an elementary model-dependent consideration involving GPE as a positive quantity with zero in the bottoms of gravitational potentials. For the computation of the GPE between two point bodies, we can integrate the gravitational force between these two bodies, whose magnitude is given by Newton's law of gravitation [4], concerning the distance between them. Using that definition, the gravitational potential energy of a two-body system of masses m [kg] and M [kg] at a distance

r [m] between them, using gravitational constant $G = 6.67408 \times 10^{-11}$ [m^{3}kg^{-1}s^{-2}] is

$$U = -\frac{GmM}{r} + K, \qquad (1)$$

where K is an integration constant. It is generally considered that only differences have physical importance for all potential energy, therefore, the choice of zero point of GPE is arbitrary, therefore K is considered according to convention zero ($K = 0$) and GPE is considered negative [5]. The convention can be justifiable in gravitationally bound systems with only shallow gravitational potential, like the Solar system, where a mass of GPE is very low in comparison with a mass of standard matter of the system in agreement with Einstein relation [6]:

$$U/c^2 = m_{GPE},$$

where c [m/s] is the speed of light. It is strange, that this convention is held up to nowadays, especially in cosmology, in systems with many BHs, like galaxies, galactic clusters, and the universe, where GPE constitutes an important part of the systems.

It follows from the Friedman equations [7] and measurements of cosmic microwave background that the density of the universe is about $9.9 \cdot 10^{-27}$ [kg/m^3], see [8]. The mass of standard matter is only about 5 % of this value. The rest of the universe mass is an unknown substance in cosmological models with negative GPE like the main-stream Lambda-CDM model [9], a zero-energy universe [10], and the MOND theory [11]. About 25 % of the unknown universe's mass has been called DM. It is observed in large structures only gravitationally. Scientists have searched for particles of DM unsuccessfully for more than 20 years [12]. About 70 % of an unknown mass of the universe has been called DE. It is represented by the cosmological constant Λ with uniform mass distribution in the universe in the main-stream Lambda-CDM model. It is supposed that DE causes accelerating expansion of the universe [13]. No one knows what DE is. There are only speculations. Therefore, there are enough reasons to study a cosmological model with positive GPE.

2. Positive gravitational potential energy

We will consider GPE between bodies of standard matter only in the following. Real bodies in the universe, which are sources of significant gravitational potentials, have spherical or nearly spherical shapes with radii always larger than zero. Owing to the simplicity of the following calculations let us use the equation (1) and suppose that the GPE of two gravitationally bound bodies is zero when the bodies merge. BHs have the deepest gravitational potentials in the universe, therefore systems with them have the largest GPE. Let us suppose that the bottoms of gravitational potentials of BHs are at their event horizons. A radius R_s [m] of an event horizon for the Schwarzschild (no rotating and charged) BH [14] with mass M is

$$R_s = \frac{2GM}{c^2}. \qquad (2)$$

Then the constant K in (1) is

$$K = \frac{GmM}{R_s} = \frac{mc^2}{2},\tag{3}$$

for two-body systems with a body with mass m and a BH with mass M in Euclidean non-wrapped space. But the real space is wrapped in the vicinity of massive bodies according to relativity theory, therefore the constant K is larger. Let us suppose that the value of K is identical to the maximum quantity of energy calculated by Hawking [15] which is released when two Schwarzschild BHs with identical masses M are merged

$$K = (2 - \sqrt{2})Mc^2 \approx 0.5858Mc^2.\tag{4}$$

Regardless the GPE the value K can be considerably larger for rotating BHs [16], the value of K in (4) will be used in the following.

2.1. Where is GPE stored?

Theories with negative GPE suppose that GPE is stored in volumes of gravitationally bound bodies (including BHs), because negative mass energy cannot be at any point of space-time. When the bodies are spiraling to merge and generate gravitational waves (GW) their masses are decreasing [15], [17]. But there is not any proven theory how GPE can be squeezed from BH masses under the event horizon when BH is moving towards deeper gravitational potential. Nevertheless, there are objects which would give information about the tiny change of their rest masses in positions with different gravitational potential. They are free atoms with their electromagnetic spectral lines. Assuming that both electrons and nucleus lost the same percentage value of their rest masses in a place with deeper gravitational potential, then such loss of the rest mass would change their electromagnetic spectral lines. The difference between the GPE mass of an object with mass m on the Sun's surface and Earth's surface is about $0.000001\ m$. Such change in the rest masses of the electron and nucleus would change the optical spectra of the atoms. But astronomers do not observe such changes. They observe only the Doppler and gravitational shifts in spectra of stars [18]. Therefore, we can conclude that GPE could not be stored in the rest masses of gravitationally bound objects. Therefore, the space-time is the only possibility where GPE can be stored.

Let us suppose that the GPE of two gravitationally bound bodies can be imagined as a scalar field of elastic deformation of two spherically symmetrical vector gravitational fields (VGF) of two bodies in space-time. The highest violation of spherical symmetry of the VGF is in the surroundings of a connecting line between the two bodies and the highest density and mass of GPE is there. The violation of spherical symmetry of VGF of two gravitationally bound bodies can reach infinity in principle. Therefore, GPE and its mass can be far from the two bodies. The value of the elastic deformation of the VGF and consequently GPE distribution in
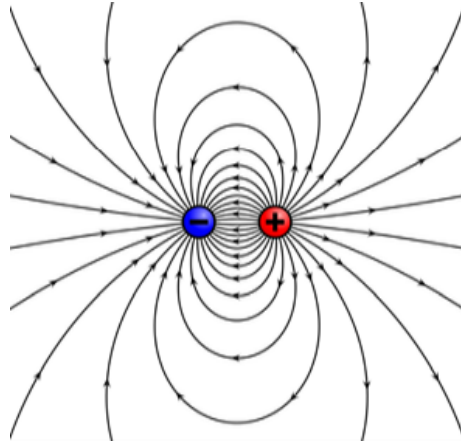
Figure 1: Illustration of the electric field surrounding a positive (red) and a negative (blue) charge. Source –
`https://www.iitjeephysics4u.com/2019/03/electric-field-lines.html`.

space-time would be the same as the density of force lines of an electrostatic field between two bodies with plus and minus charges of the same value (see Figure 1).

The equation (1) can be rewritten as

$$U = \frac{-mV_M(x_m) + K}{2} + \frac{-MV_m(x_M) + K}{2}, \tag{5}$$

where $V_m(x_M) = -Gm/r$ is the gravitational potential of the body m in the place of the body M, $V_M(x_m) = -GM/r$ is the gravitational potential of the body M in the place of the body m and r is a distance between the bodies. In such a case, we have

$$mV_M(x_m) = MV_m(x_M). \tag{6}$$

The equation (6) tells that the same amounts of GPE are at both bodies m and M independently of their masses. The GPE between them has the highest density and is similar to a filament. If the body M is the Schwarzschild BH with mass $M \gg m$ and the distance $r \gg R_s$, then their GPE mass is close to $(2 - \sqrt{2})m$ see equation (4) [15].

2.2. Thought experiment: Calculation of positive GPE in galaxies and the observable universe

Let us start from a thought experiment with a gravitationally bound and hierarchically structured system of 32 Schwarzschild BHs (see Figure 2), every with the same rest mass $M_0 = 10 M_{\text{sun}}$, with the event horizon radius $R_s = 2.97 \cdot 10^4$ m and with distances between them $r \gg R_s$.

Let us suppose that:

1. 16 pairs of the closest BHs have merged and created 16 new BHs, each with the rest mass of $2M_0$. By (4) mass of GPE $\approx 16 \cdot 0.5858 M_0$ has been released during this process.
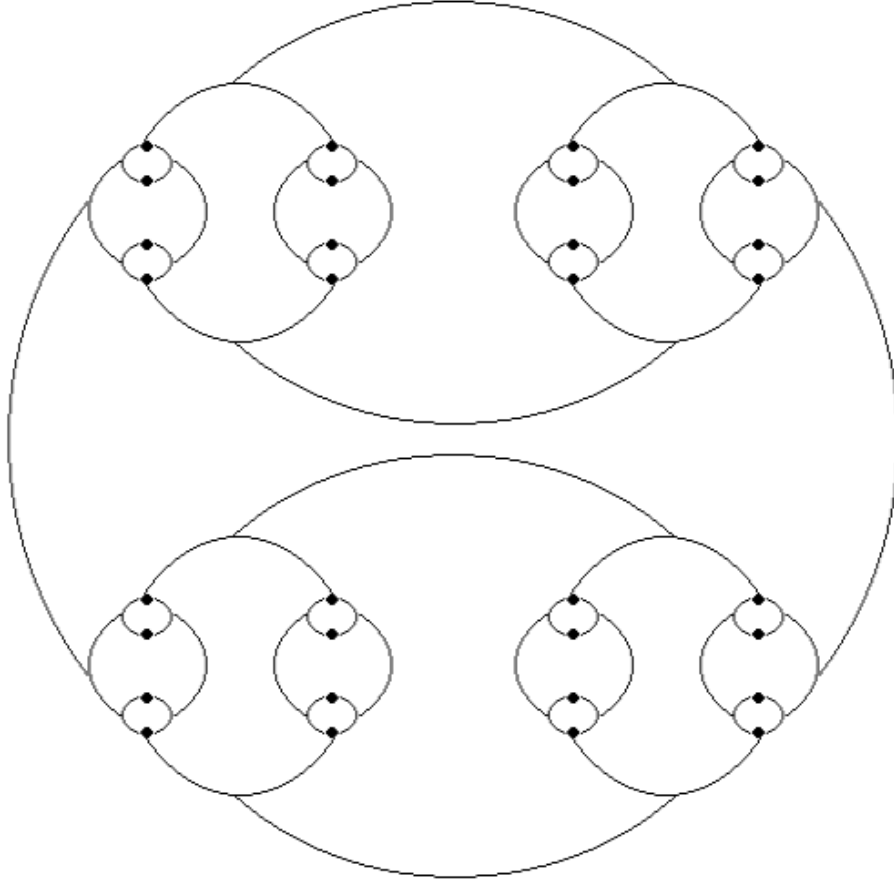
Figure 2: A model example of the hierarchically structured system of 32 gravitationally bound BHs. The BHs are indicated by the black points, the arcs indicate the BH orbitals of individual hierarchic levels.

2. In the resulting system, 8 pairs of the closest BHs have merged again and created 8 new BHs with the rest mass of $4M_0$. The mass of GPE $\approx 16 \cdot 0.5858M_0$ has been released again during this process.

3. In the resulting system, 4 pairs of the closest BHs have merged again and created 4 new BHs with the rest mass of $8M_0$. The mass of GPE $\approx 16 \cdot 0.5858M_0$ has been released again during this process.

4. In the resulting system, 2 pairs of the closest BHs have merged again and created 2 new BHs with the rest mass of $16M_0$. The mass of GPE $\approx 16 \cdot 0.5858M_0$ has been released again during this process.

5. In the resulting system, the pair of the resulting BHs have merged again and created 1 new BH with the rest mass of $32M_0$. The mass of GPE $\approx 16 \cdot 0.5858M_0$ has been released again during this process.

The total mass of GPE $\approx 80 \cdot 0.5858 M_0 \approx 46.864 M_0$ has been released in these 5 steps. It is ≈ 1.465 times longer than the sum of the rest masses of all 32 BHs. It means that this system of 32 BHs each with mass M_0 has the total mass $\approx 78.864 M_0$ for an outside observer. He can see the mass of $32 M_0$ as standard matter and the mass of $46.864 M_0$ as mysterious DM.

It is evident, that this method is possible to use for the calculation of GPE of far larger hierarchically structured systems. For example, GPE masses for similar systems with 1 024 (2^{10}); 1 048 576 (2^{20}); 1 073 741 824 (2^{30}); ... hierarchically structured BHs are nearly 2.929 times; 5.858 times; 8.787 times; ... correspondingly, higher than the sum of rest masses of the BHs in the corresponding systems. Moreover, if every BHs is surrounded by standard baryon matter with a total mass considerably larger than the mass of the corresponding BH, then it is necessary to add the value of 0.586 to the GPE mass for the corresponding BH system. It is followed from the thought experiment, that DM in galaxies and galaxy clusters can be explained by a certain quantity of the hierarchically structured BHs.

2.3. Distribution of GPE in galaxies and the universe

It is estimated that there are about 10^8 stellar-mass BHs in the Milky way [19, 20]. Galaxies are made of dense central bulges, peripheral areas with spiral arms and spherical halo. Heavy objects including BHs are more likely in central parts than in remote peripheral parts. Remote parts of galaxies contain predominantly sparse galactic gas with hydrogen. It has been shown above in equation (6) that amount of GPE near two gravitationally bound bodies is the same and it does not depend on their masses. Therefore, the dependence of the amount of GPE on distance from the center of the galaxies is decreasing considerably more slowly than the same dependence of the standard matter. As a result, the mass of GPE considerably
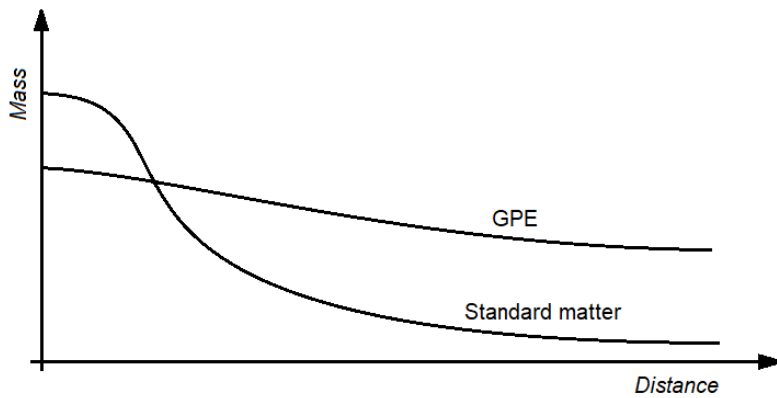

Figure 3: A comparison of possible mass distributions of standard matter and positive GPE in galaxies.
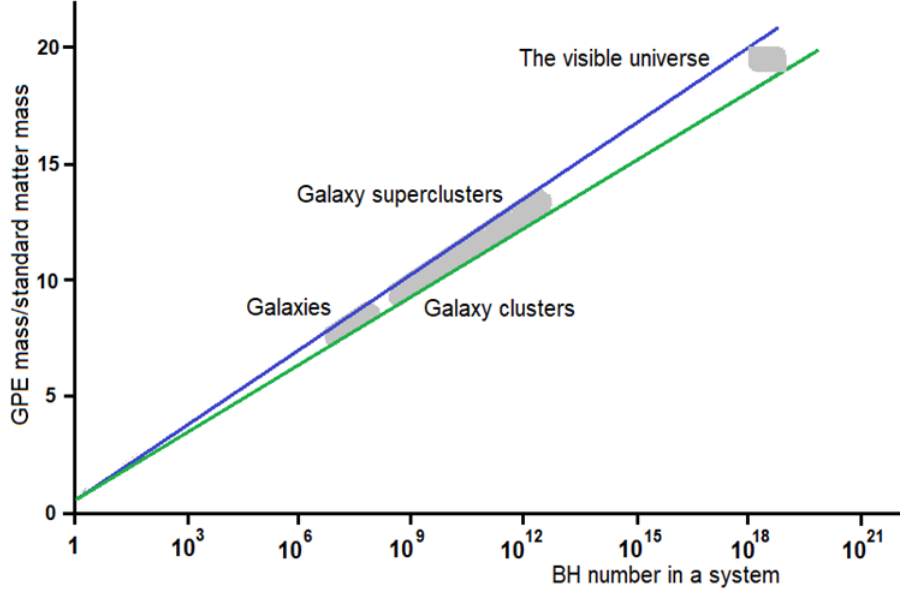
Figure 4: Dependences of ratio (GPE mass)/(mass of standard matter) versus BH quantity in a system. Lower line represents Schwarzschild BHs ($K \approx 0.5858mc^2$). Upper line represents Kerr (rotating) BHs ($K \approx 0.6441mc^2$).

exceeds the mass of standard matter and in peripheral parts of galaxies (see Figure 3). This fact causes rotational velocities of peripheral regions of galaxies to be much higher than it corresponds to distribution of standard mass. It also causes observed gravitational lensing of light coming from remote galaxies.

There are approximately 10^{11} galaxies in the observable universe [19] and it is supposed that the galaxies contain about 10^7–10^8 BHs on average. Therefore, it is supposed that there are approximately 10^{18}–10^{19} BHs in the observable universe and they represent approximately 0.01–0.1 % of the standard mass of the universe. In Figure 4, one can see the dependence of ratio (mass of GPE)/(mass of standard matter) versus quantity of BHs in systems. Altogether 10^{19} Schwarzschild BHs (in (1) $K \approx 0.5858mc^2$) together with other standard matter is the source of GPE mass which is about 19 times larger than the standard matter mass of the universe. This ratio is identical to the ratio of the sum of DM and DE mass (95 %) versus standard matter mass (5 %) in the universe. Note that 10^{18} Kerr BHs [20] (in (1) $K \approx 0.6441mc^2$) together with other standard matter is the source of GPE with mass which is about 20 times larger than the standard matter of the universe.

3. Concluding remarks and summary

Only bodies with shallow (no deep) gravitational potentials like planets and stars of the sun type there had been known in the universe in the first half of the 20th cen-

tury. GPE mass of the bodies is negligible in comparison with standard mass of the bodies. Therefore, the consensus, that GPE has no physical importance, GPE had been considered negative and acceptable at that time. It is strange, that this consensus is held up nowadays, because it is estimated that there are 10^{18}–10^{19} BHs with very deep gravitational potentials in the universe [19] and, therefore, the assumption, that GPE has no physical importance cannot be valid at present. Moreover, there are several problems in models with negative GPE. It is supposed that GPE is deposed in volumes of a gravitationally bound body in the cosmological models with negative GPE, since negative energy cannot be deposed in an empty space-time [21]. As a result, the rest masses of bodies and particles cannot be invariant in positions with different gravitational potentials. The universe of all cosmological models with negative GPE has a large mass deficit called DM and DE, because negative GPE mass is subtracted from the positive mass of all bodies, particles, fields, and energies. An extreme is "The universe from nothing" [10], where the whole mass of the universe is zero.

The presented cosmological model with positive GPE has moved zero of GPE from infinity into the bottoms of the gravitational potentials of the gravitationally bound bodies. The place of deposition of GPE has been moved from volumes of gravitationally bound bodies into space-time. Rest masses of bodies remain invariant in positions with different gravitational potentials in the presented model. Bodies with the deepest gravitational potentials are BHs and therefore the mass of GPE of systems with a large number of hierarchically structured BHs can be considerably larger than the mass of standard matter including the BHs that constituted the system. It explains weak lensing observations of 1E 0657-558 a unique cluster merger [22], where are galaxy clusters separated from hot intergalactic gas. The gravitational lensing of the galaxy clusters is considerably larger than the neighboring intergalactic gas despite the cluster standard masses being several times smaller. GPE quantity of two gravitationally bound bodies is the same at both bodies independently of their masses. It explains a higher rotational velocity of galaxy rotations in their peripherical parts than it corresponds to standard matter mass distributions in galaxies. The largest density of GPE is in the nearest vicinity of the connecting line of gravitationally bond bodies or systems. It explains fibers and walls of gravitational lensing DM between galaxies galactic clusters and superclusters [23]. GPE of a large number of BHs can explain both the quantity and space distribution of both DM and DE in the observable universe.

References

[1] Rubin, V., Thonnard, N., Ford, W. K. Jr.: Rotational properties of 21 Sc galaxies with a large range of luminosities and radii from NGC 4605 (R=4kpc) to UGC 2885 (R=122kpc). Astrophys. J. 238 (1980), 471–487.

[2] Taylor, A. N. et al.: Gravitational lens magnification and the mass of Abell 1689. Astrophys. J. 501 (2) (1998), 539–55.

[3] Kowalski, M. et al.: Improved cosmological constraints from new, old and combined supernova datasets. Astrophys. J. 686 (2) (2008), 749–778.

[4] Newton, I.: The principia: mathematical principles of natural philosophy. Preceded by A guide to Newton's principia, by I. Bernard Cohen. University of California Press, 1999.

[5] https://courses.lumenlearning.com/boundless-physics/chapter/gravitational-potential-energy/

[6] Einstein, A.: Ist die Trägheit eines Körpers von seinem Energieinhalt abhängig? [Does the inertia of a body depend upon its energy-content?]. Ann. Phys. (In German). 323 (13) (1905), 639–641.

[7] Friedman, A.: Über die Krümmung des Raumes. Z. Phys. 10 (1) (1922) 377–386. (English translation: Friedman, A. (1999). On the curvature of space. General Relativity and Gravitation 31 (12) (1922) 1991–2000.

[8] NASA/WMAP Science Team.: Universe 101: What is the universe made of? (2014).

[9] Liddle, A.: An introduction to modern cosmology (2nd ed.), London, Wiley, 2003.

[10] Kraus, L. M.: A universe from nothing. Simon and Schuster US, 2013.

[11] Kroupa, P., Pawlowski, M., Milgrom, M.: The failures of the standard model of cosmology require a new paradigm. Internat. J. Mod. Phys. D 21 (14) (2012), 1230003.

[12] Davis, J. H.: The past and future of light dark matter direct detection. Int. J. Mod. Phys. A 30 (15) (2015), 1530038.

[13] Peebles, P. J. E., Ratra, B.: The cosmological constant and dark energy. Rev. Mod. Phys. 75 (2) (2003), 559–606.

[14] Schwarzschild, K.: Über das Gravitationsfeld eines Massenpunktes nach der Einsteinschen Theorie. Sitzungsberichte der Deutschen Akademie der Wissenschaften zu Berlin, Klasse fur Mathematik, Physik, und Technik (1916), pp. 189.

[15] Hawking, S. W.: Gravitational radiation form colliding black holes. Phys. Rev. Lett. 26, (21), (1971), 1344–1346.

[16] Visser, M.: The Kerr spacetime: A brief introduction, 2008, `arxiv.org/abs/0706.0622`.

[17] Abbott, R. et al.: (LIGO Scientific Collaboration and Virgo Collaboration), GW190521: A binary black hole merger with a total mass of 150 M_{sun}. Phys. Rev. Lett. 125, 101102 (2020). List of gravitational wave observations - wikipedia.

[18] Hernández, J. I. et al.: The solar gravitational redshift from HARPS-LFC Moon spectra – A test of the general theory of relativity. Astron. Astrophys. **643**: A146 (2020).

[19] `https://phys.org/news/2014-06-universe-black-holes.html`

[20] Kerr, R. P.: Gravitational field of a spinning mass as an example of algebraically special metrics. Phys. Rev. Lett. 11 (1963), 237.

[21] Maxwell, J. C.: The Scientific Papers of James Clerk Maxwell, Volume 1, p. 571, W. D. Niven (ed.), Cambridge University Press, (1890).

[22] Clowe, D. et al.: A direct empirical proof of the existence of dark matter. Astrophys. J. Lett. 648 (2) (2006), 109–113.

[23] Tully, R. B., Courtois, H., Hoffman, Y., Pomarède, D.: The Laniakea supercluster of galaxies. Nature 513 (2014), 7–73.

LIST OF PARTICIPANTS

Elena Asencio
Helmholtz-Institut für Strahlen und Kernphysik, University of Bonn, Nussallee 14–16,
D-53115 Bonn, Germany
s6elena(at)uni-bonn.de

Hana Bílková
Institute of Mathematics, Czech Academy of Sciences, Žitná 25, CZ-115 67 Prague 1,
Czech Republic
hbilkova(at)math.cas.cz

John C. Botke
1200 N. Mariposa Road, no. 405, Nogales, Arizona, 85621, U.S.A.
jcbotke(at)gmail.com

Kirill A. Bronnikov
VNIIMS, 46 Ozyornaya St., Moscow 119461, Russia
kb20(at)yandex.ru

Roberto A. Capuzzo Dolcetta
Department of Physics, University of Roma La Sapienza, Piazzale A. Moro 5, Italy
roberto.capuzzodolcetta(at)uniroma1.it

Giovanni Carraro
Padova University, Vicolo Osservatorio 3, I-35122 Padova, Italy
giovanni.carraro(at)unipd.it

Sergey L. Cherkas
Institute for Nuclear Problems, Belarus University, Bobruiskaya 11, Minsk 220006,
Belarus
cherkas(at)inp.bsu.by

Jörg Dabringhausen
Astronomical Institute, Faculty of Mathematics and Physics, Charles University,
V Holešovičkách 2/747, CZ-180 00 Praha, Czech Republic
joerg(at)sirrah.troja.mff.cuni.cz

Juan De Vicente

CIEMAT, Av. Complutense 40, Madrid 28040, Spain

`juan.vicente(at)ciemat.es`

Yurii V. Dumin

P. K . Sternberg Astronomical Institute of M. V. Lomonosov Moscow State University, Universitetskii pr. 13, R-119 234 Moscow, Russia; Space Research Institute, Russian Academy of Sciences, Profsoyznaya str. 84/32, R-117 997 Moscow, Russia

`dumin(at)sai.msu.ru`, `dumin(at)yahoo.com`

Antonín Dvořák

Kovoprojekta Brno a.s., Poznaňská 22, CZ-616 00 Brno, Czech Republic

`antonin.dvorak(at)centrum.cz, advorak(at)kovoprojekta.cz`

David Fernández-Arenas

Instituto Nacional de Astrofísica, Óptica y Electrónica (INAOE), Luis Enrique Erro # 1, Sta María Tonanzintla, 72840 San Andrés Cholula, Pue, Mexico

`arenas(at)inaoep.mx`

Ismael Ferrero

Institute of Theoretical Astrophysics, University of Oslo, Duehaugveien 6b, Oslo, Norway

`s.i.ferrero(at)astro.uio.no`

Mina Ghodsi Yengejeh

Shahid Beheshti University, Karaj, Alborz, 3193939865 Iran

`m.ghodsi.y(at)gmail.com`

Itzhak Goldman

Afeka Engineering College and Tel Aviv University, Mivtza Kadesh 38, Tel Aviv, Israel

`goldman(at)afeka.ac.il`

Vesselin Gueorguiev

Institute for Advanced Physical Studies, Montevideo Street, Sofia 1618, Bulgaria; Ronin Institute for Independent Scholarship, 127 Haddon Pl., Montclair, NJ 07043, U.S.A.

`Vesselin(at)MailAPS.org`

Moritz Haslbauer

Helmholtz-Institut fuer Strahlen- und Kernphysik, University of Bonn; Max-Planck-Institut fuer Radioastronomie, Auf dem Huegel 69, D-53121 Bonn, Germany

`mhaslbauer(at)astro.uni-bonn.de`

Xavier Hernandez

Instituto de Astronomía, Universidad Nacional Autónoma de México, Apartado Postal 70–264 C.P., 04510 Mexico

`xavier(at)astro.unam.mx`

Čestmír Hradečný

IQS Group, s.r.o., Hlavní 130, 250 68 Řež, Czech Republic

`cestmir.hradecny(at)iqstructures.cz, hradecnyc(at)seznam.cz`

Ahmad Hujeirat

University of Heilelberg, Berlinerstr. 41, D-69120 Heidelberg, Germany

`AHujeirat(at)urz.uni-hd.de`

Igor Dmitrievich Karachentsev

Special Astrophysical Observatory, Russian Academy of Sciences, Nizhnij Arkhyz, Zelenchukski region, Karachai-Cherkessian Republic, R-369 167 Russia

`ikar(at)sao.ru`

Nandita Khetan

DARK Cosmology Centre, Niels Bohr Institute, Niels Bohr Building, Jagtvej 128, 2. floor, University of Copenhagen, 2200 Copenhagen N., Denmark

`nkhetan(at)nbi.ku.dk`

Roman Knobloch

Department of Mathematics, Technical University of Liberec, Studentská 2, Liberec, Czech Republic

`Roman.Knobloch(at)tul.cz`

Kurt Koltko

P. O. Box 100595, Denver, CO 80250, U.S.A.

`g8cpt(at)protonmail.com`

Sergei Kopeikin

Department of Physics and Astronomy, 322 Physics Bldg, University of Missouri in Columbia, MO 65211, U.S.A.

`kopeikinS(at)missouri.edu`

Michal Křížek

Institute of Mathematics, Czech Academy of Sciences, Žitná 25, CZ-115 67 Prague 1, Czech Republic

`krizek(at)cesnet.cz, krizek(at)math.cas.cz`

Pavel Kroupa

Astronomical Institute, Faculty of Mathematics and Physics, Charles University, V Holešovičkách 2, CZ-180 00 Praha, Czech Republic; University of Bonn, Helmholtz-Institut für Strahlen- und Kemphysik, Nussallee 14–16, D-53115 Bonn, Germany
`pavel(at)astro.uni-bonn.de`, `pkroupa(at)uni-bonn.de`,

Pavel Kůs

Institute of Physics, Czech Academy of Sciences, Pod Vodárenskou věží, CZ-182 21 Prague 8, Czech Republic
`pavel.kus(at)fzu.cz`,

Frederic Lassiaille

Nice, Massena, France
`lumimi2003(at)hotmail.com`

Namhyung Lee

Faculty of Physics, Columbia Southern University, 21982 University Lane, Orange Beach, AL 36561, U.S.A.
`Namhyuang.Lee(at)columbiasouthern.edu`

František Lomoz

Sedlčany Astronomical Observatory, CZ-115 67 Sedlčany, Czech Republic
`F.Lomoz(at)seznam.cz`

Martín López-Corredoira

Instituto de Astrofisica de Canarias, C/.Vía Láctea, s/n, E-38205 La Laguna, Tenerife, Spain
`martin(at)lopez-corredoira.com`

André Maeder

Geneva Observatory, 19, chemin des Marais, CH-1234 Vessy, Switzerland
`Andre.Maeder(at)unige.ch`

Jan Maršák

Pedagogical Institute, Prague, Czech Republic
`jmarsak(at)seznam.cz`

Klaus Morawetz

FH Münster University of Applied Sciences, Department of Physical Engineering, Stegerwaldstrasse 39, D-48565 Steinfurt, Germany
`morawetz(at)fh-muenster.de`

Luboš Neslušan

Astronomical Institute, Slovak Academy of Sciences, SK-05960 Tatranská Lomnica, Slovakia

ne(at)ta3.sk

Vladimír Novotný

Cosmological Section of the Czech Astronomical Society, Jašíkova 1533/4, CZ-149 00 Prague 4, Czech Republic

nasa(at)seznam.cz

Marek Nowakovski

Departamento de Fisica, Universidad de los Andes, Cra 1E, 18A-10, Bogota, Colombia

mnowakos(at)uniandes.edu.co

Wolfgang Oehm

An Quirinusbrunnen 14, D-53129 Bonn, Germany

physik(at)wolfgang-oehm.com

Tomáš Ondro

Mendel University in Brno, Zemědělská 1665/1, Brno, CZ-613 00 Czech Republic

tomas.ondro(at)mendelu.cz

Ziad G. Sakr

Institut für Theoretische Physik, Philosophenweg 16, D-69120, Heidelberg, Germany; IRAP Toulouse, France; USJ Beirut, Lebanon

sakr(at)thphys.uni-heidelberg.de

Nikolaos Samaras

Astronomical Institute, Faculty of Mathematics and Physics, Charles University, V Holešovičkách 2/747, CZ-180 00 Praha, Czech Republic

nicksam(at)sirrah.troja.mff.cuni.cz

Heikki J. Sipilä

Physics Foundations Society, Hannuksenkuja 1 C, 02270 Espoo, Finland

hjsipila(at)gmail.com

Lawrence Somer

Department of Mathematics, Catholic University of America, Washington, D.C., 20064, U.S.A.

somer(at)cua.cz

Daniele Sorini
Institute for Astronomy, University of Edinburgh, Royal Observatory, Blackford Hill,
EH9 3HJ, Edinburgh, United Kingdom
`sorini(at)roe.ac.uk`

Alessandro D. A. M. Spallicci
Université d'Orléans, Observatoire des Sciences de l'Univers, Campus CNRS, 3A Av.
de la Recherche Scientifique, F-45071 Orléans, France
`spallicci(at)cnrs-orleans.fr`

Alexei A. Starobinsky
L. D. Landau Institute for Theoretical Physics, Russian Academy of Sciences,
2, Kosygina, R-119 334 Moscow, Russian Federation
`alstar(at)landau.ac.ru`

Tuomo Suntola
Physics Foundations Society, Vasamatie 25, 02630 Espoo, Finland
`tuomo.suntola(at)gmail.com`

Charles Sven
41242 North Westlake Avenue, Antioch, Illinois 60002, U.S.A.
`cjsven(at)allnewuniverse.com`

Emilie Těšínská
Institute of Contemporary History, Czech Academy of Sciences, Czech Republic
`tesinska(at)cesnet.cz`

Václav Vavryčuk
Institute of Geophysics, Czech Academy of Sciences, Boční II, CZ-141 00 Prague 4,
Czech Republic
`vv(at)ig.cas.cz`

Tomáš Vejchodský
Institute of Mathematics, Czech Academy of Sciences, Žitná 25, CZ-115 67 Prague 1,
Czech Republic
`vejchod(at)math.cas.cz`

Asher Zvi Yahalom
Department of Electrical and Electronic Engineering, Center for Astrophysics, Geo-
physics, and Space Sciences, Ariel University, P.O.B. 3, Ariel 40700, Israel
`asya(at)ariel.ac.il`

Suk-Jin Yoon
Department of Astronomy, Yonsei University, Yonsei-ro 50, Seoul 03722, South Korea
`sjyoon0691(at)yonsei.ac.kr`

PROGRAM OF THE CONFERENCE

Wednesday, September 21

12:00–13:00 Registration

13:00–13:20 Opening (Michal Křížek and Yurii Dumin)

Chair: Michal Křížek

13:20–14:10 **André Maeder**, New perspectives in the Scale Invariant Vacuum theory

14:10–15:00 **Václav Vavryčuk**, Expansion of the Universe and the cosmological redshift

15:00–15:30 **Martín López-Corredoira**, Fundamental ideas in cosmology. Scientific, philosophical and sociological critical perspectives

15:30–16:00 <u>Coffee Break</u>

Chair: André Maeder

16:00–16:30 **Elena Asencio**, El Gordo: a massive blow to ΛCDM cosmology

16:30–17:00 **David Fernández-Arenas**, Determination of the local value of Hubble constant and cosmological constraints with local giant HII regions and high-redshift HII galaxies

17:00–17:20 **Roberto A. Capuzzo Dolcetta, Giovanni Carraro**, A possible alternative to dark matter on galactic scales

17:20–18:00 **Pavel Kroupa**, The star-formation histories of nearby galaxies raises questions on cosmology

18:00–18:05 **Wolfgang Oehm**, A possible constraint on the validity of GR for very strong gravitational fields (Poster presentation)

Thursday, September 22

Chair: Tuomo Suntola

9:00–9:45 **John C. Botke**, A different cosmology

9:45–10:15 **Asher Yahalom**, The weak field approximation of general relativity, retardation, and the problem of precession of the perihelion for Mercury

10:15–10:45 <u>Coffee Break</u>

Chair: Martín López-Corredoira

10:45–11:15 **Heikki Sipilä**, Recalculation of the Moon retreat velocity supports expansion of gravitationally bound local systems

11:15–11:45 **Tuomo Suntola**, In a holistic perspective everything in space is interconnected

11:45–12:05 **Joerg Dabringhausen**, The integrated galaxy-wide stellar initial mass function over the radial acceleration range of early-type galaxies

12:05–14:00 <u>Lunch Break</u>

Chair: Wolfgang Oehm

14:00-14:30 **Martín López-Corredoira, José Ignacio Calvo-Torel**, Fitting of supernovae without dark energy

14:30–15:00 **Itzhak Goldman**, Neutron stars constraints on a late transition of the gravitational constant

15:00–15:30 **Ahmad Hujeirat**, Why the energy density in our universe must be upper-limited? – observations confront theory

15:30–16:00 <u>Conference photo - Coffee Break</u>

Chair: Václav Vavryčuk

16:00–16:30 **Moritz Haslbauer**, The KBC void and Hubble tension in ΛCDM and Milgromian dynamics

16:30–17:00 **Luboš Neslušan**, A demonstration of the difference between the normalized and non-limited solutions of the field equations in the modeling of relativistic compact objects

17:00–17:30 **Xavier Hernandez**, A covariant description of local gravitational anomalies and its cosmological implications

17:30–18:00 **Ziad G. Sakr**, Untying the growth rate sigma 8 disentanglement

18:00–18:20 **Yurii Dumin**, Lambda-instability of Keplerian orbits and the problem of hypervelocity stars

Friday, September 23

Chair: Heikki Sipilä

9:00–9:30 **Klaus Morawetz**, Consistent solution of Einstein-Cartan equations with torsion outside matter – consequences for dark matter

9:30–10:00 **Juan De Vicente**, A comprehensible view of the Hubble tension

10:00–10:30 **Václav Vavryčuk**, Physical properties of the conformal FLRW metric

10:30–11:00 Coffee Break

Chair: Luboš Neslušan

11:00–11:40 **Charles J. Sven**, Evidence of dark energy using 3D physics

11:40–12:00 **Čestmír Hradečný**, Cosmology model with positive gravitational potential energy

12:00–14:00 Lunch Break

Chair: Asher Yahalom

14:00–14:30 **Vesselin G. Gueorguiev**, An alternative explanation of the orbital expansion of Titan and other bodies in the Solar system

14:30–15:00 **Yurii V. Dumin**, What can we learn from the low-multipole part of the CMB spectrum?

15:00–15:20 **Nikolaos Samaras**, Cosmological simulations with Milgromian dynamics

15:20–15:40 **Frederic Lassiaille**, Discrete relativity: current status of the research

15:40–16:00 **Michal Křížek**, 100 years of the Friedmann equation

16:00–16:30 Coffee Break

Chair: Pavel Kroupa

16:30–17:00 **Igor V. Karachentsev**, Dark-to-luminous matter ratio in the local volume galaxies (ZOOM presentation)

17:00–17:30 **Alexei Starobinsky**, Inflationary models with large peaks in primordial perturbation spectra at small scales (ZOOM presentation)

17:30–18:00 **Kirill A. Bronnikov**, Wormholes in a Friedmann universe (ZOOM presentation)

18:00–18:20 **Kurt Koltko**, Gauge CPT experimental predictions

9:00–12:00 Excursion to the astronomical and cosmological sights of Prague guided by **Michal Křížek** (total length about 6 km):

In the footsteps of Albert Einstein in Prague

We will meet at 9:00 in front of the main gate of the Institute of Mathematics at Žitná 25. From here we shall shortly walk to the Faculty of Science of Charles University at Viničná Street no. 7/1594. A memorial plaque (see Figure 1) dedicated to Albert Einstein is located in the lobby at the ground floor. It was unveiled on the 10th anniversary of his death in 1965 and recalls that Einstein worked in this building in 1911–1912. Einstein had his office there, where he found the calm necessary to formulate basic ideas of his General Theory of Relativity. In this building, Einstein also taught his seminar on theoretical physics for students and met the famous Professor of mathematics Georg Pick (1859–1942) with whom he became friends soon after arriving in Prague. Pick worked on non-Euclidean geometries and taught Einstein mainly foundations of tensor calculus. In Prague, Einstein got his first full professorship and was at the beginning of his fame. His stay there meant an important working period in his life. Note that at the turn of 1879/1880, the Institute of Physics (headed by Ernst Mach) of the German University moved from Ovocný trh to the building in Viničná.
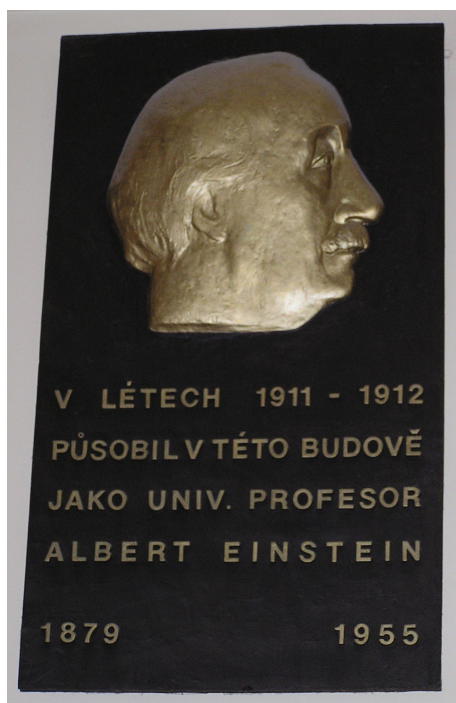

Figure 1: Memorial plaque dedicated to Albert Einstein in Viničná Street 7.

Figure 2: Memorial plaque with bust dedicated to Albert Einstein.

Then we will visit another memorial plaque with Einstein's bust (see Figure 2) in Lesnická Street no. 7/1215 in Smíchov (in 1911 this street was called Třebízského). In this house, Einstein lived with his family, in particular, his wife Mileva (born Marić) and two sons Hans Albert and Eduard. This bronze memorial plaque was unveiled in 1979 on the 100th anniversary of Einstein's birth.

The third memorial plaque dedicated to Einstein [4] was unveiled on the 14th March 1999 (see Figure 3) on the occasion of the 120th Einstein's anniversary in the Old Town Square (Staroměstské náměstí) no. 17/551. The plaque contains the following English (and also Czech) text:

"Here, in the salon of Mrs. Berta Fanta, ALBERT EINSTEIN, Professor at Prague University in 1911 to 1912, founder of the Theory of Relativity, Nobel Prize Winner, played the violin and met his friends, famous writers Max Brod and Franz Kafka."

Figure 3: Installation of the memorial plaque dedicated to Albert Einstein in the Old Town Square 17.

After his arrival in Prague in 1911, Einstein often visited this house and met there the Jewish intellectuals Max Brod, Hugo Bergmann, Felix Weltsch, and also Franz Kafka, see [1, pp. 153, 186], [6, p. 402], [7, p. 7]. He took part in Tuesday's evening lectures and philosophical debates on diverse topics. Franz Kafka gradually stopped going there until 1914 (see [1, p. 152]), when Einstein was not anymore in Prague.

It was the above-mentioned Georg Pick who introduced Einstein into this company. In particular, two topics brought Pick and Einstein together. The first of them was discussion about mathematical methods that later Einstein used to formulate his General Theory of Relativity. Their second common interest was music. Max Brod recalls that in the Salon of Berta Fantová[1] he played on piano and was accompanied by Einstein on violin performing together the Mozart violin sonata (see [1, p. 153]). They also took part in philosophical discussions in that Salon.

The relief of the plaque recalls the time of Einstein's Prague residence, his first considerations about the General Theory of Relativity, namely, bending of the light beam nearby the Sun (see Figure 4). This is represented by a curve above the Charles Bridge, where Einstein walked and thought of his own lectures on physics. Old Town Bridge Tower on the left depicting the Aristotelian cosmological idea of the universe reminds us that Einstein had no idea at that time that his theory will become the

---

[1]Berta Fantová (1865–1918), the mother of Professor Otto Fanta, see the letter of Max Brod to Franz Kafka from the 20th December 1918 in [6, p. 212].
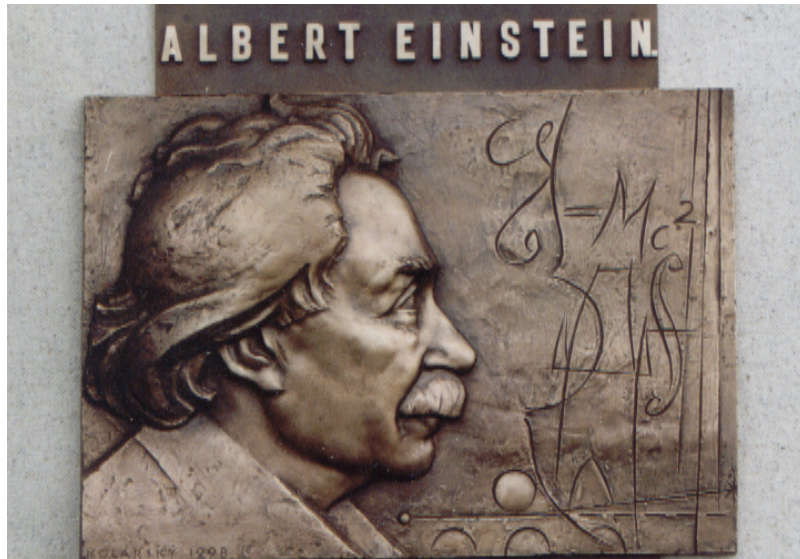
Figure 4: Artistic design of the main ideas of Albert Einstein.

basis of modern cosmology. The formula $\mathcal{E} = \mathcal{M}c^2$ on the plaque resemble Einstein's handwriting. Einstein used unusual today symbol $\mathcal{M}$ for the mass, see [2]. The curved hole in violin advocates the symbol for a double integral.

The artistic processing of the plaque was done in 1998 by Zdeněk Kolářský under documentation and consultations with Michal Křížek and Alena Šolcová. This project was supported by the Union of Czech Mathematicians and Physicists and the City Hall of Prague, which is marked at the bottom of the plaque.

The painting on the next Storch House no. 16/552 recalls the half-a-year long visit paid to Prague by Giordano Bruno in 1588. A memorial plaque placed at the Planetum in Prague recognizes his work.

Professor of physics Ernst Mach had lived for some time in the house no. 19/549 situated on the right part of the Einstein memorial plaque. A bust honoring Mach is located at Ovocný trh no. 7/562.

The Old Town Square is one of the most famous and important places in Prague. It is located in the very historical center of the city. Since the 11th and 12th centuries, when it was a crossroad of merchant roads and the marketplace, the Square has witnessed both the most glorious and also the most tragic events in the history of the Czech lands.

The most admired and sought-after monument there is obviously the Astronomical Clock on the Old-Town Hall, also known as the Prague Horologe. It consists of three units: moving statutes of the 12 apostles that appear each hour in two small windows in the upper part of the Clock, the astronomical clock with its dial, and a round calendar dial with the signs of the zodiac. The mathematical model of the Astronomical Clock was developed by the Czech astronomer and mathematician Jan Ondřejův called Šindel, professor and also the rector of Prague University.

227

The astronomical clock was constructed around the year 1409 by clock-master Mikuláš of Kadaň under Šindel's supervision. In about 1490, the calendar dial was placed under the astronomical dial. In the centuries which followed, the complex mechanism was enhanced and new statues were added.

The astronomical dial is an astrolabe on the clock face using a stereographic projection with the center on the North Pole of the celestial sphere. The dial shows various ways of measuring time over the course of centuries. The outer black ring bears gold Arabic numerals showing the old Czech hours counted from the sunset of the previous day. Roman numerals stand for what is called the German (or Italian) time introduced in the period of Emperor Rudolf II. Black Arabic numerals mark uneven planet hours, the length of which changes during the year. Three rotating pointers show the place of the Sun on the ecliptic, the movement and phases of the Moon as well as the rising, culmination and setting of individual signs of the Zodiac. The pointer decorated with a small golden star indicates the celestial time. In [5, pp. 225–252], you can find which mathematics is hidden behind Prague's Horologe.

After you get seen enough of the Prague Astronomical Clock, look down at the pavement to see the Prague Meridian which was formerly used by Prague citizens to determine the time. It was defined by the shadow cast of the column of Our Lady at Noon [Mariánský sloup]. Unfortunately, the original column was destroyed in 1918, but at present there is a replica. The metal memorial plaque on the pavement reads: *"Meridianus quo olim tempus Pragense dirigebatur"* [The meriadian according to which the time used to be defined.] Later time began to be measured more exactly at the Astronomical Tower of Klementinum which you will be invited to visit later.

The Old Town Square and its surrounding streets also commemorate a number of outstanding scientists and artists who lived in Prague. For example, the Church of Our Lady (Týnský chrám) is the final resting place of the great Danish astronomer Tycho Brahe (1546–1601). He was probably the best observer of the heavens before the invention of telescope. He is buried in front and to the right of the altar. The nearest pillar holds a tombstone made of rose marble from nearby Slivenec, portraying Tycho Brahe in relief and accompanied with the following inscriptions in Latin:

"Esse potius, quam haberi" [Rather to be somebody than only to give such an impression] and *" Nec fasces, nec opes, sola artis sceptra perennant"* [Neither power, nor riches, only the sceptre of knowledge persits.]

The house on the corner of Maiselova and Kaprova Streets is where the above-mentioned famous Czech writer Franz Kafka was born. A memorial plaque has been placed on this house. This location is called Franz Kafka Square.

The campus of Charles University at Celetná Street incorporates Karolinum which is also accessible from Železná Street. It is the main historical building of Charles University, founded by the Czech king and Roman emperor Charles IV in 1348 and being the first university in Central Europe. Although Karolinum is a national historical monument, it continues to serve as an important university building. Its Great Hall is where graduation ceremonies and other important events

still take place. In another hall of Karolinum – its Vlastenecký sál [Hall of Patriots] – a famous lecture *"Über das farbige Licht der Doppelsterne"* [On the color light of binary stars] was given by Christian Doppler (1804–1853) in 1842. There he presented his concept of the phenomenon that was later given his name – the Doppler effect. In 2006, a memorial plaque honoring Doppler was placed on the house at U Obecního dvora no. 7/799, where he lived from 1843 to 1847.

A bust of mathematician and philosopher Bernard Bolzano (1781–1848), who was also among those who heard Doppler's famous lecture, is placed to the right of the main entrance to the Hall of Patriots of Karolinum. A memorial plaque in honor of Bernard Bolzano was placed on the house called "The Four Stone Columns" in Celetná Street no. 25/590, where he spent his last years. Bolzano wrote among others an interesting treatise: *Paradoxes of infinity.* He also constructed a continuous function which has no derivative at any point.

The former university hall of residence on Ovocný trh no. 12/573 was where Johannes Kepler lived between the years 1604 and 1607. It was where he discovered that the orbit of Mars is elliptical. In 1604, he observed the supernova in the constellation Ophiuchus from the wooden observational tower in the garden of that university building. A memorial plaque was placed on the left side of the passage.

Eminent Czech physicist, mathematician, astronomer, and physician Jan Marek Marci from Kronland stayed in a home on Melantrichova Street no. 12/472 in the period 1635–1667. Twenty years before Newton, he carefully described the dispersion and diffraction of light, studied the color spectrum of the rainbow, etc.

In 1911, the Montmartre cabaret was opened in Řetězová Street no. 7/224. Albert Einstein and his older colleague Georg Pick were frequent visitors there. Not far away, in Husova street no. 5/240, one can find a new plaque dedicated to Professor Friedrich Reinitzer who discovered the first liquid crystal, see [3].

In Prague's Old Town Klementinum you can find an observatory dating back to mid-18th century and the oldest meteorological station in Central Europe which keeps an uninterrupted record of meteorological data since 1775. Klementinum was originally a Dominican monastery. In the 16th century, it became the seat of a Jesuit College and University. Today Klementinum is a national cultural monument and the seat of the National Library of the Czech Republic. The whole large complex of buildings is dominated by the 52-meter high Astronomical Tower, which was completed in 1722. It is topped with a lead sculpture of Atlas bearing on his shoulders an armilar sphere (the symbol of astronomy). Due to the prominent Jesuit mathematician, physicist and astronomer Josef Stepling, the tower was equipped with various astronomical instruments. Fifteen sundials can be found on the premises of Klementinum. After an independent Czechoslovakia was formed in 1918, the Klementinum observatory became the seat of of the Czechoslovak Astronomical Society for some period.

Leaving Klementinum, you catch sight of the Old Town Bridge Tower which is a gateway to the famous Charles Bridge. The tower is richly decorated with sculptures. Its decorations include the Aristotelian cosmological model of the universe.

It was probably designed by Emperor Charles IV together with Master Havel from Strahov. The upper part depicts the stable sphere of stars, under which there are a supra-lunar and sub-lunar spheres accompanied with representations of human vices. The number of decorations is connected with periods of time: the number of months in a year, days in a week and hours in a day. The year, date and time chosen for the construction of the Bridge Tower is also remarkable: 1357. If these numbers are completed as follows

$$1\,3\,5\,7\,9\,7\,5\,3\,1,$$

one creates what is called a palindrome comprising all one-figure odd natural numbers [5, p. 113]. Emperor Charles IV chose that special sequence on the recommendation of Master Havel from Strahov as the best moment to lay the cornerstone of the Stone Bridge (from 1870 named the Charles Bridge), namely, in 1357 of the Julian calendar on the 9th July at 5 o'clock 31 minutes.

References

[1] M. Brod: *Život plný bojů*, Nakl. Franze Kafky, Praha, 1966.

[2] A. Einstein: *Elementary derivation of mass and energy*, Schwadron Collection, J. N. U. L., Jerusalem, 1946.

[3] J. Janko, E. Tešínská: *Reinitzer's discovery of liquid crystals*, DVT 22 (1989), 65–78.

[4] M. Křížek, A. Šolcová, M. Toepell: *Neues Einstein-Denkmal in Prag 1999*, MNU (Der mathematische und naturwissenschaftliche Unterricht) 53 (2000), H4, 252–253; see also Pokroky Mat. Fyz. Astronom. 44 (1999), 258–261.

[5] M. Křížek, L. Somer, A. Šolcová: *From Great Discoveries in Number Theory to Applications*, Springer, Cham, 2021.

[6] M Pasley: *Franz Kafka & Max Brod, přátelství, korespondence*, Hynek, Praha, 1998.

[7] S. Strohs: *Josef Winternitz a teorie relativity*, Filosofia, Praha, 1995.